A forward genetic approach to identify new loci controlling wheat starch digestibility

Petros Zafeiriou

Quadram Institute Bioscience

A thesis submitted in fulfilment of the

requirements for the degree of

Doctor of Philosophy

University of East Anglia

School of Biological Science

December 2022

Abstract

Reducing the rate and extent of starch digestibility in wheat-based foods can help maintain healthy blood glucose levels, which is important for preventing and managing chronic diseases (e.g., obesity, diabetes). To manipulate starch digestibility in wheat (and other crops in general), there have been two key strategies, processing raw materials and modifying starch biosynthesis in planta. Both approaches have shown promise for reducing the starch digestibility of staple foods, but many challenges still remain in producing sustainable products due to increased costs of processing or penalties on yield or crop quality. A forward screening approach, which aims to identify genetic loci underpinning natural variation, opens the possibility of discovering new genes that influence starch digestibility.

This PhD project aimed to develop an improved method for measuring starch digestibility in a diverse wheat germplasm collection with the ultimate aim of discovering new loci that could be used to breed wheat varieties with improved health benefits.

To achieve this, 1) a high-throughput screening tool was developed to enable the screening of large germplasm resources; 2) the core Watkins collection, a historical collection of wheat landraces was screened and presented wide variation of starch digestibility; 3) in-depth analysis was conducted to investigate starch properties among selected low- and high-digestibility lines in sieved flour fractions and purified starch; 4) a stable low-digestibility line was selected, and a biparental mapping population was used to identify QTL for starch digestibility.

Acknowledgements

I am grateful to my supervisors, Dr Brittany Hazard, Dr Simon Griffiths, Dr Fred Warren and Brendan Fahy, Prof Peter Wilde and Dr David Seung, for guiding for their guidance during my 4-year PhD journey. I was on a team of experts with different notions and backgrounds.

I would like to thank all members of Brittany Hazard Group and David Seung Group for their great advice, understanding and friendship.

Thanks to the Limagrain team that hosted me during my Professional Internships for PhD Students (PIPS) and did everything they could to feel part of their team.

I would like to thank the UK Research and Innovation (UKRI) Biotechnology and Biological Sciences Research Council (BBSRC) Doctoral Training Programme for funding this project.

I would like to thank Dr George Savva, who has been a great help throughout my PhD, always providing me with statistical support and experimental guidance. I want to thank Dr Natalia Perez and Dr Peter Ryden for their noble act of selflessness when I had questions; to Dr Jennifer Ahn-Jarvis, who has always been to support me in my project and provided brainstorming sessions when needed and to Dr Cathrina Edwards, who has always been kind to advise me when I had issues with the starch digestibility assay.

I would like to thank my friends Dr Marina Corrado, Dr Raffaelle Colosimo, Dr Anabel Mulet-Cabero, Dr Kathrin Haider, Dr Trey Koev, Dr Hannah Harris, and Jennifer McClure for all the wonderful moments I have shared with them.

Thanks to my mother, who has always believed in me and is so proud of me.

Thanks to my grandfather Petros and grandmother Foteini that raised me and did everything they could to make me feel equal to other children.

I extend my gratitude to my track and field coach, Dora Ountzoudi, for giving me the confidence and motivation to achieve my goals.

Finally, I would like to thank Christina, who has always been my best friend and partner and support everything I do. I am forever grateful for quitting her job and moving with me to Norwich to do my PhD. I would like to thank Christina's parents Ioanna and Kostas, for always being there for me in times of joy and misery.

Lastly, I would like to extend my gratitude to all the people who helped me during my PhD and made this an unforgettable experience.

Presentations

"The hunt for healthier wheat, High-throughput *in vitro* starch digestion assay reveals wheat landraces with low starch digestibility"

Starch Round Table, 4-7 October 2021, Online Conference

"High-throughput in *vitro starch* digestion assay reveals wheat landraces with low starch digestibility"

Designing Future Wheat, 18 November 2021, Online Conference

"High-throughput *in vitro* starch digestion assay reveals wheat landraces with low starch digestibility"

Monogram, 4-6 April 2022, Leeds, UK

Publications

Corrado, M., **Zafeiriou, P**., Ahn-Jarvis, J.H., Savva, G.M., Edwards, C.H. and Hazard, B.A., 2022. Impact of storage on starch digestibility and texture of a high-AM wheat bread. *Food Hydrocolloids*, p.108139.

Zafeiriou, P., Savva, G.M., Ahn-Jarvis, J.H., Warren, F.J., Pasquariello, M., Griffiths, S., Seung, D. and Hazard, B.A., 2023. Mining the AE Watkins Wheat Landrace Collection for Variation in Starch Digestibility Using a New High-Throughput Assay. Foods, 12(2), p.266. (available in the supplemental section)

Table of Contents

List of Figures

List of Tables

List of Supplemental data

Abbreviations

ADP	Adenosine diphosphate
ADPG	Adenosine diphosphate glucose pyrophosphorylase
AFLP	Amplified Fragment Length Polymorphism
AGPase	ADP-glucose pyrophosphorylase
AM	Amylose
AMG	Amyloglucosidase
AP	Amylopectin
AX	Arabinoxylans
BBSRC	Biotechnology and Biological Sciences Research Council
BGC1	B-granule content 1
BPNPG7	Blocked p-nitrophenyl maltoheptaoside
CI	Confidence Interval
CIMMYT	International Maize and Wheat Improvement Center
CLD	Chain Length Distribution
cM	CentiMorgan
DAA	Days After Anthesis
DBE	Debranching Enzyme
DFP	Diisopropylfluorophosphate
DPA	Days Post Anthesis
DMSO	Dimethyl sulfoxide
DP	Degree of Polymerisation
DRI	Differential Refractive Index
DSC	Differential Scanning Calorimetry

DWB	Dry Weight Basis
EDTA	Edetic acid
EMS	Ethyl methanesulfonate
FAO	Food and Agriculture Organization
GBSS	Granule-bound Starch Synthase
GMO	Genetically Modified Organism
GRU	Germplasm Resources Unit
GSP-1	Grain softness protein-1
GI	Glycaemic Index
GWAS	Genome-Wide Association Study
G-6-P	Glucose-6-phosphate
G-6-P DH	G-6-P dehydrogenase
HK	Hexokinase
ISA1	Isoamylase I
ISA2	Isoamylase II
JIC	John Innes Centre
KASP	Kompetitive Allele-Specific PCR
LOD	Logarithm of the Odds
LOS	Logarithm of Slope
MAS	Marker-Assisted Selection
NA	Not Available
NADP	Nicotinamide-adenine dinucleotide phosphate
NAM	Nested Association Mapping
NDF	Non-Dietary Fibre
NGS	Next-Generation Sequencing

NIR	Near Infrared Reflectance
NS	Not Significant
NSP	Non-Starch Polysaccharide
PAHBAH	p-hydroxybenzoic acid hydrazide
PBS	Phosphate buffered saline
QIB	Quadram Institute Bioscience
QTL	Quantitative Trait Loci
PCR	Polymerase Chain Reaction
RAG	Rapidly Available Glucose
RAPD	Random Amplified Polymorphic DNA
RDS	Rapid Digestible Starch
REML	Restricted maximum likelihood
RFLP	Restriction Fragment Length Polymorphism
RI	Refractive Index
RIL	Recombinant Inbred Lines
RS	Resistant Starch
SBE	Starch Branching Enzyme
SBEI	Starch Branching Enzyme I
SBEII	Starch Branching Enzyme II
SCFA	Short Chain Fatty Acids
SD	Standard Deviation
SDS	Sodium Dodecyl Sulfate
SDS	Slowly Digestible Starch
SDS-PAGE	SDS- Polyacrylamide Gel Electrophoresis
SE	Standard error

SEC	Size Exclusion Chromatography
SEM	Scanning Electron Microscopy
SGLT1	Sodium-glucose cotransporter 1
SKCS	Single Kernel Characterisation System
SNP	Single Nucleotide Polymorphism
SS	Starch Synthase
SSR	Simple Sequence Repeat
SSI	Starch Synthase I
SSII	Starch Synthase II
SSIII	Starch Synthase III
TEM	Transmission Electron Microscope
TGW	Thousand Grain Weight
TILLING	Targeting Induced Local Lesions IN Genomes
TRIS	Tris(hydroxymethyl)aminomethane
TS	Total Starch
UKRI	UK Research and Innovation
UPLC-SEC	Ultra-High Performance-SEC

Symbols

$C\infty$	Product concentration or amount of starch digested at the end of digestion
Ct	Product concentration or amount of starch digested at a time, t.
n	Number
R^2	Coefficient of determination
t	Time
λ	Wavelength
k	Rate of digestion
ΔE_{400}	Difference between the reaction and blank absorbance at 400nm
Q	Heat rate flow
Δt	Temperature difference between reference and sample(s) sensors
R	Thermal resistance between the block and pans
V_h	Hydrodynamic volume
Mw	Molecular weight
N_A	Avogadro's constant
V_{el}	Elution time
S_{DRI}	V_{el} detector signals

Chapter 1 Introduction and literature review

1.1 Introduction

Genetic variation holds the key to developing future crops that are more nutritious and resilient to fluctuating environments. Wheat (*Triticum aestivum* L.) is one of the most consumed crops worldwide largely due to its unique storage protein composition (gluten) that can be formed into a dough for bread, pasta, and many other foods. Although protein is essential for function, the greatest contribution to calories in wheat is starch, which comprises ~80% of the grain (Shewry et al., 2013, Delcour, 2010).

Despite the growing demand for wheat, concerns are emerging around starch-rich wheat foods, mainly those made from refined white flour, as the overconsumption of these products could contribute to increased risk of chronic diseases (e.g., obesity and type II diabetes) (Hazard et al., 2020). Thus, recent studies have aimed to analyse starch digestibility in wheat-based foods (Corrado et al., 2022a, Sissons et al., 2020, Belobrajdic et al., 2019). Depending on the rate and extent of starch digestion, starchy foods can have different effects on human health. For instance, regular intake of foods with highly digestible starch (e.g., white bread) can impact glucose homeostasis negatively and increase the risks of vascular disease and type II diabetes (Jenkins et al., 2002). On the contrary, foods with low-digestibility starch can help maintain healthy blood glucose levels and prevent abnormal glucose tolerances and hyperglycemia (Wolever and Mehling, 2002). Foods with low-digestibility can also lead undigested starch (resistant starch (RS)) to the large intestine, where it is further used by bacteria that produce metabolites beneficial for gut health (e.g., short-chain fatty acids (SCFA): butyrate, acetate, and

propionate) (RaigondEzekiel and Raigond, 2015, Slavin, 2013, Roediger, 1982, Lupton, 2004).

To manipulate starch digestibility in wheat (and other crops in general) there have been two key strategies, processing raw materials (e.g., milling, thermal treatment) and modifying starch biosynthesis in *planta* to produce raw materials with new starch properties (e.g., high-amylose (AM) flour). Both approaches have shown promise for reducing the starch digestibility of staple foods, but many challenges still remain in producing sustainable products due to increased costs of processing or penalties on yield or crop quality (JeswaniBurkinshaw and Azapagic, 2015, Bouis and Saltzman, 2017, Hazard et al., 2015).

A third strategy, that is still relatively unexplored, is using a forward genetic approach aimed at discovering new loci affecting starch digestibility that have minimal pleiotropic effects on crop yield and quality. Despite the current advances in wheat genetics and genomics tools, this approach has been limited in wheat due to a lack of efficient and accurate assays for measuring starch digestibility on a large number of samples. Thus, this PhD project focused on developing an improved method for measuring starch digestibility in a diverse wheat germplasm collection with the ultimate aim of discovering new loci that could be used to breed wheat varieties with improved health benefits.

To begin, this chapter presents a literature review on the history of wheat domestication and breeding and highlights the potential for using diverse wheat germplasm as a source of natural variation for new trait development. This review also covers wheat grain composition, with a focus on starch including its biosynthesis, molecular structure and external factors that can influence its structure (e.g., environment and processing). Finally, the chapter ends with a

summary of starch digestion, its impact on health and strategies used to decrease starch digestibility of wheat foods so far.

1.2 Wheat domestication and breeding

The genus *Triticum* (wheat) has been cultivated in different parts of Asia and Africa since 9000 BC (Belderok et al., 2000), and it is believed that the primary ancestor of modern cultivated wheat is *Triticum monococcum* (einkorn wheat). Since then, wheat has hybridized with other wild and cultivated species to evolve into a form that can now be used commercially (Figure 1.1).

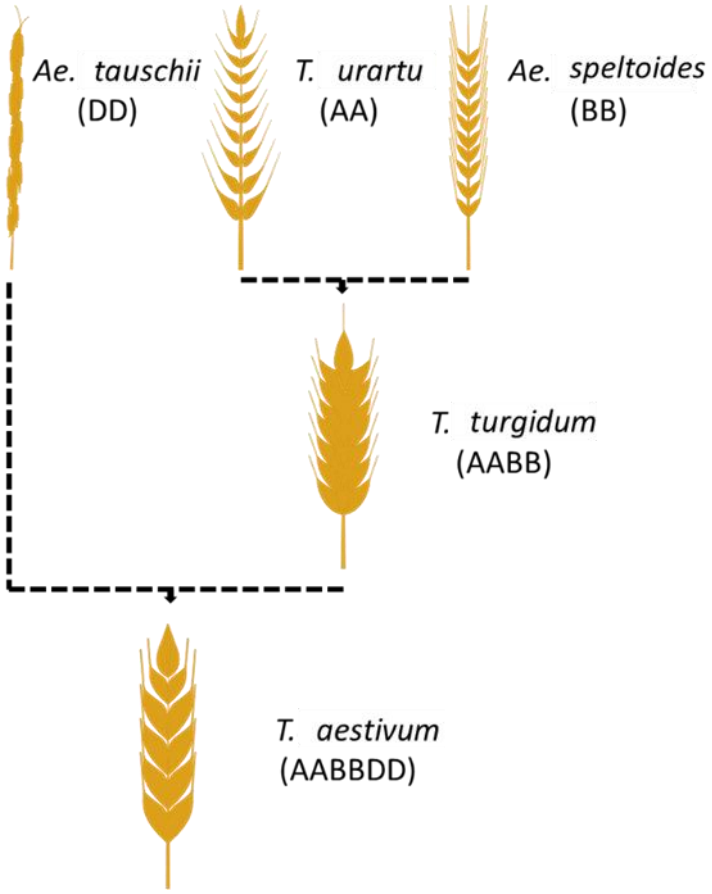

Figure 1.1. Hybridization events led to modern cultivated wheat. The hybridization of T. urartu and Ae. speltoides led to the emergence of the tetraploid species known

as T. turgidum. Then, Ae. tauschii hybridized with T. turgidum, resulting in the formation of T. aestivum. Adapted from (Pourkheirandish et al., 2020)

Today about 95% of the world's wheat production belongs to *T. aestivum* species (hexaploid wheat, AABBDD) (Lukaszewski et al., 2014), and the remaining 5% belongs to *T. turgidum* (tetraploid wheat, AABB), also known as 'durum wheat', which is used in the pasta industry. *T. aestivum* species originated around 6000 BC in the Persian region when the tetraploid species of *T. turgidum (AB-genome donor)* crossed with the diploid grass species *Aegilops tauschii* (D-genome donor) (Belderok et al., 2000, Lukaszewski et al., 2014, Petersen et al., 2006, Nesbitt, 1996). *A. tauschii* species in themselves are not of any economic interest due to the difficulty of threshing the grains and poor yield. However, the hybridization with *T. dicoccoides* led to higher yield and threshable grains (Belderok et al., 2000). *T. aestivum* species started to spread worldwide due to its adaptability to different environments and human activity; in each generation of farmers began selecting the crops with improved traits (e.g., non-shattering seed) that would meet end-user needs. This process is known as selective breeding. In combination with cultural practices, natural selection allowed wheat species to adapt to local conditions and become one of the leading food sources in an increasing human population (Zeven, 1999). These wheat species are known as landraces (locally adapted wheat lines) and were used for thousands of years in human civilisation.

Wheat species continued to develop over the years by crossing wheat plants carrying traits of interest (e.g., disease resistance, high yield) to produce varieties with multiple traits of interest, thus superior to either parent. There are several historical reports of "intentional breeding", with the first being reported in England in 1787 by Knight, who aimed to improve disease resistance in different types of

plants (Lupton, 1987, Venske et al., 2019). Most of the scientific-based work, however, started in the 20th century with Biffen's and Nilsson-Ehle's work which validated Mendel's findings on wheat crops (Nilsson-Ehle, 1910, Biffen, 1905). Wheat development continued gradually until a notable work by Norman E. Borlaug in the mid-1960s, which accelerated the advancements of wheat crops (Borlaug, 2007). During that period, International Maize and Wheat Improvement Center (CIMMYT) obtained semi-dwarf and photoperiod-insensitive wheat cultivars by incorporating reduced height and photoperiod genes in wheat (Pingali, 2012, Evenson and Gollin, 2003, Venske et al., 2019). These cultivars adapted to different environments and provided high-yield crops.

As described above, phenotypic selection was the primary method for plant breeders to create more advanced varieties for centuries. Despite success in breeding for many advantageous traits, other agriculturally important traits have been difficult to select for solely based on phenotype due to:

- the complexity of the trait (a range of phenotypes controlled by multiple genes; these traits are called quantitative traits)
- genetic linkage (if genes are close to each other, they tend to co-segregate)
- environmental interactions
- gene environment interactions

These factors led to deviations from classical Mendelian segregation patterns and therefore were difficult to deal with. In the 1980s, with the advent of DNA markers (Collard et al., 2005), breeders and researchers were able to create linkage maps in various plants and crops.

Over the years, different types of DNA markers have been developed, which have helped improve breeding accuracy and precision. These markers have been used to

identify genetic variations between individuals or populations, detect genetic diseases, and help select desirable traits for breeding (Lateef, 2015).

The most common types of DNA markers include:

- Restriction Fragment Length Polymorphisms (RFLPs): RFLPs were the first type of DNA markers used in plant breeding. These markers are based on differences in the length of DNA fragments produced by restriction enzymes (Lateef, 2015).

- AFLPs (Amplified Fragment Length Polymorphisms): AFLPs are (Polymerase Chain Reaction) PCR-based markers that use restriction enzymes to generate fragments that are then amplified and visualized by gel electrophoresis (Lateef, 2015).

- Simple Sequence Repeats (SSRs): SSRs consist of a short base-pair motif that is repeated several to many times in tandem (e.g., CAGCAGCAG). These sequences experience frequent mutations that alter the number of repeats.

- Random Amplified Polymorphic DNA (RAPDs): RAPDs are DNA fragments derived from PCR amplification of random segments of genomic DNA with single primer of arbitrary nucleotide sequence.

- Single Nucleotide Polymorphisms (SNPs): a SNP is a variation in a single nucleotide at a specific location in the genome. SNP markers have several advantages over other DNA markers and are often preferred for plant breeding. The advantages of SNP markers are:

    - Abundance: SNPs are the most common type of genetic variation in the genome, with millions of them distributed throughout the genome. This high density allows for high-resolution mapping and analysis of genetic

variation. This is an advantage compared to RFLPs and AFLPs, which are often limited in number and distribution, making them less useful for high-resolution mapping and analysis (Mammadov et al., 2012).

- Bi-allelic nature: SNPs have only two possible alleles at each locus, making them highly informative for genetic analysis. In contrast, RAPDs produce random DNA fragments, and AFLPs and SSRs can have multiple alleles at each locus, making them less informative and potentially more difficult to interpret (Mammadov et al., 2012).

- High-throughput genotyping: SNP genotyping can be done using high-throughput methods such as microarrays and sequencing, allowing for the analysis of thousands of markers in a single experiment. In contrast, genotyping with RFLPs and SSRs can be time-consuming and require specialized equipment. RAPDs and AFLPs are also PCR-based, but they require visual interpretation of gel electrophoresis, which can be subjective and time-consuming (Ganal et al., 2019).

Therefore, SNP markers have become the marker of choice for many genetic studies due to their high level of polymorphism, which makes them useful for population genetics, association mapping, and genomic selection (Yirgu et al., 2023). SNP markers have also been widely used in plant breeding for marker-assisted selection (MAS), allowing breeders to select specific traits more efficiently (Yirgu et al., 2023, HeHolme and Anthony, 2014).

A cost-effective, high-throughput, and reliable method for genotyping SNPs is the Kompetitive Allele-Specific PCR (KASP) assay. KASP assays are based on the principle of PCR amplification followed by allele-specific fluorescence detection using a fluorescence plate reader (Figure 1.2) (HeHolme and Anthony, 2014). The

fluorescence intensity is measured for each dye, and the genotypes are determined based on the presence or absence of the fluorescence signal (HeHolme and Anthony, 2014).

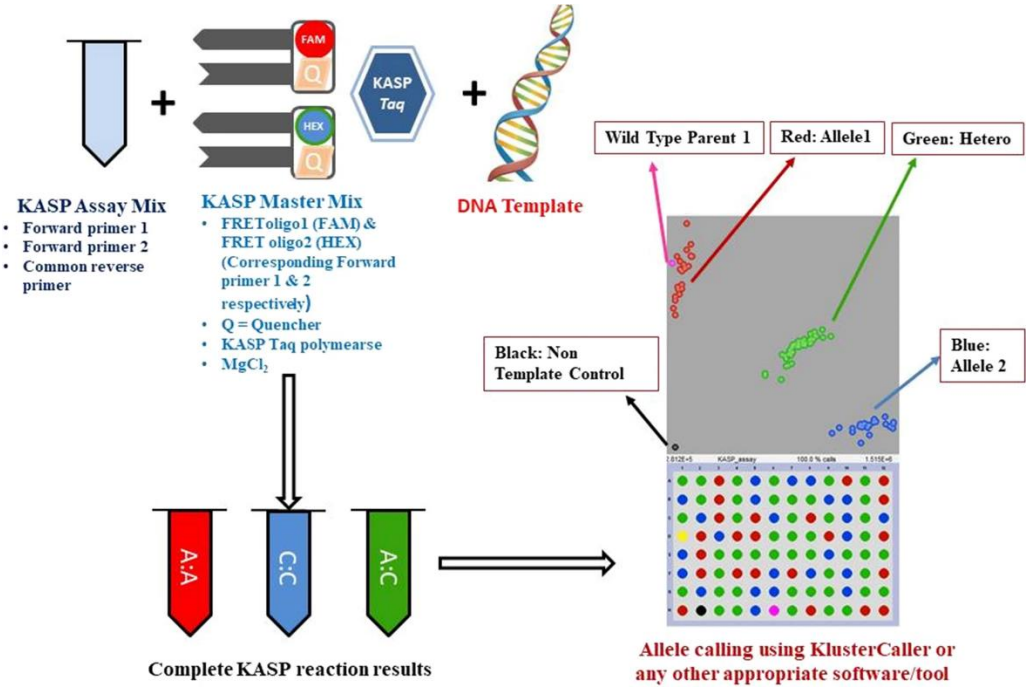

Figure 1.2. KASP mechanism overview. The allele-specific primer used in KASP that matches the SNPs upstream region binds to it and enables discrimination between the two alleles during the PCR amplification. Additionally, each allele-specific primer is against with a different fluor-labelled oligos to allow for fluorescent detection of the amplified PCR products. The amount, fluorescence intensity, of PCR product generated by each allele-specific primer is measured for each dye, and the genotypes are determined based on the presence or absence of the fluorescence signal. Figure adopted from Kaur et al. (2020).

KASPs are widely used in crop development and have become an important tool for high-throughput genotyping in breeding programs.

Mapping populations: populations derived from two or more parents differing in one or more traits, helped breeders to identify single and multiple genes linked with

the trait of interest – quantitative trait loci (QTL) by associating phenotypic scores with DNA markers.

PCR proved to be an invaluable tool in facilitating the use of MAS in breeding programs (Mullis et al., 1986, BorrillHarrington and Uauy, 2018, Ramirez-GonzalezUauy and Caccamo, 2015). MAS uses markers tightly linked to genes/QTL called diagnostic markers which are specific genetic markers that are used to identify or predict desirable characteristics in wheat and other crops. These markers are associated with important traits such as disease resistance, yield potential, quality attributes, and environmental adaptation. The principle of MAS is to select individual plants that carry a trait of interest based on a marker linked to a gene (Collard et al., 2005). The main advantages of using MAS are:

- Higher precision for selecting progeny that carries the genes of interest compared to the phenotypic selection, which can be affected by environmental conditions (Winter and Kahl, 1995)
- Ability to select individuals at a seedling stage decreases costs associated with growing plants to maturity (Collard et al., 2005)
- Possibility to combine and select multiple genes at once as well as select against deleterious or undesirable genes (Collard et al., 2005)
- Cost-effective once MAS markers have been developed compared to applying many phenotypic screenings or conducting complex field analyses (Young, 1999, Dreher et al., 2003, Collard et al., 2005)
- Ability to test for particular traits where phenotypic assessment is not possible (Collard et al., 2005)
- Ability to accelerate gene/QTL introgressions and recovery of the recurrent parent in a backcross (crossing the progeny with one of its parents)

(AndersonChao and Liu, 2007, Kumar et al., 2010a, Kumar et al., 2011, James et al., 2011).

- The ability for breeding companies to accelerate the process of releasing a variety.

In the late 90s, new 'Next-generation sequencing' (NGS) methods were developed, making it possible to obtain millions of sequences in a short time at a significantly lower cost than Sanger sequencing (Sahu et al., 2020).

The combination of low-cost, high-throughput DNA screening, less template preparation and computational development attracted breeding companies to implement the aforementioned genetic tools (NGS and MAS) in their breeding programs. For example, the low cost of sequencing enabled research institutes and breeding companies to screen larger populations to identify polymorphisms and develop DNA markers. By associating the marker data with the phenotypic data (e.g., in a QTL analysis or a genome-wide association study (GWAS)), target traits are linked with diagnostic DNA markers. Then by using MAS, breeders were able to choose parents that carried the markers linked with the target trait (Varshney et al., 2009). Lastly, from as early as the seedling stage, breeders were able to select candidate lines in the progeny that carried the diagnostic marker/s. As a result, these tools helped breeding companies to develop lines with enhanced performance to become new elite varieties.

1.3 Wheat genetic diversity and global demands

Genetic diversity is an important principle in the development of new and improved varieties. Without genetic diversity, breeders won't have access to a wide range of traits and variations and the breeding process becomes limited, leading to challenges in developing better varieties (Reif et al., 2005). Crop breeding heavily relies on genetic diversity since it offers breeders a diverse pool of genes that can be selected for improved traits (Reif et al., 2005). Genetic diversity ensures that breeders have access to a wide range of traits and variations that can be combined through hybridization to produce superior offspring (Venske et al., 2019). Breeders often use the genetic gain equation or breeder's equation (Response = Accuracy * Selection intensity * Diversity / Time) which is a mathematical formula used to describe the relationship between the response to selection and the genetic variance of a trait, considering diversity as a crucial component. This equation is employed to estimate the genetic gain that can be achieved through selection for a particular trait and can guide breeding efforts towards achieving desired outcomes. For example, a higher genetic diversity within the population is essential because it contributes to the overall potential for genetic gain. A diverse genetic pool allows breeders to explore a broader range of genetic variations, increasing the chances of identifying individuals with superior traits for selection. Therefore, genetic diversity consideration is particularly important in pre-breeding efforts to ensure that it helps broaden their genetic resources, increase their chances of finding superior traits and ultimately make more successful and sustainable breeding choices.

Today all elite wheat varieties carry genes underlying agriculturally important characteristics (e.g., high yield, disease resistance, flowering time, protein content, and threshing properties). This was achieved through many years of crossing and selecting markers for preferred phenotypes. Despite the improvements in agronomically important traits, selection has led to an overall decrease in genetic diversity, which may pose challenges for future breeding to reach global demands for food (Dijk et al., 2021).

Today both pasta and bread wheat carry only 30% of the genetic diversity of the wheat wild relatives (Gaut et al., 2018). According to some studies on wheat genetic diversity, the first reduction of gene diversity started as early as the initial domestication of wild emmer (Dubcovsky and Dvorak, 2007, BucklerThornsberry and Kresovich, 2001, BorrillHarrington and Uauy, 2018, Balla et al., 2022). The second "domestication bottleneck" of wheat was during the hybridization of a small set of domesticated emmer (*T. Turgidum*) (4n = 28 chromosomes, AABB) and *Ae. tauschii* (2n = 14, DD) (Figure 1.1). This natural hybridization that occurred about 10,000 years ago further decreased the genetic diversity of the AB genome (contained ~30% of the wild emmer diversity) and D genome (contained less than 15% of the *Ae.tauchii diversity*) (Dvorak et al., 1998, BorrillHarrington and Uauy, 2018). As wheat species started to spread and become landraces, many crosses occurred between emmer and hexaploid wheat, *T. aestivum* (6n = 6x = 42 chromosomes, AABBDD). This caused an increase in the genetic diversity of hexaploid wheat by re-introducing part of the remaining genetic diversity of the domesticated emmer (BorrillHarrington and Uauy, 2018). The genetic diversity of these landraces started to narrow again over the years due to genetic drift and human selection (DoebleyGaut and Smith, 2006, Wingen et al., 2014, Reif et al., 2005). Especially during the 'green revolution' (the 1950s-1960s), many breeders

focused on specific genes to improve yield, resistance to diseases, and quality to create elite cultivars (Winfield et al., 2018).

At the beginning of the 2000s, the advent of genetic tools in plant breeding caused a further reduction in the genetic diversity of bread wheat. New tools allowed breeders to target and select specific genes in a population. A study that examined the genetic diversity of modern cultivars of bread wheat in the UK, USA and Australia showed that UK wheat had the lowest genetic diversity between 1940 and 2005 (White et al., 2008, Roussel et al., 2005). However, this reduction of germplasm diversity depended on the breeding program. For example, in the same period, the USA and Australia had more diversity in their modern bread cultivars (White et al., 2008). Conversely, CIMMYT wheat varieties showed a decrease in genetic diversity between 1949 and 1989 but increased diversity between 1990 and 1997 (Reif et al., 2005). Later, studies comparing wheat landraces with elite varieties showed a loss of phenotypic and genetic diversity. For instance, the whole Watkins collection, 826 landrace cultivars acquired in the 1930s by A.E. Watkins from 32 countries from Asia and Europe and Africa (currently held at the germplasm resources unit (GRU) Seedstor at the John Innes Centre (JIC): https://www.seedstor.ac.uk), showed a greater level of genetic diversity compared to modern European bread wheat varieties as well as more variability in agronomically important phenotypes (Wingen et al., 2014, Bansal et al., 2011, Bansal et al., 2013, Randhawa et al., 2015, Toor et al., 2013).

Future yield trends, nutritional demand, and climate changes set high challenges for future wheat development and, as a consequence, have raised global concerns about meeting the demand using the existing diversity in wheat breeding programs.

For example, it was predicted that wheat demand would increase every year by 1.7 – 2.2% globally (Ray et al., 2013). Wheat yield, however, did not follow this trend; a study that analysed historical crop production trends showed that countries that constitute 24% of the world wheat production (Australia, France, India, Netherlands, UK) had plateaued since 1995 (GrassiniEskridge and Cassman, 2013).

Regarding nutritional demand, Food and Agriculture Organization (FAO) released a report discussing the challenges to reducing the "double burden" of malnutrition that derives from the coexistence of undernourishment and being overweight (FAO, 2018). According to FAO estimates, levels of undernourishment were decreasing until recent years, but in 2015 the levels of undernourishment grew. Together with the persistent prevalence of overweight people, this shows a warning sign for the target goal of ending all forms of malnutrition by 2030, which is less than a decade away (FAO, 2018).

Some of the causal issues leading to undernourishment and 'overnutrition' derive from a diet low in vitamins, minerals and fibre content (FAO, 2018). Supplementing the above report, a total of twenty-nine studies that looked at the dietary fibre intake in adults showed that globally the amount (g) of fibre consumed per day ranged from 15-25g in males and 14-21g in females. Based on these results, most countries – including the UK, did not reach the suggested daily recommendation of fibre (25-35g/d and 25-32g/d for adult men and women, respectively) (Stephen et al., 2017).

Considering future agricultural trends, nutritional data and evidence of low genetic diversity, it can be argued that there is a need to increase the genetic diversity of modern wheat cultivars. By increasing genetic diversity, there is a higher probability of balancing a yield growth that will catch up with the global wheat demand and meet key nutritional requirements.

1.4 Sources of natural variation in wheat

There are currently a number of wheat germplasm resources available as a source of natural genetic variation, such as synthetic hexaploid wheat, landraces, wild relatives and biparental and multiparental wheat populations.

Synthetic wheat is a recreation of hexaploid wheat by introducing a variant of *Ae. tauschii* into tetraploid wheat (Dreisigacker et al., 2008). The re-introduction of *Ae. tauschii* aims to improve the limited variation of the D genome captured in all bread wheat (BorrillHarrington and Uauy, 2018).

Landraces are wheat lines that were developed by natural selection and conventional breeding. These lines were adapted slowly to local places, and thus different landraces vary in genotype depending on the place where they were grown. The most well-known collections are those of the INRA collection, containing more than 10,000 accessions (40% of those have been studied) (Balfourier et al., 2007), the 998 accessions of hexaploid wheat (Huang et al., 2002) derived from 68 countries of five continents, the whole Watkins collection containing 826 accessions (Wingen et al., 2014) and the Mexican creole wheat collection that contains 8,416 Mexican landraces (Vikram et al., 2016). From the Watkins collection, a smaller set of 300 landraces and a core set of 118 landraces was created, representing most of the genetic variation captured in the 826

accessions (Wingen et al., 2014, Arora et al., 2023). This core set was used to generate mapping populations that can be used for both research and breeding purposes (Wingen et al., 2017). Specifically, the core Watkins was developed using a reduced set of landrace cultivars that were initially selected based on diverse phenotypes in adult plant height, heading date, and four grain characteristics (Wingen et al., 2014). The diversity of this core group was then determined using the CoreHunter software using various diversity indices such as the Cavalli-Sforza and Edwards Distance, Modified Rogers Distance, Number of Effective Alleles Index, and Shannon-Weaver Diversity Index (d_{SWI}) (Thachuk et al., 2009). To select the final core set of accessions, the d_{SWI} index was used because it produced the highest value of genetic diversity when averaged over all four diversity indices.

Modern cultivars can also be used in breeding programs as long as the traits of interest are different from those possessed by elite varieties. Several different population structures can be used: biparental populations or multiparental populations (e.g. MAGIC population) (Saintenac et al., 2018, Huang et al., 2012, Mackay et al., 2014, Milner et al., 2016, Dixon et al., 2018), nested association mapping panels (crossing a number of different lines to a common parent) and association panels consisting of a variety of cultivars (Jordan et al., 2018, Sukumaran et al., 2015, Liu et al., 2017, BorrillHarrington and Uauy, 2018).

Although all of the populations mentioned above can be used in a breeding program, there is a significant difference in the level of ease of using these sources. For example, wild relatives will contain the highest genetic diversity compared to other sources. However, the ease of recombining loci with the elite varieties will be the most challenging (Figure 1.3). On the other hand, modern wheat lines are the easiest to cross with the elite varieties, but the genetic variation is the lowest

compared to wild relatives and landraces. Acknowledging the above comparisons, landraces are considered the sweet spot for introgressing alleles into elite varieties due to the relatively larger variation that is captured compared to the modern cultivars but still easy to recombine material to the elite wheat lines (personal communication with Prof. Cristobal Uauy, JIC, UK).

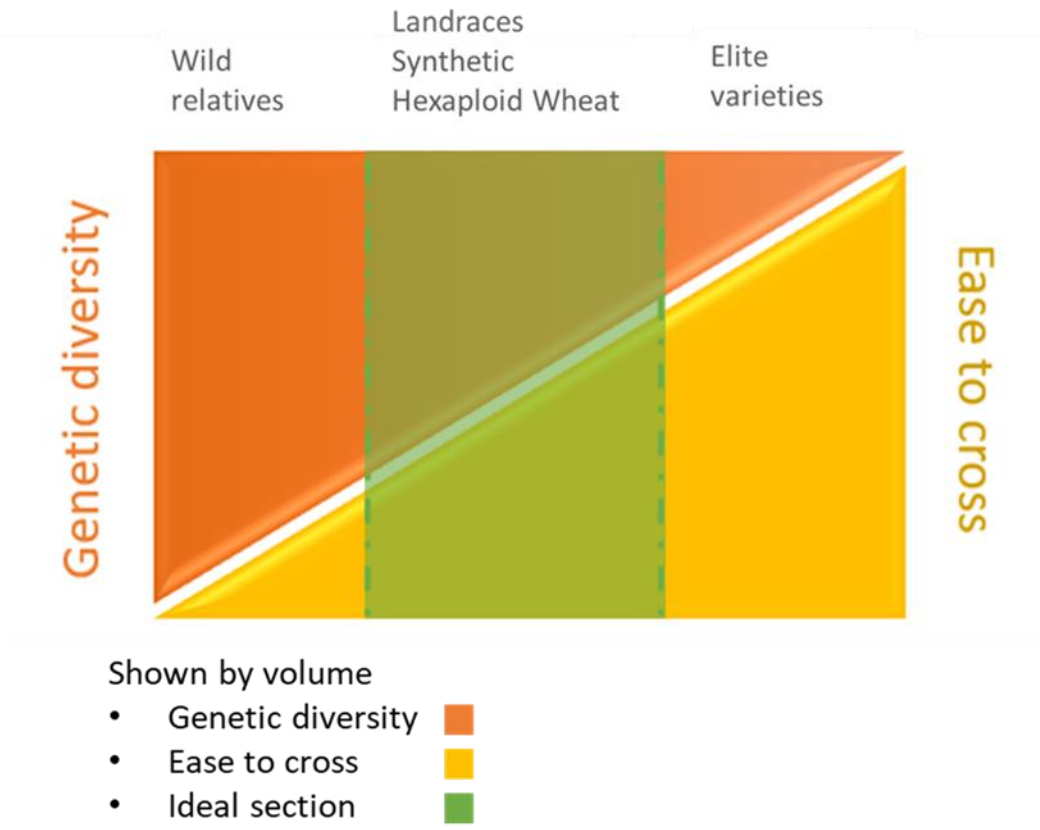

Figure 1.3. Relationship between genetic diversity and ease of crossing, as represented by volume (genetic diversity: orange, ease to cross: yellow, ideal section: green), across wild wheat relatives, landraces, hexaploid wheat, and elite wheat lines. This graph was created through personal communication with Prof. Cristobal Uauy, JIC, UK.

1.5 Induced variation in wheat

An alternative approach to introduce variation into elite varieties is induced mutagenesis. Chemical mutagenesis and radiation are two mutagenetic approaches used in the EU and produce plants that are not regulated as genetically modified organisms (GMOs)(HolmeGregersen and Brinch-Pedersen, 2019, Leitao, 2011, MbaAfza and Shu, 2012). Both types of mutagenesis induce random mutations across the whole genome. Radiation makes use of X or Gamma rays (physical treatment) and Targeting Induced Local Lesions IN Genomes (TILLING) uses chemical mutagens like ethyl methanesulfonate (EMS). The main difference between the physical and chemical approaches is density and specificity efficiency. The physical treatment provides a mixture of gene and chromosomal mutations, whereas chemical treatment mainly targets single-base substitutions (HolmeGregersen and Brinch-Pedersen, 2019). Additionally, chemical treatments provide larger mutation densities (Szarejko et al., 2017). A number of TILLING populations have been reported in wheat (DongVincent and Kate Sharp, 2009, Krasileva et al., 2017, Chen et al., 2012). Among the resources, a joint project between the University of California Davis, Rothamsted Research, The Earlham Institute, and JIC provides an *in silico* TILLING database for both tetraploid (Kronos) and hexaploid (Cadenza) wheat (Krasileva et al., 2017). Both populations exome capture using Illumina NGS (1,535 for Kronos and 1,200 for Cadenza). This TILLING resource enables users to quickly identify mutations in genes of interest for more than 90% of the wheat genes (http://www.wheat-tilling.com/). Examples of TILLING applications in wheat include improvements in starch composition, flowering time and kernel hardness (Chen and Dubcovsky, 2012, Uauy et al., 2009, Wang et al., 2008)

1.6 Wheat grain structure

Wheat grain morphology can vary significantly, but the grain typically has an oval shape and weighs approximately 45 to 50 mg (ŠramkováGregová and Šturdík, 2009) (Figure 1.4). Grain size ranges from 5 to 9mm in length, 3 to 3.5 mm in width, and 2.5-3 mm in thickness (Delcour, 2010, Arendt and Zannini, 2013, Kohyama et al., 2017).

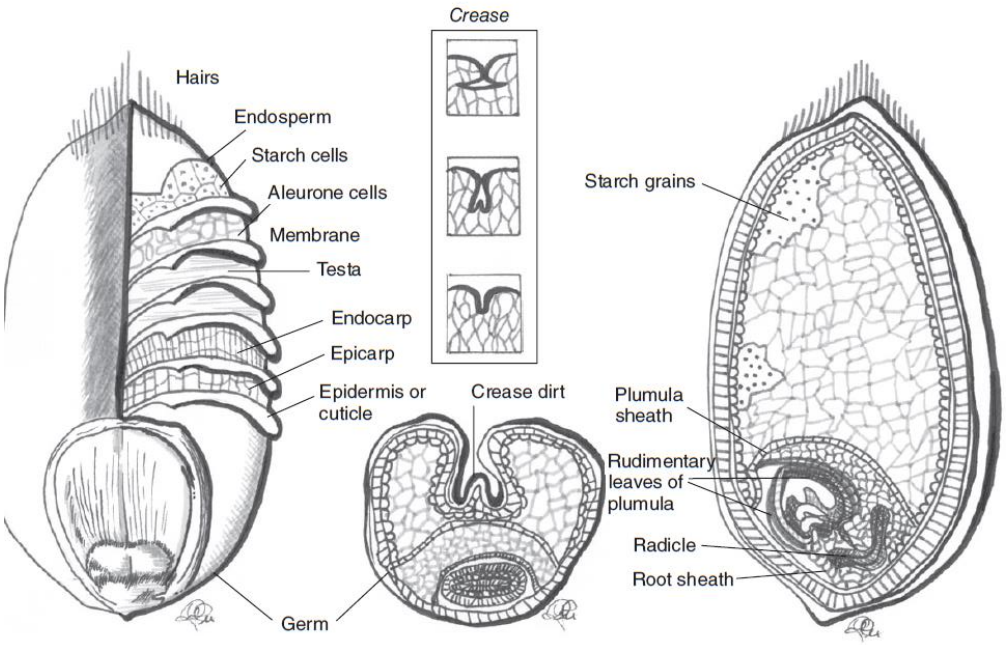

Figure 1.4. Longitudinal and cross-sections of a wheat kernel. Adapted from Arendt and Zannini (2013).

Wheat grains are comprised of an endosperm (80-85%, dry weight), an embryo (2-3%, dry weight), and a series of outer layers of cells (aleurone layer, hyaline layer, testa, pericarp) called the bran (13-17% of the total wheat grain dry weight) (Table 1.1) (Belderok et al., 2000, Evers and Millar, 2002, Arendt and Zannini, 2013). The bran is the source of most dietary fibre in wheat (Belderok et al., 2000). Below the

aleurone layer is the starchy endosperm, where most starch and protein are stored. Its primary function is to provide nutrients to the embryo, primarily in the form of starch, in order for the grain to germinate into a plant (ŠramkováGregová and Šturdík, 2009).

Table 1.1. Percentage distribution of chemical constituents in different fractions of wheat kernels, values are reported as dry weight. Data adopted from Arendt and Zannini (2013)

Fractions	% of kernel weight	Pentosans and hemicellulose	Cellulose	Starch	Protein	Fat
Bran	3.8-4.2	43.1	35.2	14.1	-	5.1-5.8
Pericarp	5.0-8.9	5.0-8.9	-	-	2.5	0.7-1.0
Testa (hyaline)	0.2-1.1	-	-	-	1.5	0.7-1.0
Aleurone	4.6-8.9	-	-	-	14.2	0.2-0.5
Endosperm	74.9-86.5	2.4	0.3	95.8	74.5	6.0-9.9
Germ	2.0-3.9	15.3	16.8	31.5	3.0	0.75-2.2

The starchy endosperm, which constitutes two-thirds of the kernel by volume, is located beneath the cell walls primarily composed of arabinoxylans (AX) and β-glucans (PhilippeSaulnier and Guillon, 2006, Hucl and Chibbar, 1996). The main constituent of the starchy endosperm and the wheat kernel is starch (Hucl and Chibbar, 1996). Starch in plants occurs in a paracrystalline (partially crystalline) form as granules. These starch granules are embedded in the endosperm together

with proteins and lipids. Protein concentration ranges significantly among wheat varieties from 6% to more than 27%, dry weight of a mature grain (Delcour, 2010). Protein in wheat is distinguished between gluten and non-gluten groups. Gluten proteins are the predominant group in wheat, accounting for 80-85% of the total protein, whereas non-gluten proteins account for the remaining 15-25% (Arendt and Zannini, 2013). Gluten proteins are further subdivided into monomeric gliadins (30000 – 80000 mW) and polymeric glutenins (>80000 mW) due to their different functions in food production. Albumins and globulins (<25000 mW) make up the non-gluten proteins (JoyeLagrain and Delcour, 2009). Proteins in the endosperm form a matrix with lipids; lipids constitute about 3-4% of the total wheat grain dry weight and are mainly phospholipids, palmitic and linoleic free fatty acid lipids (Bertoft, 2017, MorrisonMilligan and Azudin, 1984, Wrigley et al., 2015, Delcour, 2010, Arendt and Zannini, 2013).

1.7 Starch biosynthesis

In all cereals, starch, a glucose polymer in the form of AM (linear α-1,4 polymer) and amylopectin (AP) (α-1,4 and α-1,6 polymer), is synthesised in the chloroplast (photosynthetic organelles located in the leaf cells) and amyloplast (non photosynthetic organelles located in the cereal endosperm cells) of the plant (Seung and Smith, 2019). Starch synthesis is a complex process that involves many pathways and enzymes that work synergistically or individually to produce the final structure of starch. Many of the roles of the enzymes are well studied, but there is still a significant amount of research that needs to be done to solve the mechanisms involved in priming polysaccharide formation and starch granule formation (Wrigley et al., 2015). The pathway of starch synthesis involves the production of

sucrose in the plant plastids, followed by conversion to glucose-1-phosphate by phosphoglucomutase (Figure 1.5) (Esposito et al., 1999). After glucose-1-phosphate is used by adenosine diphosphate (ADP) glucose pyrophosphorylase (ADPG) enzymes, located in both the cytoplasm and amyloplast, it is converted to ADPG. ADPG is devoted to continuing the starch synthesis process in the amyloplasts (Wrigley et al., 2015). Then, three main types of enzymes have been shown to synthesise starch, starch synthases (SSs), starch branching enzymes (SBEs) and debranching enzymes (DBEs) (Figure 1.5, Table 1.2) (Wrigley et al., 2015).

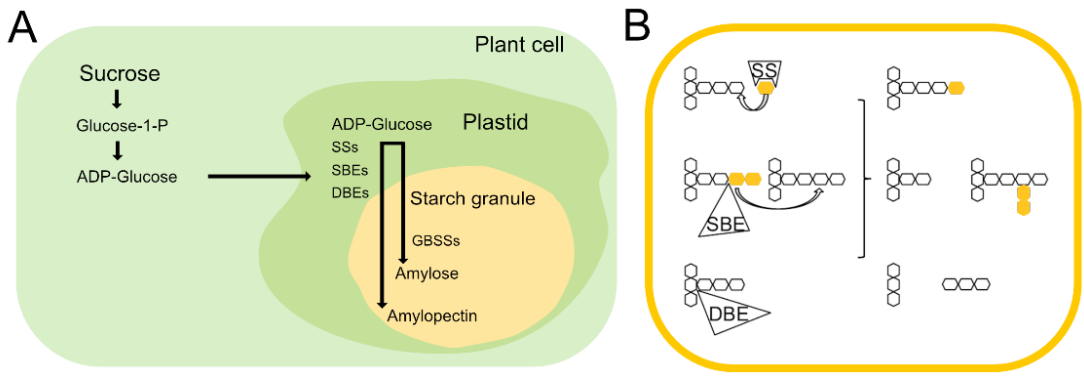

Figure 1.5. (A) Starch biosynthesis pathway; Glucose-P produced from the imported sucrose undergoes a conversion process into ADP-glucose in the plant cell and then is transferred into amyloplasts. SSs transfer ADP-glucose into starch polymers, which are then branched by SBEs and DBEs to form AP. Additionally, GBSSs form linear AM chains. (B) The main enzymatic steps to synthesise starch involve the action of SSs, SBEs and DBEs. Adapted by Li et al. (2015).

Table 1.2. *Main genes involved in wheat starch biosynthesis and their genomic location (RefSeq Annotation v1.0).*

Gene	Wheat gene name	Genomic location
	TraesCS7A02G251400	7A:235460629-235468417
	TraesCS7B02G139700	7B:175999323-176007332
ISAI	TraesCS7D02G249500	7D:220970419-220978648
	TraesCS2A02G293400	2A:504334128-504344701
	TraesCS2B02G309500	2B:442514284-442525323
SBEIIa	TraesCS2D02G290800	2D:372924177-372935106
	TraesCS2A02G310300	2A:533893908-533915882
	TraesCS2B02G327300	2B:468648740-468670922
SBEIIb	TraesCS2D02G308600	2D:395602930-395623439
	TraesCS7A02G120300	7A:77434519-77442262
	TraesCS7B02G018600	7B:15592400-15602503
SSI	TraesCS7D02G117800	7D:72936703-72947152
	TraesCS7A02G189000	7A:145465456-145472269
	TraesCS7B02G093800	7B:107604257-107611452
SSIIa	TraesCS7D02G190100	7D:144130174-144137521
	TraesCS1A02G091500	1A:84002521-84014688
	TraesCS1B02G119300	1B:141283445-141296283
SSIIIa	TraesCS1D02G100100	1D:87756557-87767085
	TraesCS1A02G353300	1A:536958431-536965909
	TraesCS1B02G368500	1B:598877339-598884411
SSIVb	TraesCS1D02G356900	1D:441067006-441074814
	TraesCS4A02G418200	4A:688097145-688100962
GBSSI	TraesCS7A02G070100	7A:35765406-35769104
	TraesCS7D02G064300	7D:35595505-35599537

Starch synthases (SSs)

The starch synthase (SS) enzyme's primary function is to transfer α-glucose molecules from ADP-glucose to the nonreducing end of the α-1,4 glucose polymer. A number of studies have shown that more than nine genes have been reported in plants which are responsible for the production of SSs. Depending on the location of the SS, the enzymes can be separated into two classes. One is the granule-bound starch synthases (GBSSs) which are bound inside the starch granules, and the other

is the soluble SSs, which are found in the amyloplast as well and distributed between the granular and stromal fraction (Wrigley et al., 2015).

For GBSS, two isoforms were reported, the GBSSI and the GBSSII. GBSSI has been shown to be the major contributor to AM synthesis (SmithDenyer and Martin, 1997). Studies on wheat, barley and rice showed that with the absence of GBSSI, a small amount of AM was identified (Patron et al., 2002, Fujita et al., 2011, Vrinten and Nakamura, 2000, Lafiandra et al., 2010). This indicates its primary importance for AM synthesis in wheat. GBSSII has been reported to play a role in the synthesis of AM only in the non-storage tissues of the plant (Al-Dhaher, 2015).

For the soluble SSs, four different isoforms were reported: SSI, SSII, SSIII and SSIV, three of which, SSII, SSIII and SSIV, were further subdivided into SSIIa, SSIIb, SSIIc, SSIIIa, SSIIIb, SSIVa and SSIVb. One of the main actions of SSs is the elongation of the α-1,4 glucan chains and possibly be involved in starch granule initiation (Pfister and Zeeman, 2016). According to Zhang et al. (2011), double knockout mutation of SSIIa and SSIIIa in rice showed a lower percentage of short and long AP chains (5-6 degree of polymerisation (DP) and 12-23 DP, respectively) and a higher percentage of medium chains (7-11 DP). Studies that mutated by knockout SSIIa in durum and hexaploid wheat reported a significant increase in AM content and lower starch content (Hogg et al., 2013, HoggMartin and Giroux, 2017). SSIIb, SSIIc and SSIIIb show very low expression in the cereal endosperm. SSIV is currently lacking much information for evaluating its function.

Starch branching enzymes (SBEs)

SBEs play a crucial role in AP synthesis; they are the major responsible enzymes for the introduction of the α-1,6 branch to the linear glucan molecule (Rydberg et al., 2001, HaworthPeat and Bourne, 1944, Tetlow and Emes, 2014). These α-1,6 branches can then be extended by the same or other enzymes (i.e., SSs) by adding α-1,4 linkages (Wrigley et al., 2015, Ball and Morell, 2003, Crofts et al., 2015). SBEs can be separated into two types due to the different sequence patterns: the SBEI and SBEII (SmithDenyer and Martin, 1997). SBEII can be further separated in cereals, SBEIIa and SBEIIb, due to the slightly different sequences of these two isoforms (Wrigley et al., 2015). The main difference between SBEI and SBEII is the substrate. SBEI transfers slightly longer chains (~15 DP) compared to the SBEII (~ 12 DP), and as substrate preference, it has AM compared to the SBEII, which prefers AP (TakedaGuan and Preiss, 1993, KurikiStewart and Preiss, 1997, Nakamura et al., 2010, Morell et al., 1997, Guan and Preiss, 1993, Rydberg et al., 2001). SBEI knockout mutants of both monocots and dicots had minimal effects on starch composition (Blauth et al., 2002, Tetlow and Emes, 2014). Xia et al. (2011) has identified that the SBEI mutants in maize altered germination; however, the study could not demonstrate a mechanism.

The SBEIIs have clearly shown their contribution to AP synthesis, and mutants for SBEII have severe effects on starch molecular structure (Hazard et al., 2014). When SBEIIa and SBEIIb are suppressed in wheat, high AM content (>70%) is reported. This is not observed in SBEIIb mutants, suggesting that both enzymes' genes should be suppressed to provide high AM wheat starch (Regina et al., 2006, Hazard et al., 2012, Li et al., 2019).

Debranching enzymes (DBEs)

In starch synthesis, DBEs have also been discovered. Their primary function is the removal of some branches attached to the glucans. Therefore, DBEs are essential for the structure of AP and thus starch structure. Depending on their substrate sensitivity, two DBEs have been identified in plants: pullulanase, also called limit dextrinase, and isoamylase (ISA), ISA1, ISA2 and ISA3 isoforms (ZeemanKossmann and Smith, 2010, RepellinBåga and Chibbar, 2008). Both of them attack the α-1,6 glucan linkages and yield α-1,4 linear chains. The pullulanase and ISA3 tend to be more active on the short external chains, and the ISA1 and ISA2 on the longer external chains (ZeemanKossmann and Smith, 2010).

1.8 Starch structure

Starch is an α-glucan polymer that is composed of AM and AP. AM and AP are two polymers that are both formed entirely from α-D-glucose and are the two structural components of the starch granules. However, the two polymers have different molecular structures due to different linkage points. Therefore, AM and AP molecules have different physicochemical properties and susceptibility to digestive enzymes. More specifically, AM is a linear, largely unbranched polymer composed of D-glucopyranose monomers connected by α-1,4 linkages and has a DP up to 6000 and molecular weight 18-37 x 10^4 Mw (Hizukuri et al., 1989, Takeda et al., 1987). A small percentage of these linkages (0.2-0.8%) showed involvement of α-1,6 D-glucose linkages that can disrupt the continuity of the linear polymer (Hizukuri et al., 1981).

On the other hand, AP is a highly branched polymer with α-1,4 and α-1,6 linkages, causing branching every 20 to 25 glucose units. In nature, AP is considered one of

the largest molecules, and its molecular weight could be up to 56.8 x 10^8 Mw (Zhong et al., 2006). In most wheat kernels, AP constitutes around 70%-80% of the starch, whereas AM constitutes 15%-30% (SajilataSinghal and Kulkarni, 2006, Soulaka and Morrison, 1985).

A widely accepted model of AP molecular structure is the cluster model developed to explain the 9nm repetition observed in X-ray diffraction studies of starch granule structure (Figure 1.6) (JenkinsCameron and Donald, 1993, Sanderson et al., 2006, Blazek et al., 2009, French, 1972). More specifically, this model separates the AP into crystalline and amorphous regions. The crystalline regions are formed of double-helical chains of neighbouring short (10-20 DP) AP chains (Imberty et al., 1991, Srichuwong et al., 2005, Wang and Copeland, 2015, Bertoft, 2004).

Each of these helical structure strands has six glycosyl units per turn, a height of 2.1 nm and a length of about 4 to 6 nm (Imberty and Pérez, 1989, Kozlov et al., 2006).

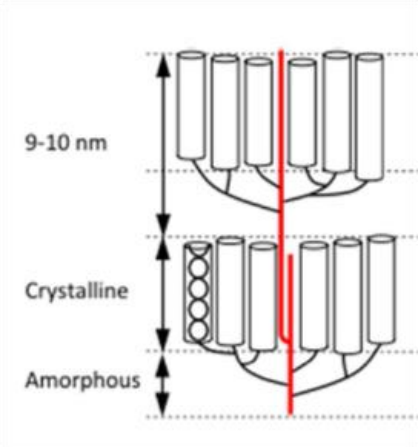

Figure 1.6. AP repeated structure based on the cluster model of Bertoft (2017).

AP structure can also be divided into two main chains: the long B-chains, which have other chains branching from them, and the short A-chains, which do not have any other chain branching from them. Additionally, the C-chain is the single chain that carries the reducing end of the molecule (Figure 1.7).

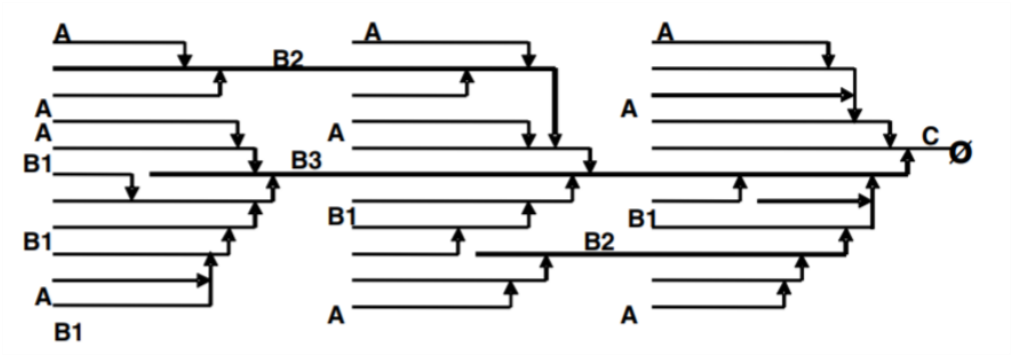

Figure 1.7. Chains of AP structure show the short A chains, long B chains and C chain that carries the reducing end of the molecule. (SajilataSinghal and Kulkarni, 2006, Soulaka and Morrison, 1985).

Granule structure

Although the position of the AM chains in the starch granules is as yet unclear, studies have shown that AM and AP create crystalline and amorphous regions dispersed throughout the starch granule in a particular pattern (Figure 1.8) (Wang and Copeland, 2013). Under X-ray diffraction, crystalline regions are mainly AP high-density side chains with AM that intertwine and create double-helical configurations, creating clusters (GallantBouchet and Baldwin, 1997, Pérez and Bertoft, 2010). Depending on their DP and how these regions crystallize, they create different crystalline structures that have been shown to affect the digestion of starch (PlanchotColonna and Buleon, 1997, Williamson et al., 1992, Cai and Shi, 2013). There are mainly two crystalline structures, the A and B types. A type has an orthogonal unit cell formation and could trap about eight water molecules per unit cell. B type has a hexagonal unit cell formation and could trap about 36 water molecules per unit cell (Ratnayake and Jackson, 2008). A-type was also found to have a shorter chain length (23-29 glucose units) compared to B-type (30-44

glucose units) (SharmaYadav and Ritika, 2008). The mixture of A and B types in crystalline regions creates the C type crystallites. A type crystalline packing occurs mainly in cereals, whereas B type occurs primarily in roots, tubers and high AM starches. C types have been identified in some fruits and roots, and legumes (LuengwilaiBeckles and chemistry, 2008, WangYu and Yu, 2008, WangSharp and Copeland, 2011). The amorphous regions of the granule are composed mainly of AM and AP branch points (endpoints) and AP long linear chains (Wang et al., 2012). The structures are separated into semi-crystalline and amorphous parts, determined by the proportion of amorphous and crystalline regions. The hilum of the granule is mainly amorphous whereas the rest of the granule is separated by peripheral 'growth rings' of amorphous (60-80 nm) and semi-crystalline regions, with steadily increasing thickness (80-160 nm to 450-550 nm) (TesterKarkalas and Qi, 2004, French, 1972, MorrisonTester and Gidley, 1994b, Vamadevan and Bertoft, 2015, Blazek et al., 2009, Koroteeva et al., 2007, Kozlov et al., 2006, Jenkins and Donald, 1995, GallantBouchet and Baldwin, 1997, Wang et al., 2012, Wang and Copeland, 2015).

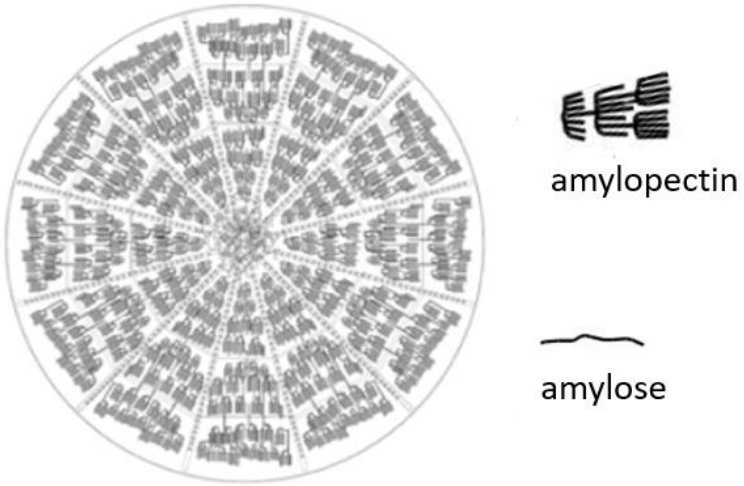

Figure 1.8. Proposed illustration of starch granule structure (Wang and Copeland, 2013, Wang et al., 2012)

Starch granules can vary significantly in size in all cereal cultivars. Starch granules are classed as A and B-type according to their diameter. Very small C-type granules have also been reported, but it remains controversial whether they can be classified as B-type or C-type due to the difficulty of defining a boundary between them (Bechtel et al., 1990, Bechtel and Wilson, 2003, Zhang et al., 2010). Average A-type granules have a diameter larger than 15-16 μm, whereas B-type granules have a diameter lower than 15-16 μm. The large A-type only constitutes around 5% of the total number of the starch granules but accounts for more than half of the total starch (TS) mass (Raeker et al., 1998, Bechtel et al., 1990, ShindeNelson and Huber, 2003, Kim et al., 2011, Zhang et al., 2010). The starch granule's shape in the endosperm is primarily lenticular for the A-type and spherical for the B-type granules; however, shape, size and ratio can vary depending on the cultivar, species, type of host cells, genotype, AM/AP ratio and environment that granules are grown in (LindeboomChang and Tyler, 2004, Nhan and Copeland, 2014,

Langeveld et al., 2000). Although some studies reported differences in the chemical composition of wheat granules, more studies need to be done to support their results (Salman et al., 2009, Liu et al., 2007, Peng et al., 1999, Raeker et al., 1998).

1.9 Environmental factors affecting wheat grain composition and structure

One of the aims of modern breeding is to decrease the variability of yield and grain composition affected by the environment. This is due to the need to develop wheat varieties for particular markets that are stable over the years and to reduce the risk of not fulfilling market requirements. Environmental changes significantly affect wheat yield, composition, and chemical structure (Leng and Hall, 2019, Schleussner et al., 2016, Liu et al., 2011). Several studies suggest that temperature, drought and soil nitrogen are the main environmental factors affecting wheat grain characteristics.

The majority of wheat varieties grow optimally in the range of 20-25^{o}C (Keeling et al., 1994). Temperatures above that range can significantly affect yield and starch content. According to Liu et al. (2011), two wheat varieties (Yangmai 9 and Yangmai 12) had an average decrease of 9.54% and 11.77% of the starch concentration in each days after anthesis (DAA) stage (19-21, 25-27, 33-35) in the year 2003/04 and next year an average decrease of 11.88% and 11.94% in the same DAA stages when the temperature was kept at 40^{o}C compared to 25^{o}C during grain development. For the grain filling, there was an average decrease of 11.28% and 12.02% in each DAA stage in 2003/04 and 14.04% and 16.21% in 2004/05 when the temperature was kept at 40^{o}C instead of 25^{o}C. In terms of the granule size, both lines had significantly reduced A granules. For example, Yangmai 9 decreased 50% and 53% of the A and

B starch granule ratio on 2003/04 and 2004/05, whereas Yangmai 12 decreased 37% and 33% when plants were kept at 40^{o}C. An explanation for this phenomenon is the reduction of the activity of biosynthetic enzymes such as SS, GBSS, and SSS, as well as the reduction of the transcriptional expression of the genes encoding ADP-glucose pyrophosphorylase (AGPase), SS, GBSS, and SBE (Zhao et al., 2008, Keeling et al., 1994, Lu et al., 2019).

Drought is another factor influencing the starch content and yield negatively. If there is a water deficit during grain development, biosynthetic enzyme activity (SSs, AGPase and GBSS) is significantly reduced (CaleyDuffus and Jeffcoat, 1990, JennerUgalde and Aspinall, 1991, Ahmadi and Baker, 2001). This causes alterations in grain starch which is also considered a leading indicator for reduced yield in drought environments (Thitisaksakul et al., 2012). Water stress has also been shown to alter granule size and AM content. According to Lu et al. (2014), water deficit conditions decreased the size of the small starch granules in the wheat endosperm of a high-yield winter cultivar (Zhengmai 366). Another study examining five different wheat varieties on starch characteristics and protein reported an overall decrease in apparent AM content at 8 and 15 days post anthesis (DPA) when plants were kept under water stress (Singh et al., 2008). These results could be explained due to a decrease in the GBSSs activity, which is a significant contributor to the synthesis of AM (SmithDenyer and Martin, 1997).

Soil nitrogen is one of the vital components for crops to grow. Nitrogen has been shown to influence grain composition, mainly protein and starch content. A study examining the effect of nitrogen on grain characteristics and yield on different soil nitrogen conditions on five different Australian varieties reported a strong positive

correlation with protein content and a moderate negative correlation with starch content (Nhan and Copeland, 2014).

All the above studies suggest that if a trait of interest is influenced significantly by environmental factors, it is important to consider the environmental conditions if these are beyond their optimal range for the execution of a forward and reverse genetic approach study.

1.10 Processing and structural changes of starch

Humans mainly process starch before its consumption by mixing it with other compounds and cooking it to improve its flavour and texture (TesterKarkalas and Qi, 2007), but this impacts its functional properties. Starch under the right conditions (enough water or other solvent, high temperature) will undergo gelatinisation and eventually retrogradation (BelitzGrosch and Schieberle, 2009).

Gelatinisation and Shearing

Starch constituents are held together primarily by Van der Waals forces and inter and intramolecular hydrogen bonds between their hydroxyl groups. When starch is heated under sufficient water quantities (in most cases greater than 60%), the energy barrier that holds the constituents together is overcome by the input of heat energy allowing the water to disrupt the hydrogen bonding between hydroxyl groups of the starch molecules (Wang et al., 1991). Water molecules first interact with the amorphous regions as these require less energy to be disrupted compared to the crystalline areas that have a higher energy barrier (Singh et al., 2003). As the amorphous areas get hydrated, they start to destabilise the crystalline regions

(Ratnayake and Jackson, 2008, Wang and Copeland, 2013, BeMiller, 2011). This causes the crystalline structure to become amorphous, resulting in more exposed hydroxyl groups. The granules swell more and absorb more water molecules that interact again with AM and AP via hydrogen bonding. This leads to the loss of the crystalline structure and unravelling of double helices. This irreversible process is called gelatinisation (Liu et al., 2009, LimWu and Reid, 2000, Atwell et al., 1988, Lelievre, 1974, SvihusUhlen and Harstad, 2005, Donald, 2001, Wang and Copeland, 2013).

As granules absorb more water and increase in size several times (each gram of starch granule can absorb 20-40 g of water), some AM components start to leach out (hypothesised to be lower molecular weight AM). This creates a colloidal system that includes swollen granules, granule fragments and AM components which are all dispersed and solubilised in water (LimWu and Reid, 2000, Singh et al., 2003, BelitzGrosch and Schieberle, 2009, Banks and Greenwood, 1975, Gidley and Bulpin, 1989, Han and Hamaker, 2001, LiGidley and Dhital, 2019).

A similar loss of starch crystallinity can be induced by shearing using high mechanical energy. The mechanical energy can disrupt the molecular bonds, whereas heating provides thermal energy for the water molecules to overpass the energy barrier of the AM and AP bonding (WenRodis and Wasserman, 1990). The combination of both energies (mechanical and thermal) makes water molecules transfer faster to the starch components and disrupt the structure. Thus, less water content is required to obtain complete gelatinisation of the starch under shear compared to the equivalent static system (BurrosYoung and Carroad, 1987).

Retrogradation

When a gelatinised starch paste cools down, the dispersed starch forms crosslinks. AM has been shown to preferentially form structures compared to AP chains due to its longer linear polymorphic form allowing it to have higher free energy and thus a higher tendency to form hydrogen bonds and higher Van der Waals attraction (Tian et al., 2009). As AM forms hydrogen bonds with other AM components, it gradually develops a double helical structure (40-70 glucose units) (Jane and Robyt, 1984, Singh et al., 2003). For AP molecules, the outermost short branches are the primary areas that undergo re-crystallisation (Ring et al., 1987). As starch molecule reassociation increases, junction zones (the areas where starch constituents interact) increase (Figure 1.9). Over time, junction zones continue to grow in size until they squeeze water out of the water-filled gaps. This process is called syneresis and is one of the stages of retrogradation.

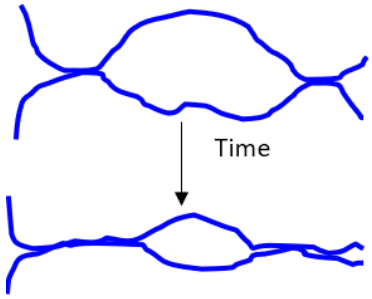

Figure 1.9. Junction zones between glucan chains increase over time in the retrogradation process.

By cooling starch, the degree of digestibility decreases significantly, and more RS can be obtained. This decrease in digestion rate is primarily due to the re-association of molecules that contribute to the re-crystallisation of the starch structure (Berry, 1986, SharmaYadav and Ritika, 2008, SvihusUhlen and Harstad, 2005, Zhou and Lim, 2012, ChungLim and Lim, 2006).

1.11 Starch digestibility and absorption

Starch accounts for approximately 45% to 60% of the calories consumed (Boron and Boulpaep, 2012). Food is our primary energy source, and many digestive processes are required to ensure our food is modified to a form in which nutrients can be absorbed. Hydrolytic enzymes are one of the main actions to convert dietary food into an absorbed form.

Digestive enzymes

In humans and other mammals, starch hydrolysis in the digestive tract is achieved by several glucosidases, including α-amylases and brush border enzymes (maltase-glucoamylase, sucrase-isomaltase) (LinHamaker and Nichols Jr, 2012). α-amylase occurs mainly in two isoforms: salivary α-amylase and pancreatic α-amylase. Both α-amylases have a very similar function and differ only about 6% in their amino acid sequence (Boron and Boulpaep, 2012). Salivary and pancreatic α-amylases are endo-enzymes in action, meaning that both cleave the internal α-1,4 links in the glucose polymers and not the terminal ones (Whitcomb and Lowe, 2007).

Maltase-glucoamylase and sucrase-isomaltase are located at the brush-border membrane. Both are double-headed, and their function is to release glucose molecules by cleaving the α-1,4 links and α-1,6 linkages (LinHamaker and Nichols Jr, 2012). Sucrase's role is to cleave the α-1,2 glycosidic linkages of the sucrose molecules (Boron and Boulpaep, 2009).

Digestion of starch in the human gastrointestinal tract

The first step of starch digestion starts within the mouth (Figure 1.10). There, food containing α-1,4 glucose polymers is cleaved by salivary α-amylases releasing maltose, maltotriose, and minor amounts of glucose (ButterworthWarren and Ellis, 2011). As food is masticated, it is transformed into a bolus by continuous comminution and lubrication in the mouth (Bornhorst and Singh, 2012).

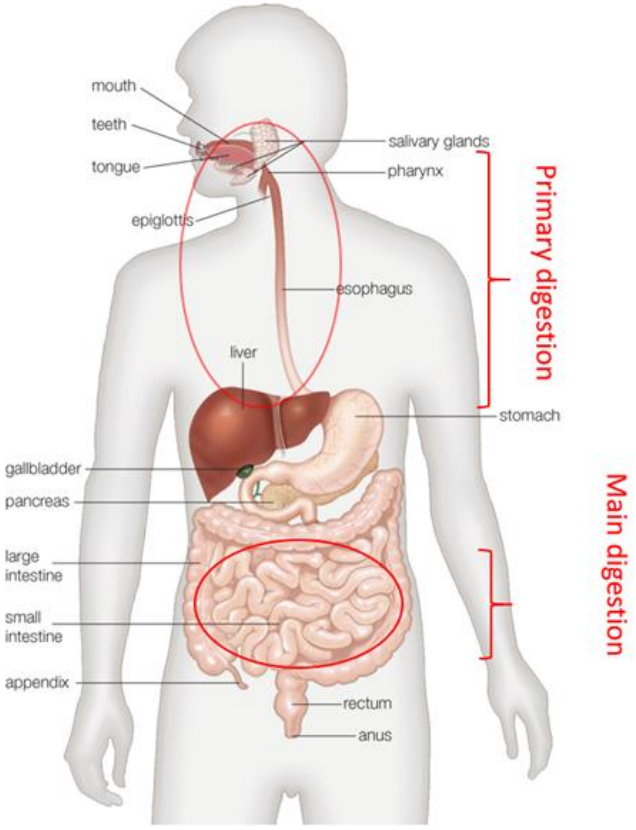

Figure 1.10. Starch digestion areas in the human GI tract. (Britannica, 2019).

The enzymatic digestion process is continued until the salivary α-amylase is exposed to the stomach acid, which has a pH of 1.5 – 3.5 and creates unfavourable conditions for the function of the α- amylase (Boron and Boulpaep, 2012). The digestion at this stage can vary significantly regarding the properties of food as well as between individuals due to dentition status, gender, facial anatomy, personality type, chewing time and speed, and time of eating (Bornhorst and Singh, 2012). Due

to the food bolus structure, some amounts of the α-amylase can be trapped in the food matrix, and thus a delay in its exposure to the stomach acid will occur (Boron and Boulpaep, 2012).

Afterwards, chyme, a mixture of food components inside the stomach, passes through the first section of the small intestine called the duodenum. There, a combination of pancreatic α-amylase and bicarbonate products produced by the pancreas enter the lumen through the hepatopancreatic sphincter and enable the enzymatic process again by neutralising the pH to the optimum conditions (Smith, 2004).

Although maltose and maltotriose derived from α-amylase digestion and branched dextrins are released in the small intestine, humans and other mammals are not able to absorb oligosaccharides molecules (Newey, 1967, Whitcomb and Lowe, 2007). Therefore, brush border enzymes which can convert the oligosaccharides and branched dextrins into monosaccharides, make starch amylolysis products available for absorption; this step is called membrane digestion (Lin et al., 2012).

Absorption

Once the starch amylolysis products are in the small intestine and converted to glucose molecules, Na^+ and specific glucose transporter proteins, sodium-glucose co-transporter (SGLT1/2), transport glucose to the enterocytes (Figure 1.11). SGLT1 transfers only D-isomers of hexoses, and its performance is highly dependent on the concentration of Na^+, where a high concentration increases the absorption rate (Wright, 1993). Most of the glucose the enterocytes take up is transferred out of

the cell through facilitated diffusion by GLUT2 proteins and then into the bloodstream (Smith, 2004).

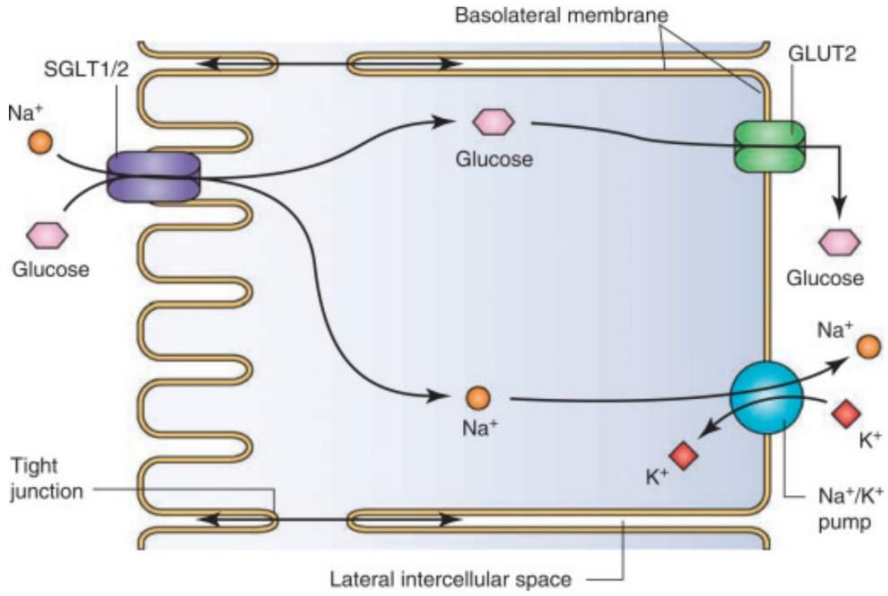

Figure 1.11. Glucose transport process across the brush border membrane. (Wright et al., 2004, Mather and Pollock, 2011).

The first characterisation of starch digestion was reported by Englyst and Cummings (1985) in an *in vitro* study where they concluded that starch could be classified as rapidly digestible starch (RDS), slowly digestible starch (SDS), and RS depending on its digestion behaviour with pancreatic α-amylase. Subsequent studies (EnglystVeenstra and Hudson, 1996, Englyst et al., 1999) found a positive relationship between rapidly available glucose (RAG) and rapidly digestible starch (RDS) with glycaemic index (GI). This relation was supported later by several studies testing different cereal starches in different types of food products and processes (Kim et al., 2003, Hu et al., 2004, Leeman et al., 2006, Capriles et al., 2008, King et al., 2008, Nilsson et al., 2008, Dona et al., 2010, Alsaffar, 2011). Recent studies have used a more rigorous approach to analyse starch digestion using first-order kinetics

as this is a more rigorous approach than analysing fractions of starches (Patel et al., 2014, ButterworthWarren and Ellis, 2011).

1.12 Healthy aspects of low-digestibility starch and Resistant Starch

The rate and extent of starch digestibility play a significant role in our diet and general health. When blood glucose concentrations increase during absorption, insulin, a peptide hormone produced by pancreatic beta cells, triggers the increase of cellular glucose uptake to maintain blood glucose concentration within normal levels. When glucose is not used directly, it is stored in muscles and the liver in the form of glycogen. Repeatedly high glucose concentration levels in the blood due to high carbohydrate diets and high-digestibility products can affect glucose homeostasis (resulting in anomalous glucose tolerance and insulin sensitivity). This can sequentially lead to the development of vascular disease and type II diabetes (Jenkins et al., 2002).

Balancing a diet with lower-digestibility products can reduce the risks of hyperglycemia and potentially prevent the development of metabolic diseases (Wolever and Mehling, 2002). A study that measured the starch digestibility profile of high AM pasta made from *sbella* durum wheat reported a lower digestibility profile than a wild type. This study also showed evidence that low-digestibility pasta had a lower effect on the GI than a wild type when measured *in vivo* (Sissons et al., 2020). A similar analysis looking at high-AM bread and its effect on postprandial glycemia reported a lower rise in GI when high-AM bread was consumed compared to conventional bread (Belobrajdic et al., 2019).

The remaining starch that has not been absorbed in the small intestine during digestion is determined as RS. Therefore, RS is the only starch that reaches the large intestine together with most of the non-starch polysaccharides (NSP), which escape digestion in the small intestine (KleinCohn and Alpers, 1998, EnglystKingman and Cummings, 1992). There, the colonic bacteria ferment the RS and most of the NSP and produce metabolites such as short-chain fatty acids (SCFA) (acetate, butyrate, propionate- together they comprise 95% of the SCFAs in the colon), gases (hydrogen, carbon dioxide, methane) and lactate as well as heat (Topping and Clifton, 2001, Cummings, 1997, SharmaYadav and Ritika, 2008, Topping et al., 2008).

Interestingly, studies that examined the percentage of RS fermented in the large intestine reported that around 70-90% of the RS is fermented compared to 40-60% of the NSP (Phillips et al., 1995, Cummings, 1984). The higher fermentation of RS is translated to a higher by-product production (Lupton, 2004).

Metabolites produced in the gastrointestinal tract have been shown to provide many health benefits (Slavin, 2013). Butyrate, a SCFA, is the preferred energy source for colonic epithelial cells (Roediger, 1982). Studies have also shown that butyrate is one of the main determinants of the metabolic activity and vitality of the epithelial cells and may play a crucial role against colonic disorders (Hague et al., 1993, HeerdtHouston and Augenlicht, 1994, Lupton, 2004).

Acetate has been shown to provide a considerable energy source for the brain as well as the skeletal and cardiac muscles (Lindeneg et al., 1964, Lundquist et al., 1973, Juhlin-Dannfelt, 1977, Skutches et al., 1979, FernandesVogt and Wolever, 2014). Also, acetate is one of the major compounds to increase cholesterol synthesis. Propionate works as an inhibitor of cholesterol synthesis, and both work

synergistically to balance cholesterol production, which plays a vital role in cardiovascular action (Slavin, 2013).

An additional benefit of SCFAs is their function to lower the luminal and faecal pH, which inhibits the development of pathogenic organisms (Slavin, 2013, Wrigley et al., 2015). Together, the SCFAs contribute about 7-8% of the daily energy requirements (Slavin, 2013, Wong et al., 2006).

1.13 Approaches to decrease starch digestibility

1.13.1 Processing approaches

There are two main approaches to manipulate starch digestibility. The first approach is to modify starch digestibility by processing and the second approach is to produce new raw materials with lower digestibility by manipulating starch biosynthesis *in planta*.

Staple wheat foods like bread, biscuits, pasta and other confectionaries require some processing to improve their flavour and texture before consumption. The main processes that wheat undergoes are milling, mixing with other ingredients, cooking and cooling (Figure 1.12). All of these processes impact starch functional properties and may influence its digestibility.

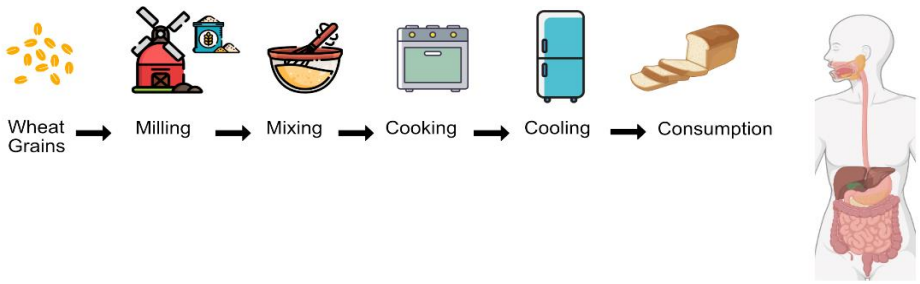

Figure 1.12. Main processes before consumption of staple foods include milling, mixing, cooking and cooling.

For example, during milling, starch granules which are embedded in the endosperm are prone to damage, making them more accessible to digestive enzymes (Edwards et al., 2015). During mixing, food compounds could create complexes with starch (e.g. fatty acids) which could affect its digestibility (Okumus et al., 2018).

During cooking, the heat energy input and mixing cause the starch to gelatinise, and starch polymers leach out in the colloidal phase. The exposure of the starch constituents in the colloidal phase makes them more available for hydrolysis by digestive enzymes. Several studies have shown that when starch is gelatinised, its digestion rate increases significantly (Wang and Copeland, 2013, ChungLim and Lim, 2006, Parada and Aguilera, 2009, Holm et al., 1988). If gelatinised starch in wheat is not consumed and is allowed to cool down, the dispersed starch forms crosslinks, and retrogradation occurs (Tian et al., 2009). Consequently, the digestibility rate decreases when starch is retrograded, and higher RS levels can be obtained (Wang et al., 2015).

The majority of staple wheat foods are made with white flour, a product of milling which removes the outer layers (bran) and embryo of the grain, instead of wholemeal flour, a product of milling whole wheat grains. The bran components present in wholemeal flour can negatively impact dough functional properties; bran constituents disrupt the 'protein-starch matrix' of the dough and impair its rheological properties (elasticity and extensibility) (Boita et al., 2016). This can make it difficult to achieve the desired crumb structure, volume, and overall appearance of the baked product. In addition to disrupting the protein-starch matrix and impairing the rheological properties of the dough, the presence of bran

components in wholemeal flour can also negatively impact other sensory properties of baked goods, such as flavour. For example, bran contains bitter compounds such as phenolic acids, which can affect the taste and aroma of the final product (LaddomadaCaretto and Mita, 2015). Lastly, the presence of bran in flour can also affect the shelf life of the baked goods (Taglieri et al., 2021). The fat present in the bran can oxidize and become rancid over time, leading to off-flavors and unpleasant odours in the baked goods (Wang et al., 2014).

Despite the negative impacts on quality, wholemeal flour has more fibre (12–18% dry weight basis (DWB)) compared to white flour (2-3% dry weight) (Andersson et al., 2013, Lovegrove et al., 2020, Gebruers et al., 2008).

In order to increase the dietary fibre of wheat-based products, many studies have focused on adding exogenous dietary fibre ingredients or modifying processes to decrease digestibility and obtain higher amounts of RS.

Depending on the mill type (hammer mills, roller mills, ball mills, disc mills- wet or dry), the temperature of milling (e.g. cryogenic milling), different cutting techniques (cutting on rear, cutting on cutting, rear on rear, rear on cutting) and different degrees of comminution, starch granules are damaged to a different extent, and thus the digestibility of starch is affected (Darlington et al., 2000, Greenwell, 1986, MorrisonTester and Gidley, 1994a, DhitalShrestha and Gidley, 2010, Devi et al., 2009, Wrigley et al., 2015, Edwards et al., 2015).

Water accessibility, while starch is heated during gelatinisation, has also been shown to affect starch digestibility. Studies that measured the digestion rate of starch after gelatinisation in different water conditions reported decreased digestion rates when water was limited (SajilataSinghal and Kulkarni, 2006, Tester and Sommerville, 2001, Wang et al., 2017, Sievert and Pomeranz, 1989). Repeated

cycles of cooking and cooling in excess water have also been shown to increase RS amounts in wheat flour (Arcila and Rose, 2015).

In terms of additives, a number of listed ingredients can be added to flour to decrease starch digestibility. Compounds such as polyphenols, lipids, metal ions, carbohydrate-binding proteins, cellulose and phytate have been shown to reduce starch hydrolysis by inhibiting the enzymatic activities of starch glycosidases (Kan et al., 2020, Tian and Sun, 2020, Ji et al., 2018, Kumar et al., 2010b). Soluble fibre (AX and β-glucans- the main dietary fibre components of wheat white flour deriving from the cell walls) has also been shown to decrease the digestion rate of starch by its ability to increase the viscosity of the media (Dhital et al., 2014).

Although several studies use processing techniques and additives to increase dietary fibre and reduce digestibility in starch-based products, most of them are product specific, not economically favoured, and not environmentally friendly for long-term use (JeswaniBurkinshaw and Azapagic, 2015, Bouis and Saltzman, 2017).

1.13.2 Genetic approaches

In plants, both forward and reverse genetic approaches have their advantages and can be used in combination to gain a comprehensive understanding of gene function in wheat and other crops. A forward genetic approach involves identifying genes responsible for observed phenotypic differences. On the other hand, reverse genetics involves starting with a known gene sequence and manipulating it to observe the resulting phenotypic changes (Bahuguna et al., 2018).

Reverse genetic approaches

Another key strategy to reduce starch digestibility and increase RS in wheat is the use of crop genetics approaches to generate new starch properties in the grain. Native starch granule structure and composition have been shown to influence its digestibility. For example, higher AM in starches has been shown to be associated with more RS (Hazard et al., 2015, Schönhofen et al., 2016). Therefore, many wheat improvement programs have focused on using reverse genetic approaches to modify genes encoding starch biosynthesis enzymes which control the amount, composition and structure of starch in the grain in order to alter the digestibility of the starch (Regina et al., 2015, Slade et al., 2012). Below are some examples of studies that have reduced wheat's digestibility by mutating genes encoding starch biosynthetic enzymes.

Several studies in wheat SSIIa mutants reported an increase in AM content but lower starch content. The increase in AM was also associated with an increase in RS (Hogg et al., 2013, HoggMartin and Giroux, 2017, Yamamori et al., 2006). Another study that examined high AM wheat with elevated levels of GBSS reported a decrease in both the extent and rate of starch digestion (*in vitro*) compared with wild type wheat (Li et al., 2020b). These polymeric changes obtained by manipulating the enzymes mentioned above showed decreased starch digestibility. However, studies have reported undesirable effects of the mutants, including reduced starch content leading to yield penalties (Hazard et al., 2015). This reduction in yield has been a deterrent factor for breeding companies that need to prioritise yield and disease resistance to meet production demands. Therefore, identifying genes that provide desirable starch characteristics (i.e., reduced digestibility) with minimal impacts on yield is an important strategy for improving nutritional traits of wheat.

Forward genetic approaches

Starch digestibility is a quantitative trait that is controlled by many genes. Although many of these genes are involved directly in starch biosynthesis, there is a possibility that a number of other genes control factors affecting the starch properties and the composition of the starchy endosperm, which could impact starch digestibility.

For example, the firmness of wheat grains known as grain hardness, a significant characteristic that impacts the milling and baking properties of wheat, can impact starch digestibility and is mainly affected by the protein content (mainly by puroindoline (Pin) proteins) and composition in the endosperm (Morris, 2002, Shewry, 2023). The primary factor influencing the trait of grain hardness in wheat is determined by a group of three closely associated genes located at the Hardness (Ha-D) locus on chromosome 5DS (Shaaf et al., 2016). These genes are known as puroindoline a, puroindoline b, and Grain softness protein-1 (Gsp-1) (Shaaf et al., 2016). Hard wheat endosperm is more susceptible to damage and requires higher milling energy compared to soft wheat. This is mainly due to the protein-starch interactions on the surface of the starch granules (Darlington et al., 2000, Shewry, 2023). More starch damage is obtained during the milling of hard wheat, which leads to more accessible starch during digestion (Yu et al., 2015). Another factor that has been shown to affect starch digestibility is the limited accessibility of starch due to its native encapsulation by intact cell walls. According to Bhattarai et al. (2018), intact cell wall structure led to a reduced digestibility *in vitro* in both uncooked and cooked wheat samples compared to deliberately broken cell wall

wheat samples. Legumes as chickpeas and peas, which generally have thicker cell walls than wheat starch endosperm cell walls, exhibit this effect to a greater degree. For instance, chickpeas have a cell wall thickness estimated between 1-2 µm, whereas wheat endosperm is ≤1 µm (Edwards et al., 2021). After 6 hours *of in vitro* digestion, the structural integrity of the intact chickpea macroparticles remained mostly unchanged, while the wheat endosperm cells near the particle edge were ruptured, and their starch was assumed to have been digested (Edwards et al., 2021). In another study on peas, the digestibility of starch of seeds and flour was compared. The study found that pea seeds with less damaged cell walls had lower water absorption and reduced accessibility for α-amylase compared to flour, resulting in a lower blood plasma glucose concentrations compared to flour (Petropoulou et al., 2020).

These examples highlight that genes underlying other grain properties could be targeted to modulate starch digestibility and have further pleiotropic effects on processing which could also impact starch digestibility. Forward genetics approaches can be used to identify underlying genes controlling phenotypes of interest (Bahuguna et al., 2018). More specifically, the benefits of utilizing a forward genetic approach are:

- Genome complexity: A forward genetic approach can help to identify the genes responsible for specific traits without prior knowledge of their sequence. This becomes important because wheat has a large and complex genome which makes it challenging to identify and manipulate.
- Gene discovery: Wheat has a high degree of genetic redundancy, where multiple genes can control a single trait. In such cases, reverse genetic approaches are limited to candidate target genes whereas forward genetics

is open to new gene discovery. Many genes in wheat remain uncharacterized, and their functions are unknown. A forward genetic approach can help identify these genes and determine their roles in various traits and pathways.

- Natural variation: Wheat has significant natural variation, which can be exploited through a forward genetic approach to identify useful traits for crop improvement.

A major bottleneck in forward genetic studies is the lack of availability of high throughput phenotypic screens. Researchers are aiming to develop such high-throughput methods to screen multiple traits reproducibly, non-invasively and flexibly (Mir et al., 2019).

Most of the tools developed so far are designed for field-related traits such as leaf phenology, root structure, plant height, micronutrients, water uptake efficiency, and biomass. In terms of starch digestibility, little has been developed over the years, mainly due to the complexity of many factors (starch synthesis, environment, processing, storage and digestion) that determine starch digestibility. However, some studies have focused on developing high-throughput methods for starch characterisation. For example, a 96-sample method has been developed that estimates the ratio of AM and AP in starch by an iodine-binding assay (Kaufman et al., 2015). Another method used for starch characterisation is size exclusion chromatography (SEC) (Perez-Moral et al., 2018). The principle of this method is to separate molecules by size; chains are cleaved by ISA, which hydrolyses the α-1,6 glycosidic bonds of the starch constituents to obtain linear glucan chains that can then be screened by SEC to obtain their chain length distribution (CLD). The AM and AP ratio can also be estimated- AM usually has longer chains than AP, which has

many short chains. However, SEC and iodine-binding assays are very time-consuming due to the extended time required for the starch isolation, debranching process and glucan chain separation. Recently a Ultra High Performance (UPLC)-SEC was developed and reported to successfully decrease the running time of chain separation (Perez-Moral et al., 2018).

Some attempts have also been made to estimate starch digestibility directly. These methods focused on hydrolysing the substrate, starch, and measuring the products of the digestion, oligosaccharides and glucose. These methods can also integrate hydrothermal processes and use milled whole grains or final food products that provide more realistic information in terms of starch digestibility (Minekus et al., 2014, Guerra et al., 2012). The negative aspect of these methods is the high chemical demand and the multiple steps involved. To overcome these bottlenecks, some studies developed methods that involve fewer steps and consumables (Toutounji et al., 2019, Edwards et al., 2014). These protocols simplified more complex starch digestion methods by using a pseudo-first-order reaction and a single enzyme to hydrolyse starch. This is done by standardising equally in all samples the units of α-amylase, in which 1 U is defined as the amount of the enzyme that catalyzes the conversion of one micromole of substrate per min under the specified conditions of the assay method (Labuda et al., 2018).

As in most enzyme-catalysed reactions, the reaction rate decreases with time as the substrate diminishes. Therefore, in order to follow and plot the reaction, an initial fit of the experimental data to a first-order kinetic equation (Equation 1) is commonly used. In this mathematical equation, C_t is the quantity of starch digested at time t, k is the amylolysis rate constant, and C_∞ is the extent of digestion. This equation may be transformed into a logarithmic form which can be plotted in a

form referred to as a Logarithm of Slope (LOS) plot to allow the calculation of kinetic parameters (Equation 2) (Edwards et al., 2019, Edwards et al., 2014, Butterworth et al., 2012). The logarithmic form allows expression of the relationship of k; the rate of digestion, C_∞; the extent of digestion, and t ; the time of amylolysis (Edwards et al., 2018).

$$Ct = C_\infty(1 - e^{-kt}) \text{ (Eq 1)} \qquad \ln\left(\frac{dC}{dt}\right) = -kt + \ln\left(C_{\infty k}\right) \text{ (Eq 2)}$$

According to the Edwards et al. (2019) protocol, a high correlation was observed between the simplified *in vitro* starch digestibility indices and GI values of matched food products allowing a simpler method to be used and work as an indicator for potential GI profile. The main limiting factor of these methods is the number of samples that can be used in each assay because of the multiple time points and a single pipette during digestion. Therefore, even though many available germplasm resources and advancements in genomics have been developed recently, there is still a need to develop more efficient methods to screen wheat and other crops for starch digestibility if forward approach studies are to be conducted.

In a forward screening approach, starch digestibility data will allow the identification of novel loci/genes that would be challenging to achieve through different approaches. Developing a high-throughput assay for starch digestibility will enable the screening of germplasm resources to conduct QTL analysis on the selection of low- and high-digestibility lines. The high- and low-digestibility lines can be studied further to understand mechanisms affecting starch digestibility. Additionally, if low- and high- digestibility lines are selected, a segregating biparental population can be obtained between these two parents, and a QTL analysis can be conducted. The QTL analysis will allow the discovery of loci controlling the trait of interest (starch digestibility) and development of markers

that can be used for breeding and research purposes to develop future lines with low-digestibility.

1.14 Aims of the project

This project aims to enable the use of natural variation to decrease starch digestibility in future breeding programs. To achieve that, a high-throughput screening tool was developed to enable the screening of large germplasm resources (Figure 1.13). The core Watkins collection was used as a the germplasm resource to uncover novel variation in starch digestibility (Table 1.3). Throughout this thesis the core Watkins will be referred as Watkins. High and low-starch digestibility lines were selected to further dissect grain and chemical components associated with starch structure and starch digestibility. Lastly, a low-digestibility line was selected, and a previously generated biparental population using this line was grown and used for a QTL analysis to locate potential loci controlling starch digestibility.

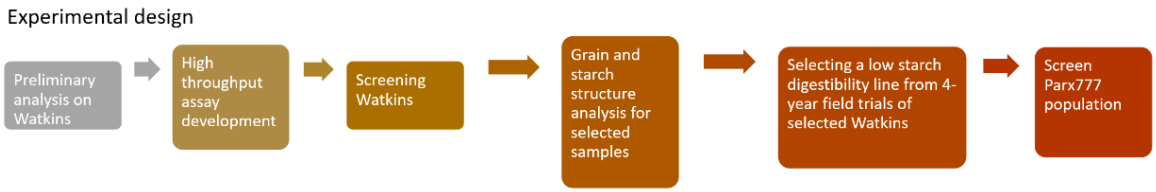

Figure 1.13. Developing an experimental approach for a thesis project. Preliminary analysis on AM content on selected Watkins. Development of a high throughput screening assay for starch digestibility. Screening the Watkins for grain characteristics, sample preparation and starch digestibility and TS. Grain and structural analysis for selected samples on starch digestibility, TS, DSC, endogenous α-amylase, CLD, protein analysis and particle size analysis on wholemeal flour and purified starch. Selecting a low digestibility line by screening the starch digestibility

and TS of 4-year field trials on selected Watkins. Screening the Paragon x 777 on grain characteristics, starch digestibility and TS and conducting a QTL analysis.

Table 1.3. Germplasm used and analysis.

Germplasm	Year grown	Number of lines	Field trial location	Plot size (m^2)	Material used	Analysis	Provided by
Watkins	2018	118	Church Farm, Norfolk UK	1	Grains	NIR	GRU
					Whole meal flour	Starch digestibility, TS	
Elite varieties	2013	8	Morley Farm, Norfolk, UK	1.5	Grains	NIR	Brendan Fahy
					Whole meal flour	Starch digestibility, TS	
Selected Watkins and elite varieties (subset of above 'Watkins' and 'Elite varieties')		8			Whole meal flour	Starch digestibility, TS, DSC, endogenous α-amylase, particle size analysis & SEM, protein analysis	GRU Brendan Fahy
					White flour	Starch digestibility, TS	
					Purified starch	Starch digestibility, TS, DSC, CLD, starch granule size distribution	
Watkins	2010	26	Barn Field, Norfolk, UK	1	White flour	Starch digestibility, TS	Dr. Alison Lovegrove
	2012	28	Coopers Field, Norfolk, UK	6	White flour	Starch digestibility, TS	Dr. Alison Lovegrove
	2013	28	Bylands, Yorkshire, UK	1	White flour	Starch digestibility, TS	Dr. Alison Lovegrove
	2014	21	Coopers Field, Norfolk, UK	1	White flour	Starch digestibility, TS, AM content,	Dr. Alison Lovegrove
Paragon x W777 Nested Association Mapping (NAM) population	2020	96	Church Farm, Norfolk UK	1	Grains	NIR, Marvin	Dr. Simon Griffiths
					Whole meal flour	Starch digestibility, TS, QTL analysis	

Required amount per sample	
NIR	15-30 gr
Marvin	15-30 gr
Starch digestibility	5-10 mg
AM	5 mg
TS	5-10 mg
DSC	200 mg
Endogenous – α amylase	60 mg
SEC (CLD)	10 mg
Particle size analysis & SEM	5-10 mg
Protein analysis	10 mg

Chapter 2 Development of a high-throughput assay for starch digestibility and screening of the Watkins collection

2.1 Introduction

Reducing the rate and extent of starch digestibility in wheat-based foods can help to maintain healthy blood glucose levels, which is important for the prevention and management of chronic diseases (e.g., obesity, diabetes) (Blaak et al., 2012). Furthermore, there is substantial evidence that consumption of RS, the starch that escapes digestion in the small intestine and reaches the colon, can reduce blood glucose levels and help to maintain a healthy gut (Corrado et al., 2022a, Belobrajdic et al., 2019, Hughes et al., 2021). Thus, breeding for wheat with less digestible starch is an important strategy to develop healthier staple foods. So far, reverse genetic studies in wheat have demonstrated potential for increasing RS levels using induced mutations in starch biosynthesis genes (Botticella et al., 2018, SchonhofenZhang and Dubcovsky, 2017, Fahy et al., 2022, Hazard et al., 2015). However, initial analyses of some mutants have shown detrimental effects on yield and on pasta and bread-making quality. Thus, identifying additional sources of genetic variation for starch digestibility could support the development of improved traits for commercial breeding applications (SchonhofenZhang and Dubcovsky, 2017, Hazard et al., 2015).

Wheat landraces, locally adapted lines that have not been modified through modern breeding techniques, represent untapped reservoirs of genetic diversity that can be directly crossed to modern cultivars. Of special note is the entire

Watkins collection (Wingen et al., 2014) encompassing 826 bread wheat landraces collected in the 1920s and 1930s from a wide geographic distribution. This collection contains variation for a number of important agronomic traits and has been successfully used for identifying resistance genes for a variety of diseases (Dyck and Jedel, 1989, Bansal et al., 2011, Bansal et al., 2013, Burt et al., 2014). The Watkins lines have been purified by single-seed descent from which many genomic and genetic resources have been developed; a core set of 118 accessions was used to generate nested association mapping populations, all of which were genotyped, have genetic maps available, and are free to access (http://wisplandracepillar.jic.ac.uk/) (Wingen et al., 2017).

Despite the availability of diverse wheat germplasm resources like the Watkins collection, forward screening approaches for starch digestibility have been limited due to the lack of informative, accurate, and efficient phenotyping methods. Screening methods based on AM content, which has a positive association with RS content, have proven useful for identifying lines with high levels of RS in other cereals, but they have failed to identify other factors that may cause resistance to digestive enzymes (Chen et al., 2017, Mishra et al., 2016). Only a few studies have developed methods to screen large populations for starch digestibility and they have focused on analysing purified starch (Wang et al., 2022). However, other components of the wheat flour matrix could potentially impact starch digestibility (Edwards et al., 2014, Sissons et al., 2021, QiYi and Li, 2022), but no studies have screened flour samples of germplasm collections.

Recently, a new *in vitro* method of starch digestibility was published which produces results that are well correlated with the glycaemic response to foods (Edwards et al., 2019). This method has proven useful for measuring starch digestibility in mechanistic studies (Edwards et al., 2019) and testing early-stage

food products, but modifications and improvements are required to accurately and efficiently use it for screening large wheat germplasm collections.

This chapter presents a comprehensive overview of the development and validation of a high-throughput assay for measuring starch digestibility. The optimization process of the high-throughput assay is described in detail, including the use of a thermomixer instead of traditional equipment, such as a cabinet incubator, tube rotator, and water bath. The modifications made to tailor the method for accurately and efficiently screening large wheat germplasm collections are also explained.

To validate the high-throughput assay, standard samples of wheat and maize starch were used to compare the starch digestibility profiles with those of the Edwards et al. (2019) protocol. The single enzyme system reported by Edwards et al. (2019), is an *in vitro* starch digestibility method which involves hydrolysing starch using porcine pancreatic α-amylase in a controlled environment. A specific enzyme-substrate ratio is maintained during the process. As the starch is broken down, it produces reducing sugars. The amylolysis process is stopped at predetermined intervals by transferring aliquots to a solution that deactivates the amylase enzyme. The concentration of reducing sugars formed is measured using a colourimetric assay, and this measurement is compared to maltose standards. The concentration of reducing sugars produced determines the extent of starch digestion at each time point, and this information is graphically presented to show the portion of starch digested over time. However, a significant drawback of this method is its limited sample capacity (6 samples per assay), as samples need to be placed in separate tubes and handled individually. Therefore, in this chapter the development of a 96-sample format will be discussed. The chapter also explains the criteria for using the Watkins collection as a source of natural variation. The high-throughput assay was

then applied to screen hydrothermally processed flour samples of the Watkins collection and commercial wheat lines for bread, biscuit, and animal feed (Wingen et al., 2014).

Summary of the experiments

The experiments in Chapter 2 include amylose content analysis from selected Watkins lines varying AX content (Figure 2.1 and Table 2.1). Then grain characteristics of the Watkins collection and selected elite lines were analysed using NIR. Wholemeal flour of the Watkins collection and elite varieties were also thermally processed (cooked and cooled) and analysed for total starch and starch digestibility.

Figure 2.1. Chapter 2 Experimental design. Preliminary analysis on AM content on selected Watkins. Development of a high throughput screening assay for starch digestibility. Screening the Watkins and selected elite lines for grain characteristics, starch digestibility and TS.

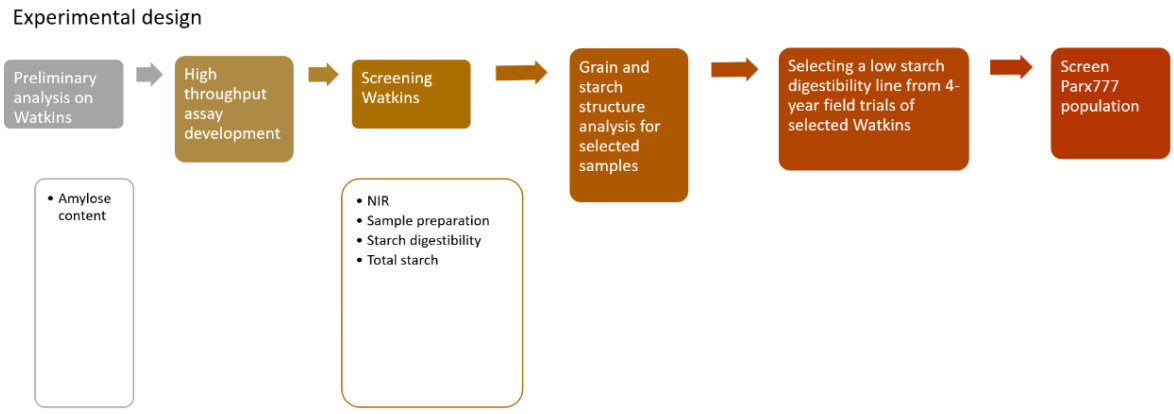

Table 2.1. Germplasm used and analysis in Chapter 2.

Germplasm	Year grown	Number of lines	Field trial location	Plot size (m^2)	Material used	Analysis	Provided by
Watkins	2014	21	Coopers Field, Norfolk, UK	1	White flour	AM content	Dr. Alison Lovegrove
	2018	118	Church Farm, Norfolk UK	1	Grains	NIR	GRU
					Whole meal flour	Starch digestibility, TS	
Elite varieties	2013	8	Morley Farm, Norfolk, UK	1.5	Grains	NIR	Brendan Fahy
					Whole meal flour	Starch digestibility, TS	
Required amount per sample							
AM	5 mg						
NIR	15-30 gr						
Starch digestibility	5-10 mg						
TS	5-10 mg						

2.2 Materials and methods

2.2.1 Plant material

For the results presented in this chapter, the Watkins collection grains analysed were ordered from the GRU (JIC, UK) using the publicly accessible SeedStor system https://www.seedstor.ac.uk/; permission to use the materials for research purposes was obtained. Grains from elite varieties of the bread, biscuit, and animal feed commercial groups of the UK Agriculture and Horticulture Development Board Recommended List (https://ahdb.org.uk/) (Cougar, Crusoe, Dickens, Diego, Myriad, Paragon, Santiago, Skyfall) were kindly provided by Fahy et al. (2018). Elite varieties were grown in 2013 in 1.5m^2 plots (one per genotype) at Morley Farm, Norfolk, UK (52°33'15.57"N 1°10'58.956"E). Dr Alison Lovegrove (Rothamsted Research) provided white flour samples (prepared using a Chopin CD1 mill, KPM, UK) from a subset of Watkins lines showing variation in AX content (Wingen et al., 2014, Shewry et al., 2015). The selected Watkins lines were sown in 1m^2 plots in autumn at Coopers Field, Church Farm in Bawburgh, Norfolk, UK, for the year 2014 (Supplemental Figure 2.1 and Supplemental Table 2.1).

2.2.2 Chemicals

Chemicals used in this study: 4-Hydroxybenzhydrazide (PAHBAH) (CAS: 5351-23-5), Tris(hydroxymethyl)aminomethane (TRIS) (77-86-1), Edetic acid (EDTA) (60-00-4), Sodium Dodecyl Sulfate (SDS) (151-21-3), Dithiothreitol (DTT) (3483-12-3), Phosphate buffered saline (PBS) (P4417-100), Sodium Carbonate (497-19-8), Dimethyl sulfoxide DMSO (67-68-5), maltose (6363-53-7), AM (CAS: 9005-82-7), sodium hydroxide (1310-73-2) and porcine pancreatic α-amylase (EC 3.2.1.1, supplied in a diisopropylfluorophosphate (DFP)-treated suspension of 2.9 M NaCl containing 2mM $CaCl_2$, A6255, Type I-A, 647-015-00-4) were purchased from Sigma-Aldrich Company Ltd., Poole, UK.

2.2.3 Field design

The 118 Watkins lines were grown in Autumn 2018 in 1 m^2 plots at Church Farm, Norfolk UK (52°37'49.2"N 1°10'40.2"E) using standard agronomic practices and harvested late summer 2019 (field map available in Supplemental Table 2.2). One plot per line was used for most lines, however, for known lower-yielding lines, additional plots were sown. The yield of the Watkins lines was expected to vary significantly between the lines based on the previous yield data of the Watkins lines grown at the same location in 2011 (Figure 2.2). Therefore, lines that had previously yielded less than 1200g of grain per 1m^2 in 2011 (627, 690, 811, 685, 591, 471, 313, 700, 568, 742, 816, 34, 694, 731, 468, 705, 698, 729, 199, 209) were grown in two plots, and one line (827) that yielded 201g of grain per 1m^2 was sown in three plots to ensure adequate quantities of grains for starch analysis.

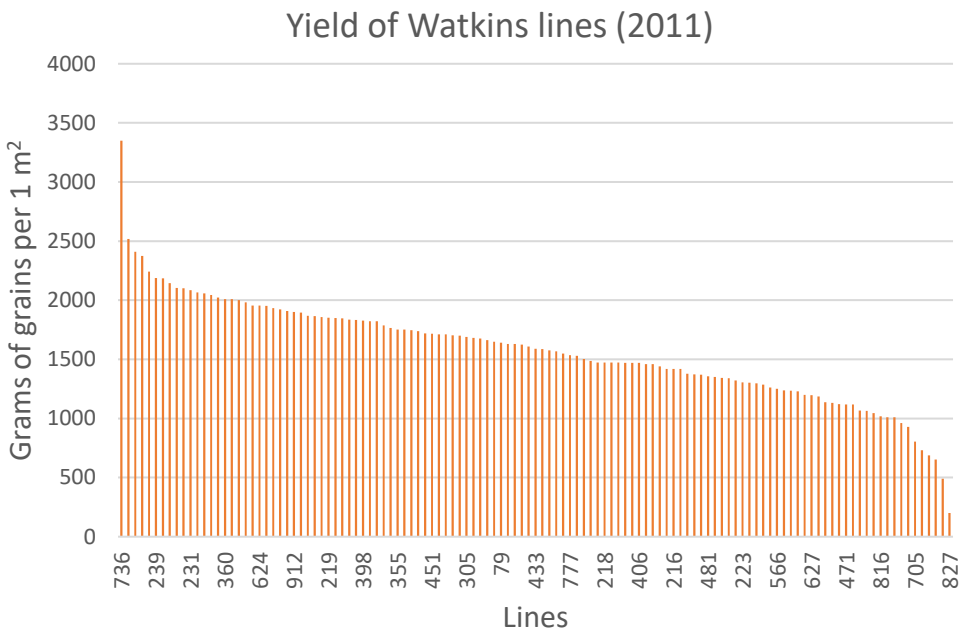

Figure 2.2. Yield of Watkins collection (2011). Data provided by GRU, Norwich, UK.

2.2.4 Seed analysis

The grain protein content, starch content, non-dietary and fibre content were measured using a NIR Instrument (DA 7250 At-line) by the GRU (JIC). Three technical replicates were used and values expressed as mean.

NIR spectroscopy is a spectroscopic method based on the use of the near-infrared region of the electromagnetic spectrum to determine the material's properties. More specifically, NIR emits light to illuminate the sample (Figure 2.3). Depending on the sample's composition, the light absorption will differ (minerals and most inorganic compounds do not absorb infrared light, whereas water and organic compounds do). The remaining light which has not been absorbed will be reflected in the device, which separates it by wavelength, and each wavelength is measured by a detector. In this study, the NIR instrument used was equipped with a diode

array technology; thus, the diode detector measured the wavelength. The infrared absorption data is then expressed in the material's properties based on calculations with reference data which has been used for NIR calibration. In this study, the NIR used was calibrated with more than 4000 samples for moisture content (ranging from 7.3-22.1%, 0.97 R^2), more than 4200 samples for protein content (ranging from 8.2-22.8%, 0.98 R^2), more than 1200 samples for starch content (ranging from 61.5-83%, 0.97 R^2) and more than 100 samples for hardness (ranging from 12.9 to 87.2 Single Kernel Characterisation System (SKCS), 0.81 R^2).

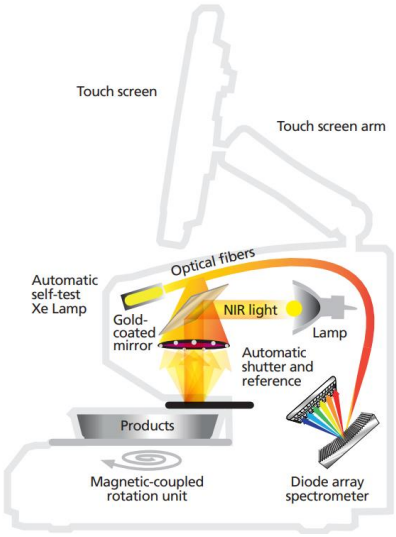

Figure 2.3. Diagram showing the diode array NIR analysis system used in the GRU, JIC. (https://www.perkinelmer.com/).

For grain hardness of the Watkins, data was provided by Dr Alison Lovegrove (Rothamsted Research). For the analysis the Watkins lines were sown in autumn in 1m^2 plots at Barn Field, Church Farm in Bawburgh, Norfolk, UK, in the year 2010 and analysed in 2015 using a SKCS.

SKCS is a widely used method for measuring grain hardness, which is an important quality factor in determining the end-use potential of wheat for various

applications, such as milling, baking, and food processing. The SKCS measures wheat hardness by analysing the force required to crush a single kernel of wheat between two parallel plates.

In this analysis a SKCS 4100 was used to measure grain hardness of the Watkins lines. The SKCS 4100 consists of a sample hopper, which holds the wheat sample, a feeding mechanism that delivers a single kernel to the testing area, and two parallel plates that crush the kernel. The system also includes sensors that measure the force required to crush the kernel, as well as its weight, diameter, and thickness. This information is then used to calculate the hardness index of the wheat sample.

The hardness index is a measure of the average kernel hardness of the wheat sample and is calculated based on the force required to crush the kernels. The higher the force required, the harder the kernels, and the higher the hardness index.

2.2.5 Sample preparation and starch extraction

For digestibility analyses grains from the Watkins and elite varieties were coarsely milled in a cyclone mill fitted with a 0.5 mm screen (UDY Corporation). After each milled sample cyclone mill was open and dry cleaned with brush and compressed air to prevent contamination between samples. 30 minutes breaks were taken every 4 samples to prevent overheating of the mill which can lead to changes in the starch damage and moisture levels of the samples. Milled samples were passed through a 0.3 mm sieve to produce 'wholemeal' flour samples (Figure 2.4). The flour samples were kept in a vacuum desiccator for five days before the analysis. A single biological replicate was used for the milling and sieving process.

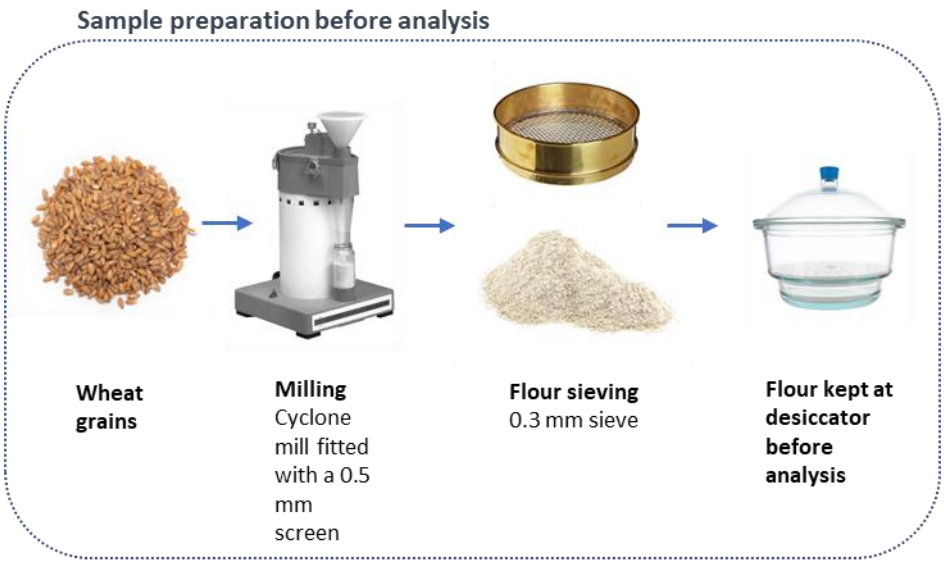

Figure 2.4. Sample preparation before analysis. *A cyclone mill was used to coarse-mill wheat grains fitted with 0.5 mm screen. Milled samples were passed through a 0.3 mm sieve to produce the 'wholemeal' flour samples. Afterwards, the flour samples were stored in a vacuum desiccator for 5 days before analysis.*

Samples of starch derived from hard (e.g., Skyfall) and soft (e.g., Myriad) wheat grains were prepared using a cyclone mill equipped with a 0.5 mm screen (UDY Corporation) and by mortar grinding. For mortar grinding, grains were placed on moistened filter paper in Petri dish overnight at 4^{o}C and then crushed in a mortar using a pestle. Milled and ground samples were filtered through Miracloth and washed using water. The filtered solutions were then centrifuged, and the supernatant was discarded. The pellet was resuspended in 30mL of 2% (w/v) SDS, centrifuged, and the supernatant was discarded again; this process was repeated three times. Then, cold acetone was added to remove lipid constituents, followed by centrifugation and discarding of the supernatant. This process was repeated three times in total. Samples were left overnight without a lid in a fume hood to allow the remaining acetone to evaporate. Two technical replicates were used for the milling and mortar grinding process.

2.2.6 High-throughput starch digestibility assay and developmental steps

Single enzyme system

The single enzyme system by Edwards et al. (2019) was adopted in this study and modified to increase the throughput of the method. The single enzyme system involves weighing samples into 15mL tubes containing 100 ± 2 mg of starch suspended in 10 mL of PBS (pH 7.4). The tubes are then mixed at 37°C for 20 minutes (Figure 2.5). A 200 µL 'blank' aliquot is taken from each sample, mixed with 'stop solution' (0.3 M Na_2CO_3, pH 9) and set aside. Porcine pancreatic α-amylase solution is added to each sample to achieve an activity of 4U/mL, and the tubes are returned to the mixer and are incubated at 37°C for various times. Aliquots are collected from the mixture at each time point, mixed with stop solution, centrifuged, and the supernatants are stored at −20°C for later analysis of starch amylolysis products.

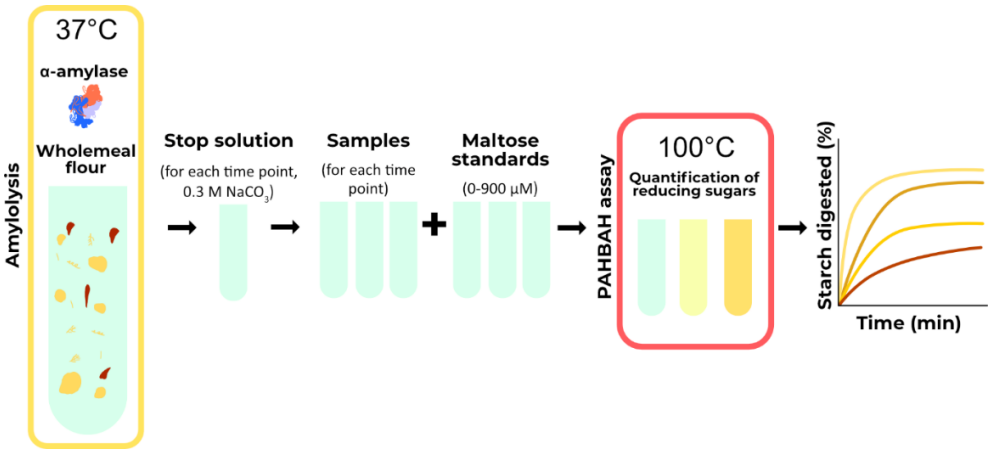

Figure 2.5. Single enzyme system. The weighed samples of starch are mixed in PBS at 37°C and then porcine pancreatic α-amylase is added. During starch digestion aliquots at predetermined time points are collected and analysis of starch amylolysis products is conducted by PAHBAH assay.

To determine the concentration of reducing sugars produced from starch amylolysis in the aliquots, a PAHBAH assay is used. The stored supernatants are diluted in deionized water (1:10) and 100 µL of the diluted sample is transferred to a 1.5 mL tube. Freshly prepared PAHBAH is added, and the tubes are vortexed, incubated, and equilibrated before absorbance measurement at λ = 405 nm. Standards containing known concentrations of maltose are also prepared and react with PAHBAH. The reducing sugar concentration in each sample is then expressed as maltose equivalents by reference to the standard curve.

24-sample format starch digestibility assay

Starch samples were prepared in a solution with PBS (phosphate-buffered saline, pH 7.4), where an amount of starch was weighed into pre-labelled 15mL tubes, and PBS was added to reach a concentration 5.7 mg/mL solution of starch. Samples

were then mixed and transferred to a 99°C water bath for 10 min to simulate the boiling conditions typically encountered during food preparation (Corrado et al., 2020). After the heat treatment, samples were vortex mixed to prevent gel granule formation and then left for 15 min at room temperature. Samples were then re-mixed, and 1.67mL was transferred into 2.2mL Eppendorf tubes. Tubes were then left to incubate for 10 min at 800rpm into a 37°C preheated thermomixer. After the 10 min of incubation, mixing was stopped for 10 sec, and 100µL of the sample was transferred into a 2mL tube (0 timepoint) which contained 100µL of stop solution (0.3M Na_2CO_3, pH 9). Then, 167µL of pancreatic α-amylase (2 U/mL) was added to the sample in the thermomixer and continuously mixed at 800rpm. Samples for selected timepoints (0, 3, 6, 9, 12, 15, 18, 20, 25, 30, 60, 90 min) were transferred to the stop solution. At the end of digestion (last time point), the samples in the stop solution were centrifuged at 1500*g* for 5 min. Then 10µL of each sample was transferred into a new 1.5mL tube, and 90µL of water was added to reach a final volume of 100µL.

To determine the maltose content, 1mL of PAHBAH solution (9.5% 0.5M HCL and 90% 0.5M NaOH) was added to each tube and maltose standards. Samples were then transferred to the water bath for 5 min at 99°C. Then samples were left to cool down for 15 min, and 200µL was transferred to a 96 microwell plate and measured at 405nm in a microplate reader (Bio-Rad Benchmark Plus, Waukegan, Illinois, USA). Samples were measured in three technical replicates.

Minimising dilution steps

This section describes the stages involved in decreasing the number of dilution steps in the Edwards protocol. According to the 24-sample format assay described

above, a stop solution of 1:1 (digestion sample: stop solution) is made and then it is centrifuged. Then a 1:10 dilution of supernatant to water is made before performing the PAHBAH assay. An experiment was carried out to remove the dilution step. For that, the concentration of starch to PBS changed to 11.4 mg/mL (from 10 mg/mL), and the ratio of digested solution to sample changed to 1:19. This change in concentrations delivered the same maltose concentration as the Edwards protocol.

Temperature evaluation of the thermomixer

The temperature was monitored in the thermomixer using an external k-type thermocouple bead probe attached to a RS42 handheld digital thermometer (RS PRO, U.K). For the 24-sample format, the thermomixer was pre-set to 37^{o}C, then 1mL of water was added to tubes, and the temperature was recorded after 10 and 50 min. For the 96-sample format, the thermomixer was pre-set to 37^{o}C and all 96 samples were filled with 1mL of water. After 30 min at 37^{o}C at 800 rpm the temperature was recorded. For the temperature evaluation two thermomixers were tested (Thermal mixer, Bioshake iQ with a 96 adapter – NUNC® and Eppendorf ThermoMixer C with a 96 Eppendorf SmartBlock™).

To estimate the temperature evenness at higher temperatures, a set of maltose standards was prepared and aliquoted into six sets. The first two were placed in the left external columns (1,2), the other two in the middle columns of the deep well plate (6,7) and the last two in the right columns of the deep well plate (11,12). The deep well plate was then incubated for 7 min in a preheated thermomixer at 100^{o}C with the lid attached at 600rpm. After 10 min, the deep well plate was placed on ice for 10 min to allow fast and even heat transfer (cooling). Samples were then

placed on a well plate, and the colour development was measured at 405nm on a spectrophotometer.

96-sample format starch digestibility assay

Starch digestion assays were carried out on samples that were gelatinised and allowed to retrograde following a protocol by Edwards et al. (2019), modified for screening a large number of samples. Wholemeal flour samples were weighed (6 mg) and transferred into a deep well plate (96/1000 µL, Eppendorf) (Figure 2.6). PBS solution (600µL, pH 7.4) was added to each sample with a 1mm glass ball to improve mixing. The deep well plate was sealed and secured with a Cap-mat (96-well, 7 mm, Round Plug, Silicone/PTFE) and added to a preheated thermal mixer (80^{o}C) with a 96 SmartBlock™ DWP 1000n attachment (Thermomixer C, Eppendorf Ltd., Stevenage, UK) for 15 min at 1500 rpm to gelatinise the starch, then cooled at 4^{o}C for 21 h to accelerate retrogradation.

As the sealing of the plate is not as tight as that of tubes, the cooking temperature had to be reduced to 80°C to address the issue of increased liquid evaporation rate, which could result in a higher concentration of the sample. However, the cooking time was extended to 15 minutes from the original 10 minutes specified in other studies (Corrado et al., 2020). The extended cooking time and cooking temperature at 80^{o}C ensured that all starch was gelatinized, as the temperature remained above the wheat starch gelatinization temperature (most wheat starches are completely gelatinised around 64^{o}C) (Olkku and Rha, 1978).

The plate was then briefly spun in a Heraeus Megafuge 16 (100*g* for 1 min) to collect condensed liquid on the Cap-mat and placed on the thermal mixer for 30 min at 37^{o}C, 1600 rpm. Time zero samples (50µL) were collected using a 12-multichannel pipette and transferred into a 2mL deep well plate containing 1.95mL of stop

solution (17 mM Na_2CO_3). Digestion was started by adding pancreatic α-amylase (enzymes that cleave the internal α-1,4 links) suspended in PBS, targeting 2U/mL activity in the samples. Aliquots (50µL) were then taken after 6, 12, 18, 24, 40, and 90 min from the onset of digestion and transferred to the stop solution containing 17 mM Na_2CO_3. This solution was used to increase the pH and inactivate the amylase hydrolytic reaction. The PAHBAH assay was then followed for the maltose quantification.

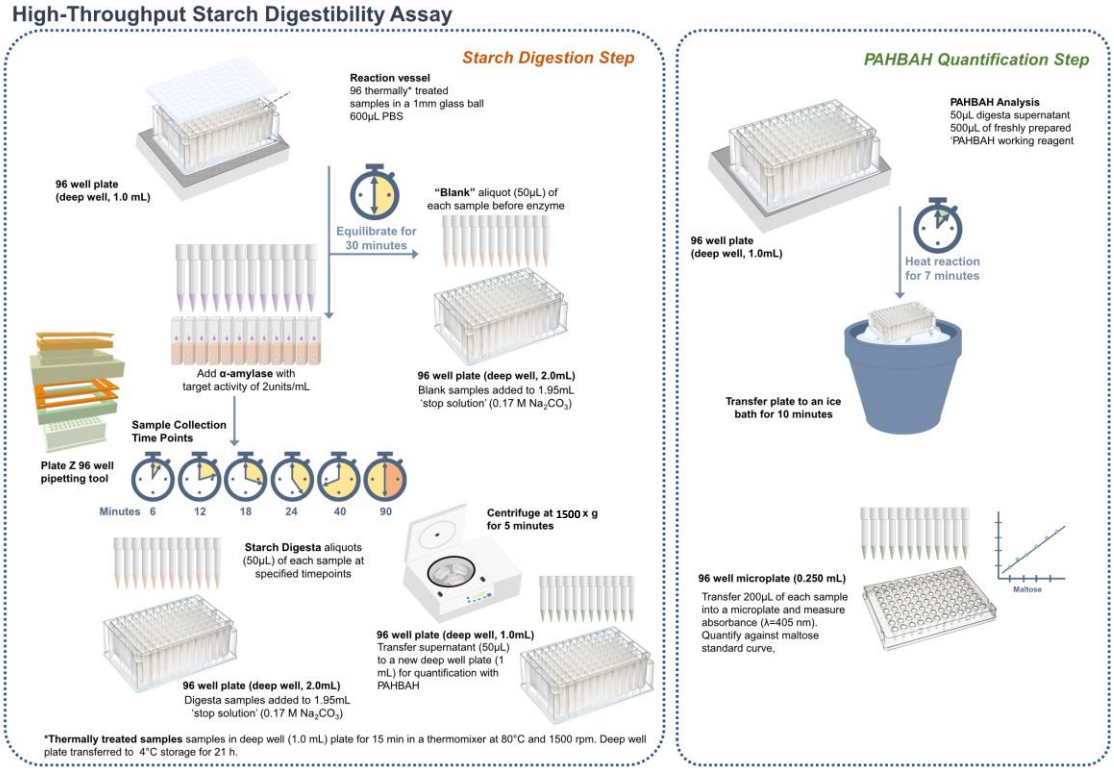

Figure 2.6. Principle of the in vitro starch digestibility method. For amylolysis, a known enzyme-substrate ratio is used, and starch is hydrolysed by porcine pancreatic α-amylase to produce reducing sugars. During amylolysis, aliquots are transferred to a 'stop solution' at predetermined time points to inactivate amylase activity. The reducing sugar concentration is quantified using a colorimetric p-PAHBAH assay and maltose standards (Lever, 1972). The portion of starch digested

for each timepoint is calculated based on reducing sugars and is then displayed against time. Adopted from Zafeiriou et al. (2023)

Maltose quantification (PAHBAH assay)

The stopped digestion reactions were centrifuged at 1500*g* for 5 min to avoid transferring any starch remnants, and 50µL of the supernatant was transferred to a new deep well plate. The PAHBAH reducing end assay was used to quantify the reducing ends released (Lever, 1972). The reaction produces a yellow colour when anionic forms of carbohydrate hydrazones are formed. This formation is achieved when the reagent containing hydrazides of benzoic acid derivatives is linked with reducing sugars in strong alkali conditions. Briefly, 0.5mL of freshly prepared reagent (2 g of PAHBAH dissolved in 38mL of 0.5 M HCl and 360mL of 0.5 M NaOH) was added to each sample. The deep-well plate was held at 100^{o}C for 7 min and then placed in an ice bath for 10 min. Samples were then transferred to a microplate, and absorbance was measured at 405 nm using a microplate reader (Bio-Rad Benchmark Plus, Waukegan, Illinois, USA). Reducing sugars were expressed as maltose equivalents, using a standard curve of maltose standards (5 – 1000 µM). Starch digestibility (%) was expressed according to Edwards et al. (2019), equation 3; each timepoint's maltose equivalents were corrected by subtracting the baseline maltose (time zero) and then divided by the maltose equivalent of TS. Four technical replicates were used, each carried out on a different day.

$$(Starch\ amylolysis\ \%)_t = \frac{[maltose]_t}{[maltose]_{substrate}} \times 100 \quad \text{(Eq 3)}$$

Validation of the high-throughput starch digestibility assay

Starch digestion profiles from the high-throughput assay and the Edwards et al. (2019) protocol were compared using standards of purified starch from standard maize, waxy maize, and high-AM maize (purchased from Merck, formerly Sigma-Aldrich, Darmstadt, Germany) and previously characterized by Koev et al. (2020), and standard wheat starch (purchased from Merck, formerly Sigma-Aldrich, Darmstadt, Germany), and two high-AM starches: *sbeII* and *ssIIIa*, previously characterized respectively by Corrado et al. (2022a) and Fahy et al. (2022). Starch samples were aliquoted to make 5.4mg of starch/mL of PBS solution and α-amylase activity was adjusted at 2U/mL. The thermal treatment procedure was followed as described above for the high-throughput starch digestibility assay. Three runs were obtained for both protocols over different days. For each run, six technical replicates per starch sample were placed randomly in the 96-well plate for the high-throughput assay, and two technical replicates were used for the Edwards protocol. For each run, starch samples and enzyme solution were prepared in stock and aliquoted for use in both the high-throughput and Edwards protocol.

Amylase activity for digestion assay

The purpose of measuring the activity of pancreatic α-amylase enzyme is to determine the units of amylase activity. One unit is defined as the amount of enzyme that catalyzes the conversion of one micromole of substrate per minute under the specified assay conditions (Labuda et al., 2018). The units of amylase activity are then used to adjust its concentration and deliver the same activity level in all samples during starch digestibility assays. The enzyme activity of the pancreatic α-amylase was determined by applying the starch amylolysis assay on gelatinised potato starch (CAS: 9005-25-8, purchased from Sigma-Aldrich Company

Ltd., Poole, UK) and obtaining the linear rate of maltose release every 3 min (mg/mL). For the digestion of potato starch, a suspension of 5mg/mL was prepared and heated (90^{o}C) with continuous stirring for 20 min to ensure the complete gelatinization of the starch. This process increases the solubility of the starch and optimizes its digestion. Three technical replicates of 5mL gelatinised starch solutions were transferred to 15mL Falcon tubes and left in an incubator (New Brunswick™ Excella® E24/E24R Shaker) with continuous end-over-end mixing (Grant rotator, settings: 30 rpm orbital, 02; 35- degree reciprocal, off; 5-degree vibration, off) for 10 min to equilibrate at the preferred temperature of digestion 37^{o}C. Time zero samples (100µL) were transferred into 1.5mL microfuge tubes containing 100µL of stop solution (0.3 M Na_2CO_3). Digestion was started by adding 50µL pancreatic α-amylase suspended in PBS (5µL into 2.5mL PBS) into the substrate solutions. Aliquots (100µL) were then taken after 3, 6, 9, 12 and 90 min from the onset of digestion and transferred to the stop solutions (100µL). Samples were then centrifuged at 12,500*g* for 5 min to avoid aspirating any starch remnants, and 10µL of supernatant was diluted in 90µL of deionised water. Reducing sugars of digestion mixtures and maltose standards were estimated using the PAHBAH assay previously described. A maltose curve was used to express reducing sugars into maltose equivalents, and a linear rate of maltose release every 3 min (mg/mL) was calculated.

2.2.7 Total starch measurement

For the starch determination, an enzymatic digestion assay was used, and the determination of glucose was achieved by measuring the absorbance of the adjusted D-glucose into hexokinase (HK)/glucose-6-phosphate

dehydrogenase/NADP+ format. The principle of the method involves the solubilisation and hydrolysis of starch by adding DMSO and thermostable α-amylase that releases branched and unbranched maltodextrins. Then AMG is added to convert the maltodextrins to D-glucose. To determine the D-glucose of the sample, HK enzyme and adenosine-5'-triphosphate (ATP) is added to first phosphorylate glucose to glucose-6-phosphate (G-6-P) and ADP (Figure 2.7). Then, by adding the enzyme glucose-6-phosphate dehydrogenase (G6P-DH), G-6-P is oxidized by nicotinamide-adenine dinucleotide phosphate (NADP+) to gluconate-6-phosphate and reduced nicotinamide-adenine dinucleotide phosphate (NADPH). The amount of NADPH is measured on a spectrophotometer at 340 nm and is stoichiometric with the amount of D-glucose. Starch content can then be calculated by converting the absorbance of samples to the amount of glucose released using a standard curve from glucose standards and taking into account the weight of the sample, volumes used, and dilutions.

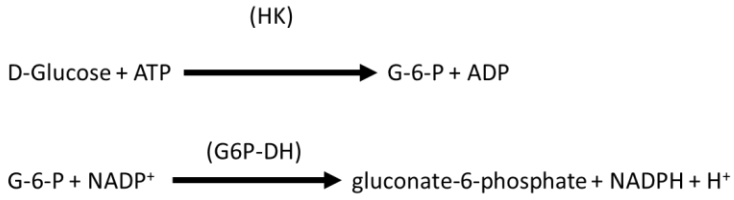

Figure 2.7. Illustration of glucose determination by HK assay. *The method involves phosphorylating glucose to G-6-P using HK enzyme and ATP, followed by oxidizing G-6-P to gluconate-6-phosphate and NADPH using G6P-DH enzyme.*

Wholemeal flour samples were weighed (~8 mg) and transferred into a deep well plate (96/1000 µL, Eppendorf), each well containing 20µL of DMSO and a 1mm glass ball to improve mixing. The plate was mixed for 5 min at 1600 rpm to disperse the samples before adding 500µL of a thermostable α-amylase to each sample. The

thermostable α-amylase was solubilised at 1:30 (v/v) in 100 mM sodium acetate buffer, pH 5.0 (TS HK kit; Megazyme, Bray, IE). The deep well plate was sealed and secured with a Cap-mat (96-well, 7 mm, Round Plug, Silicone/PTFE). Samples were heated at 90^{o}C for 10 min at 1600 rpm using a thermal mixer with a 96 SmartBlock™ DWP 1000n attachment (Thermomixer C, Eppendorf Ltd., Stevenage, UK). The deep well plate was then cooled at 50 ^{o}C, and 20µL of AMG was added to each sample and left to incubate at that temperature for 35 min at 1600 rpm. After incubation, the deep well plate was centrifuged at 14,000 rpm (20800*g*) for 10 min, and 50µL of supernatant was transferred to a new tube containing 500µL water to dilute the samples. To each plate well, a solution (containing 195µL of 100µL of 100mM bicine (pH 7.7), 5mM $MgCl_2$, 10µL of ($NADP^+$ / ATP) and 85µL of water) was added. Then 5µL of glucose samples or blank or glucose standards (0-100nmol) were added to each well, and absorbance was read at 340 nm with 10-sec pre-shake. Then 2.0 µL of (HK/G-6PDH) was added to each well, and absorbance was re-measured until values were stable. Glucose values were obtained using a glucose curve and subtracting the absorbance before adding G-6PDH from the absorbance after addition. Glucose values were then expressed by converting glucose into starch, where 1 µmol glucose is equivalent to 162 µg of starch and by including the incubation volume and dilution steps. Samples were measured in three technical replicates.

2.2.8 Amylose estimation method

The principle of the iodine method is the formation of the complex with AM and long linear chains and, under the presence of water, the development of a blue colour that can be measured by a colorimeter. More specifically, when iodine is mixed with DMSO, a base solvent, triiodide ions are formed under this basic pH.

This is necessary for the initiation of the AM-iodine complex (Knutson and Grove, 1994, Knutson, 1986). DMSO is also used for increasing the solubility of starch as it has been shown to be an effective starch solvent (Wolf et al., 1970). Then by adding deionised water, a blue colour is formed depending on the AM content of the sample, and it can be measured colorimetrically to obtain the apparent AM using a standard curve from pure AM (>88%) (Knutson and Grove, 1994). The equation to obtain the AM % is shown below (Equation 4) and is used to adjust the detected AM for AP binding iodine (Knutson, 1986).

$$\%\ Amylose = \frac{\%\ apparent\ amylose - 6.2}{93.8} \text{ (Eq 4)}$$

A modified method from Knutson (1986), Knutson and Grove (1994) was used to estimate the AM content as a preliminary analysis on selected Watkins lines. Starch samples of 5 mg of a subset of Watkins lines (29 lines provided by Dr. Alison Lovegrove previously chosen based on their varying AX content) were used and 10mL of iodine solution (6mM iodine/DMSO) was added. Tubes were placed on a blood rotator (Grant, PTR-35) at 35 rpm and left overnight to allow the starch to dissolve. 20 hours later, 20µL of the solution and 180µL of distilled water were transferred from each tube to a well in a 96-well microplate (two technical reps for each sample). Samples were left for 30 min in a dry place for the development of a stable colour. Then the plate was read by a spectrophotometer at 600 nm (BIO RAD, Benchmark Plus). The content of AM was calculated by a standard curve using AM standards (1-5mg potato AM type III, Sigma-Aldrich). Samples were measured in three technical replicates.

2.2.9 Tools

During the optimisation of the high-throughput assay, a low-cost 3D-printed pipetting tool was developed, which allowed for manageable weighing and transferring of samples into 96-sample deep well plates and improved speed and control of pipette aspiration (Plate Z). The Plate Z 3D design is available to download and print for free (https://www.hackster.io/386082/high-throughput-pipetting-plate-z-bde2c7).

2.2.10 Data analysis

Statistical analyses and graphs were obtained with Excel (version 2022), Jamovi (version 1.0.7.0) and R (R version 4.2.1). Plots were made using Excel and the ggplot2 R package (version 3.3.6) (Wickham, 2016).

Datasets of the validation of the high-throughput *in vitro* starch digestibility assay were analysed using the packages lme4 (v 1.1-30) and lmerTest (v 3.1-3) for a mixed model fit (KunzetsovaBrockhoff and Christensen, 2017, Bates et al., 2015, Pinheiro et al., 2022). For validation of the high-throughput assay, the methods were compared by plotting the estimated starch digestion profiles and by comparing the estimated starch digested at 90 min. The bias (difference in estimates between methods) and variation in starch digested at 90 min measured by the high-throughput assay was estimated using linear mixed models, including the type of starch as a fixed effect and sample batch as a random effect.

A linear mixed model including line as a fixed effect and experimental run as a random effect was used for analysis of *in vitro* starch digestibility of the Watkins lines and elite varieties. Marginal means with standard errors (SE) (calculated using a pooled standard deviation) are plotted for each line.

One-way ANOVA was used for analysis of AM, *in vitro* starch digestibility and TS of the Watkins lines and elite varieties; a *p-value < 0.05* was adopted for statistical significance.

The correlation between starch digestibility and TS was estimated using a linear regression model. All values reported represent the mean ± SE of three technical replicates unless stated otherwise in the description of the corresponding figure and supplemental datasets. For boxplot graphs, red points represent the average and black horizontal lines represent the median.

2.3 Results

2.3.1 Development of the high-throughput assay

Starch digestibility is a quantitative trait controlled by many genes but can also be affected by external factors (endogenous, processing and digestion) (Hazard et al., 2015, Parada and Aguilera, 2009, Wang et al., 2015, Tian et al., 2009, HoggMartin and Giroux, 2017). Thus, a strategy to measure starch digestibility directly was employed rather than measuring specific underlying factors.

This project focused on developing a high-throughput assay to measure starch digestibility in a processed matrix like wholemeal flour, which to the current knowledge, has not been available yet. The method was adapted from the protocol presented by Edwards et al. (2019) as this protocol, compared to other *in vitro* digestion methods (Minekus et al., 2014, Guerra et al., 2012), has advantages such as fewer steps, low need for consumables, and non-specialised equipment. Despite the advantages of this protocol, the number of samples that can be run in a day is limited (approximately 6) due to each sample being handled individually. To adapt

the method to a high-throughput assay, the project focused on increasing its handling capacity, minimising procedure steps and optimising sample preparation for starch digestibility. The developmental steps used to increase the throughput of the protocol are described below.

Increasing handling capacity

The use of an incubator in a starch digestibility assay limits the number of samples that can be handled (by pipetting) simultaneously. Laboratory thermomixers solve this issue as they have been designed to carry 24 and 96-format samples and thus allow the use of a multichannel pipette. For this reason, the development of the high-throughput assay was carried out using a thermomixer as a medium of temperature distribution and mixing. Having an even temperature in all samples is critical because amylase activity is temperature-sensitive. Mixing is also important for adequately distributing starch constituents in the solution during digestion and maintaining similar colloidal composition during pipetting.

An initial trial of a thermomixer was carried out with 2.2mL tubes using a 24-sample format. For temperature control, a target range of 36.8^{o}C to 39 ^{o}C was selected based on the optimal activity of porcine pancreatic α-amylase (Miłek, 2021). The temperature recorded varied from 36.8 ^{o}C to 37.1 ^{o}C, and no uneven heat distribution patterns were identified (Table 2.2).

Table 2.2. Temperature record of water samples after 10min (top table) and 50min (bottom table) of heating in thermomixer set at 37 °C.

10 min	36.8	36.9	37	36.8	37.1	37
	36.9	36.8	36.8	37	37.1	37
	37	36.8	36.9	37	37	36.8
	37.1	37.1	36.9	37	37	37.1

50min	36.8	37.1	36.8	37	37	36.8
	36.9	36.9	36.9	36.9	37.1	37.1
	37	37.1	37	37.1	37	37.1
	37	36.8	36.9	36.8	36.8	37.1

For testing the mixing efficiency of the 24-sample format thermomixer, an oil-stained with Sudan black was used as an indicator for the movement of the sample and the colour dispersion was evaluated by observation. The oil was distributed in the tube during the mixing process (800 rpm), suggesting that samples can be appropriately mixed during digestion (Figure 2.8).

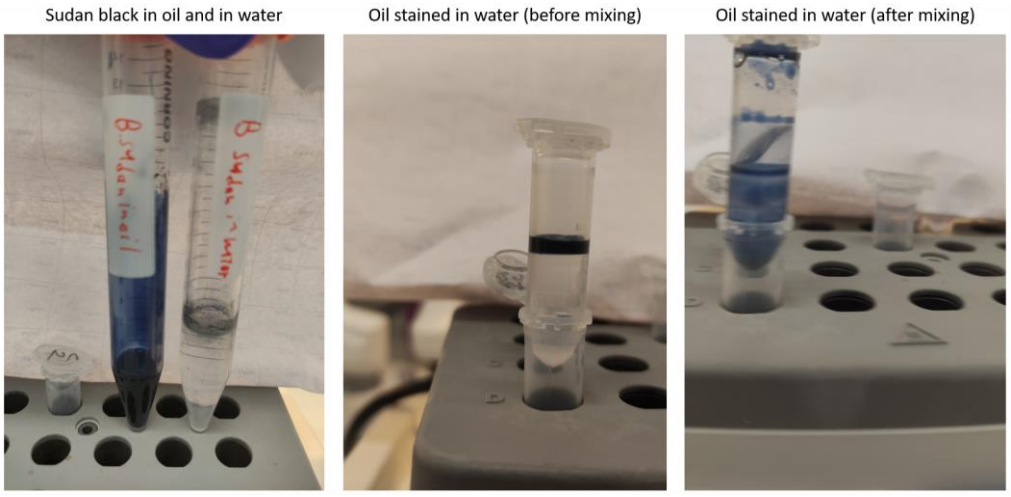

Figure 2.8. Sudan black used for mixing assessment on the thermomixer. The left picture indicates the dissolving ability of Sudan black in oil (left tube) and water (right tube). The middle picture indicates the heterogeneous solution of oil-stained with Sudan black. The right picture indicates the mixing ability of the thermomixer.

Subsequent experiments aimed to further increase the handling capacity to a 96-sample format. For the temperature control, a thermomixer (Thermal mixer, Bioshake iQ with a 96 adapter – NUNC® & Axygen® deep well 96/2.0mL) and a 2.2mL Nunc deep well plate was used (Figure 2.9).

A

B

	1	2	3	4	5	6	7	8	9	10	11	12
A	37.5	37.1	37.4	37.3	37.6	37.6	37.3	37.6	37.8	37.8	37.6	37.3
B	37.8	37.3	37.5	37.8	37.9	37.8	37.6	38	38	38.1	37.9	37.5
C	37.5	37.7	37.9	38	38.1	38	37.8	38.1	38.3	38.3	38.1	38.2
D	37.3	37.7	37.9	37.9	38.2	38.2	38	38.2	38.3	38.3	38.2	38
E	37.3	37.7	38	38.1	38.1	38	38	38.2	38.3	38.3	38.2	38
F	37.7	37.6	37.7	37.9	37.9	38	37.9	38.2	38.3	38	38.2	37.8
G	37.2	37.3	37.5	37.6	37.6	37.7	38	38.1	38.1	37.9	38	37.4
H	37.9	37.2	37.3	37.6	37.6	37.5	37.7	37.8	37.8	37.8	37.6	37

Figure 2.9. Temperature measurement on a 96-sample format using a Bioshake iQ thermomixer set at 37°C. (A) shows the measurement of the temperature, and (B) table shows the temperature results.

Results showed that the temperature was not even throughout the 96-well plate. An increased temperature trend was identified in the middle right (7-12th column) area of the deep well plate, and the outer part was the coldest compared to the inner part of the deep well plate. This can be partially explained due to the slower heat transfer to the environment (heat loss) on the inner part compared to the external parts.

To address this issue, a different thermomixer (Thermal mixer, Eppendorf ThermoMixer C with a 96 Eppendorf SmartBlock™ DWP 1000n attachment) was tested. This thermomixer was designed to have deeper deep well plate fitting (manufacturer deep well plates designed to fit better to the designated thermomixer), potentially improving the thermal evenness. Additionally, it was supplied with a lid to improve even heat distribution. For the 37°C temperature measurement, a 1.1mL deep well plate was used, and the procedure was repeated as stated above. Temperature results measured by the thermometer showed that

after 30 min, the temperature difference among samples was minor (±0.1°C), (Figure 2.10).

A

B

	1	2	3	4	5	6	7	8	9	10	11	12
A	37	37	37	37	37.1	37	37	37.1	37.1	37.1	37	37.1
B	37	37.2	37	37	37	37	37	37	37	37	37	36.9
C	37	37	37	37	37	37	37	36.9	37	37	37	37
D	37	37	37.1	37	37	37	37	37	37	37.2	37	37
E	37	37	37	37	37	37	37	37	37	37	37	37
F	37	37.1	37	37	37	37.2	37	37	37.1	37	37	37
G	37	37	36.9	37	37	37	37	37	37	37	37.2	37
H	37.1	37	37	37	37	37	37.1	37.1	37	37	37	37

Figure 2.10. Temperature measurement of a 96-sample format using an Eppendorf thermomixer. (A) measurement of the temperature; (B) table shows the temperature results across the plate.

A higher temperature was subsequently tested to determine if the thermomixer was a suitable alternative to a waterbath which is used in the Edwards protocol for the PAHBAH assay. For this experiment, a set of maltose standards was prepared and aliquoted into six sets across a 96-well plate to determine if absorbances were consistent.

m.st (µM)	1	2	5	7	11	12	SD
0	0.07	0.06	0.05	0.06	0.06	0.11	0.02
5	0.09	0.07	0.08	0.07	0.07	0.12	0.02
10	0.12	0.07	0.07	0.07	0.07	0.11	0.02
100	0.17	0.16	0.20	0.17	0.15	0.20	0.02
250	0.37	0.34	0.37	0.32	0.30	0.34	0.02
500	0.61	0.61	0.69	0.55	0.55	0.58	0.05
750	0.81	0.86	0.90	0.86	0.87	0.74	0.05
1000	1.09	1.10	1.06	1.09	0.99	1.04	0.04

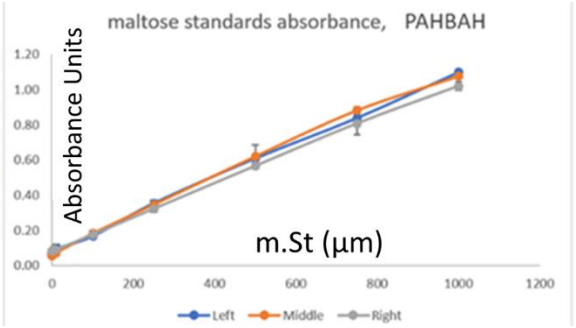

Figure 2.11. Absorbance of maltose standards using PAHBAH assay.

The variation in the absorbances of maltose standards was small (max SD of 0.05), and no clear trend was identified across the plate (Figure 2.11). Based on the above results, no major differences in temperature were observed among different sides of the plate when high heat was applied. Therefore, it was concluded that a

thermomixer can be used as an alternative to a water bath to analyse released maltose units (PAHBAH assay) after starch digestion. In terms of the limited volume per sample (600 µL), this assay had to decrease the number of time points (7 time points) to effectively get a sufficient amount of sample for the PAHBAH assay. These modifications increased the throughput of the assay as more samples could be analysed simultaneously.

To test the mixing ability of the 96-sample format on the thermomixer, the same technique using a stained oil (Sudan black) and mixing rotation at 1500rpm was used. The Sudan black stained only a small fraction of the tubes, leaving a large fraction non-mixed. This was due to smaller tube dimensions causing weaker fluid motions which were unable to cause an adequate bottom turbulent flow (Figure 2.12). To improve the mixing ability of the fluid, a 1mm glass ball was added, and the experiment was repeated. The glass ball improved the mixing ability by providing a stronger turbulent flow on the middle and bottom part of the tube, which, with a combination of upper fluid motion and mixing pipetting, would allow the hydrocolloid solution to be mixed during all the time of the digestion assay (Figure 2.12).

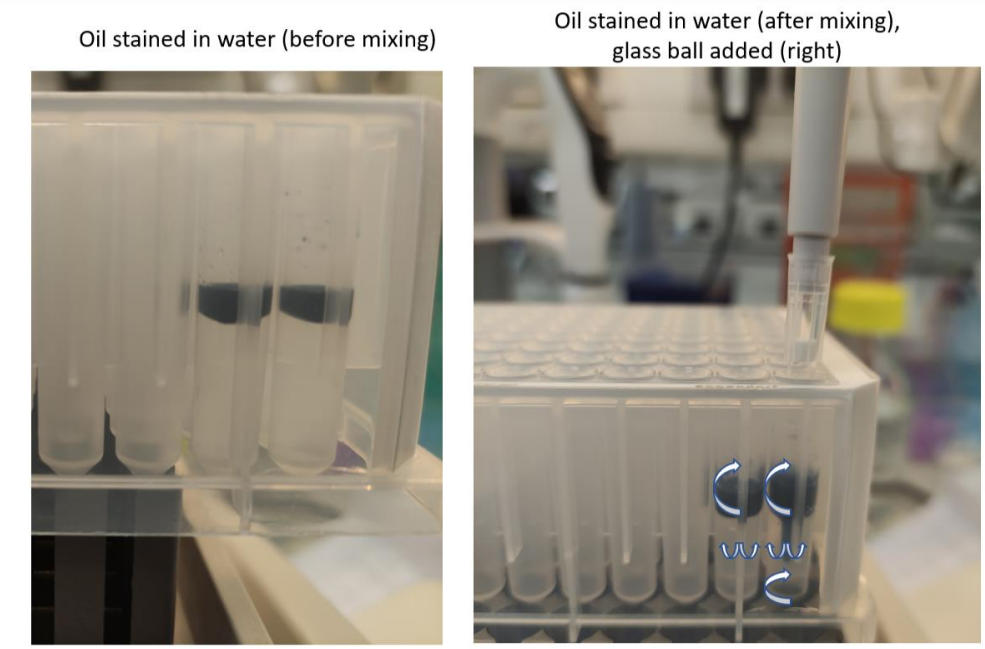

Figure 2.12. Evaluating the mixing ability of samples in a deep well plate using stained oil and the Eppendorf thermomixer.

Tubes of the same dimension containing wholemeal flour were also tested. The 1.2mL tubes, containing the wholemeal flour, were mixed (with and without a glass ball) at 1500rpm after being heated (80^{o}C for 7 min) on a thermomixer and cooled (4^{o}C for 21 hours) to simulate the thermal conditions required for the starch digestion assay (Figure 2.13). The glass ball improved the samples' mixing ability by dispersing the hydrocolloid solution compared to the sample with no glass ball. Additionally, the glass ball was able to disrupt any gel formation during gelatinisation and retrogradation of the starch and thus provide better overall sample mixing.

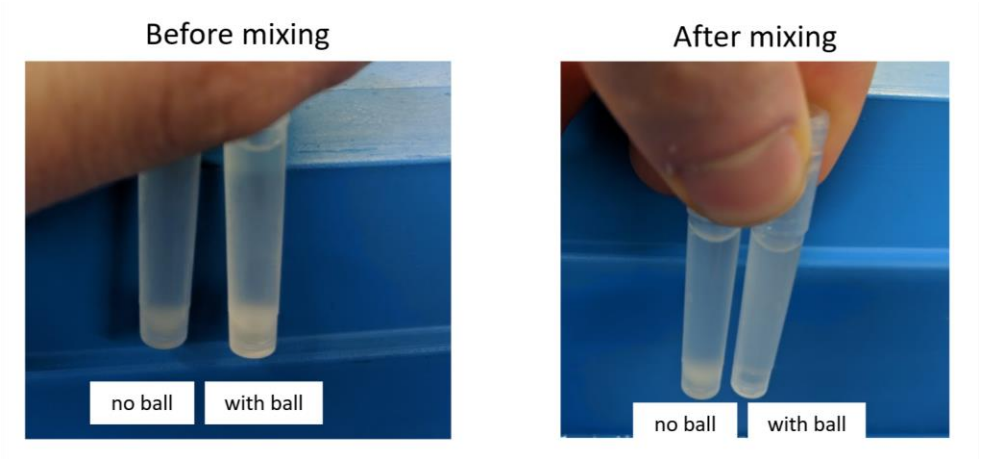

Figure 2.13. Evaluating the mixing ability of the thermomixer (Eppendorf) with gelatinised and retrograded samples.

Another aim was to minimise the evaporation of samples on the deep well plate. When samples were heated in the thermomixer at 80°C, the liquid evaporation rate increased, and the concentration of the sample increased. This issue was addressed using adhesive tape to seal the sample, and a small hole was made with a needle to release the pressure created during heating (Figure 2.14). When samples were gelatinised and cooled, the deep well plate was then centrifuged at low speed for 1 min to recover the droplets formed on the top of the tape.

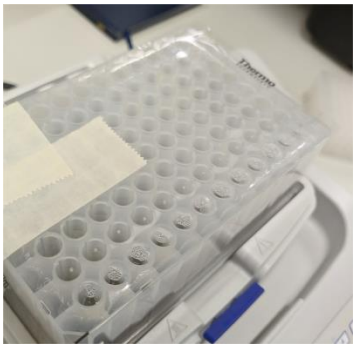

Figure 2.14. Using adhesive tape on the deep well plate and creating holes to release pressure.

Scaling down the protocol and minimising procedure steps

To scale down the starch digestibility assay protocol, an aliquot of sample in PBS was obtained from the 15mL tubes, used in the Edwards protocol, and the use of 2.2mL Eppendorf tubes was tested initially for the 24-sample format. For the trial, three starch standards were used (potato starch, wheat starch and high-AM maize starch (70% of AM)) (Figure 2.15).

6 sample format	24 sample format
Weigh samples ~(6)	Weigh samples (24)
Add PBS	Create a stock solution (PBS)
Thermal Processing	Thermal Processing
Transfer samples to 37°C	Transfer samples to 2.2mL tubes for digestion
Take blank and add enzyme	Take blank and add enzyme
Take samples for each timepoint to a "stop solution"	Take samples for each timepoint to a "stop solution"
Centrifuge samples	Centrifuge samples
Take supernatant	Take supernatant
Dilute supernatant	Dilute supernatant
Add PAHBAH to both samples	Add PAHBAH to both samples
Transfer to waterbath 99°C	Transfer to waterbath 99°C
Transfer samples to a 96 well	Transfer samples to a 96 well
Measure absorbance	Measure absorbance

Figure 2.15. Starch digestion method development (24-sample format). The left list depicts the Edwards protocol, and the right list depicts the modified assay. The blue font shows the modified steps.

For the starch digestion, standards followed a normal digestibility curve (Figure 2.16). Starch from potato was the most digestible starch compared to wheat and maize starch, reaching a plateau after 15min of digestion. On the contrary, high-AM maize was the least digestible sample; only 24% of the starch was digested compared to potato and wheat, with 76% and 70% digested, respectively.

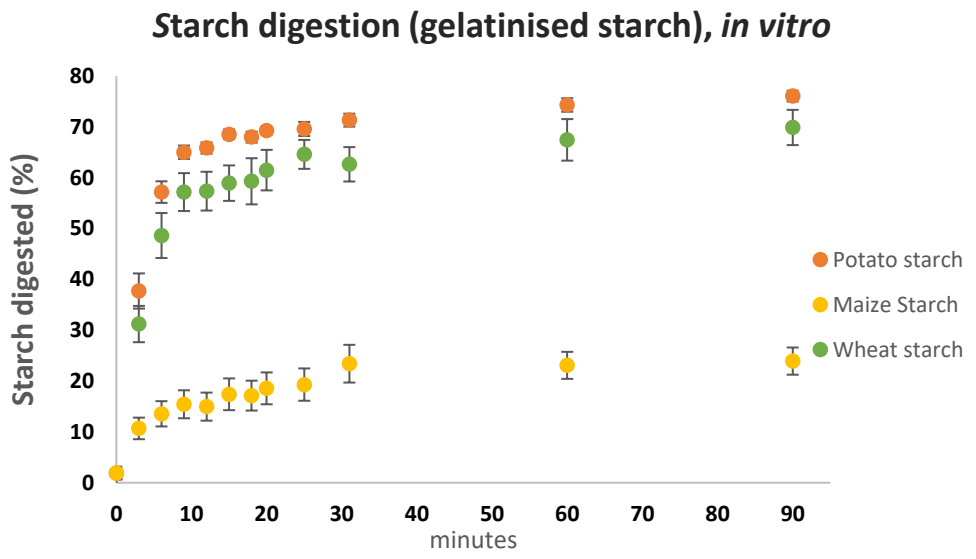

Figure 2.16. In vitro starch digestion of different sources of starches using 2.2mL sample tubes. The activity of pancreatic α-amylase was set to 2U/mL. Values represent mean ± SD of n = 3 technical replicates.

To decrease the materials needed and minimize pipette handling (Figure 2.17), a dilution step was removed. Potato starch was digested following the Edwards protocol, and the modified protocol with the dilution step removed produced comparable digestion profiles (Figure 2.18) Only the 12 min time point showed a statistically significance difference in % starch digested between the protocols (*p* value <0.05) and the differences were minor.

24 sample format	
	Weigh samples ~(8)
	Create a stock solution (PBS)
	Thermal Processing
	Transfer samples to 2.2mL tubes for digestion
	Take blank and add enzyme
	Take samples for each timepoint to a "stop solution"
	Centrifuge samples
	Take supernatant
	Dilute supernatant
	Add PAHBAH to both samples
	Transfer to waterbath 99°C
	Transfer samples to a 96 well
	Measure absorbance

24 sample format (d. dilution step)	
	Weigh samples ~(8)
	Create a stock solution (PBS)
	Thermal Processing
	Transfer samples to 2.2mL tubes for digestion
	Take blank and add enzyme
	Take samples for each timepoint to a "stop solution"
	Centrifuge samples
	Take supernatant
	Dilute supernatant (step removed)
	Add PAHBAH to both samples
	Transfer to waterbath 99°C
	Transfer samples to a 96 well
	Measure absorbance

Figure 2.17. Starch digestion assay development (dilution step removal). The blue highlight shows the step modification.

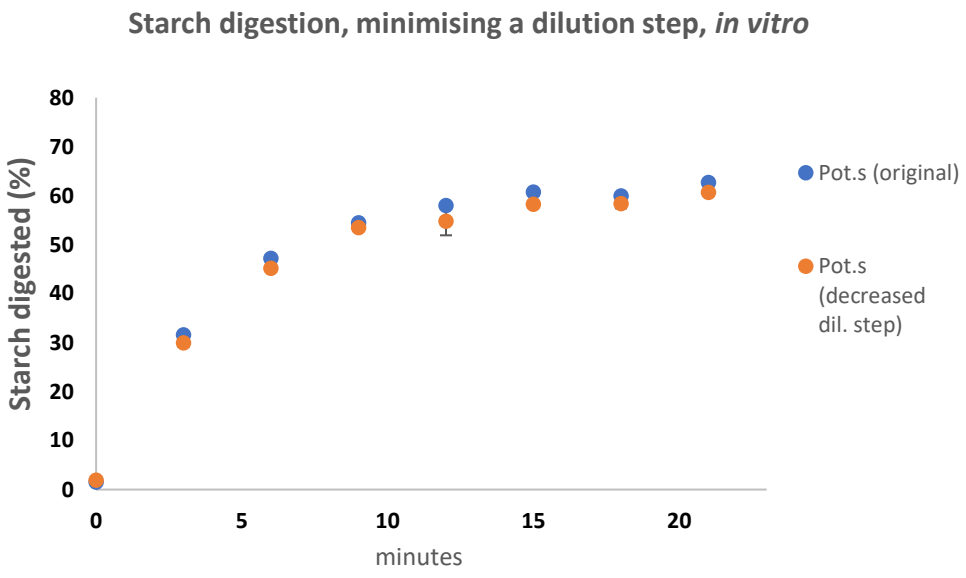

Figure 2.18. In vitro starch digestion of potato starch comparing the removal of dilution step and non-removal dilution step assay. The activity of pancreatic α-amylase was set to 1U/mL. Values represent mean ± SD of n = 2 technical replicates.

Optimising sample preparation

The following set of experiments aimed to test the effects of different sample preparation techniques on starch digestibility, including milling and mortar grinding and processing (cooking and cooling) wholemeal flour and purified starch.

Hard and soft wheat samples were prepared using coarse milling and mortar grinding followed by starch isolation. Starch digestibility has been shown to be affected by the particle size of the substrate and the hardness of wheat (Edwards et al., 2015, KorompokisDe Brier and Delcour, 2019, Darlington et al., 2000). Fine milling on hard wheat, wheat that contains a high amount of proteins or a different ratio of specific proteins (e.g., puroindolines), causes higher starch granule damage, which could affect its digestion. Grinding in a mortar is considered one of the milder methods to avoid starch granule damage. However, grinding in a mortar by hand is a low-throughput method and is less consistent than milling.

For the estimation of starch digestibility of the milled and mortar-ground samples, the same *in vitro* digestibility assay as above was repeated (assay illustrated in Figure 2.17) and samples were run in duplicates (Figure 2.19).

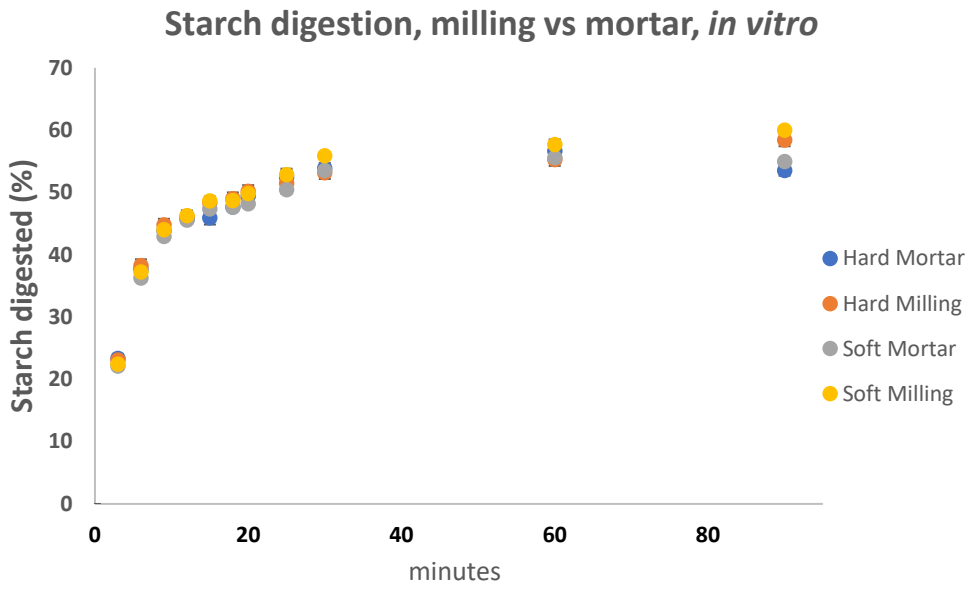

Figure 2.19. In vitro starch digestion of milled and mortar-ground wheat starch samples. The activity of pancreatic α-amylase was set to 2U/mL. Values represent mean ± SD of n = 2 technical replicates.

Both hard and soft wheat starch samples obtained from coarse milling and mortar grinding showed small differences in starch digestibility; the only observed difference was at 90 min. These small differences may be due to the complete gelatinization of the starch granules, which occurs at high temperatures (most wheat starches are completely gelatinised around 64°C) and high-water accessibility (BelitzGrosch and Schieberle, 2009), despite any starch damage that may have occurred during milling or grinding (Olkku and Rha, 1978). Considering the small differences in the starch digestibility, it was concluded that samples had minor differences when milled or hand-ground. Thus, coarse milling was selected as the most efficient method to prepare samples for analysis.

Subsequently, starch digestibility profiles of purified starch and wholemeal flour were compared and the effects of thermal processing (gelatinised and retrograded

samples) were analysed as they would be most relevant for predicting digestibility in wheat foods. More specifically, cooked samples were gelatinised and kept at 18°C for 21hr, and retrograded samples were cooked and cooled to accelerate re-crystallisation (kept at 4°C for 21 hr) (Figure 2.20).

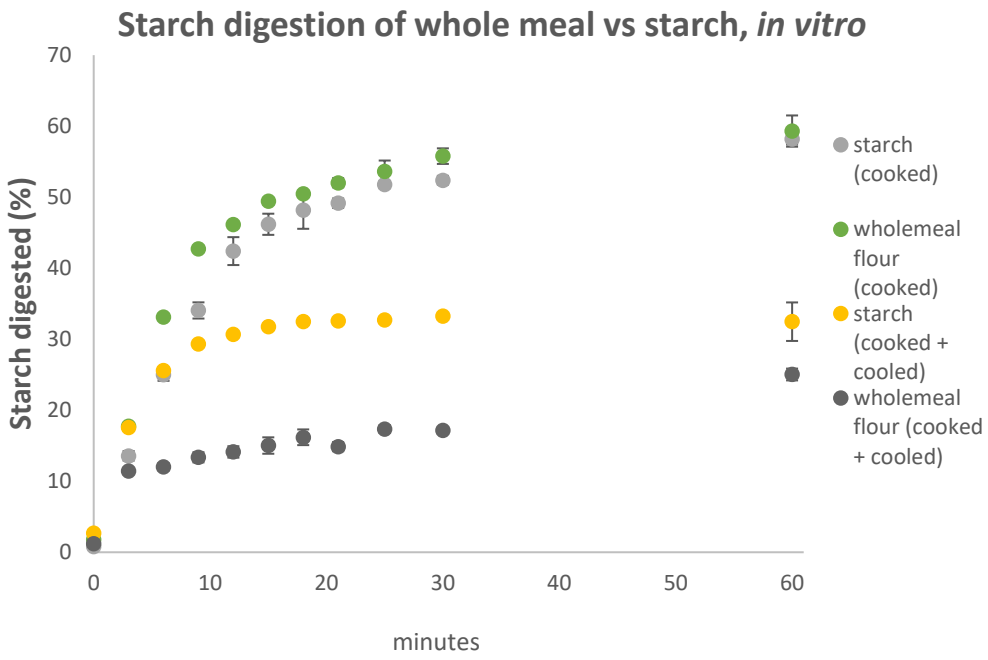

Figure 2.20. In vitro starch digestion of purified starch and wholemeal flour. Selected Watkins lines (2018) are gelatinised or gelatinised and retrograded. The activity of pancreatic α-amylase was set to 2U/mL. Values represent mean ± SE of n = 3 technical replicates.

Samples kept at 4°C ('cooked and cooled') were less digestible than samples kept at 18°C ('cooked'). For samples kept at 18°C the % of starch digested at 60 min was 58.2% (for starch) and 59.3% (for wholemeal flour), whereas samples kept at 4°C had 32.5% (for starch) and 25% (for wholemeal flour) starch digested at 60 min. Additionally, the starch and wholemeal flour kept at 18°C had smaller differences; only 3, 6 and 9 min were statistically significantly different (p <0.01, p <0.01 and

p<0.05, respectively), compared to starch and wholemeal flour kept at 4°C, in which all time points were statistically significantly different (p <0.01 for 3 min, p<0.001 for 9-30 min and p<0.05 for 60 min).

Another aim was to measure flour samples and transfer them to a 96-deep well plate to directly apply a hydrothermal treatment in the sample plate used for the digestion assay. However, weighing samples directly onto a plate posed a challenge since most balances cannot accommodate plates and adding weight can affect sensitivity. To address the issue of directly weighing samples into a deep-well plate, 3D-printed caps were designed to fit in the deep-well plate sampling area. With these caps, flour samples could be successfully transferred with minimal material loss (~0.1mg maximum loss during the measurements of 10 samples of wholemeal flour). Figure 2.21 illustrates the process of weighing and transferring the samples. Firstly, a clean 3D-printed cap is placed on the scale and wholemeal flour is weighed. Next, the 3D caps are placed on top of each well and tapped multiple times to remove any remaining material. To prevent sample mixing and contamination, the 3D caps are left on the deep well plate until all weighing is complete and are then removed prior to analysis.

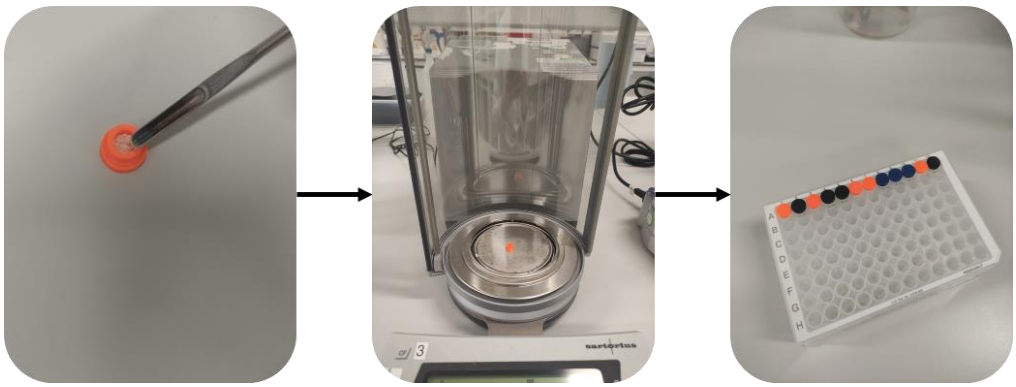

Figure 2.21. 3D printed caps for weighing and transferring flour samples to the deep well plate.

Optimising sampling

Another challenge identified during the high-throughput assay development was the aspiration of samples during multiple sample handling. The digestion samples (mixture of wheat flour, PBS solution and pancreatic α-amylase) exist in a colloidal system containing different sizes of solid particles suspended in a liquid solution during digestion. Before obtaining a sample during predetermined time points, mixing pauses, allowing samples to sediment. If the fluid solution remains the same (e.g., viscosity and density), the rate of settling depends on the size, shape and density of the particle. Therefore, if the solid particles have not been settled yet during sampling, there is a chance of being aspirated. If a large particle is aspirated, it can cause blocking of the pipette tip or change the composition of the digesta as it might contain large amounts of a substrate, leading to a change to the substrate -enzyme ratio. To make sampling more consistent, a 3D printed tool was developed to always aspirate samples from the exact height of the well (Plate Z, available free to download from hackster.io). Plate Z was developed to simulate the action of a liquid handling robot and make it able to obtain samples of the top-end of the digestion liquid, thus increasing the evenness of pipetting by ensuring that all samples have been taken from the same height (Figure 2.22).

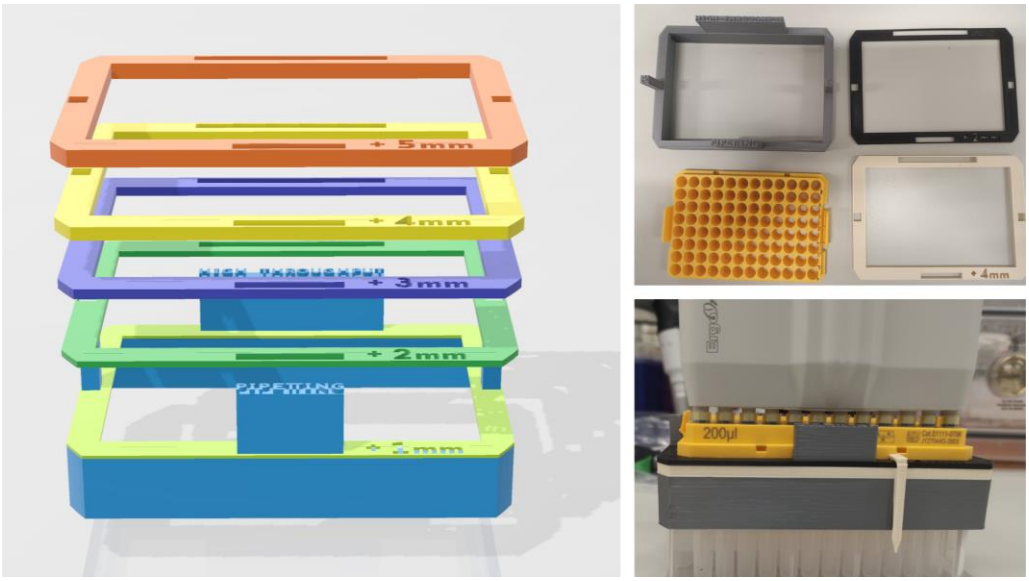

Figure 2.22. Plate Z, 3D printed high-throughput pipetting tool showing the plate attachment, tip holder and different size layers to control the aspiration height during pipetting.

2.3.2 Validation of the assay

The 96-format digestion assay was validated using high, medium and low AM content starches from maize and wheat and comparing to results using the Edwards et al. (2019) protocol (Figure 2.23).

In this analysis, the digestion profiles of maize and wheat starch standards were comparable to those generated using the Edwards protocol (Figure 2.24, Supplemental Table 2.3), particularly with respect to the variance. For example, the difference in the average estimates at 90 min from the two methods was -0.72 percentage points, and the variation observed at 90 min within the runs was 2.1 percentage points in the high-throughput assay and 2.2 percentage points in the Edwards protocol. There were no significant differences in the percent of starch digested at all the time points measured between the Edwards protocol and the

high-throughput assay. Thus, the high-throughput assay provided comparisons between samples that were accurate and reproducible, and the reliability of the assay was deemed sufficient for use as a screening tool to aid in the selection of low- and high-digestibility samples. For future work, it will be important to consider improving the efficiency of upstream steps, including milling, sieving, and weighing samples which present additional bottlenecks.

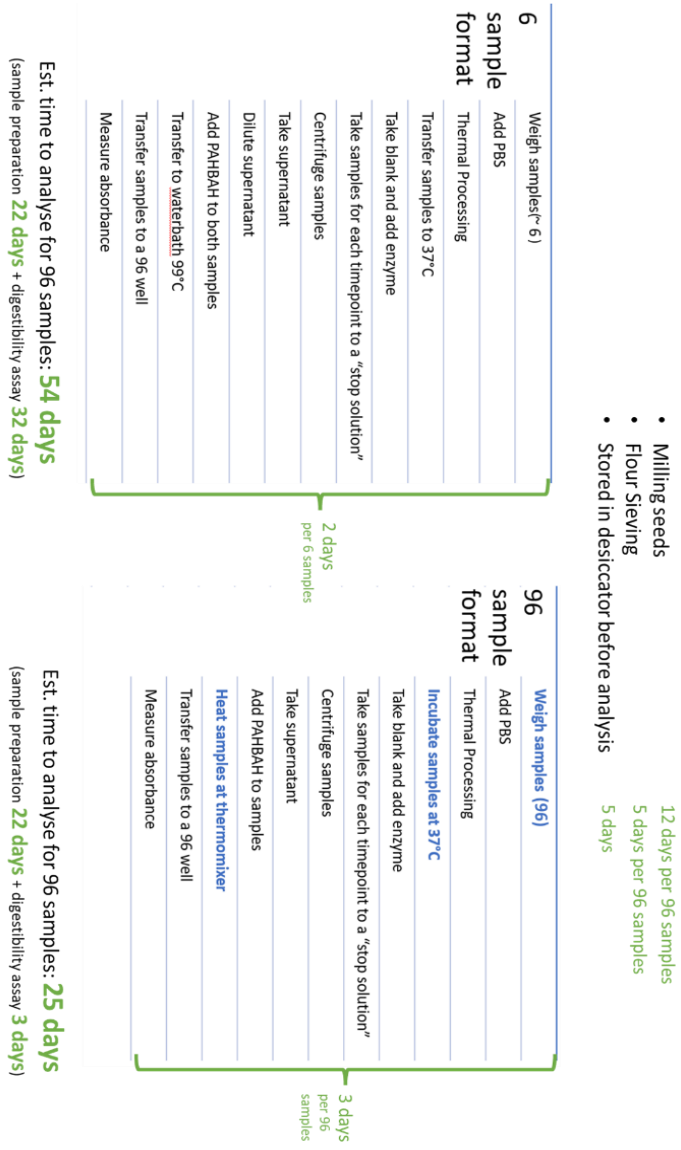

Figure 2.23. Starch digestion assay development (96-sample format). The blue highlights show the step modification. Green highlights show the estimated time for each step of the analysis.

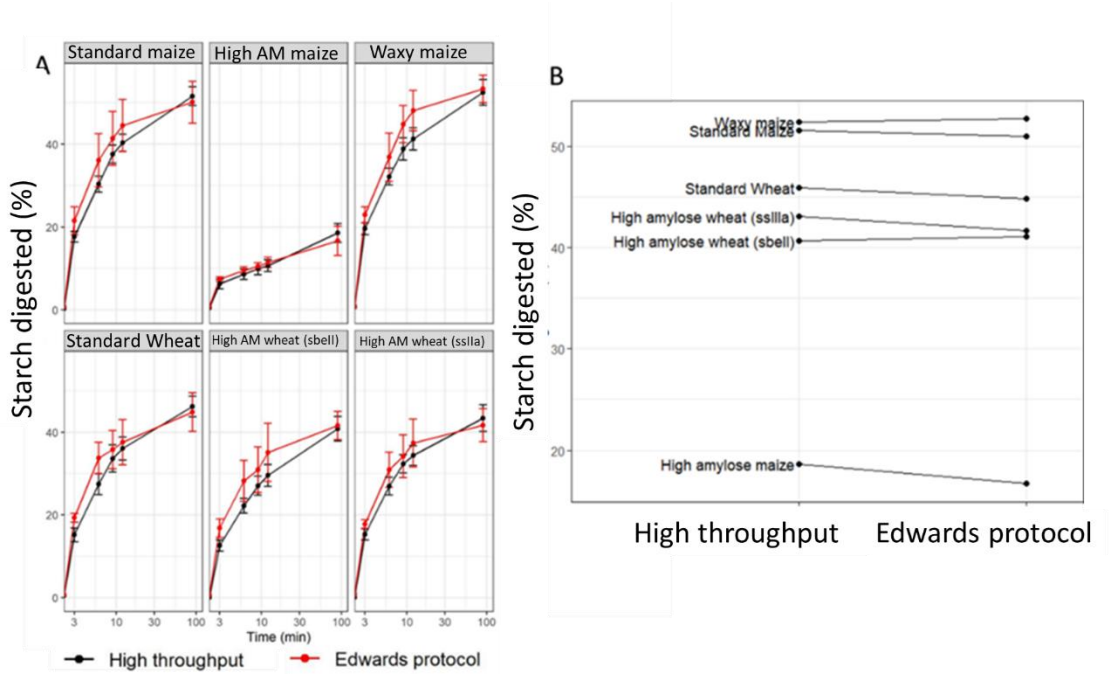

Figure 2.24. Comparison of the high-throughput starch digestibility assay to the Edwards protocol. ***A.*** *Digestibility profiles of purified maize and wheat starch produced by the high-throughput assay (black) and the Edwards protocol (red).* ***B.*** *Starch digested (%) at 90 min, ranking comparison of the high-throughput assay (left) to the Edwards protocol (right). Values represent the mean ± SD of n = 18 technical replicates for the high-throughput assay and n = 6 technical replicates for the Edwards protocol.*

2.3.3 Natural variation in the starch of a Watkins subset

The Watkins collection was hypothesised to be a good source of variation for starch digestibility based on previous studies that showed its large genetic and phenotypic diversity (Wingen et al., 2014, Bansal et al., 2011, Bansal et al., 2013, Randhawa et al., 2015, Toor et al., 2013, Shewry et al., 2015). Therefore, as a preliminary analysis, AM content was measured for white flour samples of selected Watkins lines to determine the potential for identifying variation in starch molecular structure, as

prior studies have shown elevated levels of AM to contribute to a reduced starch digestibility (Hazard et al., 2014, Schönhofen et al., 2016, Hazard et al., 2015, Corrado et al., 2022a). This subset was selected based on previously identified variation in AX content (Shewry and Lovegrove, 2014) and obtained from Rothamsted Research, UK.

The analysis revealed a statistically significant difference in AM content ($p < 0.0001$) among the Watkins lines (Figure 2.25). AM content varied in normal range between 20% to 29% (g/100g of starch) in Watkins lines grown in 2014. The highest AM line recorded was W551, WATDE0070 (29.4 g ± 0.61 SE per 100g starch), and the lowest AM was in W32, WATDE0004 (20.1 g ± 1.04 SE per 100g starch).

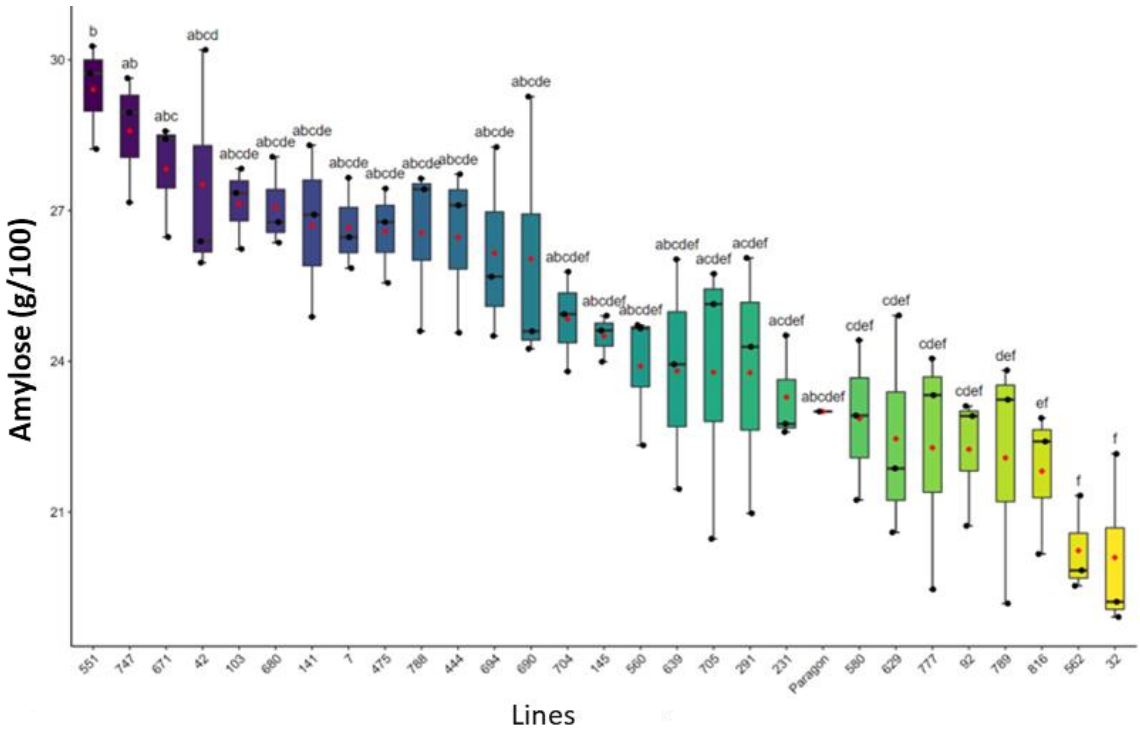

Figure 2.25. AM content (% starch) of Watkins lines and Paragon measured by iodine dye-binding method. n = 3 technical replicates

2.3.4 Natural variation in starch digestibility of Watkins lines and elite UK wheat varieties

After establishing the high-throughput assay, the next step was to use it as a screening tool to discover the variation in the starch digestibility of the Watkins collection and compare it with elite UK commercial wheat lines selected to represent each commercial group (animal feed, biscuit and bread quality).

For the starch digestibility analysis, whole wheat flour samples were weighed (6 mg) and transferred into deep well plates. Before starting the starch digestion assay, deep-well plates with samples were kept for five days in a desiccator. The assay for the starch digestibility was the same as described above (section 2.3.2) with a modification of time points (0, 6, 12, 18, 24, 40, and 90 min) and sample type (wholemeal flour).

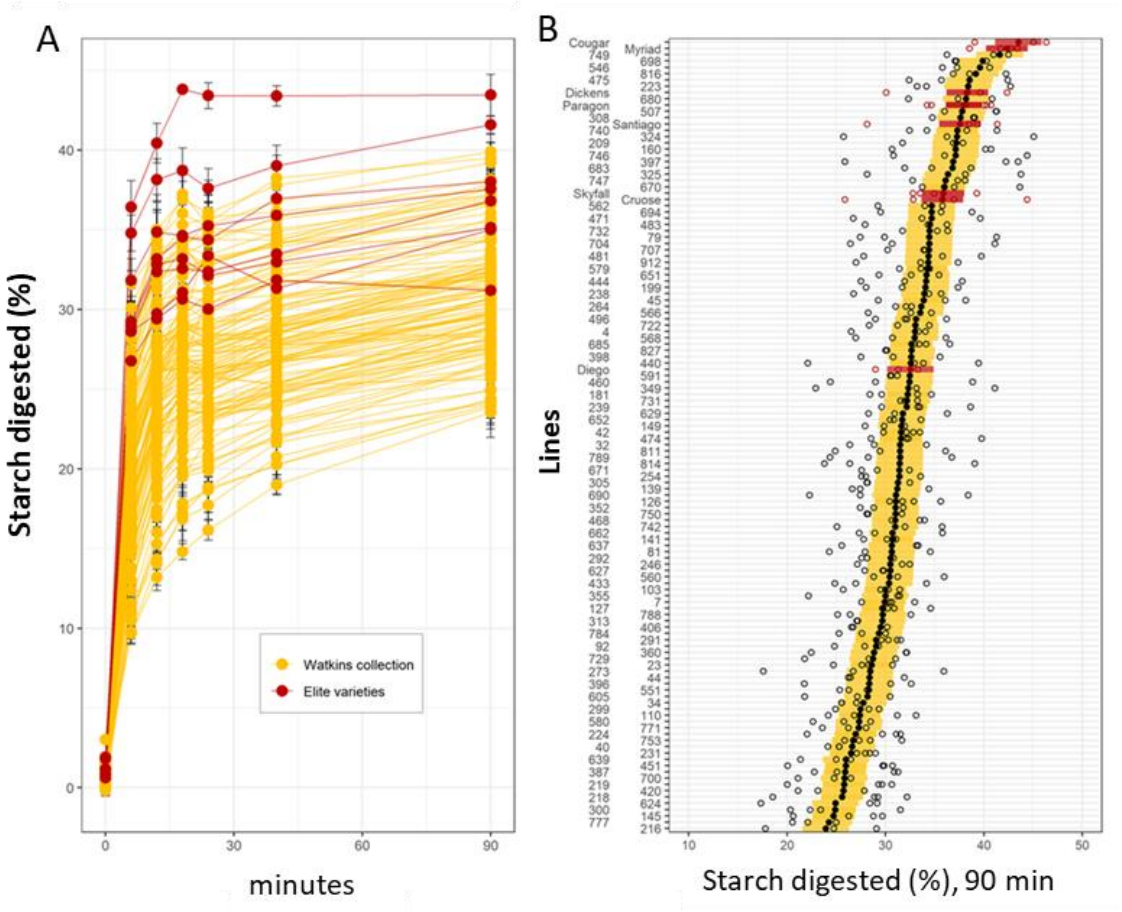

Figure 2.26. Starch digestibility of Watkins lines (yellow) and elite varieties (red) of wholemeal flour. A. Starch digested (%) for Watkins (yellow) and elite varieties (red). Points and lines represent the mean and SE from between 3 and 6 technical replicates per line. B. Starch digested (%) at 90 min. Individual data points from technical replicates are shown in white dots, and marginal mean values from a mixed effects model with line as a fixed effect and experimental run as a random effect are shown in black (Watkins) and red dots (elite). The SE estimated from the model is displayed as yellow (Watkins) and red (elite) bars. Values represent mean ± SE of n ≥3 technical replicates. Adapted from Zafeiriou et al. (2023).

Results of the high-throughput assay revealed a wide range of variation in starch digestibility among Watkins lines ($p \leq 0.001$), (Figure 2.26, Supplemental Table 2.4); starch digestibility profiles formed a gradient of low to high digestibility rather than

two distinct groups, which is expected from complex traits. More specifically, the Watkins lines differed for the 6 min timepoint between 9.7-31.6% starch digested, 13.2-35% for the 12 min, 14.8-37.2% for the 18 min, 16.2-36.1% for the 24 min, 19-37.8% for the 40 min and 23.5-39.9% for the 90 min (Table 2.3). The Watkins 777 line had the lowest starch digestibility, whereas Watkins 325 had the highest starch digestibility at 6 min, Watkins 816 was at 18 min, and Watkins 749 was at 12, 24, 40 and 90 min time points. Elite varieties differed significantly in timepoints ranging between 12-40 min ($p < 0.05$) but showed less variation than Watkins collection. More specifically, elite varieties varied for the 6 min timepoint between 26.8-36.4% starch digested, 29.4-40.4% for the 12 min, 30.6-43.8% for the 18 min, 30-43.4% for the 24 min, 31.3-43.4% for the 40 min and 31.2-43.5% for the 90 min (Table 2.3). The elite line Diego had the lowest starch digestibility in most time points (6-24, 90 min), whereas Cougar was the highest digested line in all time points. Lastly, elite wheat lines formed a group at the top end of the graph as high-digestibility lines, whereas Watkins lines formed a gradient of low to high-digestibility lines.

Table 2.3. Range of starch digestibility of Watkins lines and elite varieties of wholemeal flour. The p-value shown derives from the one-way ANOVA.

Timepoint (min)	iD	Range of starch digested (%)	p value
6	Watkins	9.7-31.6	≤ 0.001
	Elite	26.8-36.4	< 0.05
12	Watkins	13.2-35	≤ 0.001
	Elite	29.4-40.4	< 0.05
18	Watkins	14.8-37.2	≤ 0.001
	Elite	30.6-43.8	< 0.05
24	Watkins	16.2-36.1	≤ 0.001
	Elite	30-43.4	< 0.05
40	Watkins	19-37.8	≤ 0.001
	Elite	31.3-43.4	< 0.05
90	Watkins	23.5-39.9	≤ 0.001
	Elite	31.2-43.5	ns

Furthermore, there was no evidence for a relationship between the position of Watkins line plots in the field and the starch digestibility at 90 min, as no trend has been observed between field rows and columns (Figure 2.27).

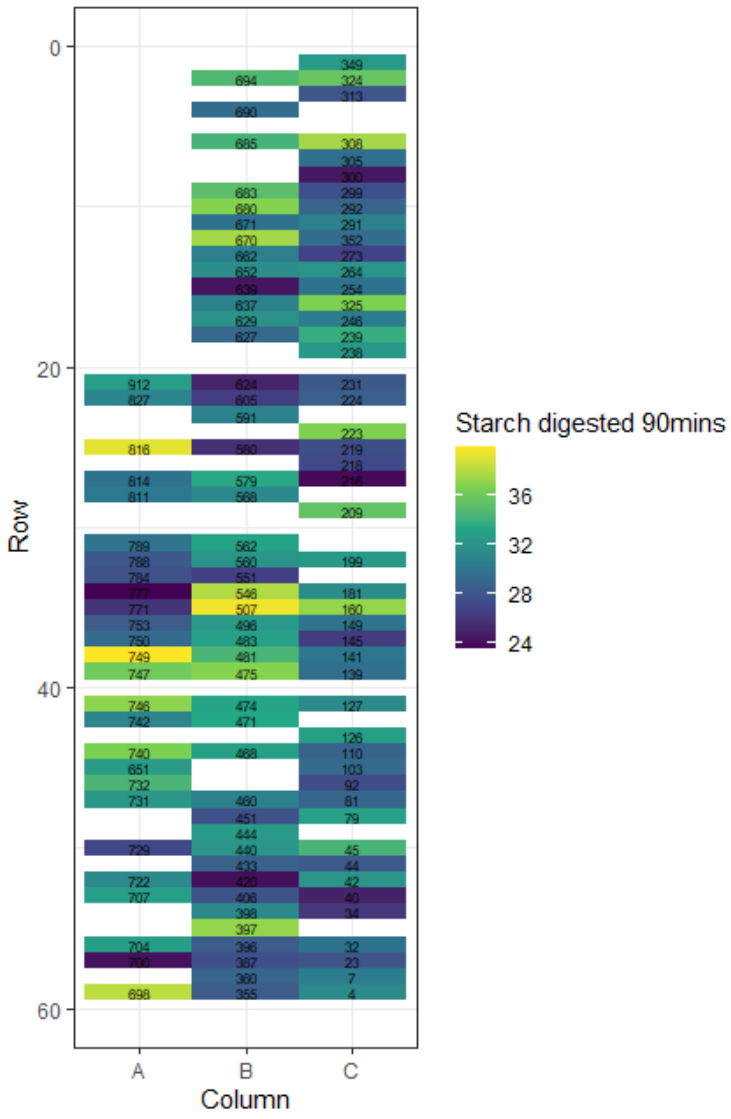

Figure 2.27. Field design of Watkins collection and starch digested (%) at 90 min.

TS content was measured for wholemeal flour samples using a 96-format thermomixer. The digestion efficiency was assessed with the addition of iodine at the end of digestion to observe whether any remaining non-digested starch was present (Figure 2.28). No colour development was observed in the sample after the

TS assay, which indicates that the digestion of starch using a 96-format was efficient.

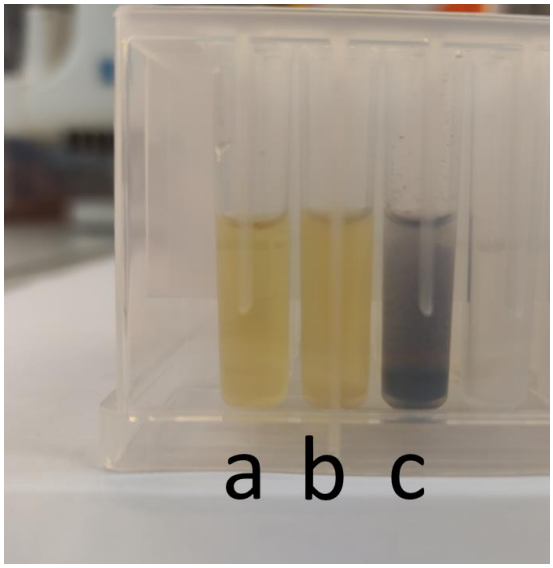

Figure 2.28. Iodine colour development in the presence of water. *(a) Blank, (b) digested wholemeal flour sample, (c) non-digested wholemeal flour sample using a 96-format TS HK assay.*

TS content of wholemeal flour differed significantly for Watkins lines (43 ± 3.3 g/100 flour to 61 ± 2.4 g/100 flour, mean ± SE, $p \leq 0.001$), and the elite varieties (46 ± 3.6 g/100 flour to 61 ± 0.9 g/100 flour, $p \leq 0.05$) (Figure 2.29, Supplemental Table 2.5). The elite variety Diego had the highest TS content (61 ± 0.9 g/100 flour), and the Watkins line 651 had the lowest (43 ± 3.3 g/100 flour). Most of the samples had a TS content between 47 to 57 g/100 flour.

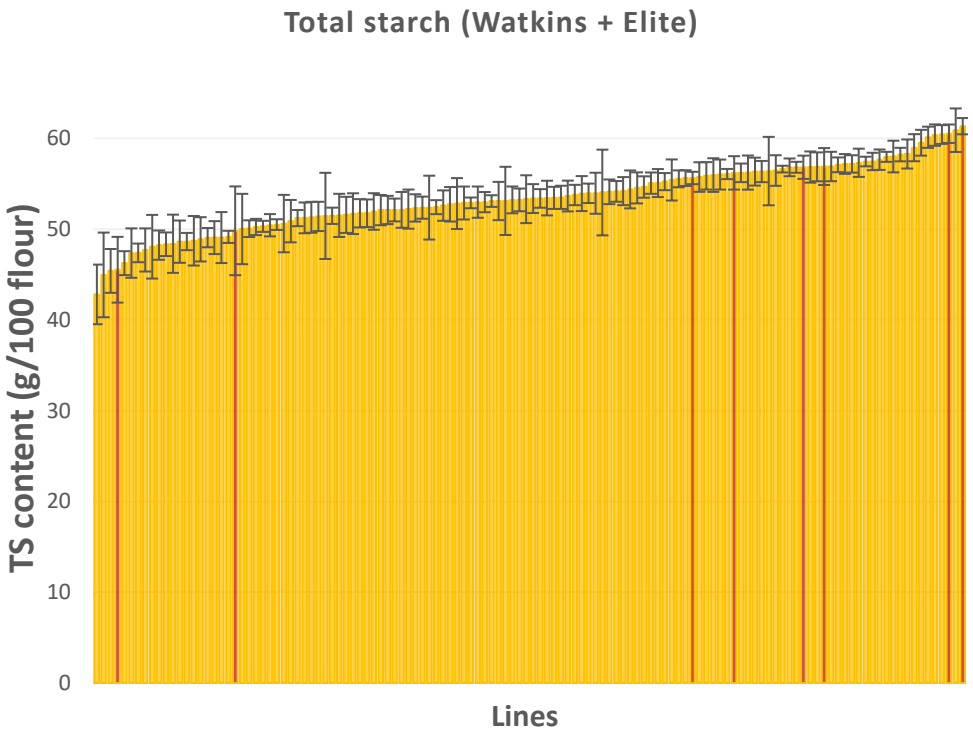

Figure 2.29. TS content (% w/w, as is) of the Watkins lines (yellow) and selected elite varieties (red). Ordered from highest to lowest starch digestibility results. Values represent mean ± SE of n = 3 technical replicates.

Linear regression analysis showed that TS content only weakly correlated ($R^2 = 0.03$) with starch digested at 90 min which suggests the differences in TS content cannot explain the variation observed for starch digestibility (Figure 2.30).

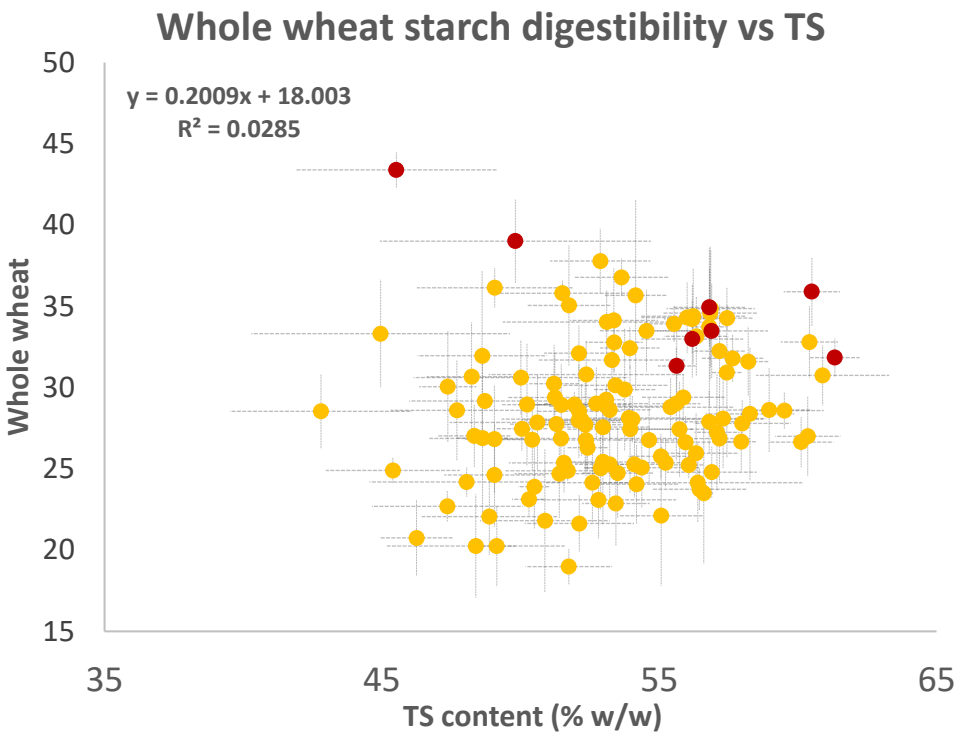

Figure 2.30. Linear regression of whole wheat starch digestibility and TS. Watkins' lines are shown in yellow, whereas elite varieties are shown in red. Values represent mean ± SE of n ≥ 3 technical replicates.

2.3.5 Seed analysis

The grains from the Watkins' collection harvested in 2019 and grains from elite varieties obtained from SeedStor, JIC, UK (Cougar, Skyfall, Myriad, Dickens, Diego, Santiago, Crusoe and Paragon) were screened with NIR to measure protein, moisture, starch, ash and non-dietary fibre (NDF) dry basis % (https://www.seedstor.ac.uk/). Results are attached in the supplemental data (Supplemental Table 2.6). Based on the measured grain characteristics there was a weak correlation between ash content and starch digestibility ($r = -0.26$, $p < 0.01$) (Table 2.4). However, no significant correlation was observed between any other parameters.

Comparing the TS of wholemeal flour measured with the Megazyme HK assay and the TS of grain measured with NIR using a paired t-test, showed a significant difference between the two methods ($p < 0.001$), (Figure 2.31)

Lastly, there was no significant correlation ($r = 0.18$, ns) between the kernel hardness index, which was obtained from a field trial conducted in 2010, and the starch digestibility (measured at the 90-minute timepoint) of the wholemeal flour derived from the Watkins lines (Supplemental Table 2.7).

Table 2.4. Pearson correlation of the Watkins and elite varieties on starch digestibility % (90 min) and grain characteristics measured by NIR.

Parameters (dry basis %)	r	p value
Protein	-0.17	ns
Starch	0.16	ns
NDF	0.07	ns
Ash	-0.26	<0.01
Moisture	-0.13	ns

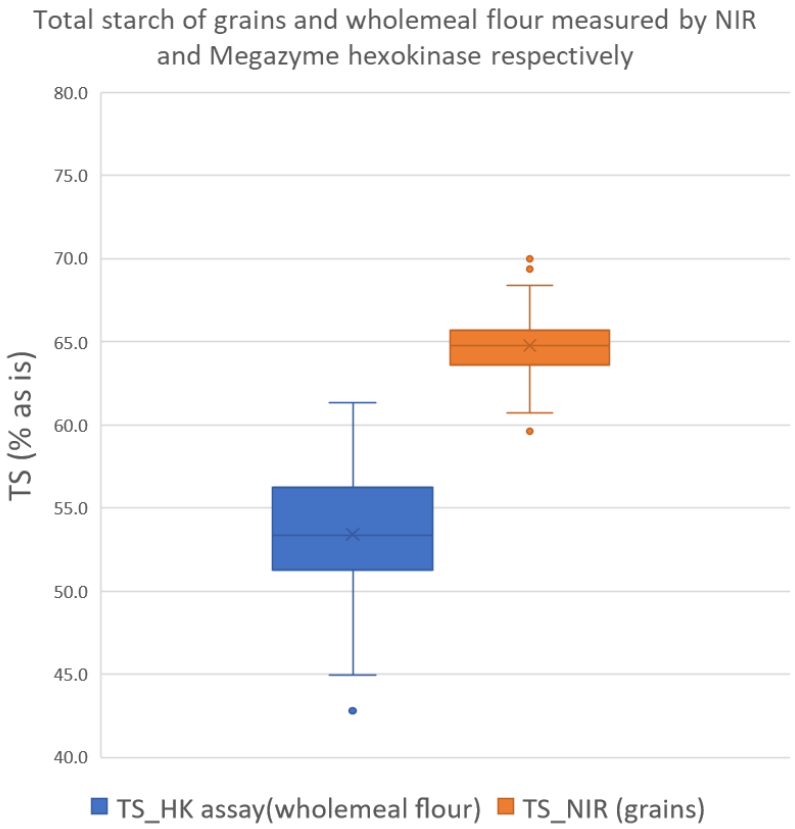

Figure 2.31. TS measurements (%, as is) on grains and wholemeal flour on the Watkins and elite varieties. Wholemeal flour was measured by Megazyme HK assay (blue) and grains were measured by NIR (yellow). Mean values of 3 technical replicates were used for the paired t-test.

2.4 Discussion

2.4.1 Development of the high-throughput assay to screen samples for starch digestibility

This chapter focused on determining the extent of natural phenotypic variation in starch digestibility of the Watkins collection and elite wheat varieties which required the development of a high-throughput assay.

Initially, the existing protocol underwent modifications to increase the sample format from 6 to 24, which resulted in increasing the throughput of the assay and helped to transition from an incubator to a thermomixer, as individual tubes could be tracked during processing and digestion. For example, during the assay individual tubes could be removed from the thermomixer to check whether samples were completely dispersed which was not possible to do with a 96-well plate format. Despite the expanded sample format (from 6 to 24), analysing germplasm collections remained inefficient due to numerous steps and the inability to use a multichannel pipette due to tip spacing. For instance, centrifuging "stop solution samples" required multiple dilutions before the PAHBAH assay, and individual tubes were needed for the colour development reaction. To address these issues, a 96-sample format using deep well plates was introduced to replace tubes. This modification enabled the processing and handling of multiple samples simultaneously. Additionally, the thermomixer used in the high-throughput assay replaced traditional equipment such as a cabinet incubator, tube rotator, and water bath. This modification made the process easier to run, more standardized, and more suitable for researchers to conduct such experiments and compare their findings. Consequently, the high-throughput starch digestibility assay substantially shortened the analysis time for studying 96 samples from 32 days to 3 days. It is important however to highlight that the preparation of these samples before conducting the assay remains a significant bottleneck, requiring approximately 22 days to prepare 96 samples. The major issues identified were the mixing ability of each sample in the 96-deep well plate and the volume of each sample. More specifically, samples had lower fluid motion in the 1mL tubes than in 15mL or 50mL tubes and were affected less by the applied kinetic energy. To address this mixing issue, a combination of a glass ball in each tube and an increase in rpm was applied.

One limitation of that assay is that the number of time points is limited due to the small sample volume.

Recent studies have also focused on increasing the throughput of starch digestibility assays. However, the throughput of these methods is still a bottleneck to conducting studies with many samples (Edwards et al., 2014, Toutounji et al., 2019). An example is a recent study from Toutounji et al. (2019), which developed a high-throughput *in vitro* assay for screening the starch digestibility of rice cultivars. Although this protocol decreased the operational steps of the method, samples still had to be handled individually, which required a single pipette. A single pipette system limits the number of samples that can be run simultaneously and thus decreases the overall throughput of the method. An alternative approach to increase the throughput has been taken by Wang et al. (2022). In this study, a 96-format high-throughput assay was developed for starch digestibility to screen isolated wheat starch samples of a wheat MAGIC population. However, this study focused on classifying samples into groups based on their digestibility profile and starch structure properties and there have been no reports of using this method to analyse wholemeal flour samples or hydrothermally treated samples. A number of studies have shown significant effects on starch digestibility when heat treatment on starch is applied. For example, studies that looked at the gelatinisation and retrogradation of starch and its effect on starch digestibility found an increasing rate of starch digestibility when starch has been gelatinised and a decreasing rate when starch has been retrograded (Wang and Copeland, 2013, ChungLim and Lim, 2006, Parada and Aguilera, 2009, Holm et al., 1988, Wang et al., 2015). In terms of the wheat grain matrix and its effect on starch digestibility, a study that compared the estimated GI of whole wheat bread and white bread found a lower estimated GI for the whole wheat bread (Whitney and Simsek, 2017).

In this study, starch amylolysis of a processed matrix was measured directly, using wholemeal flour samples that were hydrothermally treated, which may be more relevant to what people consume in wheat-based foods. Optimisations of the assay were also required to maintain the mixing ability of samples and produce adequate sample volumes for analysis. The development of 3D printed tools allowed faster sample handling during sample preparation and pipetting during starch digestibility. Lastly, the high-throughput assay was validated by comparing the results with the Edwards et al. (2019) protocol, which has previously correlated well with glycaemic response *in vivo.*

2.4.2 Variation in starch digestibility of the Watkins collection

The screening of the Watkins collection presented a wide variation in starch digestibility and TS among different landraces; these results suggest potential for identifying underlying genetic diversity. The elite varieties used in the screening were selected to represent each commercial group (animal feed, biscuit and bread quality). These elite varieties showed a smaller contribution to the overall variation of starch digestibility and TS and lower starch digestibility compared to the overall variation in most landraces. Additionally, the landraces formed a high-to-low digestibility gradient rather than two distinct groups, suggesting that starch digestibility is a complex trait. A larger variation in starch digestibility observed in the Watkins may suggest that the trait has narrowed over time. However, there were two limitations of the current study which prevent validation of the above hypothesis. The first limitation is that the study used a small number of elite varieties (8). This implies that the results of the study may not be fully representative of the broader population of elite varieties, and there may be other

elite varieties that could exhibit different characteristics or responses. To address this limitation, subsequent trials should include more elite varieties (at least 5 lines from each 4 commercial groups on the UK Agriculture and Horticulture Development Board Recommended List), which will provide a more comprehensive understanding of the elite variety population and the potential applications of the study's findings. The second limitation is that the elite varieties were not grown in the same year as the Watkins collection, making it difficult to capture information on environmental effects. This could potentially affect the validity of the results since the environmental conditions in different fields could affect the growth and development of the crops. To address this limitation, future field trials need to be conducted in multiple locations, where the same elite varieties can be grown alongside the Watkins collection. Findings from other studies support the above hypothesis by showing a reduction in the germplasm diversity of wheat due to genetic drift and selection (Reif et al., 2005, Wingen et al., 2014, Bansal et al., 2011, Bansal et al., 2013, Randhawa et al., 2015, Toor et al., 2013). These studies have demonstrated higher genetic diversity in the Watkins collection than in modern European bread wheat varieties and increased variation in agronomically desirable traits, such as stripe, leaf, and stem rust resistance, as well as grain surface area and grain width.

The study found no strong correlation between the measured grain characteristics and the starch digestibility of the Watkins wholemeal flour. One possible explanation for this is that the grains underwent milling and sieving (0.3 mm), resulting in the removal of specific grain fractions and components, which changed the initial grain composition. This was evident when comparing the TS of wholemeal flour measured with the Megazyme HK assay and the TS of grain

measured with NIR. Additionally, the NIR calibration may not accurately fit Watkins grains as it was originally calibrated with commercial-use wheat grains.

While the hardness of the grains can affect starch digestibility due to the increased susceptibility of starch granules to damage in hard wheat endosperm, hardness was found to be a non-significant factor in this study, as the starch granules had already undergone complete gelatinisation during cooking.

To further investigate factors affecting starch digestibility, endogenous α-amylase and AM content could be conducted and a correlation analysis with starch digestibility could be performed. Due to time constraints, this analysis was not carried out on the Watkins collection. Although there is an existing high-throughput assay for AM estimation developed by Kaufman et al. (2015), starch purification is necessary before analysis which is a highly time-consuming method. However, a grain and starch structure analysis, which included an analysis of endogenous α-amylase and AM, was conducted on a smaller sample set of high and low-digestibility starch samples (described in Chapter 3).

Given the significant amount of time required for sample preparation and analysis of the wheat samples (e.g., field trial, labelling, milling, sieving, and weighing), the whole Watkins collection or the 300 Watkins set was not screened (i.e. 826 or 300 accessions x 3 replicates). Therefore a GWAS could not be conducted due to the small sample size (118 lines in the Watkins collection). Consequently, as the project's main goal was to develop a high-throughput assay for starch digestibility and identify a low digestibility line for QTL analysis using a biparental population, a decision was made to screen a pre-milled selection of the Watkins collection from four field trials (described in Chapter 4) rather than repeating the process with a second year of drilling.

Chapter 3 Natural variation in starch molecular structure and grain composition

3.1 Introduction

Starch has been the staple dietary carbohydrate in human diets for millions of years (Hardy et al., 2017, Hardy et al., 2012). The starch polymers, AP and AM, form partially crystalline starch granules in their native state, which are difficult for humans to digest. Thus, starch-based foods are typically cooked prior to consumption. Heating starch in the presence of water leads to starch gelatinisation making starch polymers more accessible to digestive enzymes (Wang and Copeland, 2013, ChungLim and Lim, 2006, Parada and Aguilera, 2009). Subsequent cooling leads to retrogradation, and the starch polymers form complexes that are less digestible in the human digestive tract (Wang et al., 2015).

Intrinsic factors like molecular structure and composition can also influence starch digestibility, specifically the length of glucan chains, frequency of branch points, AM-to-AP ratio, and extent of crystallinity (Hazard et al., 2015, Schönhofen et al., 2016, Anugerah et al., 2022). The protein content and NSP in cereals are additional factors that have been shown to affect starch digestibility (Dhital et al., 2014); proteins have been reported to interact directly and indirectly with α-amylase and starch components. For example, proteins may function as physical barriers or adsorbed constituents to α-amylase or behave as water absorption antagonists to starch components (DhitalBrennan and Gidley, 2019, BhattaraiDhital and Gidley, 2016).

Few studies on cereals have focused on discovering natural variation in nutritional traits (Alomari et al., 2018, Ward et al., 2008, Shewry et al., 2015). Therefore, limited knowledge exists for aiding in the selection of factors that affect starch digestibility. The purpose of this chapter is to examine whether the properties of starch in the selected three low- and five high-digestibility lines are related to changes in starch digestibility. In addition, this chapter explores the potential impact of protein content and particle size of flour on starch digestibility. By investigating these factors, the chapter aims to explore the underlying mechanisms of starch digestion and whether these factors could be used as phenotypic markers for selecting low-digestibility starch lines in the Watkins collection.

Summary of the experiments

In Chapter 3, a series of experiments were conducted on both low- and high-digestibility lines. The experiments carried out were starch digestibility of thermally processed flour on different flour fractions, an analysis of starch content and an examination of the thermal properties of starch using wholemeal flour (Figure 3.1 and Table 3.1). Furthermore, the particle size measured by Coulter counter of the selected wholemeal flour samples was analysed and SEM micrographs were obtained to investigate aggregate formations above 120µm. Additionally, the selected wholemeal flour samples were analysed for endogenous α-amylase activity and protein content measured by an Elemental Analyser. Finally, the starch granule size distribution, measured by Coulter counter, and CLD were measured by SEC, were conducted on purified starch samples of the selected lines.

Figure 3.1. Chapter 3 Experimental design. Grain and structural analysis for selected samples on starch digestibility, TS, DSC, endogenous α-amylase, CLD, protein analysis and particle size analysis on wholemeal flour and purified starch.

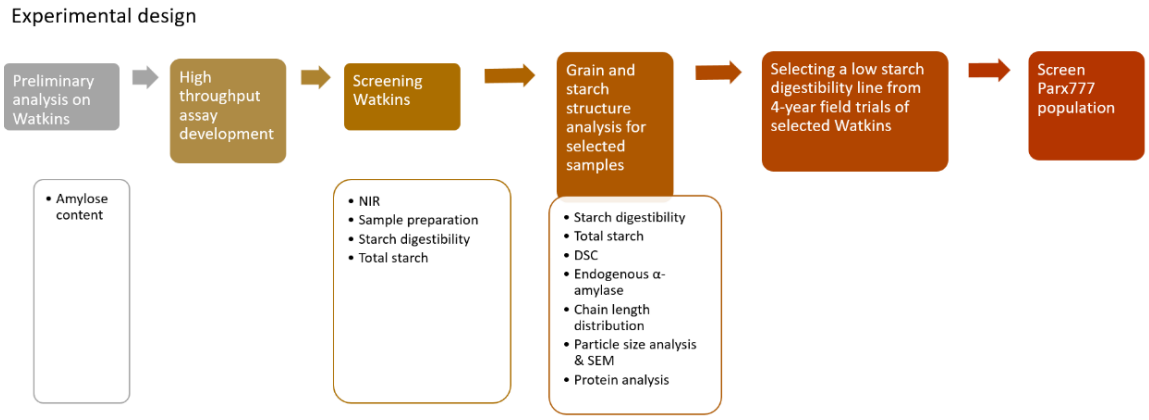

Table 3.1. Germplasm used and analysis in Chapter 3.

Germplasm	Year grown	Number of lines	Field trial location	Plot size (m^2)	Material used	Analysis	Provided by
Selected Watkins *	2018	3	Church Farm, Norfolk UK	1	Whole meal flour (Watkins & elite)	Starch digestibility, TS, DSC, endogenous α-amylase, particle size analysis & SEM, protein analysis	GRU
Elite varieties *	2013	5	Morley Farm, Norfolk, UK	1.5			Brendan Fahy
					White flour (Watkins & elite)	Starch digestibility, TS	
*(subset of the 'Watkins' and 'Elite varieties')					Purified starch (Watkins & elite)	Starch digestibility, TS, DSC, CLD, starch granule size distribution	

Required amount per sample	
Starch digestibility	5-10 mg
TS	5-10 mg
DSC	200 mg
Endogenous – α amylase	60 mg
SEC (CLD)	10 mg
Particle size analysis & SEM	5-10 mg
Protein analysis	10 mg

3.2 Materials and methods

3.2.1 Plant material

A total of eight lines, five from the Watkins collection (816, 308, 639. 216 and 777) and three from elite varieties (Dickens, Myriad, Paragon), were selected for further analysis. The grains of the lines from the Watkins collection were ordered from the GRU (JIC, UK) and gains from elite varieties were kindly provided by Fahy et al. (2018). The selected Watkins lines were grown in Autumn 2018 in $1m^2$ plots at Church Farm, Norfolk UK (52°37'49.2"N 1°10'40.2"E) and elite varieties were grown in 2013 in $1.5m^2$ plots at Morley Farm, Norfolk, UK (52°33'15.57"N 1°10'58.956"E).

3.2.2 Chemicals

Chemicals used in this study: Percoll (17-0891-01, GE Healthcare), PAHBAH (5351-23-5), TRIS (77-86-1), EDTA (60-00-4), SDS (151-21-3), DTT (3483-12-3), PBS (P4417-100), Sodium Carbonate (497-19-8), DMSO (67-68-5), maltose (6363-53-7), sodium hydroxide (1310-73-2) and porcine pancreatic α-amylase (EC 3.2.1.1, supplied in a DFP-treated suspension of 2.9 M NaCl containing 2 mM $CaCl_2$, A6255, Type I-A, 647-015-00-4) were purchased from Sigma-Aldrich Company Ltd., Poole, UK.

3.2.3 Milling and sieving

Grains from the Watkins (grown in 2018) and elite varieties (grown in 2013) were coarsely milled in a cyclone mill fitted with a 0.5 mm screen (UDY Corporation). Milled samples were passed through a 0.3 mm sieve to produce wholemeal flour samples, and selected lines were passed through a 0.053 mm sieve to produce 'sieved flour' samples. The flour samples were kept in a vacuum desiccator

containing silicon dioxide for five days before analysis. A single biological replicate was used for the milling and sieving process.

3.2.4 High-throughput starch digestibility assay

Starch digestion assays were carried out on samples that were gelatinised and allowed to retrograde following the protocol from Chapter 2, section 2.2.6. Samples were measured in three technical replicates.

3.2.5 Amylase activity for digestion assay

The enzyme activity of the pancreatic α-amylase (for use in the starch digestibility assay) was determined following the protocol from Chapter 2, section 2.2.6.

3.2.6 Endogenous α-amylase

Endogenous α-amylase levels present in wholemeal flour samples were determined using the Ceralpha assay procedure following manufacturing instructions (α-Amylase Assay Kit (Ceralpha Method, R-CAAR4 05/12); Megazyme, Bray, IE). To measure the endogenous α-amylase flour extracts were obtained using extraction buffer (sodium malate 1M, sodium chloride 1M and calcium chloride 40mM, content diluted to 1L of distilled water, pH 5.2). Then extract containing the endogenous α-amylase is added to a Ceralpha substrate mixture (non-reducing end-blocked p-nitrophenyl maltoheptaoside (BPNPG7), 54.5 mg and α-glucosidase 100 U and glucoamylase 100 U at pH 5.2, content diluted in 10mL distilled water). Endogenous α-amylase then acts on BPNPG7, whereas the other two enzymes do not take action due to the presence of the blocking group. When p-nitrophenyl

maltosaccharide is present from the hydrolysis by endogenous α-amylase, glucoamylase and α-glucosidase act on the substrate to release glucose and free p-nitrophenyl. Finally, a stop reagent containing Trizma base (20% w/v tri-sodium phosphate solution, pH ~ 11, content diluted to 500mL distilled water) is used, and the phenolate colour development of the samples is read on the spectrophotometer and expressed as Ceralpha Units/g flour.

Wholemeal and white flour samples (60mg) were suspended in extraction buffer (600µL) with occasional stirring for 6 min at room temperature to allow enzyme extraction. Samples were then centrifuged at 1000*g* for 10 min. Aliquots of 200µL Ceralpha substrate and flour extracts were placed into separate test tubes and pre-incubated for 5 min at 40°C. Then 200µL of flour extracts were added to 200µL of Ceralpha substrate and left to incubate for 10 min at 40°C. To stop the hydrolysis, 3mL of stopping reagent was added to each solution, and the absorbance of the solutions and the reaction blank were read on a spectrophotometer (400 nm) against distilled water. The equation to calculate the Units/g flour is shown below (Equation 5), where ΔE_{400} is the difference between the reaction and blank absorbance and E_mM of p-nitrophenol in 1% Trizma base is 18.1. Samples were measured in two technical replicates.

$$Units/g\ flour = \frac{\Delta E_{400}}{\frac{Incubation}{time}} \times \frac{\frac{Total\ volume}{in\ Cell}}{Aliquot\ Assayed} \times \frac{1}{E_mM} \times \frac{\frac{Extraction}{Volume}}{\frac{Sample}{Weight}} \times Dilution$$

(Eq 5)

3.2.7 Starch isolation

Starch was isolated using an adapted method reported by Hawkins et al. (2021).

Three technical replicates of the wholemeal flour samples were first filtered through a 100 µm cell strainer (BD Falcon #352360) with water to remove larger

particles (i.e, bran) or impurities that may be present in the sample. The resulting filtrate, containing starch granules, was then centrifuged at 3000*g* for 5 min to remove low-density constituents (i.e., broken cells). The pellet containing starch was resuspended in 2mL of water and the starch suspension was then overlayed into a Percoll solution (90% v/v) and centrifuged at 2500*g* for 15 min. Percoll creates a density gradient that allows for further separation of the starch granules from other cell wall debris and proteins. Therefore, starch granules will migrate through Percoll solution to form a distinct layer at the bottom of the tube, while the cell walls and proteins remain in the upper layers. The pellets were then washed three times with 1mL of water and centrifuged at 4000*g* for 1 min to help remove any remaining buffer components. Then starch pellets were washed once with 100% ethanol to remove any residual water and speed up the drying of the pellets. Samples were then kept for one day in the fume hood, followed by five days in a desiccator containing silicon dioxide prior to analysis.

3.2.8 Total starch measurement

TS assay (HK) was carried out on sieved flour samples following the protocol from Chapter 2, section 2.2.7. Samples were measured in three technical replicates.

3.2.9 Particle size analysis of flour and starch

Particle size analysis of wholemeal wheat flour (milled and sieved) and purified starch granules was carried out using a Multisizer 4e Coulter counter (Beckman Coulter, Indianapolis, US). The Coulter counter principle for counting and sizing particles is based on measuring electrical impedance. The instrument consists of a tube with a small aperture (the size of the aperture can be adapted to the size of

the particles of interest) that carries one internal electrode. The tube with the aperture is placed in a beaker containing a suspension of a low-concentration electrolyte, particles, and a second electrode. Particles suspended in the electrolyte are pumped through the aperture, while an electrical current is generated between the two electrodes. As each particle moves through the aperture, it causes a change in electrical resistance, and the impedance is measured. The magnitude of this voltage pulse is proportional to the particle volume and can be converted into volumetric units to generate the particle size distribution, assuming constant particle density. For the starch granules the density is approximately 1.5 g/cm^3 and according to studies on wheat, native starch granules have minimal density changes (Su et al., 2020, DengateBaruch and Meredith, 1978, BrustOrzechowski and Fettke, 2020). For the analysis, samples (5 mg of flour or 10 mg of purified starch) were suspended in 1mL of deionised water and mixed for 15 min on a rotating wheel. Suspensions were filtered through a sieve (200 µm nylon mesh for the flour and 70 µm nylon mesh for the starch) into 100mL of Isoton II electrolyte solution (Beckman Coulter) before the analysis. The aperture tube used was 200 µm for wholemeal flour and 70 µm for the purified starch. A minimum of 100,000 particles were quantified. For starch samples, the mean diameter of A- and B-type granules and relative volumes were calculated by fitting a mixture of two log-normal distributions in R (cite as a reference script available https://github.com/JIC-CSB/Coulter_counter_fitting) (Hawkins et al., 2021). All measurements were conducted with logarithmic bin spacing but are presented on a linear x-axis for clarity. Wholemeal flour samples were measured in three technical replicates, and starch samples were measured in ≥ 6 replicates depending on the observed variation.

3.2.10 Scanning electron microscopy (SEM)

Scanning electron microscopy (SEM) is obtained by an electron beam to image a sample under a vacuum. When electrons are fired to the target sample, they reflect with lower energy when they reach the sample's surface. The angle of these electrons is detected, and the typology of the sample is obtained. Due to the low or no conductivity of biological samples, a gold coating is added by sputtering to improve the image quality. In this study, three technical replicates of wholemeal flour sample for each selected line were brushed onto a carbon tab and fixed to an SEM pin stub. Samples were analysed by Dr David Seung (JIC Group Leader). SEM pin stubs were sputter coated with ~15 nm gold particles in a high-resolution sputter-coater (Agar Scientific Ltd) and were visualised using a Nova NanoSEM 450 (FEI) SEM.

3.2.11 Differential scanning calorimetry

The thermal properties of both wholemeal flour and purified starch were investigated using a Heat Flux Differential Scanning Calorimeter (DSC). Differential Scanning Calorimetry is a thermoanalytical technique utilized to observe changes in starch structure by heating and cooling it. This technique relies on the difference in heat flow between the sample and the reference during controlled heating or cooling. DSC has a constant-temperature furnace chamber surrounding the sample and reference pan (air), which are both held in Hastelloy ampoules. When sample and reference pans are placed on the blocked heated holders, the heating or cooling rate in both pans occurs at a linear rate. During heating or cooling, the sample can exhibit endothermic (heat absorption) or exothermic (heat release) phenomena, and the resulting transitions are quantified as energy (J or J/g).

Equation 6 describes the differential behaviour between the sample and reference, where Q represents the heat rate flow, and Δt represents the temperature difference between the reference and sample sensors and R describes the thermal resistance between the block and pans (Menczel and Prime, 2009).

$$Q = \frac{\Delta T}{R} \qquad \text{(Eq 6).}$$

The parameters expressed for every endothermic or exothermic event during a DSC experiment are expressed as onset and peak temperature (*T*o and *T*m) and enthalpy of transition (ΔH).

In the experiments involving wholemeal flour, a multicell differential scanning calorimeter (TA Instruments, New Castle, US) equipped with four 1mL capacity Hastelloy ampoules was used. Wholemeal flour samples (200 mg) were accurately weighed into the DSC ampoules with 1000µL of deionised degassed water. A reference pan was compared containing only 1000µL of deionised water. The furnace was flushed with dry nitrogen at a rate of 50mL/min. Thermal cycles were defined to mimic the processing of samples for the digestibility assay: Cycle 1 to mimic gelatinisation, heating from 10 to 80^{o}C at 2^{o}C/min and holding at 80^{o}C for 15 min; Cycle 2 to mimic retrogradation, cooling from 80 to 4^{o}C at 2^{o}C/min, holding at 4^{o}C for 21hr, then heating from 4 to 150 ^{o}C at 1^{o}C/min to analyse the effect of retrogradation.

To determine the gelatinisation parameters of starch, a DSC 2500 (TA Instruments, New Castle, US) was used with one reference pan (TZERO lids and aluminium pans, TA Instruments, New Castle, US) containing degassed deionised water and one sample pan. The DSC 2500 has the advantage of requiring significantly less sample material for the analysis than the Heat Flux DSC, which typically uses 1mL Hastelloy ampoules. However, due to the different structure of the pans, the aluminium lid

of the DSC 2500 does not provide a hermetic seal, and the liquid solution it contains cannot exceed 100°C. As a result, the same thermal conditions as used in the larger DSC scale could not be applied.

The furnace was flushed with dry nitrogen at a rate of 50mL/min and was calibrated for temperature and enthalpy using Indium. A deionised degassed water solution containing 4 mg of purified starch was added to the sample pan. The calorimetric measurements were conducted over one heating cycle of 40°C to 90°C at 2°C/min. The thermal conditions of this analysis did not simulate the conditions applied using the wholemeal flour due to the different structure of the pans.

Wholemeal flour and starch samples were measured in three technical replicates, and peaks were integrated with the TA Universal Analysis software (version 4.5A) to calculate onset temperature and peak temperature.

3.2.12 Protein content

The protein content of wholemeal flour was measured using the AACC 46-30 Crude protein – combustion method (AACC, 2010) on a CE440 Elemental Analyser (Exeter Analytical, https://www.exeteranalytical.co.uk/) by Antony Hinchliffe (University of East Anglia). Briefly, wholemeal samples were dried, ground, and redried. Nitrogen composition was ascertained, and all nitrogen results were multiplied by the protein conversion factor 5.7. Reference material was used alongside samples. Samples were measured in three technical replicates.

3.2.13 Size Exclusion Chromatography (SEC)

SEC was used to determine the chain-length distribution of debranched starch for selected samples. Samples were analysed by Dr Jennifer Ahn-Jarvis (QIB Research

scientist). A Waters Alliance e2695 HPLC (Milford, US) equipped with a refractive index detector (RI), autosampler (40°C), and column heater (90°C) was used for peak resolution by size exclusion. An isocratic mobile phase of DMSO with 0.5% LiBr (w/w) at 0.5mL/min flow rate was used. The stationary phase was a guard column (8x50mm, GRAM; Polymer Standard Service, Mainz, DE) followed by two analytical columns in series (10um; 300 Å followed by 30 Å; 8x300mm, GRAM; Polymer Standard Service, Mainz, DE). The total run time was 65 min and the injection volume for each sample was 50µL. Calibration curves were generated using pullulan standards (PSS-pulkit, Polymer Standard Service, Mainz, DE) with peak molecular weights ranging from 342 to 708,000 Da and correlation coefficients of R^2 = 0.9993 ± 0.0005. Purified starch was solubilised and debranched enzymatically using methods adapted from Perez-Moral et al. (2018) and WuLi and Gilbert (2014). Debranched starch samples were solubilized at a concentration of 8 mg/mL and standards at 2 mg/mL with DMSO containing 0.5% LiBr (w/w). All samples and standards were vortexed and stored at 80°C overnight prior to analysis to ensure complete dissolution and dispersion of glucose polymer chains.

For the analysis, the SEC separates different sizes of debranched samples by hydrodynamic volume (V_h), which is defined as the volume of a hypothetical impenetrable sphere displaying in a hydrodynamic field the same frictional effect as an actual polymer molecule (Jones et al., 2009). Therefore, size-separation data is reported in terms of V_h and not as elution time, as the elution time depends on the instrument set-up and day-to-day variability. The V_h is obtained by the instrument calibration based on the molecular weight, intrinsic viscosity for a given molecular weight (Mw) and Avogadro's constant (N_A) of glucose polymers (Equation 7).

$$V_h = \frac{2}{5}\frac{M_W\,[\eta]_{Mw}}{N_A} \quad \text{(Eq 7)}$$

V_h and Mw are then fitted to the Mark-Houwink relation (Equation 8), where an (exponent) and *K* (constant) depend on the polymer-solvent-temperature system.

$$V_h = \frac{2}{5}\frac{KM_{W^{1+a}}}{N_A} \qquad \text{(Eq 8)}$$

The samples diluted in a DMSO solution pass through a column containing different size pores. Depending on the V_h, of each sample, the elution time can differ. The elution time is different due to the different sizes of the pores where large molecules cannot fit through the small pores, and their time (t_{el}) is faster compared to a small molecule which can fit in several pores, and the elution time is slower. Therefore, depending on the standard elution, a relation is achieved between elution volume (V_{el}) and *V*h.

SEC protocols can use different types of detectors; in this study, the detector used was a Differential Refractive Index (DRI). DRI yields the weight distribution of the polymer $w(\log V_h)$, which derives from the difference in refractive Index (RI) of the solvent and the polymer solution. Equation 9 is used to obtain $w(\log V_h)$, where $S_{DRI}(V_{el})$ is the V_{el} detector signal.

$$w(logV_h) = S_{DRI}(V_{el})\frac{\Delta V_{el}}{\Delta logV_h} \quad \text{(Eq 9)}$$

For the subsequent chain-length distribution analysis on SEC data, both AP and AM chains were divided into short- and long-chain fractions based on their DP (<37 DP and >37-100 DP for AP; 100-1000 and >1000 DP for AM). Then the area under the curve was calculated for each line. To compare the samples, ratios of long/short AP, long/short AM and AM/AP were used. Samples were measured in three technical replicates.

3.2.14 Data analysis

Statistical analyses and graphs were obtained with Excel (version 2202), Jamovi (version 1.0.7.0) and R (R version 4.2.1). Plots were made using Excel and the ggplot2 R package (version 3.3.6) (Wickham, 2016). One-way ANOVA was used for the analysis of selected lines; a p-value < 0.05 was adopted for statistical significance. Chain-length distribution of debranched starch was analysed by using a mixture model, mixdist R package (version 0.5-5). The distribution components were estimated using constrained values of the DP. The correlation between protein content (wholemeal flour), endogenous α-amylase (wholemeal flour) particle size (wholemeal flour and starch), thermal properties of starch (wholemeal and starch), CLD (starch) and starch digestibility was estimated using Pearson correlation. All values reported represent the mean ± SE of three technical replicates unless stated otherwise in the description of the corresponding figure and supplemental datasets. For boxplot graphs, red points represent the average, and black horizontal lines represent the median.

3.3 Results

3.3.1 Digestibility of selected lines as wholemeal flour, sieved flour and purified starch

Three low-digestibility Watkins lines (777, 216, and 639) and five high-digestibility lines, including two Watkins lines (816, 308) and three elite varieties (Myriad, Dickens, Paragon) were selected for further analysis. The selection was based on the results of the high-throughput starch digestibility assay, specifically, the ranking

(low to high), to represent the variation observed in the screen and the reproducibility of starch digestibility data.

This experiment aimed to gain insight into possible intrinsic and extrinsic factors contributing to variation in starch digestibility. The same high-throughput assay used in the starch digestibility screen (Chapter 2, section 2.3.4) was used to analyse sieved flour and purified starch from the selected lines. Starch digestibility profiles differed considerably for wholemeal flour, sieved flour, and purified starch, suggesting that other flour components besides starch contributed to the variation in starch digestibility observed (Figure 3.2, Table 3.2). For example, two of the three low-digestibility lines (216 and 639) had a significantly higher digestibility *($p < 0.05$)* for most of the time points in sieved flour compared to wholemeal flour, whereas starch digestibility of line 777 did not differ between wholemeal and sieved flour. For purified starch samples, the low-digestibility lines were significantly more digestible *($p < 0.001$)* at all time points compared to wholemeal flour. The high-digestibility lines did not differ for most time points when comparing wholemeal and sieved flour apart from 6 min, where Myriad and Paragon had a lower starch digestibility. The digestibility of purified starch increased relative to wholemeal flour samples for all high-digestibility lines *($p < 0.05$)*.

Wholemeal flour samples

Wholemeal flour samples of low- and high- digestibility lines differed significantly at all time points *($p < 0.01$)*. Starch digested in low-digestibility lines ranged between 9.7-10.5%, 13.2-15.3%, 14.8-17.6%, 16.2-18.8%, 19-21.6% and 23.5-24.3% at 6, 12, 18, 24, 40 and 90 min respectively (Table 3.2); there were no statistically

significant differences among low-digestibility lines. High-digestibility lines ranged between 26.7-34.8%, 33-38.1%, 34.6-38.7%, 34.4-37.6%, 35.9-39%, 37.6-41.6% of starch digested at 6, 12, 18, 24, 40 and 90 min respectively (Table 3.2); there was no statistically significant difference among the selected lines.

Sieved flour samples

Sieved flour samples of low- and high-digestibility lines differed significantly for all time points *(p* < 0.05). Low- digestibility lines varied between 6.3-11.7%, 10.1-21.8%, 11.2-25%, 13-27.4%, 17.4-31.3%, 26-37.3% of starch digested for the 6, 12, 18, 24, 40 and 90 min (Table 3.2), respectively. Line 777 had a significantly lower starch digestibility within low-digestibility lines compared to 216 and 639 at all time points *(p* < 0.05). The high-digestibility lines varied between 19.3-27.5%, 29.5-35.7%, 30.8-35.8%, 32.2-37%, 35.5-40.7%, 38.1-42.7% of starch digested for the 6, 12, 18, 24, 40 and 90 min (Table 3.2). Within high-digestibility lines, only Paragon and 308 had a significant difference with Myriad and Dickens at the beginning of digestion (6 min timepoint) (*p* < 0.001).

Purified starch samples

For purified starch samples, low and high-digestibility lines were digested very similarly, and there was no statistically significant difference between the groups. Additionally, all starch samples showed a higher digestion extent compared to wholemeal and sieved flour at 90 min *(p* < 0.001). Purified starch of low digestibility samples varied between 34.6-35%, 38.3-38.5%, 39.9-40.7%, 41-42%, 42.6-43.5%, 47.6-49.2% of starch digested for the 6, 12, 18, 24, 40 and 90 min (Table 3.2),

respectively. Purified starch of high digestibility samples varied between 33.5-37.5%, 37.2-41.8%, 38.5-44.1%, 39.1-45.3%, 41.5-47.1% and 46.9-52.3% of starch digested for the 6, 12, 18, 24, 40 and 90 min (Table 3.2), respectively.

The high-throughput starch digestibility assay showed that purified starch had higher digestibility when compared to wholemeal and sieved flour, and there were no differences in starch digestibility among selected lines. These results suggest that for the selected lines, multiple components in wheat flour samples contribute to the reduction in starch digestibility, and different lines may have different underlying factors influencing their digestibility.

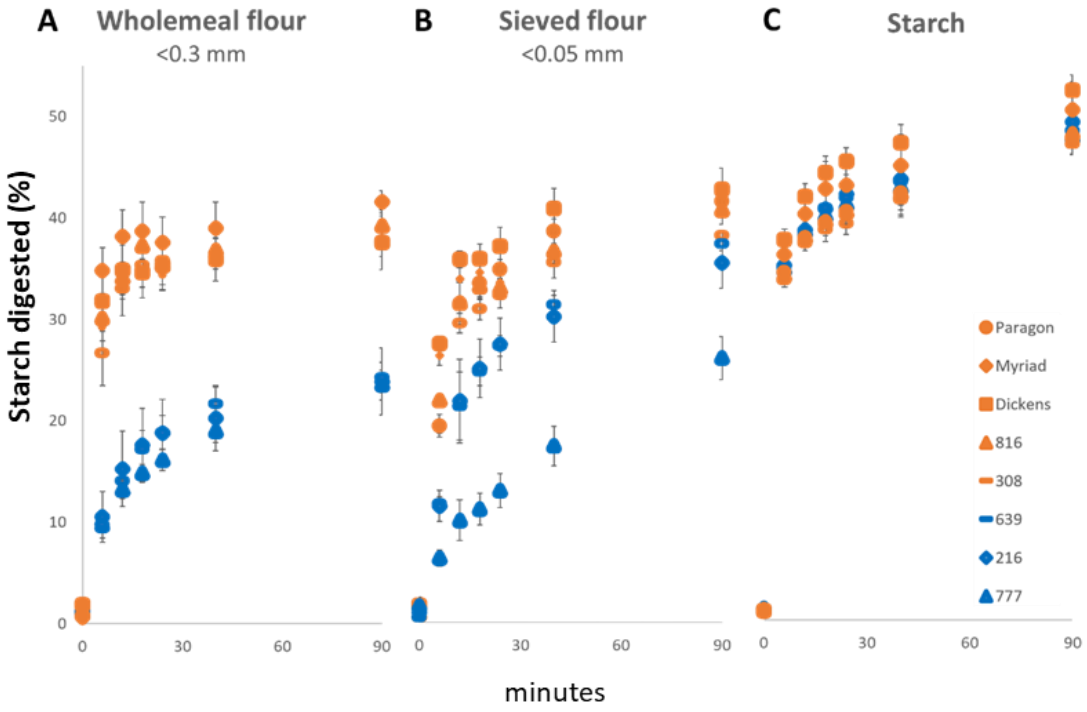

Figure 3.2. Starch digestibility of selected low- and high-digestibility lines as measured in wholemeal flour (A), sieved flour (B), and purified starch (C) using the high-throughput assay. The activity of pancreatic α-amylase was set to 2U/mL. Samples in blue represent the low-digestibility lines, and samples in orange represent the high-digestibility lines, n = 3 technical replicates.

Table 3.2. Range of starch digestibility of high and low-digestibility lines of wholemeal, sieved flour and purified starch. The p-value shown derives from the one-way ANOVA. Low refers to the three low-starch digestibility lines (639, 216, and 777). High refers to the five high-starch digestibility lines (Paragon, Myriad, Dickens, 816, and 308).

Timepoint (min)	Type of flour	Selected lines	Starch digested (%) min-max	p-value
6	Wholemeal	Low	9.7-10.5	ns
		High	26.7-34.8	ns
	Sieved	Low	6.3-11.7	< 0.05
		High	19.3-27.5	< 0.001
	Starch	Low	34.6-35	ns
		High	33.5-37.5	ns
12	Wholemeal	Low	13.2-15.3	ns
		High	33-38.1	ns
	Sieved	Low	10.1-21.8	< 0.05
		High	29.5-35.7	ns
	Starch	Low	38.3-38.5	ns
		High	37.2-41.8	ns
18	Wholemeal	Low	14.8-17.6	ns
		High	34.6-38.7	ns
	Sieved	Low	11.2-25	< 0.05
		High	30.8-35.8	ns
	Starch	Low	39.9-40.7	ns
		High	38.5-44.1	ns
24	Wholemeal	Low	16.2-18.8	ns
		High	34.4-37.6	ns
	Sieved	Low	13-27.4	< 0.05
		High	32.2-37	ns
	Starch	Low	41-42	ns
		High	39.1-45.3	ns
40	Wholemeal	Low	19-21.6	ns
		High	35.9-39	ns
	Sieved	Low	17.4-31.3	< 0.05
		High	35.5-40.7	ns
	Starch	Low	42.6-43.5	ns
		High	41.5-47.1	ns
90	Wholemeal	Low	23.5-24.3	ns
		High	37.6-41.6	ns
	Sieved	Low	26-37.3	< 0.05
		High	38.1-42.7	ns
	Starch	Low	47.6-49.2	ns
		High	46.9-52.3	ns

3.3.2 Endogenous α-amylase

Elevated amounts of endogenous α-amylase in cereals are an indication of a stressful growing environment for the plant, which could trigger early starch amylolysis in the endosperm and thus affect starch digestibility (Newberry et al., 2018, Derkx and Mares, 2020). Thus, the amount of endogenous α-amylase was measured in wholemeal flour samples of the selected lines. The activity of endogenous α-amylase in low- and high-digestibility lines differed significantly *(p* <0.05), (Supplemental Table 3.1). However values were within a normal range (<0.2 Ceralpha Units/g) according to prior studies (McCleary et al., 2002, Derkx and Mares, 2020) and there was no significant correlation with % starch digested (90 min) (r = -0.66, ns) (Figure 3.3, Supplemental Table 3.2). The activity of endogenous α-amylase in low-digestibility lines ranged from 0.06 ± 0.01 to 0.15 ± 0.01 Ceralpha Units/g of flour, mean ± SD, with the lowest being line 639 and the highest line 216. High-digestibility lines varied from 0.05 ± 0.01 to 0.13 ± 0.01 Ceralpha Units/g of flour, Paragon being the lowest and line 308 the highest.

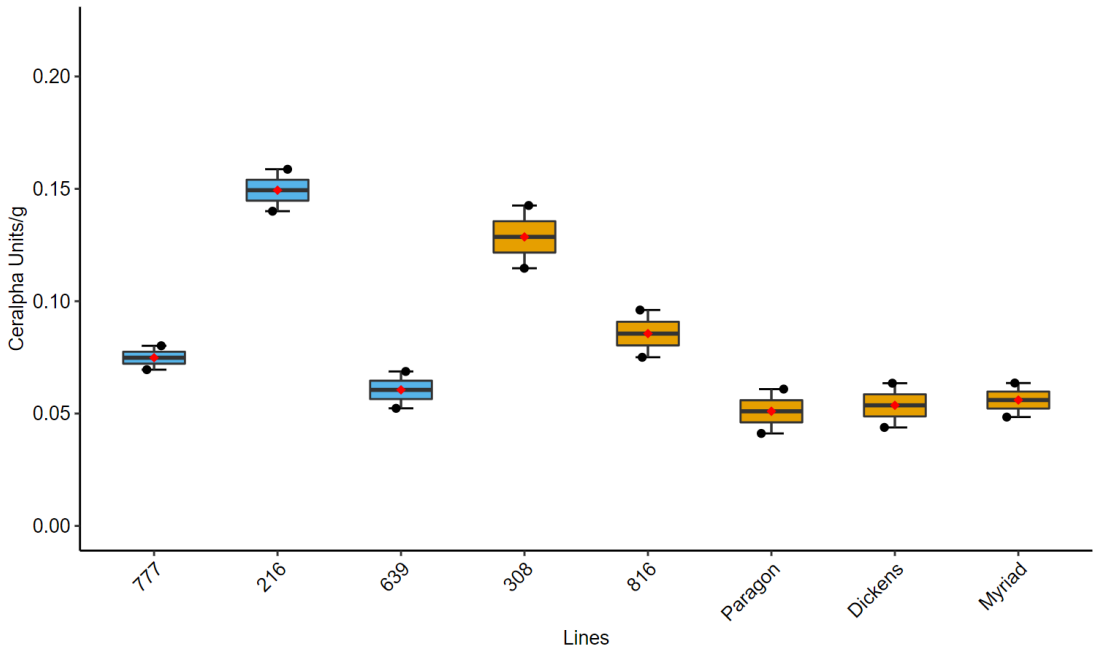

Figure 3.3. Endogenous α-amylase (Ceralpha Units/g of flour) of wholemeal flour samples from selected lines. Samples in blue represent the low-digestibility lines, and samples in orange represent the high-digestibility lines. Values represent mean ± SD of n = 2 technical replicates.

3.3.3 Particle size of wholemeal flour

Variation in milling efficiency could affect flour particle size; thus, a particle size analysis of flour was used to determine if there were any associations with the starch digestibility profiles. A combination of Coulter counter analysis and SEM was used due to the limitations of the Coulter counter to screen above 120 µm diameter. There was a statistically significant difference ($p < 0.003$), where line 639 had more particles in the range of 14-20 µm, whereas Paragon showed a slightly smaller number of particles in that range (Figure 3.4). However, no major difference in particle sizes of wholemeal flour among samples was otherwise observed, and there was no significant correlation with % starch digested (90 min) (r = -0.14, ns).

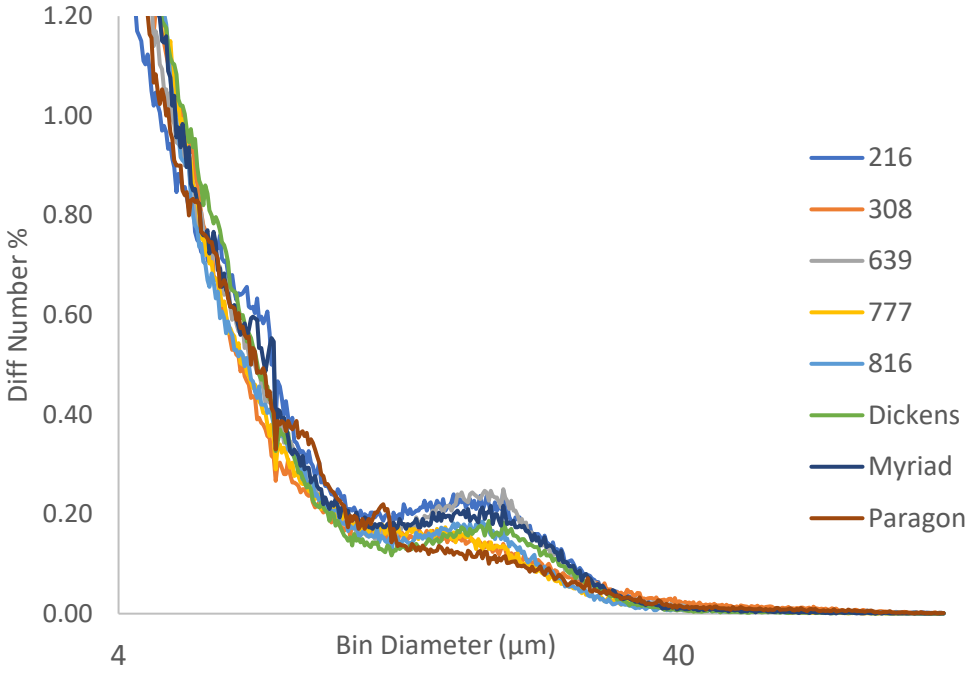

Figure 3.4. Differential Particle Size Distribution of wholemeal flour particles by Coulter counter analysis, data is shown on a log scale in the x-axis, n = 3 technical replicates.

In SEM micrographs, aggregate formations ≥ 120µm were detected in all lines apart from the low-digestibility line 639, which only had particles smaller than 120µm (Figure 3.5). This data suggests that the milling efficiency was similar in all lines apart from 639, and thus there is no evidence linking the particle size of the raw wholemeal flour with their starch digestibility profile.

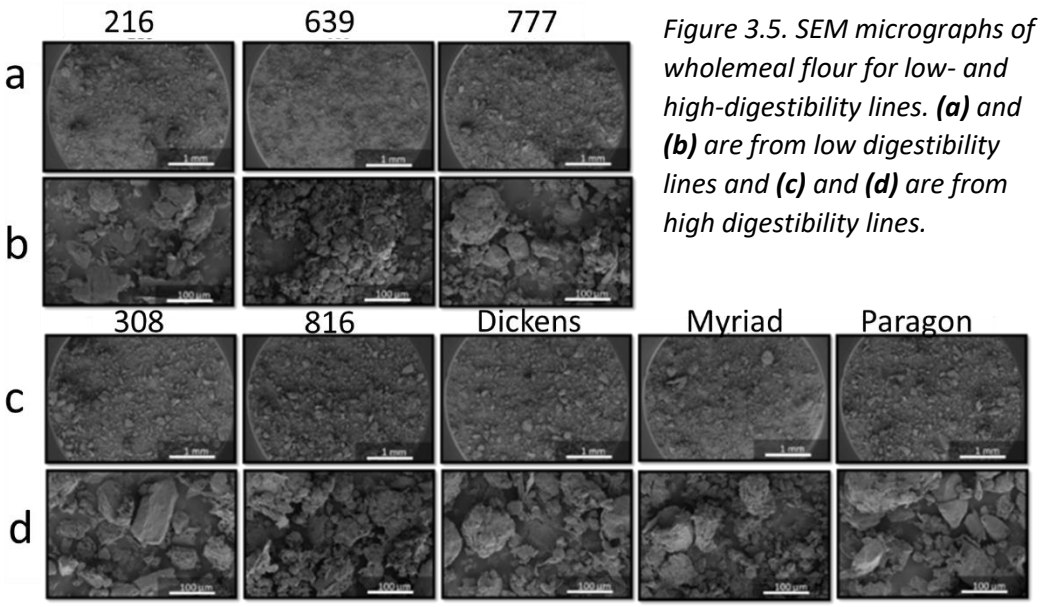

Figure 3.5. SEM micrographs of wholemeal flour for low- and high-digestibility lines. ***(a)*** *and* ***(b)*** *are from low digestibility lines and* ***(c)*** *and* ***(d)*** *are from high digestibility lines.*

3.3.4 Thermal properties of wholemeal flour and starch

Both starch structure and other non-starch components can affect the gelatinisation and retrogradation of starch and, thus, its digestibility profile (Li et al., 2019, Li et al., 2020a, Mohamed and Rayas-Duarte, 2003).

Thermal properties of wholemeal flour measured by DSC were used to examine the relationship between onset, peak temperature and enthalpy of starch with starch digestibility; thermal treatment was applied to mimic the thermal conditions of the starch digestibility assay.

The thermal properties of wholemeal flour samples varied among low- and high-digestibility lines and had associations with starch digestibility profiles. During the first thermal cycle (to mimic gelatinization), the range of onset temperature (54.5 to 58.4^{o}C, $p < 0.001$), peak temperature (62.1 to 65.6^{o}C, $p < 0.001$) and enthalpy (9 to 11.5 J/g, $p < 0.001$) differed among samples significantly (Figure 3.6, 1st cycle, Supplemental Table 3.3). Starch digestibility of low and high lines at 90 min had a

weak correlation to the onset temperature (r = 0.37, ns) and a moderate correlation to the peak temperature (r = 0.50, ns) and enthalpy (r = 0.56, ns), (Supplemental Table 3.2). To analyse the effect of retrogradation on starch structure, samples were cooled and then reheated. The onset temperature (76.4 to 81.3°C, $p < 0.05$), peak temperature (91.7 to 93°C, $p < 0.001$) and enthalpy (6.3 to 10.2 J/g, $p < 0.001$) varied significantly as shown in Figure 3.6 (2nd cycle), (Supplemental Table 3.3). There were strong negative correlations with % starch digested (90 min) and onset temperature (r = -0.77, $p < 0.05$), peak temperature (r = -0.65, ns) and enthalpy (r = -0.73, $p < 0.05$) (Supplemental Table 3.2). Overall, parameters measured in the second heating cycle had the strongest correlations with the starch digestibility of wholemeal flours.

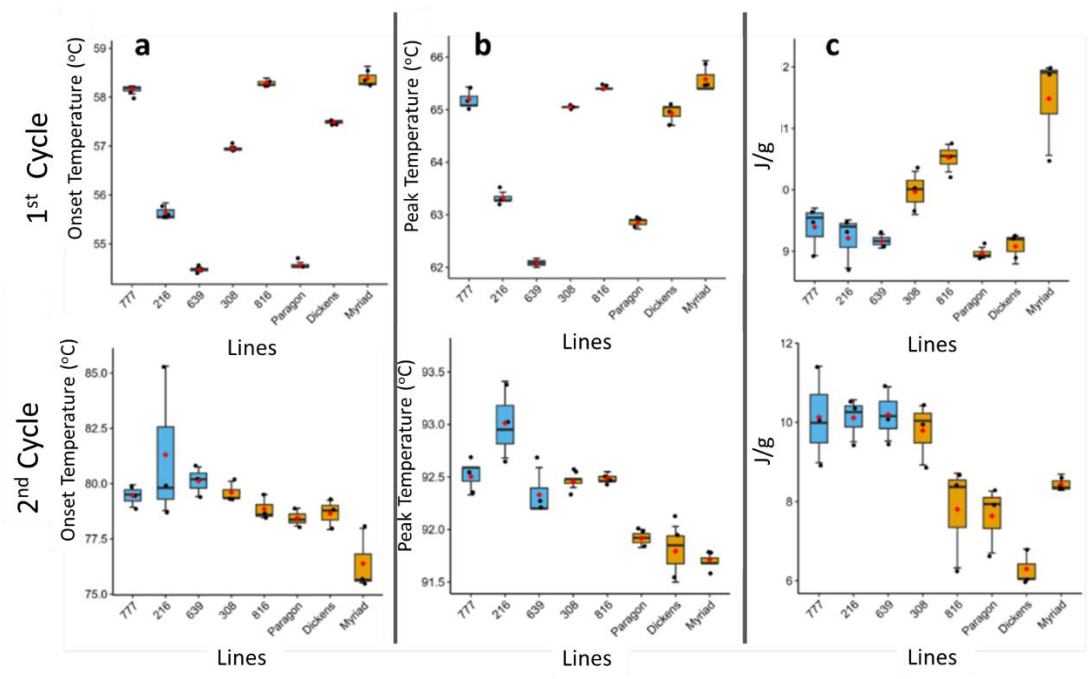

Figure 3.6. DSC parameters measured for wholemeal flour samples of low- (777, 216, 639, shown in blue) and high-digestibility (308, 816, Paragon, Dickens, Myriad, shown in orange) lines. The measurements were conducted using two thermal cycles, and the Onset temperature (a), Peak temperature (b), and Enthalpy (c) were determined, n = 3 technical replicates.

DSC analysis of purified starch was also performed to determine if the thermal properties observed in the wholemeal flour were associated with the starch. Both onset and peak temperatures for purified starch had a strong correlation with those of the wholemeal flour (R^2 = 0.95 and R^2 = 0.97, respectively, Supplemental Figure 3.1), verifying the observed thermal properties were associated with starch.

3.3.5 Protein analysis

The protein content of wholemeal flour from the selected lines differed significantly ($p < 0.001$); low-digestibility lines ranged from 13.97 – 18.53 g/100 flour, and high-digestibility lines ranged from 10.32 – 17.55 g/100 flour. The elite varieties had the lowest protein content ranging from 10.32 to 13.85 g/100 flour (Figure 3.7, Supplemental Table 3.1). Protein content had a moderate negative correlation with the % starch digested in wholemeal flour samples (r = -0.47, ns, at 90 min) and with the TS in wholemeal flour (r = - 0.45 ns) (Supplemental Table 3.2).

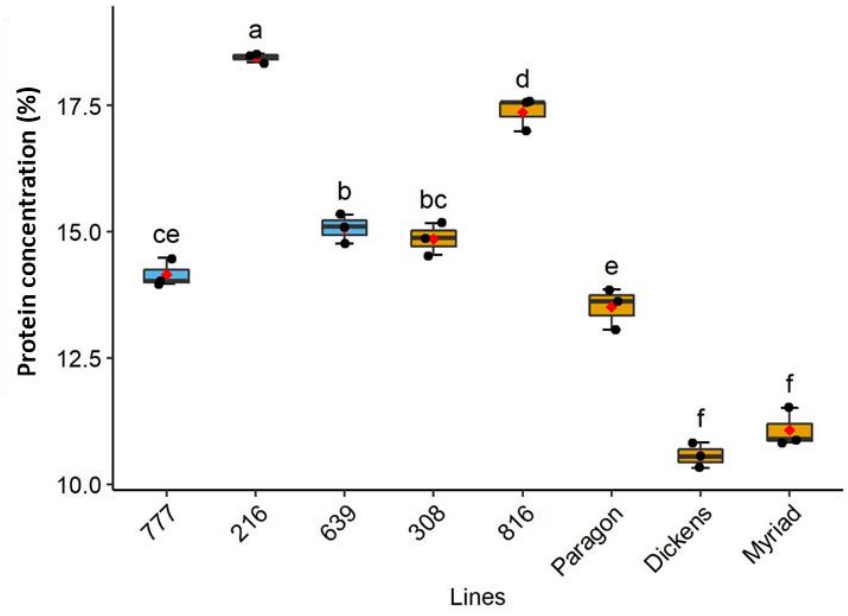

Figure 3.7. Protein analysis on selected wholemeal lines. Low digestibility lines are shown as blue and high as yellow, n = 3 technical replicates.

3.3.6 Starch structure analysis

The molecular structure of the starch can alter starch digestibility. For example, studies have shown that longer glucan chains and larger granule sizes can result in lower starch digestibility (Obadi et al., 2020, SvihusUhlen and Harstad, 2005, Corgneau et al., 2019). In this experiment, starch was isolated from selected lines, and granule sizes and CLD were analysed and compared with starch digestibility.

An examination of the starch isolation efficiency of the wholemeal wheat flour was assessed using optical microscopy (Olympus BX60 Microscope) (Figure 3.8).

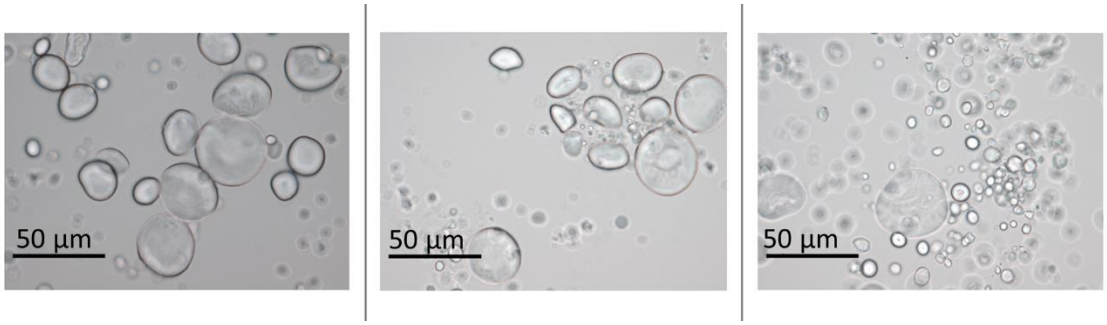

Figure 3.8. Brightfield optical microscopy images of the selected extracted starch samples stained with Sudan. A small amount of each extracted starch sample was transferred to microscopy slides. Drops of water and Sudan dye, a dye that stains lipids, were placed on the starch, and after 2 min, the samples were assessed under bright field light microscopy.

Starch extraction led to a purified starch fraction without significant impurities. Lipids did not appear to be present, as Sudan dye did not stain any material in the samples, and there was no evidence of starch granule damage.

Starch granule size distribution

Granule size distribution of purified starch using a Coulter counter revealed significant variation among starch granule diameter ($p < 0.001$), whereas minor differences were observed for the overall volume of A and B granules (Figure 3.9, Table 3.3, Supplemental Table 3.1). Low-digestibility lines showed the greatest variation in B-granule diameter, with 6 ± 0.1 µm SE for line 777 to 8.4 ± 0.2 µm SE for line 216 (40% greater). The diameter of B-granules in high-digestibility lines varied less; 816 had the highest (6.9 ± 0.2 µm SE), and 308 had the lowest (6.2 ± 0.1 µm SE). B-granule diameter had a negligible correlation with starch digestibility of the wholemeal flour samples (r = 0.23, ns). In general, similar trends were also observed for A-granule diameter, except that low-digestibility line 216 had significantly larger A-granules. The diameter of A-granules from low digestibility lines ranged from 18.2 ± 0.2 µm SE (lines 777 and 639) to 20.1 ± 0.2 µm SE (line 216). There was also significant variation in A-granule diameter among high-digestibility lines; 308 had the smallest (17.7 ± 0.04 µm SE) and Paragon the largest (20.1, ± 0.2 µm SE). A-granule diameter had a negligible correlation with the starch digestibility of the wholemeal flour (r = 0.12, ns). The volume of B-granules (%) showed a little variation for the low- (28.6% - 37.1%) and high-digestibility lines (29% - 35.3%) and had a negligible correlation with starch digestibility of the wholemeal flour (r = -0.01, ns, Supplemental Table 3.2). The same negligible correlation results apply for the A-granule (%) as it is proportional to B-granule (%).

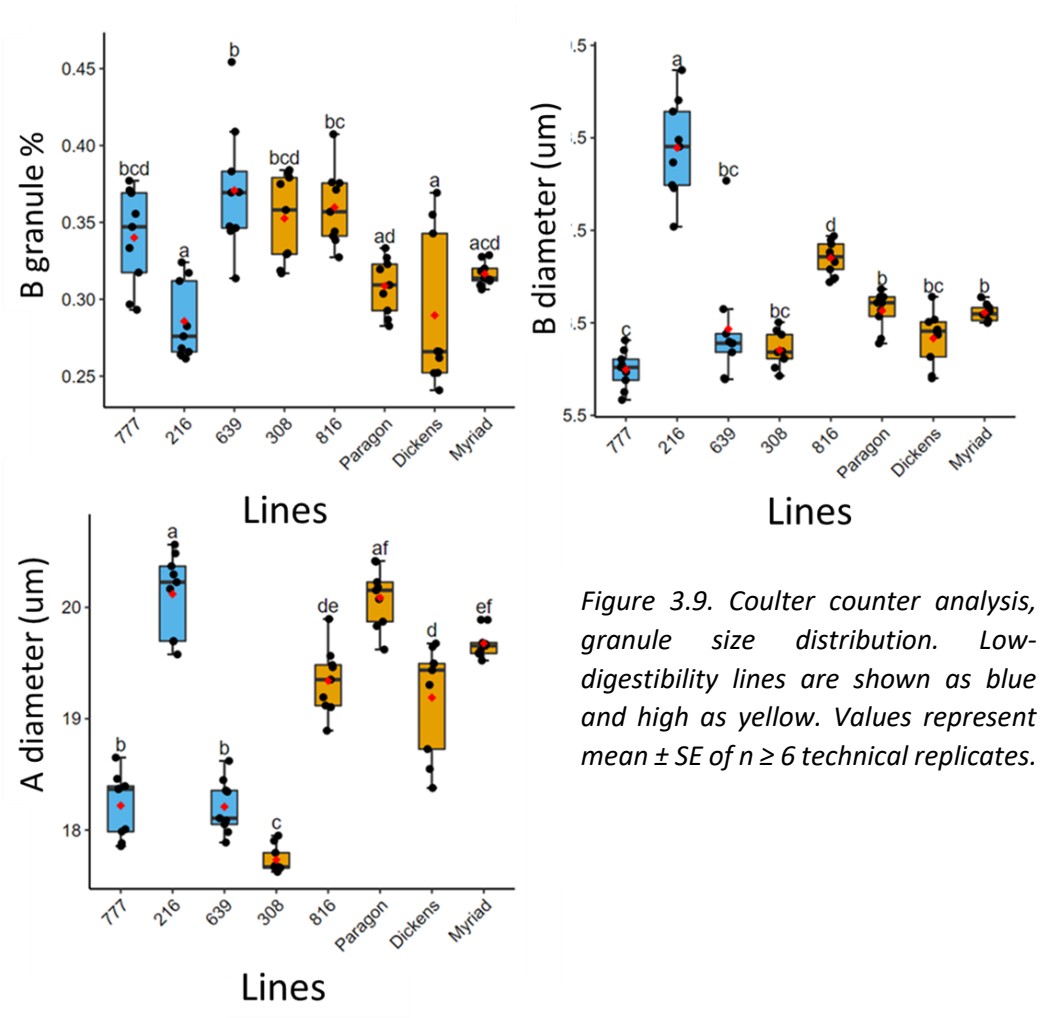

Figure 3.9. Coulter counter analysis, granule size distribution. Low-digestibility lines are shown as blue and high as yellow. Values represent mean ± SE of n ≥ 6 technical replicates.

Table 3.3. Starch granule size distribution of high and low-digestibility lines. The p-value shown derives from the one-way ANOVA. Low refers to the three low-starch digestibility lines (639, 216, and 777). High refers to the five high-starch digestibility lines (Paragon, Myriad, Dickens, 816, and 308).

Selected lines	B granule (%)	p- value	B diameter (µm)	p- value	A diameter (µm)	p value
Low	28.6-37.1	< 0.001	6-8.4	< 0.001	18.2-20.1	< 0.001
High	29-35.3	< 0.001	6.2-6.9	< 0.001	17.7-20.1	< 0.001

Starch chain-length distribution

There were significant differences in the proportion of long and short chains of AP and AM ($p < 0.001$), mainly deriving from Myriad line. No differences were observed in the overall AM:AP ratio (Figure 3.10-3.11, Supplemental Table 3.1). High-digestibility lines varied for AP long:short chains from 0.20 (line 816) to 0.25 (Myriad). Low-digestibility lines had less variation in AP fine structure, ranging from 0.23 (line 639) to 0.26 (line 216). For AM long to short-chain ratios, high-digestibility lines varied from 0.65 (line 816) to 1.16 (Paragon), whereas low digestibility lines varied only slightly from 0.93 (line 777) to 1.10 (line 216). The ratio of AM to AP ranged from 0.26 (line 308) to 0.29 (Myriad) for high-digestibility lines and 0.29 (line 216) to 0.32 (line 632) for the low-digestibility lines. Interestingly, low-digestibility lines appeared to have longer AP chains overall compared to high-digestibility lines.

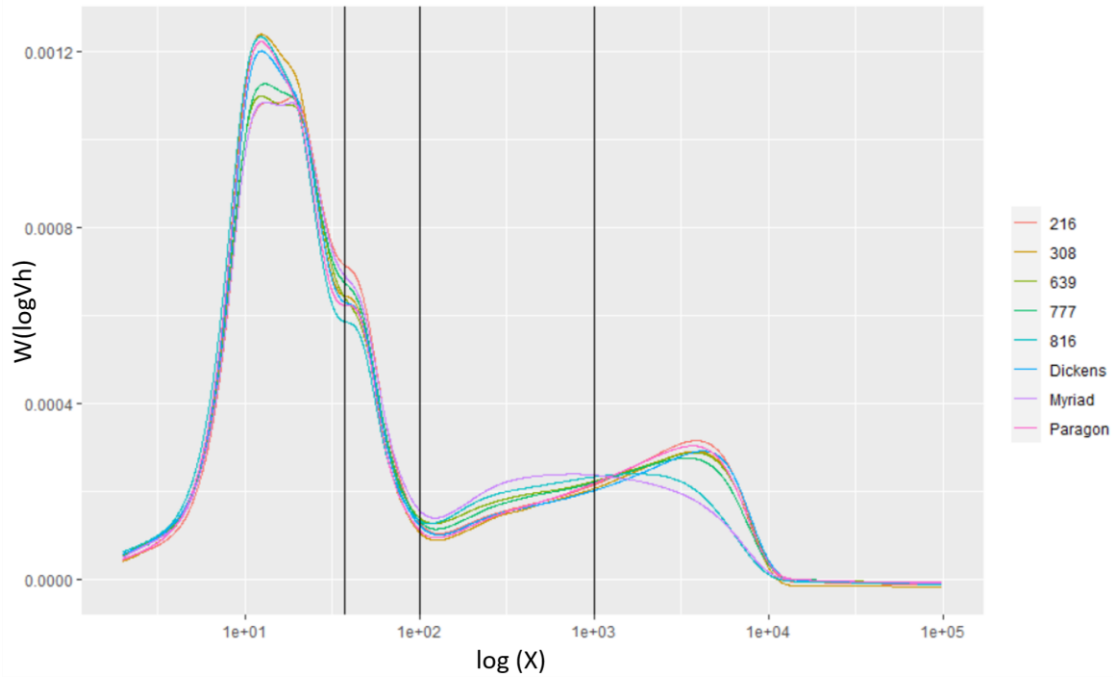

Figure 3.10. CLD of selected wheat lines (low-digestibility lines 216, 777, 639 and high-digestibility lines 308, 816, Dickens, Myriad and Paragon). The y-axis is expressed as wLogVh, whereas the x-axis is the DP and is expressed as log(X), n = 3 technical replicates.

There was a moderate negative correlation of AM/AP ratio and AP long to short-chain ratio to starch digestibility (r = -0.53, ns and r = -0.66, ns, 90 min respectively, Supplemental Table 3.2).

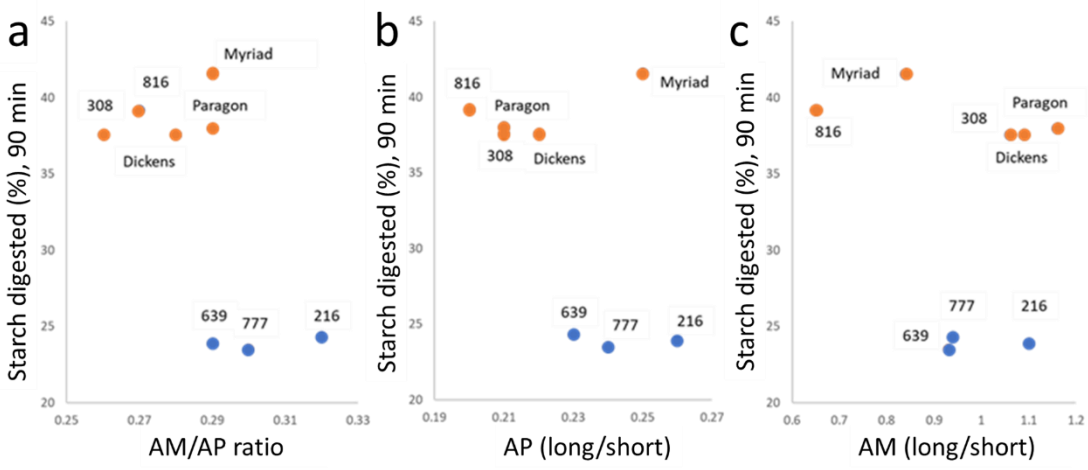

Figure 3.11. Starch digestibility % (90 min timepoint) (y-axis) versus (a) AM/AP ratio, (b) CLD ratios (long/short) of AP, and (c) CLD ratios (long/short) of AM. Low-digestibility lines are shown in blue and high-digestibility lines are shown in orange. Three technical replicates were used and values expressed as mean.

3.4 Discussion

3.4.1 For selected lines, starch properties are not the primary factors affecting digestibility but may contribute to the observed variation.

To gain insight into possible intrinsic and extrinsic factors contributing to variation in starch digestibility, a selection of low and high-digestibility lines was analysed. Starch properties, including starch CLD and granule size distribution, have previously been suggested to influence starch digestibility (Ramadoss et al., 2019).

This study used SEC to determine the starch chain-length distribution of purified debranched starch from low- and high-digestibility lines to identify correlations with starch digestibility data. There was little evidence to suggest that the chain length of glucose polymers explained the differences in starch digestibility and no evidence of starch granule size distribution affecting starch digestibility. In this study, there is limited evidence of a relationship of longer glucose polymer chains, deriving from AM and longer AP chains, to contribute on lowering the starch digestibility of wheat. An exception to that trend was the commercial line Myriad. Although Myriad had longer AP chains, it also had short AM chains, thus making it difficult to draw conclusions.

The high-throughput starch digestibility assay was used to analyse hydrothermally treated wholemeal flour, sieved flour and starch from the selected low- and high-digestibility lines. Interestingly, when starch was purified, a higher extent of digestion was observed, and there were no differences in starch digestibility among selected lines. Considering the analysis of starch structure, there is no compelling evidence that a single starch structural property defines digestibility, but it is possible that starch structure contributes to low-digestibility starch in interactions with other components of the flour matrix. However, it is possible that starch fine structure can influence starch digestibility, when the same assay and thermal treatment was applied to a high amylose starch (39 ± 1.1% apparent AM of TS, mean ± SE) obtained by a reverse genetic approach, the digestion at 90 min was 40.6 ± 1.6%, (Corrado et al., 2022b), shown in Chapter 2 section 2.3.2. In comparison, the lowest digestibility line investigated (line 308, 32 ± 0.01% of AM/AP ratio %) was digested to 46.95 ± 0.93% at 90 min. A different study that compared the starch digestion profiles of 3 wheat lines differing in AM content (26.8%, 34.6% and 63.8% AM content) reported a significant difference between

low, medium and high AM starches when the isolated starch samples were hydrolysed by pancreatic α amylase (Li et al., 2020b).

Overall, this study suggests that reverse genetic approaches may go beyond what is available in natural phenotypic variation. Limited studies have measured starch digestibility in purified starch of wheat landraces, and the current study had a small sample size and 1-year of data. An additional limitation was that the elite lines grew in different years. Therefore, it is suggested that multiple years of more purified starch samples deriving from landraces need to be screened to explore starch digestibility profiles and relation to changes in starch fine structure.

3.4.2 Multiple mechanisms affect starch digestibility

The high-throughput assay included hydrothermal processing of the wholemeal flour samples, which is known to significantly affect the starch digestibility of wheat flour (Corrado et al., 2020) and, in the production of wheat-based foods, is almost inevitable to avoid. DSC was used to detect and record the thermal transitions during the gelatinisation and retrogradation of starch. It was found that parameters measured following a period of retrogradation strongly correlated with the starch digestibility of wholemeal flour. Despite the correlations identified between DSC parameters and starch digestibility, more information is still required to define the factors causing the changes in the thermal properties. One possible example is AM lipid complexes. Several studies have used DSC to identify thermal transitions directly associated with the formation of complexes between lipids and AM and AP molecules, including fatty acids (primarily palmitic and linoleic) and phospholipids (major lipids in cereals, mostly lysophospholipids) (SvihusUhlen and Harstad, 2005, BaldwinMelia and Davies, 1997, Morrison, 1988). The fatty acids and phospholipids favour complex formation with AM due to its higher interior hydrophobicity, caused

by its longer linear chains as well as its lower steric hindrance compared to the highly branched AP molecule (Takato et al., 2017, GurayaKadan and Champagne, 1997, Bertoft et al., 2016, HasjimAi and Jane, 2013). In terms of the digestibility of starch, AM-lipid complexes have been shown to affect its breakdown rate. This is confirmed by several studies that analysed the digestibility rate of starches in different cereals. *In vitro* and *in vivo* studies concluded that AM-lipid complexes in starch decrease digestion rate (Holm et al., 1983, CroweCopeland and Seligman, 2000, Patil et al., 1998, Okumus et al., 2018, SharmaYadav and Ritika, 2008). Quantifying palmitic and linoleic fatty acids in wholemeal flour can be obtained by gas chromatography, as it can separate the individual fatty acids based on their chemical properties. This analysis has not been conducted in this study due the large amount of material needed (generally, a few grams of wheat are needed for this type of analysis (Narducci et al., 2019)), and time restrictions.

In terms of the protein complexes, surface proteins located on the granule surface act similarly to lipids but, due to their increased size and complex structure, are more difficult to form the same complexes as lipids. The non-polar amino acids cause surface proteins to behave as hydrophobic compounds, and when granules are in the presence of water, water compounds favour forming hydrogen bonds with other charged molecules or polar groups and “push away” non-polar compounds. Consequently, this effect decreases the water absorption and swelling of starch and decreases the starch digestibility as less starch will be freely exposed for hydrolysis (DhitalBrennan and Gidley, 2019). Additionally, the surface proteins may act as adsorbed constituents or physical barriers to α-amylase and decrease the starch digestibility (BhattaraiDhital and Gidley, 2016). Thermal processing also negatively affects starch digestibility in the presence of proteins. According to López-Barón et al. (2017), denatured and hydrolysed wheat proteins caused a

significant reduction in *in vitro* wheat starch digestibility. In this study, total protein showed a moderate negative correlation (ns) with starch digestibility of wholemeal flour. However, protein composition analysis was not conducted due to time constraints, which may have led to some limitations in the study. For future analysis SDS-PAGE (Polyacrylamide Gel Electrophoresis) can be used to separate and identify proteins based on their molecular size. SDS gel analysis can be used for the identification of surface starch granule proteins and endosperm proteins, such as puroindolines (approximately 14 kDa) and gliadins (approximately 25-100 kDa) (Gautier et al., 2000, PashaAnjum and Morris, 2010, Kianfar, 2021). Furthermore, the Watkins line 216 exhibited a notably high protein content, making it a promising candidate for further investigation regarding its suitability for bread-making purposes. However, due to the project's specific objectives, this analysis was not pursued at this stage.

Moreover, the use of a smaller number of samples than initially projected may have reduced the overall statistical power of the study, thus limiting the ability to explain the effect of individual factors on starch digestibility. Therefore, to obtain a more comprehensive understanding of the effect of different factors on starch digestibility in complex matrices such as wholemeal flour, a larger sample size of at least 24 or more samples is suggested. Lastly, the Watkins set couldn't be screened with the DSC method due to its low throughput and high sample requirement. For instance, the existing thermal cycles used in the method allowed a throughput of only 3 samples in 2 days. Additionally, for each line, 600mg of flour was required for three replicates which exceeded the available amount.

Although low-digestible lines showed protein content values above the overall average, two high-digestibility Watkins lines had a higher protein content than the Watkins line 777 (low-digestibility line, Figure 3.7), which was the only line that had

not been affected by sieving (sieved flour) to the same extent. This suggests that there might be different factors in the 777 affecting its digestibility compared to the other two low-digestible lines, making it a promising line for future analysis.

It was hypothesised that the presence of high levels of endogenous α-amylase can impact the digestibility of starch, leading to potential misinterpretation of experimental results. In this particular analysis, the levels of endogenous α-amylase were measured in selected lines, and a statistical difference was observed. However, it should be noted that all values remained within the normal range of below 0.2 (Ceralpha Units/g), as established by previous studies (McCleary et al., 2002, Derkx and Mares, 2020) and there was no significant correlation with starch digestibility. Furthermore, a separate study conducted on wheat flour samples from the MAGIC population reported significantly higher levels of endogenous α-amylase, ranging from 3.5 to 12.8 (Ceralpha Units/g) compared to this study. Despite these elevated levels, the study reported only minor effects on starch hydrolysis due to the high levels of endogenous α-amylase (Wang et al., 2022).

The chapter's findings suggest that there are several mechanisms that impact the digestibility of starch, and different factors in each line may influence the starch digestibility of wheat wholemeal flour. Therefore, if multiple interactions of factors affect starch digestibility levels, targeting a single factor may not be the most effective strategy. Instead, selecting based on starch digestibility assays, which can measure the actual digestibility of starch, may be a more appropriate approach.

Chapter 4 Identification of QTL for starch digestibility

4.1 Introduction

Foods with low-digestibility starch can provide health benefits (Jenkins et al., 2002, Wolever and Mehling, 2002). However, breeding for low-digestibility starch in crops has been challenging due to several genes controlling this trait of interest. A number of efforts have been made in recent years to identify candidate genes affecting starch digestibility. For example, studies using reverse genetic approaches have shown the potential for increasing RS levels in cereal crops through modifications of the starch biosynthesis pathway (Hazard et al., 2014, Fahy et al., 2022, Yang et al., 2006, Shu et al., 2009). The primary approach has involved downregulating key SSs and starch SBEs to alter the starch structure and reduce its digestibility. Most research so far has attempted to increase RS by reducing SBE activity. There is good evidence from limited trials in various crops, including wheat, that reducing the activity of SBEII genes is effective at increasing the AM: AP ratio of starch, which is associated with increased RS. For example, durum wheat and bread wheat have shown up to 10-fold increases in RS in genotypes that carry a mutation in *SBEIIa* and *SBEIIb* genes (Hazard et al., 2014, Schönhofen et al., 2016, Hazard et al., 2015). However, initial analyses of these lines showed adverse effects on crop performance in the field and on pasta and bread-making quality. Thus, it is not yet clear whether it will be possible to use *sbeII* mutants to develop wheat lines that have both increased RS and good agronomic and end-use functionality characteristics. Similarly, mutants for SSIIa have led to more RS, but adverse effects

on starch accumulation may limit use for applications in breeding (Schoen et al., 2021).

An alternative to a mutagenesis approach is forward screening, which can be used to identify genetic loci based on existing natural variation of a trait. Crude screens for AM content have proven useful for identifying RS in other cereals, but these fail to identify other variations in wheat grains that may contribute to resistance to digestive enzymes (NakamuraSatoh and Ohtsubo, 2015). Recent improvements in *in vitro* models of starch digestibility have shown potential for rapid prediction of glycaemic response and are likely to be useful in early-stage product development (Edwards et al., 2019). Therefore, selecting an *in vitro* starch digestibility assay for a forward screening approach opens the possibility of discovering new genes influencing this trait of interest. QTL analysis is a well-accepted method in crop research for identifying genomic regions associated with a trait of interest (phenotype). More specifically, the principle of a QTL analysis involves the development of a mapping population, a population derived crossing two or more parents that differ in one or more traits of interest. Using DNA markers, this population is genotyped, and the marker scores are then used to construct a linkage map in which the genome is separated into different genetic linkage groups, representing the chromosomes, and the genetic markers are ordered along those linkage groups. Then, measured phenotypic data (the trait of interest) of the mapping population is used in conjunction with the genotypic data of the same population, and the associations between marker scores and phenotype are computed. The significant associations indicate which DNA markers are linked to a QTL controlling the trait of interest (Young, 1996, Tanksley, 1993). Linked DNA markers may then be used in plant breeding programs as molecular tools for MAS to introgress the QTL into other elite backgrounds (Ribaut and Hoisington, 1998).

This study aimed to investigate natural phenotypic variation in starch digestibility as a tool for future breeding programs. Previous chapters of this thesis have shown evidence of wide variation in the Watkins collection for starch digestibility compared to selected elite wheat varieties.

Summary of the experiments

The objective of this chapter is to identify a stable low-digestibility starch line over multiple years and investigate the genetic factors underlying this trait using QTL analysis. To accomplish this objective, selected Watkins lines from four-year field trials were screened for starch digestibility and TS (Figure 4.1 and Table 4.1). Then a biparental population, generated previously, was grown, including the selected low digestibility line, and a QTL analysis on starch digestibility, TS and grain characteristics, measured by NIR and Marvin analysis, was conducted to identify potential loci that control starch digestibility.

Figure 4.1. Chapter 4 Experimental design. Selecting a low digestibility line by screening the starch digestibility and TS of 4-year field trials on selected Watkins. Screening the Paragon x 777 on grain characteristics, starch digestibility and TS and conducting a QTL analysis.

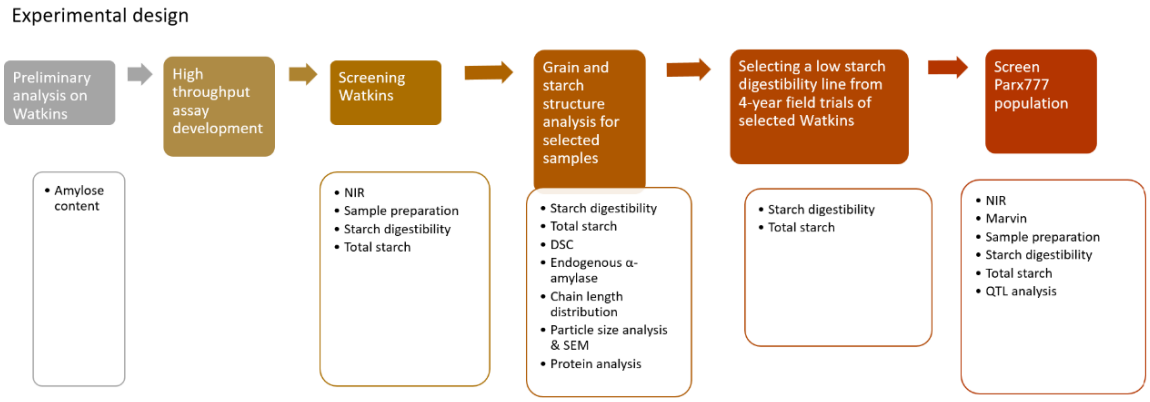

Table 4.1. Germplasm used and analysis in Chapter 4.

Germplasm	Year grown	Number of lines	Field trial location	Plot size (m^2)	Material used	Analysis	Provided by
Watkins	2010	26	Barn Field, Norfolk, UK	1	White flour	Starch digestibility, TS	Dr. Alison Lovegrove
	2012	28	Coopers Field, Norfolk, UK	6	White flour	Starch digestibility, TS	Dr. Alison Lovegrove
	2013	28	Bylands, Yorkshire, UK	1	White flour	Starch digestibility, TS	Dr. Alison Lovegrove
	2014	21	Coopers Field, Norfolk, UK	1	White flour	Starch digestibility, TS	Dr. Alison Lovegrove
Paragon x W777 Nested Association Mapping (NAM) population	2020	96	Church Farm, Norfolk UK	1	Grains	NIR, Marvin	Dr. Simon Griffiths
					Whole meal flour	Starch digestibility, TS, QTL analysis	
Required amount per sample							
NIR	15-30 gr						
Marvin	15-30 gr						
Starch digestibility	5-10 mg						
TS	5-10 mg						

4.2 Materials and methods

4.2.1 Plant material

Dr Alison Lovegrove (Rothamsted Research) provided white flour samples (prepared using a Chopin CD1 mill, KPM UK) from the genetically diverse Watkins core set of 118 lines previously showing variation in AX content (Wingen et al., 2014, Shewry et al., 2015) grown in four different years (Table 1.3). The following bread wheat lines were obtained from the GRU: Paragon and 28 Watkins accession numbers (1190007, 1190042, 1190092, 1190103, 1190141, 1190145, 1190231, 1190281, 1190291, 1190444, 1190471, 1190475, 1190551, 1190560, 1190627, 1190629, 1190639, 1190671, 1190680, 1190694, 1190704, 1190705, 1190746, 1190747, 1190777, 1190788, 1190789, 1190816), (Supplemental Table 2.1). The accession details are provided at https://www.seedstor.ac.uk/search-browseaccessions.php. In order to simplify the nomenclature, the accessions in this thesis excluded the use of the 1190 since it was repeated in all Watkins lines utilized. Consequently, throughout this thesis only the last three digits were used

to represent each accession (e.g., 1190777 is denoted as 777). The selected Watkins lines had been sown in autumn in $1m^2$ plots at Barn Field, Church Farm in Bawburgh, Norfolk, UK, for the year 2010, $6m^2$ plots at Copers Field, Church Farm in Bawburgh, Norfolk, UK, for the year 2012, $1m^2$ plots at Bylands, Yorkshire, UK, for the year 2013 and $1m^2$ plots in autumn at Copers Field, Church Farm in Bawburgh, Norfolk, UK, for the year 2014 (Supplemental Table 2.1 and Figure 2.1).

4.2.2 Field trial and awn scoring

The Paragon x Watkins 1190777 (Paragon x 777) population, 94 recombinant inbred lines (RILs) (F4 generation by single seed descent approach) was provided by the Simon Griffiths' group, JIC. Seeds of the population were sown in 1 m^2 plots in autumn 2020 at Church Farm, Norfolk UK (52°37'49.2"N 1°10'40.2"E) and grown using standard agronomic practices (low nitrogen treatment was applied to prevent lodging, 40kg/ha nitrogen fertiliser) (Wingen et al., 2017). RILs were grown in triplicates in a randomized block design, and Paragon, 777, and Soissons were used as control lines for the field screening and grain and flour analysis. The presence and absence of awns was noted before harvest to verify the field trial layout. The field trial layout is provided in Supplemental Figure 4.1.

4.2.3 Seed analysis

Grain protein content, starch content, NDF content, and hardness were measured using a Near Infrared Reflectance (NIR) Instrument (DA 7250 At-line), and grains were measured on the rotating cup attachment. Three biological reps were used

for each RIL of Paragon x 777 population and 14 and 11 biological replicates for Paragon and 777 respectively.

Thousand-grain weight, width area, and length area parameters were measured using a seed analyser (MARViN ProLine seed analyser, MARViNTECH). For the screening, the grain weights of each sample were measured using a scale, and the seed analyser was used to calculate the length and width area of the grains using a camera. The seed analyser also associated the number of grains with their weight, providing the thousand-grain weight.

For the seed analysis three biological replicates were used for each RIL of Paragon x 777population and 14 and 11 biological replicates for Paragon and 777 respectively.

4.2.4 Milling and sieving

All grain samples obtained from the field trial in 2020 (Paragon x 777) were dehusked and coarsely milled in a cyclone mill (UDY Corporation). Milled samples were then passed through a 0.3 mm sieve to produce wholemeal flour samples. The flour was kept in a vacuum desiccator for five days before analysis.

4.2.5 Endogenous α-amylase

Endogenous α-amylase (Ceralpha Method, Megazyme, Bray, IE) was carried out on white flour from selected Watkins lines of 4 field trials and wholemeal flour of Paragon x 777 population following the protocol from Chapter 3, section 3.2.6. Samples were measured in three technical replicates for white flour samples and in three biological replicates for wholemeal flour sample.

4.2.6 Total starch estimation of white and wholemeal flour

TS assay (HK) was carried out on white flour from selected Watkins lines of 4 field trials and wholemeal flour of Paragon x 777 population following the protocol from Chapter 2, section 2.2.7. Samples were measured in three technical replicates for white flour samples and in three biological replicates for wholemeal flour samples.

4.2.7 High-throughput *in vitro* starch digestion assay

Starch digestion assays were carried out on gelatinised samples and allowed to retrograde following the protocol from Chapter 2.2.6, with a modification of the sample (wholemeal flour) weight to 11 mg ± 5%. Samples were measured in three technical replicates for white flour samples (selected Watkins lines of 4 field trials) and in three biological replicates for wholemeal flour samples (Paragon x 777 population).

4.2.8 Markers and mapping

The genetic mapping and script for the QTL analysis for the Paragon x 777 population was provided by Dr Luzie Wingen (JIC Research Assistant). All steps were conducted in the R software suite (v. 3.6.1). In total, 3866 markers were used to generate a genetic map of the Paragon x 777 population. Of the 3866, 3630 were derived from the Axiom 44266 genotyping array developed by Bristol University, and 236 were run as individual KASP assays (Wingen et al., 2017). The linkage map was generated using ASMap (v. 1.0-4) using a p-value of 10^{-12} to define linkage groups as this threshold resulted in an ideal distribution of markers into the

chromosomes (Taylor and Butler, 2017). In the second round of genetic mapping, linkage groups derived from the same chromosome were attempted to be joined up using a p-value of 10^{-3}. Pictures of the genetic maps were plotted using package "LinkageMapView" (v. 2.1.2) (Ouellette et al., 2018). QTL detection was performed using package “qtl” (v. 1.44–9) (Broman et al., 2003) in two steps; the first scan determining co-factors and the second scan identifying robust QTL, taking the co-factors into account. To ensure consistency, the QTL analysis was executed three times, and repeatedly detected QTL were selected for this thesis.

4.2.9 Data analysis

Statistical analyses and graphs were obtained with R (R version 4.2.1). Datasets were curated using the package *nlme* (v 3.1-157) for the non-linear regression model to estimate C_∞ and *k* (eq 3), where the C_∞ describes the extent of digestion, and the *k* describes the natural logarithm of the rate of digestion.

$$Ct = C_\infty \left(1 - e^{-(e^k)t}\right) \text{ (eq 3)}$$

Plots were obtained using the *ggplot2* package (v 3.3.6) (Pinheiro et al., 2022, Wickham, 2016). A mixed-effect model fit by restricted maximum likelihood (REML) was used to model the effect of year on starch digestibility and TS, which estimated the parameters in a linear mixed-effect model. These parameters can be determined using the functions of the lme4 (v 1.1-30) and lmerTest (v 3.1-3) packages, in which the year was set as a fixed effect and lines as a random effect (Kunzetsova et al., 2017, Bates et al., 2015). Tests for equality of variances across groups were obtained using Levene’s and Bartlett’s tests. Further details of data analysis and statistical tests are described for each experiment in the results

section. One-way ANOVA was used for the analysis of starch digestibility, TS, grain composition and Marvin analysis; a p-value < 0.05 was adopted for statistical significance. All values reported represent the mean ± SE of three technical or biological replicates (stated in the corresponding figure) unless stated otherwise in the description of the corresponding figure and supplemental datasets. For boxplot graphs, red points represent the average and black horizontal lines represent the median.

4.3 Results

4.3.1 Selection of a low-digestibility line

The following experiments aimed to identify a stable low-digestibility line which had an appropriate established biparental population available for QTL analysis (Wingen et al., 2017). In this experiment, white flour samples from 28 wheat lines, each grown in four field trials (9 lines were grown in three trials only) of the genetically diverse Watkins set, which had previously shown variation in AX content were used (Shewry et al., 2015). These lines were analysed for starch digestibility *in vitro* and starch content. Starch digestibility data was used to select a stable low-digestibility starch line.

Starch digestibility of white flour from Watkins lines

The starch digestibility data was fitted to a non-linear regression model and expressed as C infinity (C_∞) and *k* in order to analyse the effect of year and line on starch digestibility and select a line based on these two parameters.

By visual inspection, the model fits the observed data well (Figure 4.2). There were only a few cases where the model slightly underestimated the asymptote. Due to the good fit of the model, the C_∞ and *k* parameters were taken forward into subsequent analysis instead of individual time points.

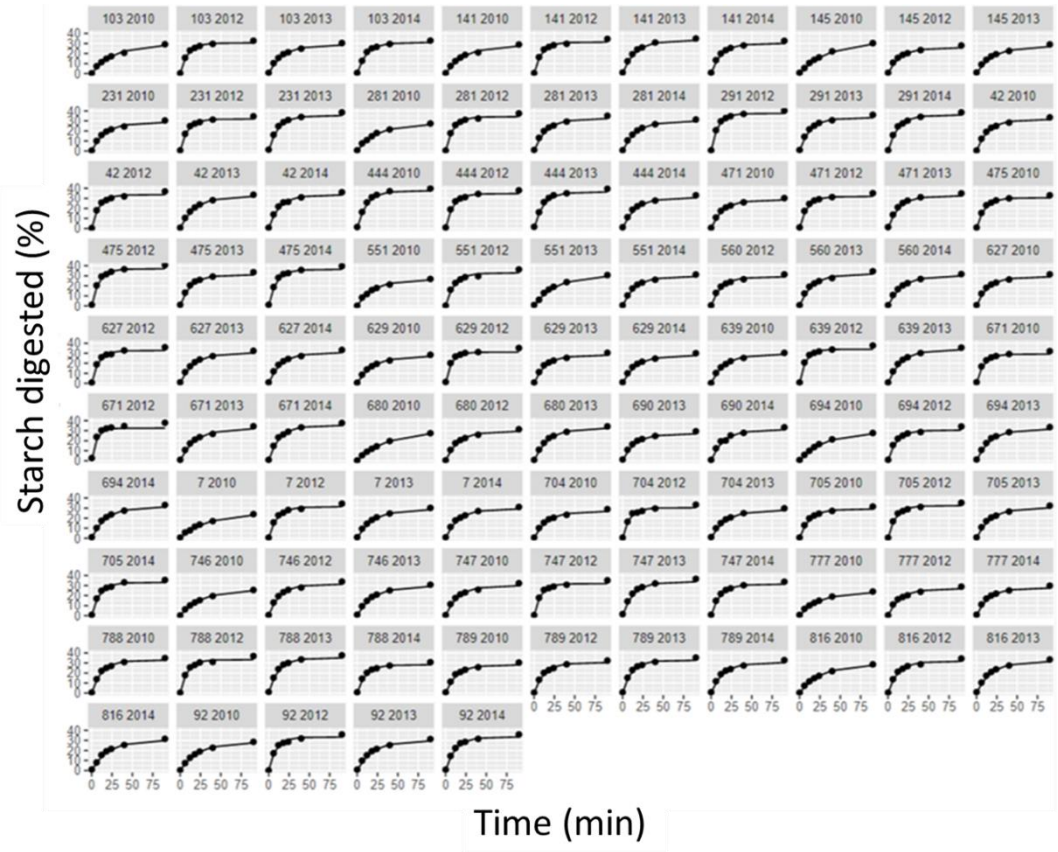

Figure 4.2. Non-linear model fitting of starch digestibility in vitro of white flour from four years' trials of selected Watkins lines from 2010, 2012, 2013, and 2014. The activity of pancreatic α-amylase was set to 2U/mL. Data has been fitted to a non-linear model. Values represent the mean of n = 3 technical replicates.

In terms of the effect of the environment (year), there was a significant difference between all years against the intercept ($p < 0.001$) for the C_∞ (Figure 4.3, Supplemental Table 4.1); the average difference between the years 2012 and 2010 (intercept) was 3.04 ± 0.54% C_∞, mean ± SE, whereas 2013 and 2014 had a difference of 2.48 ± 0.54% C_∞, and 2.28 ± 0.58% C_∞. A further test was applied to identify whether there was any evidence that the variation around the year mean differed by line, that is whether or not some lines were more variable than others, given a correction for the year mean. Levene's tests and Bartlett's tests for equality of variances across groups were used and showed no significant effect of line on starch digestibility. Therefore, there is no strong evidence that some lines are more or less affected by year than others.

k also differed significantly depending on the year, with some years having a stronger effect on the rate of digestion than others. For example, the 2012 year differed by an estimate of 0.64 ± 0.06 *k*, mean ± SE, $p < 0.01$ to year 2010 (intercept), whereas 2013 and 2014 differed by an estimate of 0.15 ± 0.06 *k*, $p < 0.05$ and 0.28 ± 0.06 *k*, $p < 0.01$ accordingly. Bartlett's and Levene's tests did not show any evidence of a difference in variances across lines. Therefore, similar to the C_∞ results, there is no strong evidence that some lines are more or less affected by year than others.

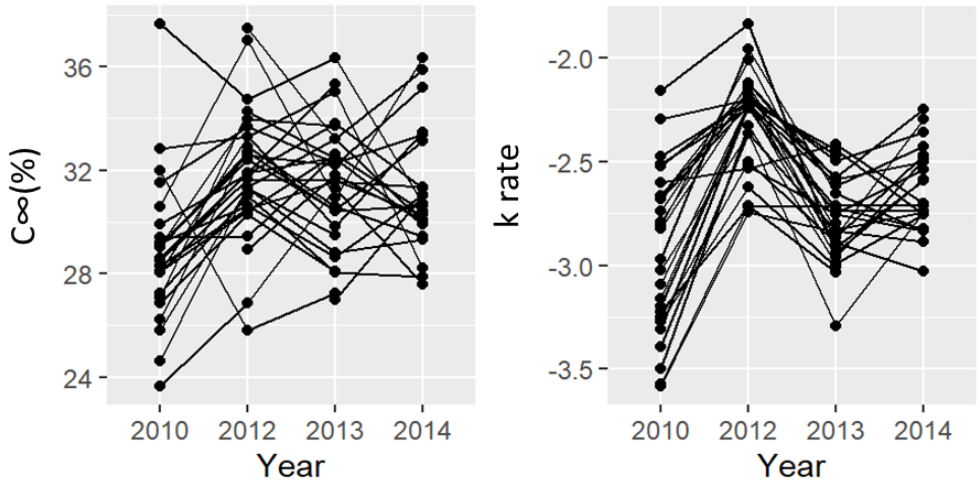

Figure 4.3. Starch digestibility of white flour samples of selected Watkins lines from 2010 (26 lines), 2012 (28 lines), 2013 (28 lines), and 2014 (21 lines). The activity of pancreatic α-amylase was set to 2U/mL. Data has been fitted to a non-linear model and expressed as C_∞ (left) and k (right). Values represent the mean of n = 3 technical replicates.

Lines were statistically different in the extent of digestion (C_∞, $p < 0.001$), whereas no statistical difference was observed in the rate of digestion *k* (Supplemental Table 4.1). The analysed Watkins lines varied from a mean of 26.5 to 36.3% over all years (Figure 4.4). The 777 line showed the lowest digestibility, and W291 was the highest. Additionally, 777 showed a lower mean for the years 2010 (28.8% C_∞), 2012 (31.9% C_∞) and 2014 (31.1% C_∞), with values of 24% C_∞, 27.2% C_∞ and 28.3% C_∞ for the mentioned years. 777 (2013) was excluded from all the analysis of starch digestibility due to its high endogenous α-amylase content (0.68 Ceralpha Units/g flour, mean, Supplemental Figure 4.2), suggesting potential poor growing or storage conditions. The findings from the analysis of three years of white flour and one year of wholemeal flour samples led to the selection of Watkins 777 as a low-digestibility line for further investigation. This particular line showed consistently low levels of starch digestibility across the years studied, making it a promising

candidate for further study. Therefore, an existing mapping population with Paragon was chosen for field trials to conduct a QTL analysis.

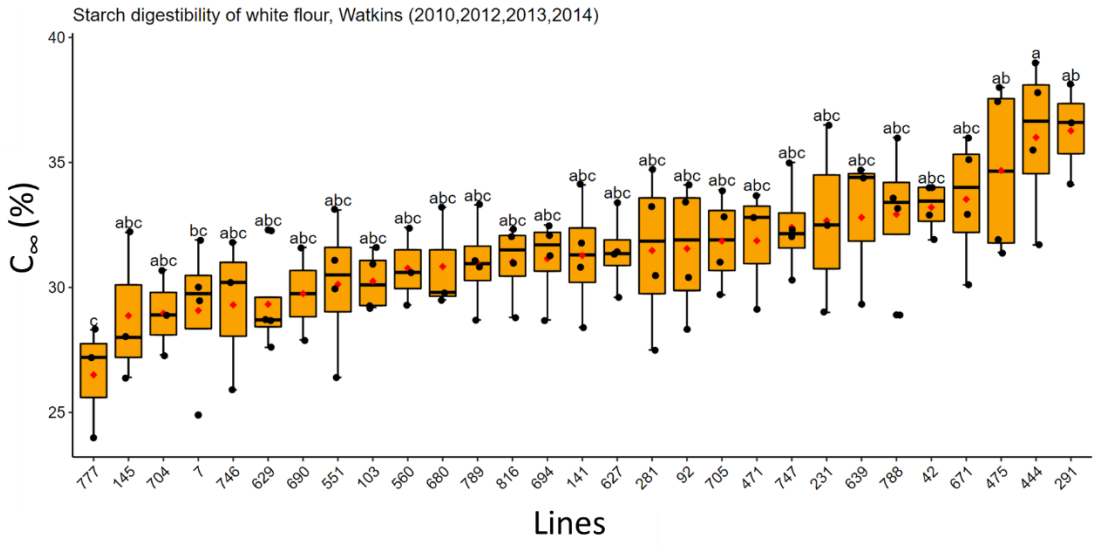

Figure 4.4. Starch digestibility in vitro of white flour of selected Watkins lines from 2010 (26 lines), 2012 (28 lines), 2013 (27 lines), and 2014 (21 lines). Data has been fitted to a non-linear model and expressed as C_∞. Black dots represent the mean of n = 3 technical replicates.

Total starch of white flour from Watkins lines

The starch content of each line was used as a TS percentage in the starch digestibility assay to obtain the starch digested % values.

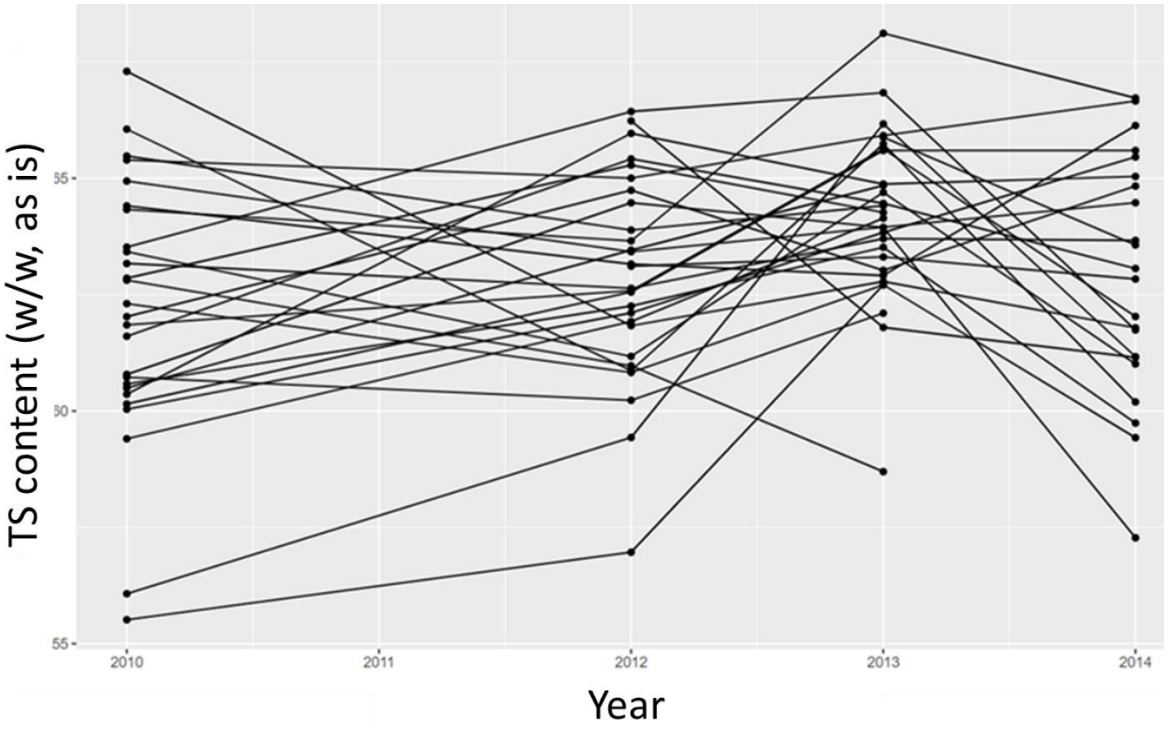

Figure 4.5. TS content of 4 years of selected Watkins lines from 2010 (26 lines), 2012 (28 lines), 2013 (28 lines), and 2014 (21 lines). Values represent the mean of n = 3 technical replicates.

The TS assay revealed a significant difference among the analysed white flour samples ($p < 0.005$) (Figure 4.5, Supplemental Table 4.2). More specifically, starch content varied from 55.5 to 67.3 (g/100 flour, mean) for samples from the 2010 trial, from 57 to 66.4 (g/100 flour) for samples from the 2012 trial, from 58.7 to 68.13 (g/100 flour) for samples from the 2013 trial and from 57.3 to 66.73 (g/100 flour) for samples from the 2014 trial. According to the mixed-effect model, there was a statistically significant difference between the years 2013 and 2010 ($p < 0.001$). However, a small difference has been observed between the year 2013 and the intercept (2010) (the average difference is 1.98 ± 0.56 TS content (g/100 flour, mean, ± SE). Bartlett's and Levene's tests (tests for homogeneity of variances) showed no evidence of a difference in variances across lines. Therefore, there is no strong evidence that some lines are more or less affected by year than others.

However, there were limitations to this experiment as one biological replicate was used for each individual line per year.

4.3.2 Field trial verification of Paragon x 777 population

A field trial check was conducted to confirm the correct drilling of the Paragon x 777 trial. A QTL analysis on the presence and absence of awns was conducted with the expectation that the genetic location of the awn-inhibitor gene on chromosome 5A would be determined.

The parent 777 presents long awns, whereas Paragon is awnless (Figure 4.6.A). Therefore, phenotypic data (awn scoring) was used for a QTL analysis to verify the field position of the RILs. QTL analysis on awns is a high-confidence field trial test. This is due to the distribution of the bimodal data and its already discovered QTL on 5A chromosome (Kato et al., 1998). Genetic analysis showed the Paragon x 777 population to have a strong QTL for the presence of awns on chromosome 5A (Figure 4.6.B). More specifically, QTL on the 5A chromosome at marker AX-643813024.5A explained 75.2% of the variability, and the increasing effect came from 777. According to the awn scores, the RIL(s) and parents' position in the field experiment verified the QTL on chromosome 5 (AX-643813024.5A), which agreed with the awn inhibitor locus identified in the 5A chromosome (LOD score = 15).

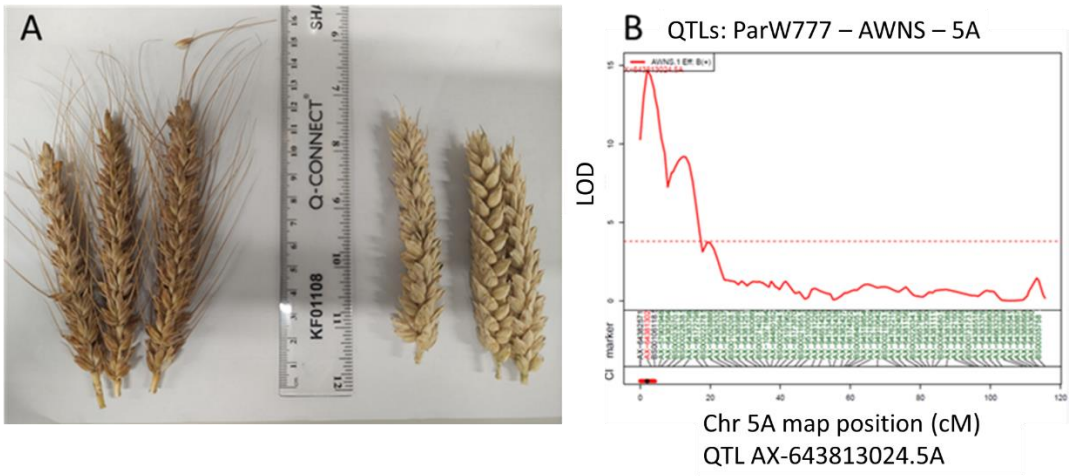

Figure 4.6. (A) Presence and absence of awns in 777 (left) and Paragon (right). (B) Awn presence QTL on chromosome 5 (AX-643813024.5A).

4.3.3 Screening the mapping population Paragon x 777 for starch digestibility

The following experiments aimed to discover the variation in starch digestibility of the biparental population for QTL analysis.

Starch digestibility of wholemeal flour of Paragon x 777 population

The wholemeal flour starch digestibility profiles differed significantly among the Paragon x 777 population at all timepoints ($p < 0.001$) (Figure 4.7, Supplemental Table 4.3). RILs differed for the 4 min timepoint between 4-15.6% starch digested, 6-26% for 8 min, 9.9-29.7% for 12 min, 9.2-31.2% for 16 min, 16.2-36.3% for 40 min and 19.9-39.4% starch digested for 90 min (Table 4.2). The mean value of the variation was 9.1% for the 4 min, 14.7% for 8 min, 19.4% for 12 min, 20.5% for 16 min, 26.4% for 40 min and 31% starch digested for 90 min. For the parents, there was a statistically significant difference in their starch digestibility profile at all time

points ($p < 0.001$). Watkins 777 had an average of 9.2% ± 0.6, 14.4% ± 1 ,18% ± 1.1, 19.8% ± 1, 25.6% ± 0.8, 30.1% ± 0.9 of starch digested, mean ± SE, whereas Paragon had an average of 13.9%, 22.2%,26.7%, 27.7%, 32.8%, 36.7% of starch digested, for the 4, 8, 12, 16, 40 and 90 min respectively.

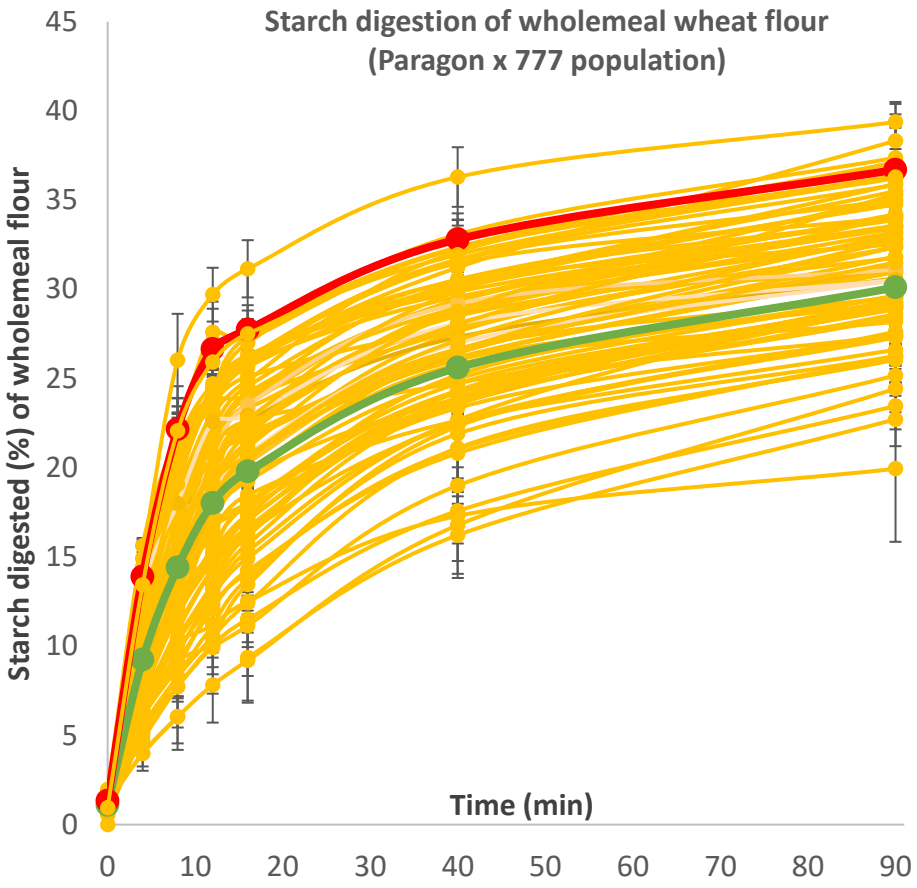

Figure 4.7. Starch digestibility of the Paragon x 777 population at six time points (4-90 minutes). The activity of pancreatic α-amylase was set to 2U/mL. Paragon is shown in red, and the 777 line is shown in green. RILs n = 3 biological replicates and Paragon and 777 n = 8 biological replicates.

Table 4.2. Starch digestibility of Paragon x 777 population. The p-value shown derives from the one-way ANOVA. The RILs are shown by the range of minimum and maximum values and the parental lines (777 and Paragon) are shown as the mean values.

Timepoint (min)	iD	Starch digested (%)	p-value
4	777	9.2	< 0.001
	Paragon	13.9	
	RILs	4-15.6	< 0.001
8	777	14.4	< 0.001
	Paragon	22.2	
	RILs	6-26	< 0.001
12	777	18	< 0.001
	Paragon	26.7	
	RILs	9.9-29.7	< 0.001
16	777	19.8	< 0.001
	Paragon	27.7	
	RILs	9.2-31.2	< 0.001
40	777	25.6	< 0.001
	Paragon	32.8	
	RILs	16.2-36.3	< 0.001
90	777	30.1	< 0.001
	Paragon	36.7	
	RILs	19.9-39.4	< 0.001

Starch digestibility data for the 90 min timepoint had a negligible correlation with protein content, starch content, NDF content, hardness, width grain area, length grain area and thousand-grain weight (TGW). None of the above factors could explain individually the variation in starch digestibility observed (Table 4.3).

Table 4.3. Pearson correlation of starch digestibility % (90 min) and flour and grain parameters.

Parameters	r	p-value
Protein dry basis %	0.11	ns
Starch dry basis %	-0.06	ns
NDF dry basis %	0.32	ns
Hardness	0.15	ns
Width grain area	-0.05	ns
Length grain area	-0.26	ns
TGW	-0.20	ns
Starch (HK method)	-0.21	ns

Total starch of wholemeal flour of Paragon x 777 Population

The starch content of the sieved (< 0.3mm) whole wheat flour differed significantly ($p < 0.001$) among the biparental population (Figure 4.8, Supplemental Table 4.3). Recombinant lines varied in starch content from 52.1 to 61.9 (g/100 flour), and the mean value of the variation was 57.6 (g/100 flour). For the parents, there was a statistically significant difference in their starch content ($p < 0.05$). More specifically, Paragon had an average of 60.7 ± 1.02 g/100 flour, mean ± SE, placing it on the high end of the variation, whereas 777 had an average of 56.8 ± 0.84 g/100 flour, placing it on the low end of the variation.

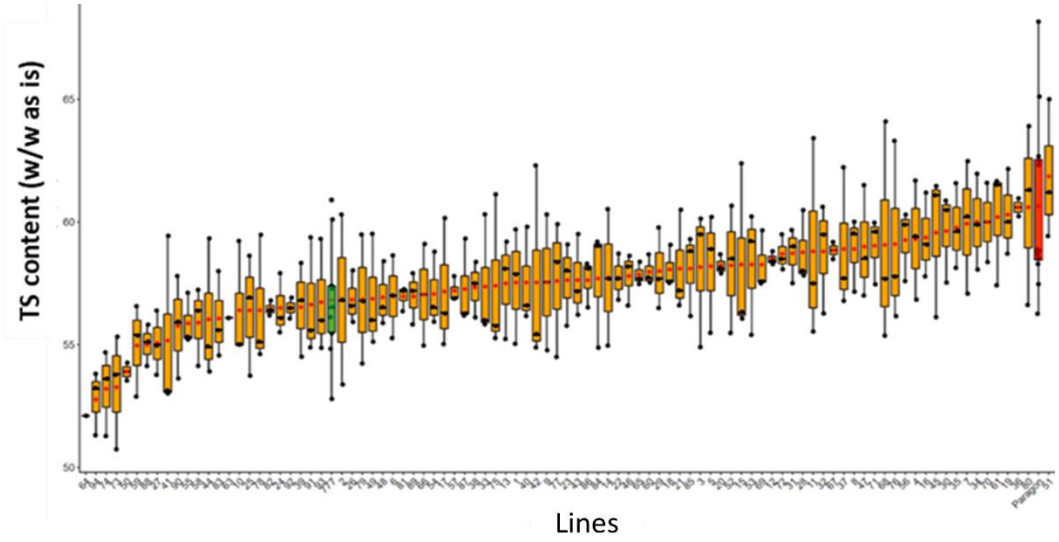

Figure 4.8. TS content (g/100 flour) of the Paragon x 777 population ordered from lowest to highest. Paragon is shown in red, and 777 line is shown in green. RILs n = 3 biological replicates and Paragon and 777 n = 8 biological replicates.

4.3.4 QTL analysis

In this study, a QTL analysis was conducted to explore the genetic association of starch digestibility in wheat. The analysis revealed the presence of 5 QTL associated with starch digestibility in wheat. These QTL were located on chromosomes 2A (QTL from timepoints 4, 8 and 40 min overlapped), 2B, 4A, 3B and 6A (QTL from timepoints 8 and 12 min overlapped), and QTL were identified using individual time points of the digestibility analysis (starch digested % in 4, 8, 12, 16, 40 and 90 min) (Table 4.4 and Figure 4.9).

Further analysis using one-way ANOVA and Tukey post hoc analysis demonstrated statistically significant differences between the RILs carrying the increasing and decreasing alleles for the 4A (BS000228161) and 6A (AX-643859306) QTL (Figures 4.9-4.38, Table 4.5). Specifically, RILs carrying the decreasing allele for the 4A QTL had a statistically lower starch digestibility at 8 min (13.1% vs. 16.5%) and 16 min

(18.8% vs. 22.5%) compared to RILs carrying the increasing allele. Similarly, RILs carrying the decreasing allele for the 6A QTL displayed significant differences in starch digestion percentages at all timepoints except for 90 min, with values of 8% vs. 10%, 12.7% vs. 16.2%, 16.2% vs. 20.1%, 18.4% vs. 22%, and 24.6% vs. 22% for the timepoints 4, 8, 12, 16, and 40 min, respectively.

Among all timepoints, the 16 min timepoint exhibited the highest variation explained, accounting for 37.6% of the observed variation (Figure 4.10). Additionally, the 16 min time point had the highest differences in starch digested compared to other time points.

Combining multiple QTL did not show a statistical difference compared to individual QTL; however, the average starch digestion was lower in combining multiple QTL (Figure 4.10, Table 4.5 and Supplemental Figures 4.3 -4.32). For instance, at the 4-minute timepoint, the RILs carrying the decreasing alleles of 2A, 3B, and 6A exhibited an average digestibility of 5.74%, whereas RILs carrying only the single decreasing allele, 6A, had an average digestibility of 8%. This combination of QTL consistently showed the lowest average starch digestibility across all timepoints. At the 8-minute timepoint, the digestibility values were 8.81% and 12.7% for the same combination compared to 6A alone. Similarly, at the 12, 16, 40, and 90-minute timepoints, the respective values were 11.7% vs. 16.2%, 13.5% vs. 18.4%, 20.4% vs. 24.6%, and 26.1% vs. 29.6% (Table 4.5).

Similarly for the increasing alleles, a higher average value on starch digestibility was observed when combining multiple QTL compared to individual QTL but there was no significant difference was between the individual QTL and combinations. Specifically, at the 4-minute timepoint, the combination of 2B, 3B, and 6A exhibited the highest starch digestibility values of 13.1% compared to 10.2% for the individual

QTL 4A, which had the highest values. At the 8, 12, 16, 40, and 90-minute timepoints, the respective values for the same combination were 21.1% vs. 16.5% for 4A, 25.1% vs. 20.2% for 4A, 26.8% vs. 22.5% for 4A, 31.9% vs. 28.1% for 4A, and 35.9% vs. 32.5% for 4A (Table 4.5).

Table 4.4. QTL above Logarithm of the odds (LOD) score 3 for starch digestibility.

For 'decreasing allele' column, A stands for Paragon, and B stands for Watkins 777.

Starch digested timepoints	Chromosome	Peak marker	Genetic position (cM)	Start marker	Genetic position (cM)	End marker	Genetic position (cM)	LOD	Add eff	Decreasing allele	Variance explained
4 min	2A	BS00078489	69.5	AX-643838458	66.6	AX-643838134	71.9	3.4	0.66	B	15.9
8 min	2A	BS00022260	70.1	AX-643868447	12.7	AX-643838134	71.9	3.6	1	B	13.8
	6A	AX-643859306	38.8	AX-643800863	37.9	AX-643859402	43.0	3.4	1.7	B	13
12 min	3B	AX-643833428	32	AX-643833198	27.9	AX-643833137	37.2	3.4	1.4	B	13.5
	6A	AX-643859306	38.8	BS00022592	35.0	AX-174260010	41.0	4.9	1.9	B	19.6
16 min	2B	AX-643816429	9.4	AX-643840802	4.5	BS00022126	11.2	5.4	0.62	A	20.1
	4A	BS00022816 1	108.1	AX-643837833	98.9	AX-643800524	114.7	4.8	1.7	B	17.5
40 min	2A	BS00078489	69.5	AX-643825790	61.8	AX-643838134	71.9	3.5	1	B	14

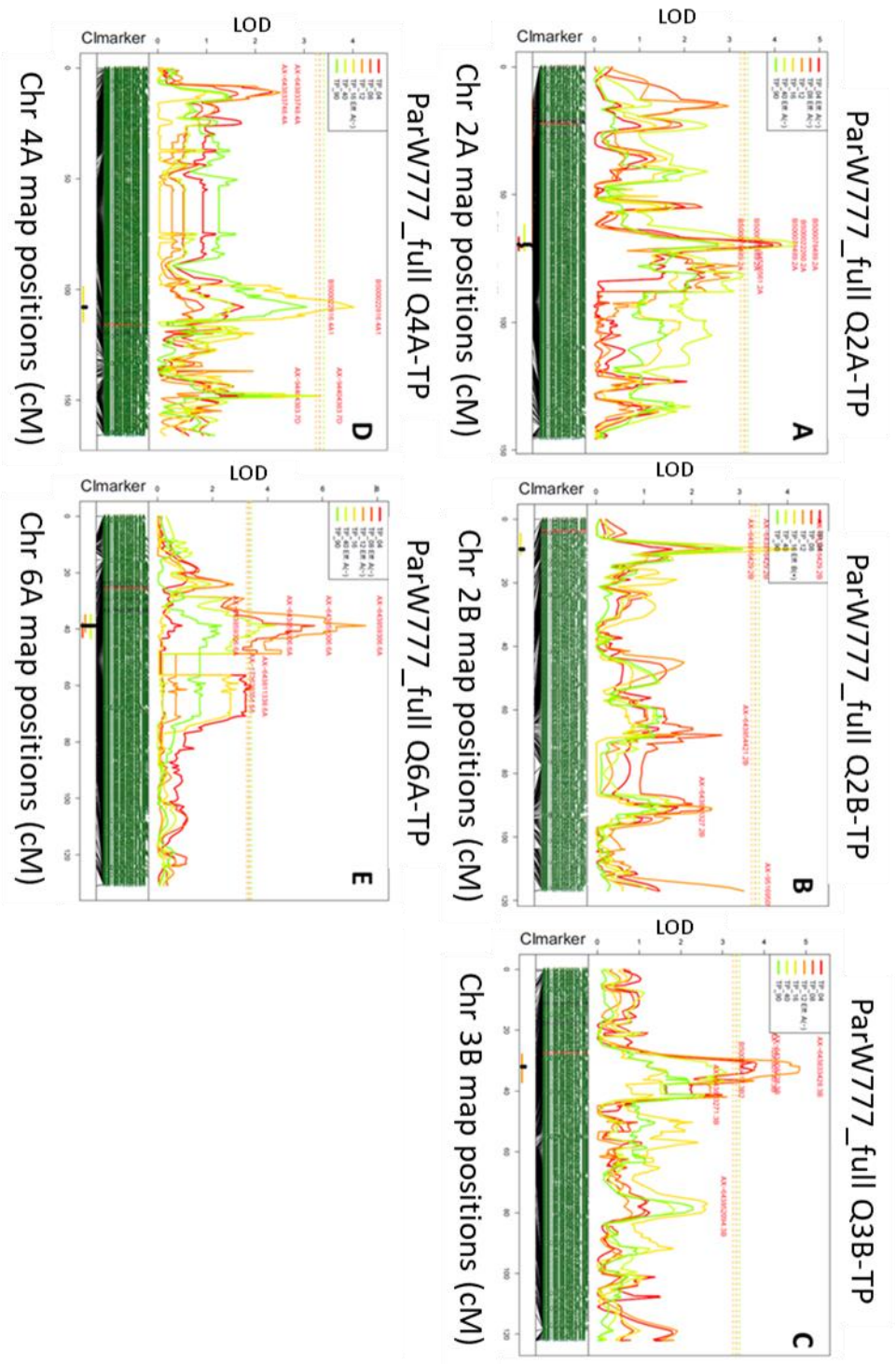

Figure 4.9. QTL interval analysis of 2A (A), 2B (B), 3B (C), 4A (D) and 6A (E) for starch digestibility of wholemeal flour. Each timepoint is represented by a distinct colour,

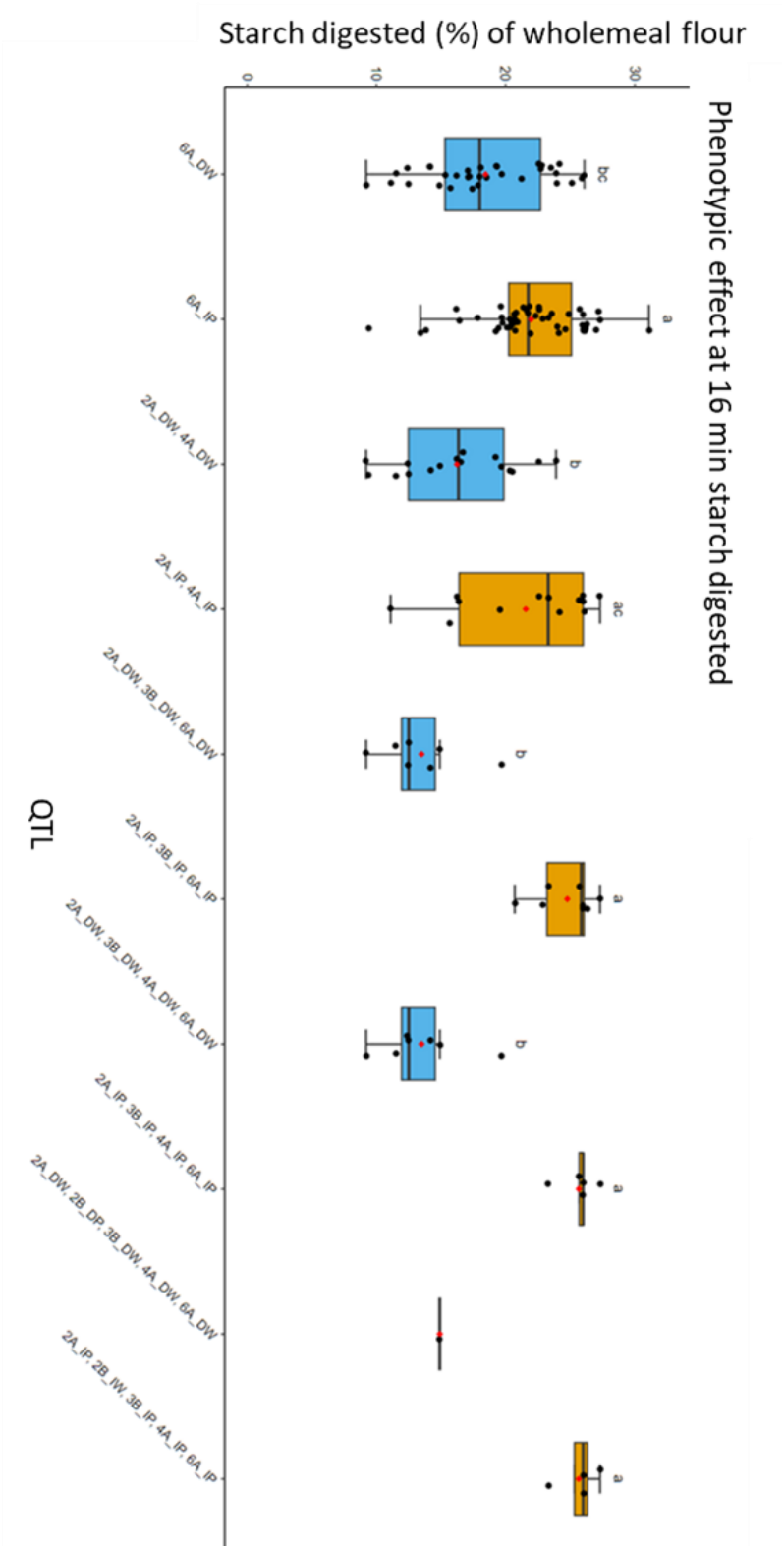

Figure 4.10. Phenotypic effect at 16 min starch digested. DW refers to the decreasing allele of Watkins 777, while DP represents the decreasing allele of Paragon. Similarly, IW stands for the increasing allele of Watkins 777, and IP stands for the increasing allele of Paragon.

Table 4.5. Phenotypic effect of different QTL combinations for starch digestibility (2A QTL used as a reference). The N refers to the number of RILs from the Paragon x 777 population carrying the specified QTL combinations. DW refers to the decreasing allele of Watkins 777, while DP represents the decreasing allele of Paragon. Similarly, IW stands for the increasing allele of Watkins 777, and IP stands for the increasing allele of Paragon.

QTL	Combinations	N	Starch digested (%), mean (SD)					
			4 min	8 min	12 min	16 min	40 min	90 min
2A	2A_DW	37	8.08 (2.29)	13 (3.7)	16.7 (4.25)	18.6 (4.37)	24.8 (3.76)	29.7 (3.59)
	2A_IP	38	9.42 (2.34)	15 (3.85)	18.7 (4.02)	20.9 (4.03)	26.8 (3.22)	31.3 (3.07)
	2A_DW, 2B_DP	19	8 (1.65)	13 (2.8)	17.1 (3.17)	19 (3.84)	25.3 (3.12)	30.2 (2.9)
	2A_IW, 2B_IP	17	10.2 (2.25)	16.5 (3.38)	20.2 (3.32)	22.5 (3.44)	28.1 (3.04)	32.4 (3.03)
	2A_DW, 3B_DW	18	7.19 (2.21)	11.8 (4.25)	15.1 (4.35)	16.5 (4.62)	23.1 (4.25)	28.3 (4.08)
	2A_IP, 3B_IP	13	10.6 (2.32)	17 (3.51)	20.7 (3.6)	23 (3.5)	28.4 (2.9)	32.7 (3.18)
	2A_DW, 4A_DW	16	6.78 (1.89)	10.7 (3.09)	14.6 (4.02)	16.2 (4.53)	22.7 (3.94)	28 (4.05)
	2A_IP, 4A_IP	14	9.81 (2.99)	16.1 (4.79)	19.3 (5.04)	21.9 (5.13)	27.6 (3.83)	32.1 (3.37)
	2A_DW, 6A_DW	16	7.08 (1.83)	11.1 (2.89)	14.5 (4)	16.8 (4.35)	23.1 (3.62)	28.3 (3.69)
	2A_IP, 6A_IP	23	10.2 (2.37)	16.2 (3.93)	19.9 (3.95)	22.1 (3.73)	27.8 (2.88)	32.1 (2.8)
	2A_DW, 2B_DP, 3B_DW	7	7.19 (1.94)	11.7 (3.39)	15.6 (3.32)	16.5 (4.11)	23.5 (3.81)	28.7 (3.27)
	2A_IP, 2B_IW, 3B_IP	9	10.5 (2.7)	16.7 (3.82)	20.3 (4.02)	22.6 (3.9)	28.1 (3.32)	32.1 (3.54)
	2A_DW, 2B_DP, 4A_DW	9	7.56 (1.91)	12.1 (3.12)	17 (3.22)	18.2 (4.43)	24.3 (3.48)	29.7 (3.39)
	2A_IP, 2B_IW, 4A_IP	9	10.3 (2.49)	17.2 (3.6)	20.6 (3.78)	23.4 (3.73)	28.9 (2.62)	33.2 (2.73)
	2A_DW, 2B_DP, 6A_DW	7	7.94 (1.51)	12.8 (2.45)	16.9 (3.69)	19.5 (3.76)	25.3 (2.32)	30.4 (2.27)
	2A_IP, 2B_IW, 6A_IP	11	11 (2.01)	17.8 (2.86)	21.5 (2.45)	23.7 (2.56)	29.2 (2.54)	33.6 (2.56)
	2A_DW, 3B_DW, 4A_DW	12	6.23 (1.68)	9.83 (2.77)	13.3 (3.4)	14.7 (3.87)	21.7 (4.02)	27 (4)
	2A_IP, 3B_IP, 4A_IP	8	10.6 (2.65)	17.5 (4.01)	20.9 (4.06)	23.5 (3.93)	29 (2.81)	33.3 (2.93)
	2A_DW, 3B_DW, 6A_DW	7	5.74 (1.41)	8.81 (1.9)	11.7 (2.93)	13.5 (3.31)	20.4 (3.5)	26.1 (4.17)
	2A_IP, 3B_IP, 6A_IP	8	11.9 (1.49)	19 (2.24)	22.9 (1.74)	24.8 (2.23)	29.7 (1.98)	33.8 (2.44)
	2A_DW, 4A_DW, 6A_DW	10	6.51 (1.93)	10.2 (3.03)	13.7 (4.56)	15.7 (4.89)	22 (3.92)	27.6 (4.53)
	2A_IP, 4A_IP, 6A_IP	9	10.7 (2.91)	17.5 (4.45)	20.8 (4.47)	23.3 (4.21)	28.7 (3.23)	33.1 (3.01)
	2A_DW, 2B_DP, 3B_DW, 4A_DW	5	6.86 (1.97)	11.1 (3.4)	15.8 (2.6)	16.1 (4.35)	23.2 (4.35)	28.8 (3.73)
	2A_IP, 2B_IW, 3B_IP, 4A_IP	7	10.4 (2.79)	17.1 (4.1)	20.5 (4.23)	23.2 (4.14)	28.9 (3)	33.2 (3.15)
	2A_DW, 2B_DP, 3B_DW, 6A_DW	1	6.3 (na)	10.3 (na)	12.9 (na)	14.9 (na)	22.7 (na)	29.5 (na)
	2A_IP, 2B_IW, 3B_IP, 6A_IP	4	12 (1.93)	19.6 (1.89)	23.3 (1.12)	25.6 (1.68)	30.6 (1.87)	34.9 (2.55)
	2A_DW, 2B_DP, 4A_DW, 6A_DW	4	7.8 (1.91)	12.5 (2.95)	17.1 (4.57)	19.4 (4.51)	24.9 (2.13)	30.8 (3.04)
	2A_IP, 2B_IW, 4A_IP, 6A_IP	5	11.4 (2.18)	19 (2.16)	22.4 (2.15)	25 (2)	30.2 (1.86)	34.6 (2.33)
	2A_DW, 3B_DW, 4A_DW, 6A_DW	7	5.74 (1.41)	8.81 (1.9)	11.7 (2.93)	13.5 (3.31)	20.4 (3.5)	26.1 (4.17)
	2A_IP, 3B_IP, 4A_IP, 6A_IP	5	12 (1.67)	19.9 (1.71)	23.3 (0.974)	25.7 (1.46)	30.5 (1.64)	34.7 (2.25)
	2A_DW, 2B_DP, 3B_DW, 4A_DW, 6A_DW	1	6.3 (na)	10.3 (na)	12.9 (na)	14.9 (na)	22.7 (na)	29.5 (na)
	2A_IP, 2B_IW, 3B_IP, 4A_IP, 6A_IP	4	12 (1.93)	19.6 (1.89)	23.3 (1.12)	25.6 (1.68)	30.6 (1.87)	34.9 (2.55)

Table continuation (2B QTL used as a reference).

QTL	Combinations	N	Starch digested (%), mean (SD)					
			4 min	8 min	12 min	16 min	40 min	90 min
2B	2B_DP	38	8.93 (2.13)	14.2 (3.49)	18.3 (3.78)	20.3 (3.99)	26.4 (3.23)	31 (3.06)
	2B_IW	34	10 (2.49)	16.3 (4)	19.9 (4.11)	22 (4.05)	27.5 (3.75)	31.9 (3.71)
	2B_DP, 2A_DW	19	8 (1.65)	13 (2.8)	17.1 (3.17)	19 (3.84)	25.3 (3.12)	30.2 (2.9)
	2B_IW, 2A_IP	17	10.2 (2.25)	16.5 (3.38)	20.2 (3.32)	22.5 (3.44)	28.1 (3.04)	32.4 (3.03)
	2B_DP, 3B_DW	20	8.57 (2.35)	13.5 (3.77)	17.5 (4.07)	19.1 (4.4)	25.6 (3.69)	30.4 (3.59)
	2B_IW, 3B_IP	15	10.9 (2.87)	17.3 (4.38)	21 (4.69)	23 (4.27)	28.4 (3.74)	32.4 (3.67)
	2B_DP, 4A_DW	17	8.31 (1.93)	13.2 (3.21)	17.5 (3.52)	19.2 (4.09)	25.5 (3.37)	30.4 (3.19)
	2B_IW, 4A_IP	18	11 (2.46)	18.1 (3.72)	21.6 (3.97)	23.9 (3.56)	29.1 (3.08)	33.6 (2.74)
	2B_DP, 6A_DW	12	8.31 (1.84)	13.2 (2.92)	17.2 (3.75)	19.6 (3.93)	25.7 (2.92)	30.7 (3.21)
	2B_IW, 6A_IP	21	10.9 (2.27)	18.1 (3.27)	21.6 (3.32)	23.7 (3.13)	29.1 (3.1)	33.5 (2.75)
	2B_DP, 2A_DW, 3B_DW	7	7.19 (1.94)	11.7 (3.39)	15.6 (3.32)	16.5 (4.11)	23.5 (3.81)	28.7 (3.27)
	2B_IW, 2A_IP, 3B_IP	9	10.5 (2.7)	16.7 (3.82)	20.3 (4.02)	22.6 (3.9)	28.1 (3.32)	32.1 (3.54)
	2B_DP, 2A_DW, 4A_DW	9	7.56 (1.91)	12.1 (3.12)	17 (3.22)	18.2 (4.43)	24.3 (3.48)	29.7 (3.39)
	2B_IW, 2A_IP, 4A_IP	9	10.3 (2.49)	17.2 (3.6)	20.6 (3.78)	23.4 (3.73)	28.9 (2.62)	33.2 (2.73)
	2B_DP, 2A_DW, 6A_DW	7	7.94 (1.51)	12.8 (2.45)	16.9 (3.69)	19.5 (3.76)	25.3 (2.32)	30.4 (2.27)
	2B_IW, 2A_IP, 6A_IP	11	11 (2.01)	17.8 (2.86)	21.5 (2.45)	23.7 (2.56)	29.2 (2.54)	33.6 (2.56)
	2B_DP, 3B_DW, 4A_DW	12	8.11 (2.06)	12.9 (3.5)	17 (3.67)	18.4 (4.29)	25.2 (3.86)	30.1 (3.46)
	2B_IW, 3B_IP, 4A_IP	11	11.4 (2.97)	18.3 (4.53)	22 (4.88)	24.1 (4.38)	29.4 (3.66)	33.6 (3.4)
	2B_DP, 3B_DW, 6A_DW	5	8.02 (2.36)	12.7 (3.67)	16.2 (4.4)	18.3 (4.71)	25 (3.84)	30.6 (4.52)
	2B_IW, 3B_IP, 6A_IP	7	13.1 (2.05)	20.7 (2.95)	24.7 (2.87)	26.3 (2.76)	31.3 (2.84)	35.1 (3.17)
	2B_DP, 4A_DW, 6A_DW	6	8.2 (1.81)	13.2 (2.75)	17.3 (3.88)	19.6 (3.9)	25.6 (2.2)	30.7 (2.46)
	2B_IW, 4A_IP, 6A_IP	12	11.6 (2.34)	19.3 (3.17)	22.9 (3.35)	25 (2.8)	30.2 (2.91)	34.7 (2.41)
	2B_DP, 2A_DW, 3B_DW, 4A_DW	5	6.86 (1.97)	11.1 (3.4)	15.8 (2.6)	16.1 (4.35)	23.2 (4.35)	28.8 (3.73)
	2B_IW, 2A_IP, 3B_IP, 4A_IP	7	10.4 (2.79)	17.1 (4.1)	20.5 (4.23)	23.2 (4.14)	28.9 (3)	33.2 (3.15)
	2B_DP, 2A_DW, 3B_DW, 6A_DW	1	6.3 (na)	10.3 (na)	12.9 (na)	14.9 (na)	22.7 (na)	29.5 (na)
	2B_IW, 2A_IP, 3B_IP, 6A_IP	5	12.2 (1.74)	19.3 (1.8)	23.2 (1.02)	25.1 (1.91)	30.1 (1.98)	34 (2.95)
	2B_DP, 2A_DW, 4A_DW, 6A_DW	4	7.8 (1.91)	12.5 (2.95)	17.1 (4.57)	19.4 (4.51)	24.9 (2.13)	30.8 (3.04)
	2B_IW, 2A_IP, 4A_IP, 6A_IP	5	11.4 (2.18)	19 (2.16)	22.4 (2.15)	25 (2)	30.2 (1.86)	34.6 (2.33)
	2B_DP, 3B_DW, 4A_DW, 6A_DW	2	7 (0.99)	11.5 (1.7)	14.1 (1.63)	16.1 (1.77)	23.9 (1.77)	29.6 (0.07)
	2B_IW, 3B_IP, 4A_IP, 6A_IP	6	13.1 (2.25)	21.1 (2.97)	25.1 (2.97)	26.8 (2.55)	31.9 (2.69)	35.9 (2.67)
	2B_DP, 2A_DW, 3B_DW, 4A_DW, 6A_DW	1	6.3 (na)	10.3 (na)	12.9 (na)	14.9 (na)	22.7 (na)	29.5 (na)
	2B_IW, 2A_IP, 3B_IP, 4A_IP, 6A_IP	4	12 (1.93)	19.6 (1.89)	23.3 (1.12)	25.6 (1.68)	30.6 (1.87)	34.9 (2.55)

Table continuation (3B QTL used as a reference).

QTL	Combinations	N	Starch digested (%), mean (SD)					
			4 min	8 min	12 min	16 min	40 min	90 min
3B	3B_DW	46	8.36 (2.31)	13.5 (4.03)	17.1 (4.33)	19 (4.64)	25.2 (4.06)	30.1 (3.85)
	3B_IP	37	10.1 (2.39)	16.2 (3.75)	20.2 (4)	22.3 (3.6)	27.8 (3.08)	32.2 (3.04)
	3B_DW, 2A_DW	18	7.19 (2.21)	11.8 (4.25)	15.1 (4.35)	16.5 (4.62)	23.1 (4.25)	28.3 (4.08)
	3B_IP, 2A_IP	13	10.6 (2.32)	17 (3.51)	20.7 (3.6)	23 (3.5)	28.4 (2.9)	32.7 (3.18)
	3B_DW, 2B_DP	20	8.57 (2.35)	13.5 (3.77)	17.5 (4.07)	19.1 (4.4)	25.6 (3.69)	30.4 (3.59)
	3B_IP, 2B_IW	15	10.9 (2.87)	17.3 (4.38)	21 (4.69)	23 (4.27)	28.4 (3.74)	32.4 (3.67)
	3B_DW, 4A_DW	25	7.8 (2.35)	12.4 (3.97)	16.1 (4.39)	17.7 (4.72)	24.3 (4.43)	29.2 (4.15)
	3B_IP, 4A_IP	23	10.5 (2.73)	17 (4.25)	20.8 (4.55)	23 (4.05)	28.6 (3.31)	32.7 (3.07)
	3B_DW, 6A_DW	15	7.03 (2.26)	11.1 (3.74)	14.3 (4.54)	16.2 (5.04)	22.8 (4.35)	28.1 (4.52)
	3B_IP, 6A_IP	18	11.4 (2.18)	18.3 (3.36)	22.3 (3.43)	24.3 (3.09)	29.5 (2.94)	33.5 (2.9)
	3B_DW, 2A_DW, 2B_DP	7	7.19 (1.94)	11.7 (3.39)	15.6 (3.32)	16.5 (4.11)	23.5 (3.81)	28.7 (3.27)
	3B_IP, 2A_IP, 2B_IW	9	10.5 (2.7)	16.7 (3.82)	20.3 (4.02)	22.6 (3.9)	28.1 (3.32)	32.1 (3.54)
	3B_DW, 2A_DW, 4A_DW	12	6.23 (1.68)	9.83 (2.77)	13.3 (3.4)	14.7 (3.87)	21.7 (4.02)	27 (4)
	3B_IP, 2A_IP, 4A_IP	8	10.6 (2.65)	17.5 (4.01)	20.9 (4.06)	23.5 (3.93)	29 (2.81)	33.3 (2.93)
	3B_DW, 2A_DW, 6A_DW	7	5.74 (1.41)	8.81 (1.9)	11.7 (2.93)	13.5 (3.31)	20.4 (3.5)	26.1 (4.17)
	3B_IP, 2A_IP, 6A_IP	8	11.9 (1.49)	19 (2.24)	22.9 (1.74)	24.8 (2.23)	29.7 (1.98)	33.8 (2.44)
	3B_DW, 2B_DP, 4A_DW	12	8.11 (2.06)	12.9 (3.5)	17 (3.67)	18.4 (4.29)	25.2 (3.86)	30.1 (3.46)
	3B_IP, 2B_IW, 4A_IP	11	11.4 (2.97)	18.3 (4.53)	22 (4.88)	24.1 (4.38)	29.4 (3.66)	33.6 (3.4)
	3B_DW, 2B_DP, 6A_DW	5	8.02 (2.36)	12.7 (3.67)	16.2 (4.4)	18.3 (4.71)	25 (3.84)	30.6 (4.52)
	3B_IP, 2B_IW, 6A_IP	7	13.1 (2.05)	20.7 (2.95)	24.7 (2.87)	26.3 (2.76)	31.3 (2.84)	35.1 (3.17)
	3B_DW, 4A_DW, 6A_DW	10	6.29 (1.46)	9.9 (2.35)	12.9 (3.11)	14.7 (3.34)	21.6 (3.45)	26.9 (3.67)
	3B_IP, 4A_IP, 6A_IP	13	11.8 (2.25)	19.1 (3.3)	23.1 (3.32)	25.1 (2.9)	30.3 (2.81)	34.4 (2.74)
	3B_DW, 2A_DW, 2B_DP, 4A_DW	5	6.86 (1.97)	11.1 (3.4)	15.8 (2.6)	16.1 (4.35)	23.2 (4.35)	28.8 (3.73)
	3B_IP, 2A_IP, 2B_IW, 4A_IP	2	10.7 (3.39)	15.6 (3.46)	19.5 (4.45)	20.7 (3.11)	25.4 (3.89)	28.6 (2.76)
	3B_DW, 2A_DW, 2B_DP, 6A_DW	1	6.3 (na)	10.3 (na)	12.9 (na)	14.9 (na)	22.7 (na)	29.5 (na)
	3B_IP, 2A_IP, 2B_IW, 6A_IP	5	12.2 (1.74)	19.3 (1.8)	23.2 (1.02)	25.1 (1.91)	30.1 (1.98)	34 (2.95)
	3B_DW, 2A_DW, 4A_DW, 6A_DW	7	5.74 (1.41)	8.81 (1.9)	11.7 (2.93)	13.5 (3.31)	20.4 (3.5)	26.1 (4.17)
	3B_IP, 2A_IP, 4A_IP, 6A_IP	5	12 (1.67)	19.9 (1.71)	23.3 (0.974)	25.7 (1.46)	30.5 (1.64)	34.7 (2.25)
	3B_DW, 2B_DP, 4A_DW, 6A_DW	2	7 (0.99)	11.5 (1.7)	14.1 (1.63)	16.1 (1.77)	23.9 (1.77)	29.6 (0.07)
	3B_IP, 2B_IW, 4A_IP, 6A_IP	6	13.1 (2.25)	21.1 (2.97)	25.1 (2.97)	26.8 (2.55)	31.9 (2.69)	35.9 (2.67)
	3B_DW, 2A_DW, 2B_DP, 4A_DW, 6A_DW	1	6.3 (na)	10.3 (na)	12.9 (na)	14.9 (na)	22.7 (na)	29.5 (na)
	3B_IP, 2A_IP, 2B_IW, 4A_IP, 6A_IP	4	12 (1.93)	19.6 (1.89)	23.3 (1.12)	25.6 (1.68)	30.6 (1.87)	34.9 (2.55)

Table continuation (4A QTL used as a reference).

QTL	Combinations	N	Starch digested (%), mean (SD)					
			4 min	8 min	12 min	16 min	40 min	90 min
4A	4A_DW	35	8.24 (2.36)	13.1 (3.83)	16.9 (4.35)	18.8 (4.6)	25 (4.09)	29.8 (3.96)
	4A_IP	37	10.2 (2.64)	16.5 (4.21)	20.2 (4.5)	22.5 (4.23)	28.1 (3.41)	32.5 (3.11)
	4A_DW, 2A_DW	16	6.78 (1.89)	10.7 (3.09)	14.6 (4.02)	16.2 (4.53)	22.7 (3.94)	28 (4.05)
	4A_IP, 2A_IP	14	9.81 (2.99)	16.1 (4.79)	19.3 (5.04)	21.9 (5.13)	27.6 (3.83)	32.1 (3.37)
	4A_DW, 2B_DP	17	8.31 (1.93)	13.2 (3.21)	17.5 (3.52)	19.2 (4.09)	25.5 (3.37)	30.4 (3.19)
	4A_IP, 2B_IW	18	11 (2.46)	18.1 (3.72)	21.6 (3.97)	23.9 (3.56)	29.1 (3.08)	33.6 (2.74)
	4A_DW, 3B_DW	25	7.8 (2.35)	12.4 (3.97)	16.1 (4.39)	17.7 (4.72)	24.3 (4.43)	29.2 (4.15)
	4A_IP, 3B_IP	23	10.5 (2.73)	17 (4.25)	20.8 (4.55)	23 (4.05)	28.6 (3.31)	32.7 (3.07)
	4A_DW, 6A_DW	17	7.21 (1.83)	11.6 (3.05)	15 (4.04)	17.1 (4.34)	23.4 (3.81)	28.5 (4.07)
	4A_IP, 6A_IP	23	10.9 (2.44)	17.9 (3.76)	21.6 (3.88)	23.8 (3.44)	29.2 (3.04)	33.6 (2.69)
	4A_DW, 2A_DW, 2B_DP	9	7.56 (1.91)	12.1 (3.12)	17 (3.22)	18.2 (4.43)	24.3 (3.48)	29.7 (3.39)
	4A_IP, 2A_IP, 2B_IW	9	10.3 (2.49)	17.2 (3.6)	20.6 (3.78)	23.4 (3.73)	28.9 (2.62)	33.2 (2.73)
	4A_DW, 2A_DW, 3B_DW	9	7.56 (1.91)	12.1 (3.12)	17 (3.22)	18.2 (4.43)	24.3 (3.48)	29.7 (3.39)
	4A_IP, 2A_IP, 3B_IP	8	10.6 (2.65)	17.5 (4.01)	20.9 (4.06)	23.5 (3.93)	29 (2.81)	33.3 (2.93)
	4A_DW, 2A_DW, 6A_DW	10	6.51 (1.93)	10.2 (3.03)	13.7 (4.56)	15.7 (4.89)	22 (3.92)	27.6 (4.53)
	4A_IP, 2A_IP, 6A_IP	9	10.7 (2.91)	17.5 (4.45)	20.8 (4.47)	23.3 (4.21)	28.7 (3.23)	33.1 (3.01)
	4A_DW, 2B_DP, 3B_DW	12	8.11 (2.06)	12.9 (3.5)	17 (3.67)	18.4 (4.29)	25.2 (3.86)	30.1 (3.46)
	4A_IP, 2B_IW, 3B_IP	11	11.4 (2.97)	18.3 (4.53)	22 (4.88)	24.1 (4.38)	29.4 (3.66)	33.6 (3.4)
	4A_DW, 2B_DP, 6A_DW	6	8.2 (1.81)	13.2 (2.75)	17.3 (3.88)	19.6 (3.9)	25.6 (2.2)	30.7 (2.46)
	4A_IP, 2B_IW, 6A_IP	12	11.6 (2.34)	19.3 (3.17)	22.9 (3.35)	25 (2.8)	30.2 (2.91)	34.7 (2.41)
	4A_DW, 3B_DW, 6A_DW	10	6.29 (1.46)	9.9 (2.35)	12.9 (3.11)	14.7 (3.34)	21.6 (3.45)	26.9 (3.67)
	4A_IP, 3B_IP, 6A_IP	13	11.8 (2.25)	19.1 (3.3)	23.1 (3.32)	25.1 (2.9)	30.3 (2.81)	34.4 (2.74)
	4A_DW, 2A_DW, 2B_DP, 3B_DW	5	6.86 (1.97)	11.1 (3.4)	15.8 (2.6)	16.1 (4.35)	23.2 (4.35)	28.8 (3.73)
	4A_IP, 2A_IP, 2B_IW, 3B_IP	7	10.4 (2.79)	17.1 (4.1)	20.5 (4.23)	23.2 (4.14)	28.9 (3)	33.2 (3.15)
	4A_DW, 2A_DW, 2B_DP, 6A_DW	4	7.8 (1.91)	12.5 (2.95)	17.1 (4.57)	19.4 (4.51)	24.9 (2.13)	30.8 (3.04)
	4A_IP, 2A_IP, 2B_IW, 6A_IP	5	11.4 (2.18)	19 (2.16)	22.4 (2.15)	25 (2)	30.2 (1.86)	34.6 (2.33)
	4A_DW, 2A_DW, 3B_DW, 6A_DW	7	5.74 (1.41)	8.81 (1.9)	11.7 (2.93)	13.5 (3.31)	20.4 (3.5)	26.1 (4.17)
	4A_IP, 2A_IP, 3B_IP, 6A_IP	5	12 (1.67)	19.9 (1.71)	23.3 (0.974)	25.7 (1.46)	30.5 (1.64)	34.7 (2.25)
	4A_DW, 2B_DP, 3B_DW, 6A_DW	2	7 (0.99)	11.5 (1.7)	14.1 (1.63)	16.1 (1.77)	23.9 (1.77)	29.6 (0.07)
	4A_IP, 2B_IW, 3B_IP, 6A_IP	6	13.1 (2.25)	21.1 (2.97)	25.1 (2.97)	26.8 (2.55)	31.9 (2.69)	35.9 (2.67)
	4A_DW, 2A_DW, 2B_DP, 3B_DW, 6A_DW	1	6.3 (na)	10.3 (na)	12.9 (na)	14.9 (na)	22.7 (na)	29.5 (na)
	4A_IP, 2A_IP, 2B_IW, 3B_IP, 6A_IP	4	12 (1.93)	19.6 (1.89)	23.3 (1.12)	25.6 (1.68)	30.6 (1.87)	34.9 (2.55)

Table continuation (6A QTL used as a reference).

QTL	Combinations	N	Starch digested (%), mean (SD)					
			4 min	8 min	12 min	16 min	40 min	90 min
6A	6A_DW	33	8.01 (2.27)	12.7 (3.66)	16.2 (4.39)	18.4 (4.61)	24.6 (3.82)	29.6 (3.84)
	6A_IP	48	10 (2.38)	16.2 (3.89)	20.1 (3.87)	22 (4.01)	27.7 (3.46)	32.2 (3.16)
	6A_DW, 2A_DW	16	7.08 (1.83)	11.1 (2.89)	14.5 (4)	16.8 (4.35)	23.1 (3.62)	28.3 (3.69)
	6A_IP, 2A_IP	23	10.2 (2.37)	16.2 (3.93)	19.9 (3.95)	22.1 (3.73)	27.8 (2.88)	32.1 (2.8)
	6A_DW, 2B_DP	12	8.31 (1.84)	13.2 (2.92)	17.2 (3.75)	19.6 (3.93)	25.7 (2.92)	30.7 (3.21)
	6A_IP, 2B_IW	21	10.9 (2.27)	18.1 (3.27)	21.6 (3.32)	23.7 (3.13)	29.1 (3.1)	33.5 (2.75)
	6A_DW, 3B_DW	15	7.03 (2.26)	11.1 (3.74)	14.3 (4.54)	16.2 (5.04)	22.8 (4.35)	28.1 (4.52)
	6A_IP, 3B_IP	18	11.4 (2.18)	18.3 (3.36)	22.3 (3.43)	24.3 (3.09)	29.5 (2.94)	33.5 (2.9)
	6A_DW, 4A_DW	17	7.21 (1.83)	11.6 (3.05)	15 (4.04)	17.1 (4.34)	23.4 (3.81)	28.5 (4.07)
	6A_IP, 4A_IP	23	10.9 (2.44)	17.9 (3.76)	21.6 (3.88)	23.8 (3.44)	29.2 (3.04)	33.6 (2.69)
	6A_DW, 2A_DW, 2B_DP	7	7.94 (1.51)	12.8 (2.45)	16.9 (3.69)	19.5 (3.76)	25.3 (2.32)	30.4 (2.27)
	6A_IP, 2A_IP, 2B_IW	11	11 (2.01)	17.8 (2.86)	21.5 (2.45)	23.7 (2.56)	29.2 (2.54)	33.6 (2.56)
	6A_DW, 2A_DW, 3B_DW	7	5.74 (1.41)	8.81 (1.9)	11.7 (2.93)	13.5 (3.31)	20.4 (3.5)	26.1 (4.17)
	6A_IP, 2A_IP, 3B_IP	8	11.9 (1.49)	19 (2.24)	22.9 (1.74)	24.8 (2.23)	29.7 (1.98)	33.8 (2.44)
	6A_DW, 2A_DW, 4A_DW	10	6.51 (1.93)	10.2 (3.03)	13.7 (4.56)	15.7 (4.89)	22 (3.92)	27.6 (4.53)
	6A_IP, 2A_IP, 4A_IP	9	10.7 (2.91)	17.5 (4.45)	20.8 (4.47)	23.3 (4.21)	28.7 (3.23)	33.1 (3.01)
	6A_DW, 2B_DP, 3B_DW	5	8.02 (2.36)	12.7 (3.67)	16.2 (4.4)	18.3 (4.71)	25 (3.84)	30.6 (4.52)
	6A_IP, 2B_IW, 3B_IP	7	13.1 (2.05)	20.7 (2.95)	24.7 (2.87)	26.3 (2.76)	31.3 (2.84)	35.1 (3.17)
	6A_DW, 2B_DP, 4A_DW	6	8.2 (1.81)	13.2 (2.75)	17.3 (3.88)	19.6 (3.9)	25.6 (2.2)	30.7 (2.46)
	6A_IP, 2B_IW, 4A_IP	12	11.6 (2.34)	19.3 (3.17)	22.9 (3.35)	25 (2.8)	30.2 (2.91)	34.7 (2.41)
	6A_DW, 3B_DW, 4A_DW	10	6.29 (1.46)	9.9 (2.35)	12.9 (3.11)	14.7 (3.34)	21.6 (3.45)	26.9 (3.67)
	6A_IP, 3B_IP, 4A_IP	13	11.8 (2.25)	19.1 (3.3)	23.1 (3.32)	25.1 (2.9)	30.3 (2.81)	34.4 (2.74)
	6A_DW, 2A_DW, 2B_DP, 3B_DW	1	6.3 (na)	10.3 (na)	12.9 (na)	14.9 (na)	22.7 (na)	29.5 (na)
	6A_IP, 2A_IP, 2B_IW, 3B_IP	5	12.2 (1.74)	19.3 (1.8)	23.2 (1.02)	25.1 (1.91)	30.1 (1.98)	34 (2.95)
	6A_DW, 2A_DW, 2B_DP, 4A_DW	4	7.8 (1.91)	12.5 (2.95)	17.1 (4.57)	19.4 (4.51)	24.9 (2.13)	30.8 (3.04)
	6A_IP, 2A_IP, 2B_IW, 4A_IP	5	11.4 (2.18)	19 (2.16)	22.4 (2.15)	25 (2)	30.2 (1.86)	34.6 (2.33)
	6A_DW, 2A_DW, 3B_DW, 4A_DW	7	5.74 (1.41)	8.81 (1.9)	11.7 (2.93)	13.5 (3.31)	20.4 (3.5)	26.1 (4.17)
	6A_IP, 2A_IP, 3B_IP, 4A_IP	5	12 (1.67)	19.9 (1.71)	23.3 (0.974)	25.7 (1.46)	30.5 (1.64)	34.7 (2.25)
	6A_DW, 2B_DP, 3B_DW, 4A_DW	2	7 (0.99)	11.5 (1.7)	14.1 (1.63)	16.1 (1.77)	23.9 (1.77)	29.6 (0.07)
	6A_IP, 2B_IW, 3B_IP, 4A_IP	6	13.1 (2.25)	21.1 (2.97)	25.1 (2.97)	26.8 (2.55)	31.9 (2.69)	35.9 (2.67)
	6A_DW, 2A_DW, 2B_DP, 3B_DW, 4A_DW	1	6.3 (na)	10.3 (na)	12.9 (na)	14.9 (na)	22.7 (na)	29.5 (na)
	6A_IP, 2A_IP, 2B_IW, 3B, 4A_IP	4	12 (1.93)	19.6 (1.89)	23.3 (1.12)	25.6 (1.68)	30.6 (1.87)	34.9 (2.55)

In this study a QTL analysis was also conducted for wheat characteristics (protein content, starch content of grain and flour, NDF content, hardness, width grain area, length grain area and TGW). The objective was to investigate potential overlap

between the QTL identified for starch digestibility and those linked to wheat characteristic traits.

In total, the study identified 3 QTL for TGW, located in chromosomes 3A, 5A, and 6A, 2 QTL for hardness in chromosomes 2A and 4A, 2 QTL for grain length in chromosomes 3A and 5A, 1 QTL for grain width in chromosome 1A, and 1 QTL for protein in chromosome 7B (Figure 4.11, Table 4.6). Among all the identified QTL, only one QTL that related to hardness, located in 4A, overlapped with a QTL identified for starch digestibility (Figure 4.12).

Table 4.6. QTL above LOD score 3 for protein, hardness, TGW, NDF and grain length and width. For 'increasing allele' column, A stands for Paragon, and B stands for Watkins 777.

Traits	Chromosome	Peak marker	Genetic position (cM)	Start marker	Genetic position (cM)	End marker	Genetic position (cM)	LOD	Add eff	Increasing allele	Variance explained
Grain width	1A	AX-86178483	26.4	AX-643837579	23.3	AX-86179448	31.6	4.0	0.05	A	18.1
Grain length	3A	BS00023087	50.0	BS00022862	24.7	AX-94481094	56.2	3.2	0.12	B	12.2
	5A	AX-643809640	91.9	BS00021939	80.6	AX-643833769	99.9	3.6	0.11	A	13.4
NDF	3B	AX-643817506	64.5	AX-643830206	58.6	AX-643798749	67.1	5.2	0.53	A	22.5
Hardness	2A	AX-643823407	92.4	AX-643812326	88.0	AX-643809408	100.9	3.9	1.9	A	14.3
	4A	AX-108781719	119.2	AX-643812800	110.2	AX-643825822	124.2	5.1	2.4	A	18.8
TGW	3A	AX-86178048	29.7	AX-643798120	29.0	BS00035364 2	35.7	3.5	0.18	B	10.3
	5A	AX-643825713	0.0	AX-643825713	0.0	BS00022864	1.8	4.2	1.5	B	13.6
	6A	AX-643797943	61.7	BS00023089	57.7	AX-643856236	72.7	3.3	1.3	B	10.6
Protein (grain)	7B	AX-94439304	49.4	AX-643869681	35.9	AX-89665432	54.4	5.1	0.01	B	22.1

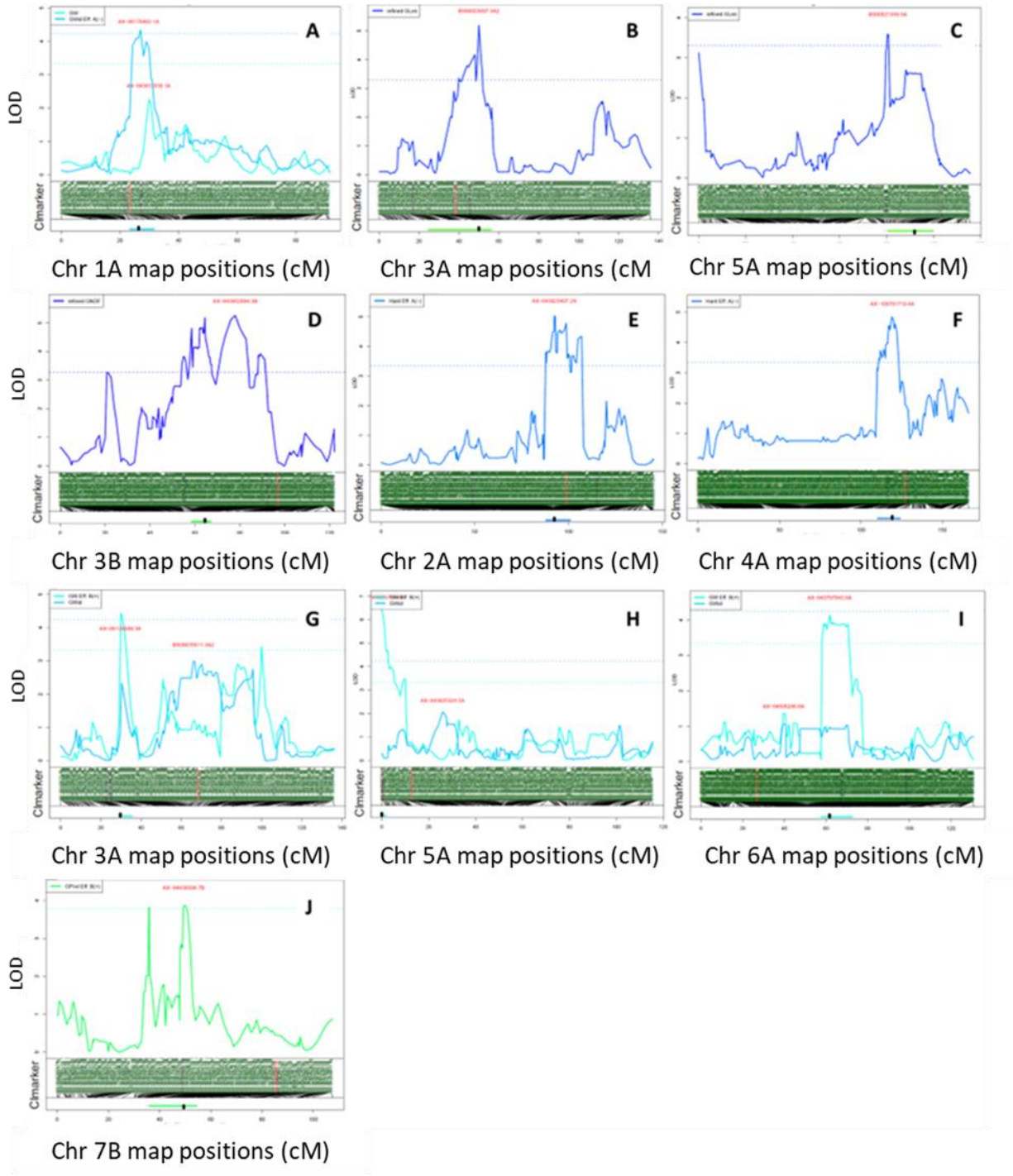

Figure 4.11. QTL interval analysis of 1A (A) for grain width, 3A (B) and 5A (C) for grain length, 3B (D) for NDF, 2A (E) and 4A (F) for hardness, 3A (G), 5A (H) and 6A (I) for TGW and 7B (J) on protein content of grains.

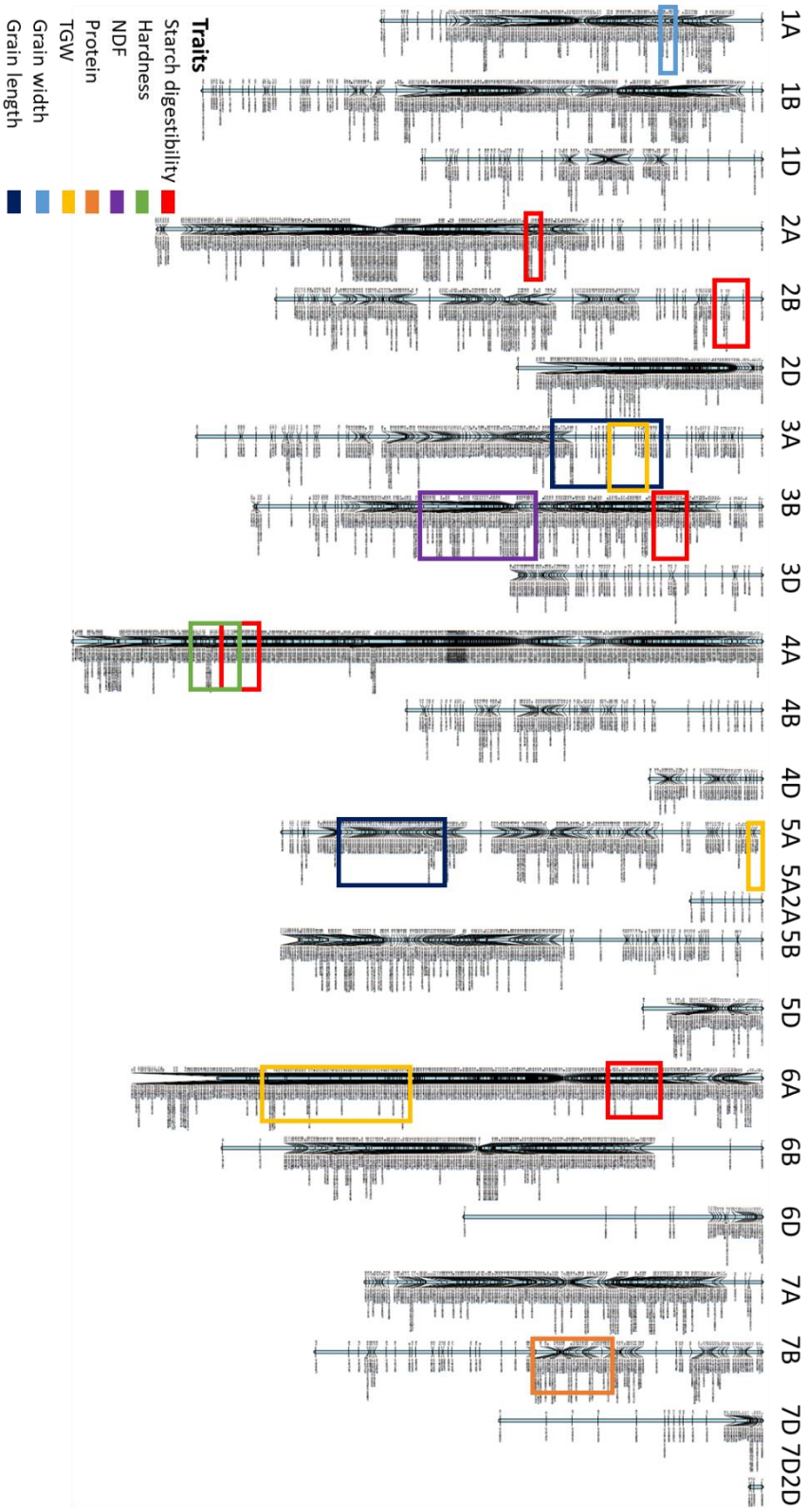

Figure 4.12. Chromosomal location of starch digestibility (6 time points), hardness, NDF, protein, TGW, Grain width and length QTL identified in the Paragon x 777 population. Chromosomes are shown in black, and markers are depicted on the right

of each chromosome bar. QTL confidence intervals are shown in red boxes for starch digestibility, green for hardness, purple for NDF, yellow for TGW, light blue for grain width, dark blue for grain length and orange for protein.

Seed compositional characteristics (NIR)

Using NIR, dehusked grains from the mapping population and parental lines were assessed for major compositional characteristics. The grains were analysed by NIR for protein, starch, NDF content, and hardness and parental lines were used as controls. There was a statistically significant difference between protein content ($p < 0.001$), starch content ($p < 0.001$), NDF content ($p < 0.05$) and hardness values ($p < 0.001$) in the mapping population (Figure 4.13).

Protein content varied between 12.4 to 17.3% dwb, and the population's average was 14.3% dwb. Paragon and 777 differed significantly ($p < 0.001$) in protein content; the protein content of Paragon (12.7% dwb) was on the low end compared to the overall variation, whereas the protein content of 777 was on the high end with 14.8% dwb. A similar trend was observed when analysing the protein content of Watkins 777 and Paragon using the crude protein–combustion method (AACC, 2010). In the case of 777, the protein content was 14.2% as is in 2018 and 14.8% dwb in 2020 and for Paragon the protein content was 13.5% as is in 2013 and 12.7% dwb in 2020.

Starch content in the mapping population varied between 64.6 to 71.6% dwb. There was a statistically significant difference between Paragon and Watkins 777 ($p < 0.001$). However, it was considered a small variation. For example, Paragon was on

the high end with 71% dwb, whereas 777 was on the middle to low end with 68.3% dwb, of the variation (the average of the population was 69.1% dwb).

NDF varied between 13.5% to 18.7% dwb. Paragon and 777 did not differ significantly, with the Paragon being on the low-middle end (16.3% dwb), whereas 777 was in the middle (17% dwb) of the variation (the average of the population was 16.7% dwb).

Hardness values varied between 60 to 85.7 SKCS. Both Paragon and 777 had similar hardness values, and there was no statistically significant difference between those. Both parents were placed on the low end of the variation (average of the population 75 SKCS). Hardness values were recorded as 62.9 for the Paragon and 65.6 for the Watkins 777.

The NIR analysis presented a high variation in the biparental population in different compositional characteristics. In half of the measured compositional characteristics (protein and starch content), parents carried significant differences contributing to the observed variation.

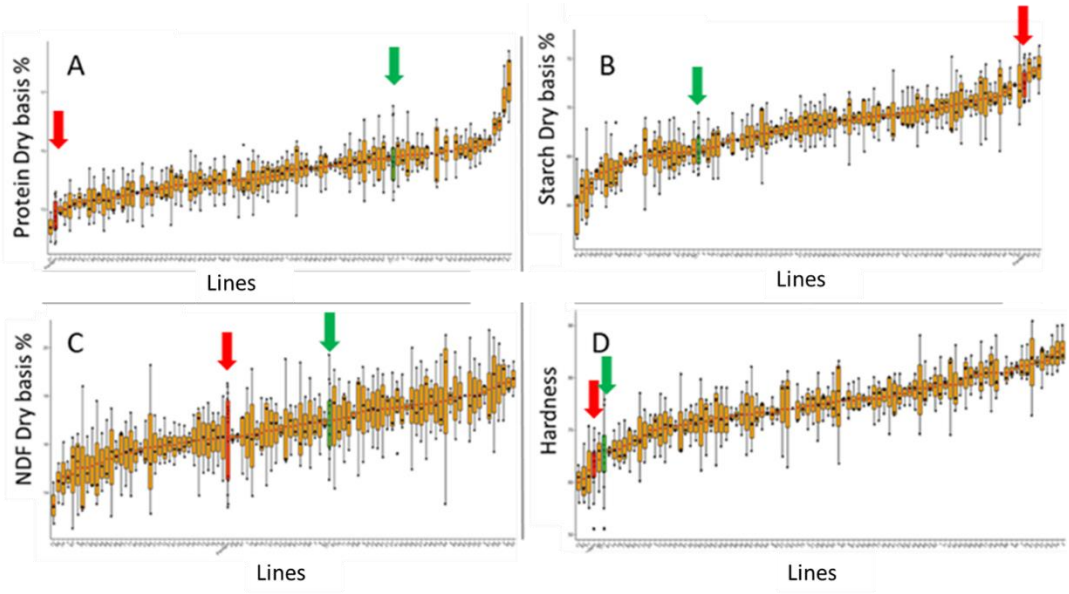

Figure 4.13. Seed analysis by NIR of the Paragon x 777 population ordered from lowest to highest on A) protein dry basis %, B) starch dry basis %, C) NDF basis % and D) hardness. Paragon is shown in red arrows and the 777 line is shown in green arrows. RILs n = 3 biological replicates and Paragon and 777 n ≥ 11 biological replicates.

Seed phenotypic characteristics (Marvin Data)

Marvin analysis was conducted on dehusked grains from the mapping population and parental lines. The analysis assessed agroeconomically important characteristics such as TGW and length and width area of the grains. There was a statistically significant difference between TGW ($p < 0.001$), width area ($p < 0.001$) and length area ($p < 0.001$) in the mapping population (Figure 4.14).

TGW varied between 35.1 to 51.3g, mean, and the population's average was 41.6g. Paragon and 777 differed significantly ($p < 0.001$) in their TGW values. More

specifically, the TGW of Paragon (47.9g) was on the high end compared to the overall variation, whereas the TGW of 777 (37.8g) was on the low end.

The length area in the mapping population varied between 5.8 to 7mm, and the average of the population was 6.4mm. Additionally, there was a statistically significant difference between Paragon and 777 ($p < 0.001$). Paragon (6.5mm) was on the middle-high end of the variation, whereas 777 (6.4mm) was in the middle.

The width area varied between 3.2 and 3.9mm, and the average of the population was 3.4mm. Paragon and 777 differed significantly in the width area ($p < 0.001$). More specifically, Paragon had seed width area values of 3.6mm, whereas 777 had values of 3.2mm. Paragon was located on the high end of the overall variation on the seed width area, and 777 was located on the low end.

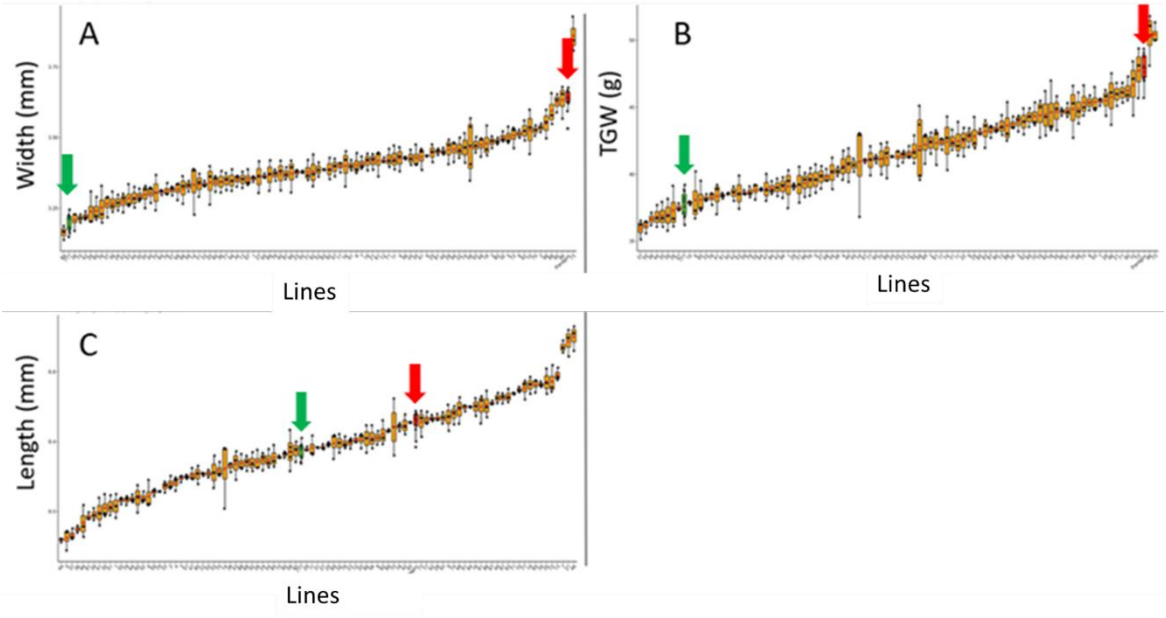

Figure 4.14. Marvin analysis on grains of the Paragon x 777 population ordered from lowest to highest on A) width (mm), B) TGW (g) and C) length (mm). Paragon is shown in red arrows, and the 777 line is shown in green arrows. RILs n = 3 biological replicates and Paragon and 777 n ≥ 11 biological replicates.

4.4 Discussion

4.4.1 Selection of a low-digestibility starch line

In cereals, the stability of a trait can be impacted by genotype x environment interactions. In particular, starch digestibility has been shown to be affected by both genotype and environment (Kaufman et al., 2018, Bach et al., 2013). However, studies suggest that genotype variation is more important in starch digestibility than environmental variance (Zhang et al., 1995, Bao et al., 2004). For wheat, there are limited studies to examine the effect of genetic and environmental variation on starch digestibility. A study which investigated the influence of variety and environment on wheat characteristics grown in Western Australia found that variety significantly influenced fast digestible starch (Kim et al., 2003). In the current thesis, starch digestibility in Watkins lines was significantly affected by year. However, there were limitations to that experiment as one biological replicate was used for each line per year. Therefore, there is no strong evidence that some lines were more or less affected by year than others. To address this issue, a similar experiment can be conducted in the future using more replicates per line and growing each line in different environmental conditions for multiple years. The main goal of this experiment was to select a stable low-digestibility line to use for QTL analysis. The Watkins line 777 presented a lower digestibility profile in 3 years of white flour and 1 year of wholemeal flour samples, making it an ideal candidate for a cross with Paragon, which has previously shown a higher digestibility profile compared to 777.

4.4.2 QTL analysis on starch digestibility

The 777 line showed a consistently lower digestibility than Paragon; however, from the 5 QTL detected, 4 QTL derived from 777 and 1 from Paragon as a decreasing allele. It is well established in QTL analysis that both parents may contribute increasing or decreasing alleles to a trait; for example Griffiths et al. (2012) identified genes controlling crop height from a double haploid population derived from the cross Savannah × Rialto which reported an increasing effect from both parents. In this starch digestibility study, the QTL located on the 2B chromosome had a decreasing allele from Paragon. When this 2B Paragon QTL was combined with other 777 QTL, it resulted in lower average starch digestibility values (Table 4.5). This is a likely explanation as to why several lines had a lower digestibility profile than the 777 and suggests the possibility of transgressive segregation. Transgressive segregation refers to the phenomenon wherein offspring or individuals within a population display trait values that surpass the range observed in either of the parent lines. Examining all the QTL combinations, the RILs carrying a combination of decreasing alleles for 2A, 3B and 6A QTL showed the lowest digestibility at timepoints 12 and 16 min. As a result, this particular combination proves to be promising for breeding purposes. Hence, the QTL identified have an additive effect on starch digestibility, and both 777 and Paragon lines carry alleles that have both decreasing and increasing effects on starch digestibility. There were few RILs that carried more than 3 QTL with decreasing alleles and only 1 RIL that carried all 5 QTL with decreasing alleles (Table 4.5). Thus, a potential limitation of the study is the small population being used, if a larger population was used this could increase the chances of recovering more RILS carrying unique combinations of decreasing and or increasing alleles which would help to assess their potential additive effect on starch digestibility. However, for breeding purposes, a selection

of fewer QTL is preferred since integrating multiple QTL for various traits in a breeding program can be expensive and complicated. Lastly, homoeology of the QTL 2A and 2B was examined to identify potential syntenic regions. However, the 2A and 2B QTL did not appear to be syntenic (homoeologous) as they seemed to fall into distinct regions.

Limited studies have conducted a forward screening approach for starch digestibility. A study from Hou et al. (2022) assessed the RS content in a GWAS population of 207 wheat varieties grown in three locations. In their study, they identified 14 genetic loci that consistently appeared in more than two environments. Particularly the SNPs associated were in chromosomes 2A (3 SNPs), 2B, 2D (2 SNPs), 3A, 4A, 4D, 5A (2 SNPs), 5B, 6A and 7B. Based on their results, they suggested four potential candidate genes that might have a relationship with RS content (*TraesCS4D03G0010800, TraesCS5A03G0943300, TraesCS6A03G1026400*, and *TraesCS7B03G0151400*). A second study by RahimKumar and Roy (2022), investigated the genetic factors influencing the gelatinization parameters of starch and the amylose-lipid complex in a diverse bread wheat collection using a GWAS analysis (n = 192). In their study, they identified 144 SNPs controlling gelatinization in wheat and proposed seven candidate genes that are potentially involved in starch gelatinization in wheat (*GSK3-alpha, RING-type domain-containing protein, Tetratricopeptide repeat, Hexosyltransferase, GLP, SNF1*, and *WRKY* transcription factor). From both studies, the SNP markers associated with RS, starch gelatinisation and amylose lipid complex were examined to determine if their genetic locations overlap with starch digestibility QTL identified in this study. However, there was no direct link between the location of SNP markers and the QTL. This suggests the possibility of additional genes affecting starch digestibility in wholemeal flour samples.

In terms of the genes involved in starch biosynthesis, a number have been reported to affect starch digestibility in crops; *SBEIIa*, *SBEIIb*, *SSI*, *SSIIa*, and *SSIIIa* (Hazard et al., 2012, Fahy et al., 2022, Wang et al., 2020, Gurunathan et al., 2019). In this project, these genes were not present in the regions of the QTL associated with starch digestibility. One starch-related gene, B-granule content 1 (*BGC1*), is located in the 4A QTL. *BGC1*, was previously shown to have an effect on starch synthesis, but there are no reports on its effects on starch digestibility (Chia et al., 2020, Saccomanno et al., 2022). The *BGC1* also has an effect on B-type starch granule content without significantly altering the total starch content (Chia et al., 2020, Saccomanno et al., 2022). In Chapter 3, section 3.3.6, the starch granule distribution analysis did not show evidence of the line 777 having a significant difference in its B-type granule content compared to Paragon. Furthermore, the digestibility of purified starch from 777 (described in Chapter 3, section 3.3.1) increased compared to wholemeal and white flour samples suggesting that other factors besides starch itself may be contributing to the lowered starch digestibility.

To explore the other potential factors influencing starch digestibility beyond starch structure, this study examined various characteristics of wheat grain and flour in the same population including protein content, starch content of grain and flour, NDF content, hardness, width grain area, length grain area, and TGW. The aim was to investigate any associations between these traits and starch digestibility. However, no significant correlations were found between the measured traits and starch digestibility. Furthermore, although the QTL analysis revealed a strong effect in terms of explained variance for these traits, only one trait showed a co-location with the QTL identified for starch digestibility. This QTL is related to hardness and it is located on the chromosome 4A. While the hardness of grains can potentially impact starch digestibility, as the starch granules are more susceptible to damage

in hard wheat endosperm, it was not considered significant in this study as granules had already undergone complete gelatinization during the cooking process. This might also explain the lack of correlation between hardness results and starch digestibility as hardness was measured in grains while the starch digestibility assay was conducted on thermally processed wholemeal flour. Therefore, it should be noted that under different sample preparations, such as analysing samples without thermal processing, hardness could correlate with starch digestibility.

Hardness is also a significant trait for quality bread characteristics. Paragon carries the increasing allele for hardness in a QTL located on chromosome 4A, while line 777 carries the decreasing allele for starch digestibility in a QTL located on the same chromosome and overlaps with the hardness QTL (Figure 4.12). The genetic distance between the peak marker for hardness and the marker associated with starch digestibility is 11.1 centiMorgan (cM). Consequently, for the purposes of breeding, it is likely feasible to separate these traits using a segregating population.

Moreover, within the current population comprising 96 RILs, a subset of 7 RILs has both the increasing allele for hardness and the decreasing allele for starch digestibility. Hence, if the preference is to select RILs possessing both QTL, these specific individuals carrying both alleles can be chosen.

A key limitation of this study is the lack of multiple field trials. Future work (described in detail in Chapter 5) should repeat the same trial in multiple environments/years and introgress the repeatedly detected QTL into the same genetic background. NILs would allow for further verification of the QTL effects and aid in the identification of causal genes. This forward genetic approach can be used for breeding and research purposes to develop future wheat lines that are more nutritious and targeted to particular applications.

Chapter 5 Future directions and conclusion

5.1 Project summary and addressing interruptions and shortcomings

This project aimed to exploit natural phenotypic variation in starch digestibility found within wheat germplasm resources. For this reason, a key aim of the project was to develop a high-throughput tool to allow for screening germplasm resources for starch digestibility, for use in this project and in future studies (Figure 5.1). As a high variation in starch digestibility was observed in the Watkins collection, the next step was to select a low-digestibility line and conduct a QTL analysis to identify genetic loci associated with starch digestibility.

The high-throughput assay for starch digestibility developed in the project significantly decreased the time required to run the assay for 96 samples from 32 days to 3 days. It is important to acknowledge that, in this study, the sample preparation stage still posed a significant bottleneck, with an estimated duration of 22 days for the preparation of 96 samples. Due to time limitations, no measures were implemented to address this particular bottleneck. In this project, the high-throughput assay was used to screen a germplasm resource called the Watkins collection (118 lines), which captures the diversity of 826 landraces collected from 32 countries with the goal to discover natural variation in starch digestibility in wheat. Additional wheat varieties were used to represent commercial elite germplasm resources. The Watkins collection presented a wide range of variation in starch digestibility which exceeded the variation that existed in elite varieties. However, a limitation of this study was that elite comparator varieties were grown

in different years. Furthermore, Watkins grown in the same year as elite lines showed a statistical difference in total starch to the other years. Therefore, if this experiment was redesigned, elite varieties would be sown in the same field trial as the Watkins.

The next aim of the project was to discover links between starch structure, wheat grain characteristics and starch digestibility. Numerous analyses were conducted on a subset of Watkins and elite varieties varying in starch digestibility in wholemeal flour, sieved flour fractions and purified starch. The key finding of the study revealed an increasing trend in starch digestibility as the sample fractions progressed towards purified starch, this suggested the lower starch digestibility observed in selected lines was due to the matrix properties of wholemeal and/or sieved flour, rather than the intrinsic properties of starch granules. One of the limitations of the study was the small number (8 lines) of selected lines used for analysing starch structure and wheat grain characteristics. This constraint hindered the statistical ability to understand the impact of individual factors on starch digestibility. The decision to reduce the number of selected lines was taken due to the time lost during the Covid lockdown as initially it was planned to include 24 samples in the subset. Therefore, if these experiments were to be redesigned, a subset of 24 (or more) samples would be investigated, based on a ranking system, comprising 12 lines with high digestibility and 12 lines with low digestibility. Additional analysis which could complement the thermoanalytical measurements conducted in this study would be SDS-PAGE. By using a subset of 24 samples this analysis could be used for potentially linking starch digestibility effects to particular protein fractions.

The next aim was to select a low starch digestibility line with an existing NAM population for QTL analysis. To achieve this, a subset of Watkins grown in 4 years (obtained for collaborators at Rothamsted Research) was screened, resulting in the selection of line 777 as a potential candidate for low starch digestibility. However, one limitation of this experiment was the absence of biological replicates, as only a single biological replicate was available for analysis. This limitation had a minor impact on the selection of the low starch digestibility line, but it significantly affected the findings regarding genotype x environment interactions. Studying the impact of genotype x environment on starch digestibility could be valuable for both research purposes and plant breeders; however, given the availability of the samples, priorities of the project and time constraints, it was decided to analyse one biological replicate per year as these samples were readily available.

The final stage of this project involved performing a QTL analysis on a NAM population with varying levels of starch digestibility. To achieve this, wholemeal flour samples from the Paragon x 777 population were screened for starch digestibility, total starch and grain characteristics. Notably, five novel QTL were identified that had not been reported in the existing literature. Due to time constraints, only a one-year field trial was screened.

In the subsequent section, a comprehensive step-by-step guide for continuing this project is provided. Additionally, alternative projects based on this current work are proposed, providing the opportunity to explore alternative pathways for exploiting starch digestibility using the existing high-throughput tool. Finally, research recommendations will be provided for potential industrial and scientific applications of the high-throughput tool, specifically focused on product development.

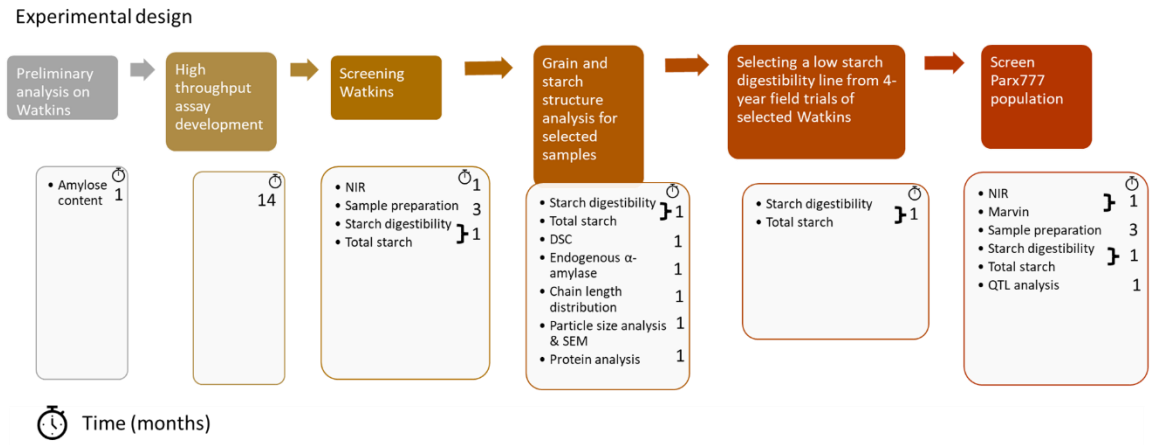

Figure 5.1. Experimental timeline estimation. Preliminary analysis on AM content on selected Watkins (1 month). Development of a high throughput screening assay for starch digestibility (14 months). Screening the Watkins for grain characteristics, sample preparation and starch digestibility and TS (5 months). Grain and structural analysis for selected samples on starch digestibility, TS, DSC, endogenous α-amylase, CLD, protein analysis and particle size analysis on wholemeal flour and purified starch (6 months). Selecting a low digestibility line by screening the starch digestibility and TS of 4-year field trials on selected Watkins (1 month). Screening the Paragon x 777 on grain characteristics, starch digestibility and TS and conducting a QTL analysis (6 months).

5.1.1 Continuing the forward genetic approach to identify causal genes affecting starch digestibility

The study proposed below involves continuing the existing project and completing the forward genetic study on starch digestibility. It is recommended to conduct two additional years of field trials, three biological replicates of $1m^2$ plots per line, of the Paragon x 777 population in multiple environments (preferably three). For each field trial, a preliminary QTL analysis on the presence and absence of awns needs

to be conducted to verify the field layout. This experiment can be repeated as the one listed in Chapter 4, section 4.3.2. Another preliminary analysis that needs to be conducted is to analyse the activity of the endogenous α-amylase of seeds in both parents, Paragon and 777. If the parents have values of endogenous α-amylase higher than 0.2 Ceralpha Units/g, it is suggested to exclude them from further analysis, and lines from the population with values above that threshold should be excluded as well. High levels of endogenous α-amylase, caused by poor growing or storage conditions, could affect the starch digestibility of the flour by hydrolysing native starch granules. This may prevent the discovery of other potential grain or starch structure characteristics that may affect starch digestibility.

The next step will be to prepare samples for starch digestibility and TS. The grains of the population need to be milled separately using a cyclone mill (UDY Corporation) with a 0.5 mm sieve and passed through an additional 0.3 mm sieve to produce wholemeal flour samples with standardised particle size. Wholemeal flour samples can then be screened for starch digestibility and TS, which is required to adjust the starch content in the starch digestibility assay. For the starch digestibility assay, it is suggested that all samples need to be thermally processed. This involves cooking the samples at 80°C for 15 minutes and cooling them at 4°C for 21 hours. Depending on the length of the project, additional analysis on DSC can be conducted to examine the thermal properties of the starch, as work in this thesis showed the 'onset temperature' and 'enthalpy' parameters of DSC had a negative correlation with the amount of starch digested at 90 minutes for selected wholemeal flour samples. Additionally, DSC analysis would be useful to validate the correlation of the thermal properties of starch with starch digestibility and add further phenotypic markers for starch digestibility.

Then a QTL analysis can be conducted on previously examined parameters to identify common QTL/s from previous field trials. If non-common QTL are identified, based on the duration of the project, an additional-year field trial can be conducted and screened again and/or further analysis of other factors, shown in other studies impacting starch digestibility, can be analysed. Potential factors to investigate include protein content and starch structural characteristics such as AM content, CLD and starch granule size distribution. In this thesis project, these factors have been obtained on a selected set of Watkins and elite varieties. However, due to the fact that there is a significant genotypic and phenotypic variation among all Watkins lines and as well as a small sample size due to time restrictions, the power to identify additional factors that impact starch digestibility was limited. By analysing the entire population (consisting of 94 RILs and parents), which exhibits less variation as it is solely derived from the parents, there is a higher likelihood of identifying individual factors that affect starch digestibility. Therefore, analysing these parameters would be useful for understanding factors affecting starch digestibility and exploring mechanisms involved in decreasing digestibility. If common QTL are identified, it is recommended to design KASP markers on differential SNPs within the QTL region(s) in order to more accurately pinpoint the genetic loci responsible for the variation in starch digestibility. Additionally, heterozygous lines should be selected in that region and selfed to create a new fine-mapping population. If non-heterozygous lines exist in the QTL region(s), it is recommended to select homozygous lines with low-digestibility starch and cross them with the high starch digestibility parent (Paragon) to create a new mapping population. The next step would be to select recombinants in the QTL region and phenotype them for starch digestibility and TS. This step would allow for refining the position of the QTL/s and could be repeated until no more recombinants are

identified or until the region is small enough, it is feasible to begin searching for candidate genes within that region, to begin looking for candidate genes. To narrow down the region of interest, more recombinants would be required within each QTL interval, but near isogenic lines would also be needed for verification of the effects of each QTL prior to fine mapping. These lines are genetically identical to each other except for the locus of interest, making it easier to verify the effects of the targeted locus. By using near isogenic lines, other effects from the Watkins 777 will be removed and the locus of interest can be studied in elite varieties currently used in breeding programs. Once candidate genes are identified, they can be tested for functionality using TILLING or gene editing approaches and the results can be used to confirm the role of the candidate genes in starch digestibility and to better understand the underlying molecular mechanisms involved (explained in section 5.1.2).

5.1.2 Gene validation and gene functionality analysis

If putative gene(s) controlling low-starch digestibility are identified, a functional genetics study utilising induced genetic variation (i.e. gene editing, TILLING) or gene expression study could be used to validate the actual role of the gene. An important functional genetics resource using induced variation is the in silico TILLING (targeted induced local lesions in genomes) database for both tetraploid (Kronos) and hexaploid (Cadenza) wheat (Krasileva et al., 2017). Exome capture was used to sequence both populations to identify mutations across the genomes; exome capture is also known as exome sequencing or target enrichment, it is a technique used in genomics to selectively capture and sequence all the protein-coding regions of the genome, known as the exome. In generating the TILLING database, a

significant number of mutations in the protein-coding sections of 2,735 mutant lines of tetraploid and hexaploid wheat were recorded. An average of 2,705 mutations and 5,351 mutations in tetraploid and hexaploid wheat were identified respectively, which corresponded to an approximately 35-40 mutations per kilobase (kb) within each population. In total the TILLING database includes more than 10 million mutations, across 1,535 Kronos mutant lines and 1,200 Cadenza mutant lines capturing more than 90% of the wheat genes. Therefore, functional genetic approaches can be used to validate putative candidate genes hypothesised to associate with starch digestibility. This would involve ordering mutants lines containing mutations in the candidate genes and investigating their effects on starch digestibility. Gene expression could also help in identifying the causal gene in loci by providing information on which genes are more expressed in several wheat lines (Adamski et al., 2020). Transgenics and gene editing tools like Clustered regularly interspaced short palindromic repeats (CRISPR)/Cas9 could also be used to increase or suppress the gene expression of all homoeologous copies of a gene in order to validate the gene action.

The same tools can be used to study the functionality of the gene. For example, with gene editing using CRISPR, it is possible to knock out one, two or all homoeologous copies in wheat to study gene behaviours (e.g., discover if the gene has functional redundancy or a dosage effect).

5.1.3 QTL analysis and GWAS analysis for low-digestibility starch using more populations

A similar approach to this project can be conducted to generate more populations from a low- and high-digestibility parent, or by utilizing other available populations

derived from the Watkins x Paragon cross. The Watkins collection presented a wide variation in starch digestibility, and multiple low-digestibility lines have been identified in this project. Examples of other potential low digestibility lines that exist in a population with Paragon are Watkins 216 and 639. Also, If additional QTL analysis is obtained (e.g., additional crosses of 777 to a different parent or another using another low-digestibility line to Paragon), the data can be used to identify common QTL among populations for low-digestibility. Then the common QTL can be validated by developing KASP SNP assays based on the peak and flanking markers associated with the detected QTL.

Further validation can be provided if needed by GWAS analysis. Compared to QTL analysis which studies the contribution of a locus to the variation of a trait, the GWAS studies the association between alleles and a trait (Adamski et al., 2020, Lovegrove et al., 2020). A GWAS analysis for starch digestibility can be conducted without the need to generate a population. However, the study would need to use larger germplasm panels than the 118 lines used in this study to provide sufficient power to detect all relevant genetic variants associated with starch digestibility. Using a larger panel size, increases the likelihood of capturing rare alleles and may capture the full extent of linkage disequilibrium blocks in the population, reducing the likelihood of false associations.

These validations increase the probability of identifying markers associated with low-digestibility and can be used in breeding programmes to develop future wheat lines with low-digestibility. An example of a successful study that followed a similar approach to identify markers linked with a health-related trait was that of Lovegrove et al. (2020). This study used 4 populations in which Yumai 34 (a high AX content cultivar) was used as one of the parents in each population. The

populations were then screened for relative viscosity, and total AX content and QTL analysis was conducted. Although many QTL were identified, only one was detected in all 4 populations. This QTL was then validated by developing KASP assays and GWAS analysis. A similar strategy can be conducted for a low-digestibility trait and RS using the high-throughput tool provided by this project.

Selecting fewer QTL associated with starch digestibility would be useful in breeding programs as it reduces the complexity. In wheat breeding, MAS is used to select traits that are controlled by multiple QTL or for traits that are difficult to select for using traditional breeding methods (Pandurangan et al., 2021). However, the practicalities of using MAS for large numbers of QTL in wheat breeding can be challenging due to the large population sizes required to stack these QTL as well as all the other agronomically important traits necessary for commercialisation.

One of the challenges of using MAS for large numbers of QTL in wheat breeding is the availability and cost of molecular markers. Developing molecular markers for every QTL of interest in large populations (large populations are needed to have enough lines carrying preferred combinations) can be time-consuming and expensive, especially for traits that are controlled by many QTL, as starch digestibility. Furthermore, the cost of genotyping large numbers of markers can be prohibitive for some breeding programs, which may have limited resources (Miedaner and Korzun, 2012, Pandurangan et al., 2021). By selecting for fewer QTL, the cost of genotyping and data analysis can be reduced, making the breeding program more cost-effective.

Another challenge of MAS for multiple QTL on starch digestibility is the genetic complexity of the trait (Pandurangan et al., 2021). Starch digestibility is influenced by multiple factors making it difficult to identify and select for the most

advantageous combination of QTL. Furthermore, some highly important traits, such as yield and disease resistance, are also controlled by many QTL (Hernandez et al., 2012, Ma et al., 2022). Moreover, certain QTL may have both positive and negative effects on different traits. This complexity poses a significant obstacle for breeding programs attempting to utilize MAS effectively, especially if the effects of individual QTL are minor or if there are epistatic interactions among them (Miedaner and Korzun, 2012). Therefore, by selecting for fewer QTL, the accuracy and efficiency of MAS can be improved, especially if the QTL are well-characterized and have large effects on the trait, and the breeding program can focus on improving the most important traits while still maintaining genetic diversity in the population.

5.1.4 Exploring phenotypic variation and selecting low-digestibility samples from large collections

Variation in wheat is critical for breeding programs to develop novel plants with advanced characteristics. As wheat evolved through history, its genetic diversity narrowed (BorrillHarrington and Uauy, 2018). Therefore, most modern polyploid wheat contains lower genetic and phenotypic variation in most traits than its wild relatives (BorrillHarrington and Uauy, 2018). In terms of starch digestibility and RS as a trait of interest, limited research and breeding programmes have been conducted to reduce the risk of losing variation in that trait over years of extensive selection on yield, disease resistance, and specific quality criteria (e.g., protein content), which could potentially decreased diversity in other traits, such as starch digestibility (Curtis and Halford, 2014, Rahman et al., 2020). Therefore, the highest variation in starch digestibility is expected to be captured in wild wheat progenitors. All genomes in hexaploid wheat do not retain most of their diversity from their wild

progenitors. However, the D genome is the one that captures the least genetic diversity found in goat grass species; 10% compared to A and B genomes that retain about 30% of the overall diversity found in wild emmer progenitors (Haudry et al., 2007, HalloranOgbonnaya and Lagudah, 2008). For that reason, many efforts have been made over the years to reintroduce the *Ae. tauschii* variation to the hexaploid wheat in order to increase the overall variation in hexaploid wheat (synthetic hexaploid wheat) (BorrillHarrington and Uauy, 2018). Using synthetic hexaploid wheat sources to discover the variation of starch digestibility is a promising project to explore whether the diversity of that trait has been retained in landraces or more variation exists in the *Ae. tauschii* accessions. A similar strategy to this project can be examined If a higher variation in starch digestibility exists. If there is, a low-digestibility line/s can be selected for further analysis. The same approach to this study can be conducted in different wheat and non-wheat variation sources. However, it is important to acknowledge that while the 96-format starch digestibility assay takes 3 days, the sample preparation currently requires 22 days. Consequently, the selection of sources should be based on the project's timeline. Some examples are:

- Natural variation wheat sources
    - 998 accessions of hexaploid wheat (Huang et al., 2002)
    - INRA collection (more than 10,000 accessions) (Balfourier et al., 2007)
    - Mexican creole wheat collection (contains 8,416 Mexican landraces) (Vikram et al., 2016)
- Different wheat population structures of modern cultivars

    - Biparental populations or multiparental populations (e.g., MAGIC population) (Saintenac et al., 2018, Huang et al., 2012, Mackay et al., 2014, Milner et al., 2016, Dixon et al., 2018)
    - NAM panels and association panels consisting of a variety of cultivars (Jordan et al., 2018, Sukumaran et al., 2015, Liu et al., 2017, BorrillHarrington and Uauy, 2018)
- Natural variation of non-wheat sources
    - Rice: International Rice Germplasm Collection, 200 tropical *japonica* accessions (Singh et al., 2022)
    - Maize: A core set of CIMMYT's global collection of 4,500 maize landraces (Gates et al., 2019)

5.1.5 Using the high-throughput assay to compare the effect and understand the mechanism of different components on starch digestibility

Most staple food products are composed of multiple ingredients apart from wheat starch, and the final products are usually processed under different conditions. Therefore, several studies have focused on examining the effect of different components and processes on starch digestibility (Copeland et al., 2009, Okumus et al., 2018, Kawai et al., 2012, DhitalGidley and Warren, 2015). The high-throughput assay developed in this project can be adjusted to support these studies and allow multiple samples to be processed and analysed on starch digestibility simultaneously.

An example is endogenous and exogenous lipids and their effect on starch digestibility. AM and lipid complexes have been shown to form in native starch granules and during processing with endogenous lipids (Morrison, 1988, Copeland et al., 2009). Both endogenous and exogenous complexes have been shown to affect the digestion rate and possibly RS (Okumus et al., 2018, Kawai et al., 2012, CroweCopeland and Seligman, 2000, Holm et al., 1983, SharmaYadav and Ritika, 2008, Patil et al., 1998). With the availability of a high-throughput starch digestion assay, multiple fatty acid structures and contents in wheat samples can now be tested under the same conditions with multiple replicates.

Several other components and molecular structures can be analysed using the high-throughput assay to understand the mechanisms affecting starch digestibility. An example is to simultaneously compare, in the same run, different protein fractions and conformations formed during processing and study their effect on starch digestibility. With the ability to include 96 samples of various protein fractions and conformations in each well while maintaining the same substrate ratio for starch, it would be possible to study the potential effects of different protein fractions and conformations on starch digestibility. Various methods can be used to isolate protein fractions in crops and other food products. One way is based on protein solubility, which involves using techniques like salt fractionation to separate proteins based on their salt solubility or ethanol precipitation to isolate proteins based on their alcohol solubility. Another approach is to use SEC to separate proteins based on their molecular weight, or ion exchange chromatography to separate them based on their net charge at a particular pH or isoelectric point (KusumahAndoyo and Rialita, 2020). Additionally, proteins in foods can exist in different conformations, which can be altered through changes in temperature and pH, resulting in partial or full denaturation (Hadnađev et al., 2017).

Another example is enzyme inhibitors such as polyphenols, lectin, cellulose, phytate, tannic acid and haemagglutinins (SharmaYadav and Ritika, 2008, Alsaffar, 2011, Thompson and Yoon, 1984, DhitalGidley and Warren, 2015). Using the high-throughput assay, these components can be compared simultaneously under different concentrations and thermal processes to better examine the different binding mechanisms to the amylase. Lastly, different cell wall thicknesses and particle sizes of flour and selected food products can be analysed simultaneously and examined on starch digestibility rate and extent using the high-throughput assay.

5.1.6 Selecting starch sources and optimising starch hydrolysis conditions for industrial and scientific applications

Depending on the starch applications, different hydrolytic rates might be desirable depending on the industry. With the development of the high-throughput assay, multiple starch sample structures can be screened and analysed for amylolysis before their use in particular applications. Below are examples of potential low and high starch amylolysis applications and how the high-throughput assay can be incorporated to support projects.

One of the advantages of low-digestibility starches is their ability to be used as encapsulation carriers to protect and deliver food ingredients to the large intestinal tract. There are numerous techniques to fabricate starches depending on the encapsulated material (phenolic compounds, β-carotene, probiotics, caffeine, etc.) (Guo et al., 2021). Examples of different techniques include aggregation, emulsification, electrohydrodynamic process, post-processing drying, and supercritical fluid (Guo et al., 2021). The high-throughput assay could assist during

the development of these starches as it will allow a quick selection and mechanistic understanding of these products during digestion.

On the contrary, high starch hydrolysis is desirable in industries such as brewing and distilling. During mashing, one of the main processes for beer and whiskey products, crushed malted grains (a multistage process to prepare grains before mashing) and controlled temperature water activates the endogenous enzymes (α and β-amylase, α-glucosidase, and limit dextrinase) (Grime and Briggs, 1996, Briggs, 1992). These enzymes start to hydrolyse the malted substrate into fermentable sugars, and the main goal is to maximise the rate of starch hydrolysis for yeast optimisation in beer and whiskey production (Fox, 2018). During mashing, multiple factors can affect the hydrolysis of starch. Examples such as water quality, grist size, grist-to-water ratio, pH, mash time, temperature and starch structure are some of the main factors that impact starch hydrolysis (GoodeUlmer and Arendt, 2005, Schur, 1980, Muller, 2000, Fox, 2018). The high-throughput assay developed for starch digestibility assays can be adjusted to serve as a tool for testing different factors simultaneously using the same substrate (up to 96 samples per run) and optimising enzyme activities for particular malted samples.

Another application for the high-throughput assay is in the stage of product development of enzymes for fermented products and other applications. Product development is a key area for enzyme manufacturers and requires substantial testing prior to use to ensure users with stable, novel and cheaper functionality. Depending on the applications, different biotechnological products can be tested and compared simultaneously in the 96-format using multiple starch substrates with the presence/absence of different components at set temperatures. An example is a production of thermostable exogenous enzymes (e.g. bacteria and

fungi), which can sustain high enzymatic activity at high temperatures on a high grist-to-water ratio during mashing (Puligundla et al., 2020).

5.2 Future trends

Low-digestibility starch crops and RS are becoming a topic of increasing interest in the scientific community due to their associated health benefits, as starches with low digestibility rates can reduce glycemic response compared to conventional starches (Roman and Martinez, 2019, Sissons et al., 2020, Belobrajdic et al., 2019). As starch is one of the most important ingredients in the food industry and consumers are becoming more educated about their diet, food manufacturers will have an increasing demand to produce healthier food products (Google trends, Figure 5.2). Therefore, to breed low-digestibility starch-based crops such as wheat, a stable and sustainable food supply chain system must first be secured. To meet this demand, a stable and sustainable supply chain of low digestibility wheat needs to be developed. This would entail breeding for starch digestibility traits that are stable across environmental conditions (locations and years) and ensuring consistency in raw materials produced (flour) for food producers.

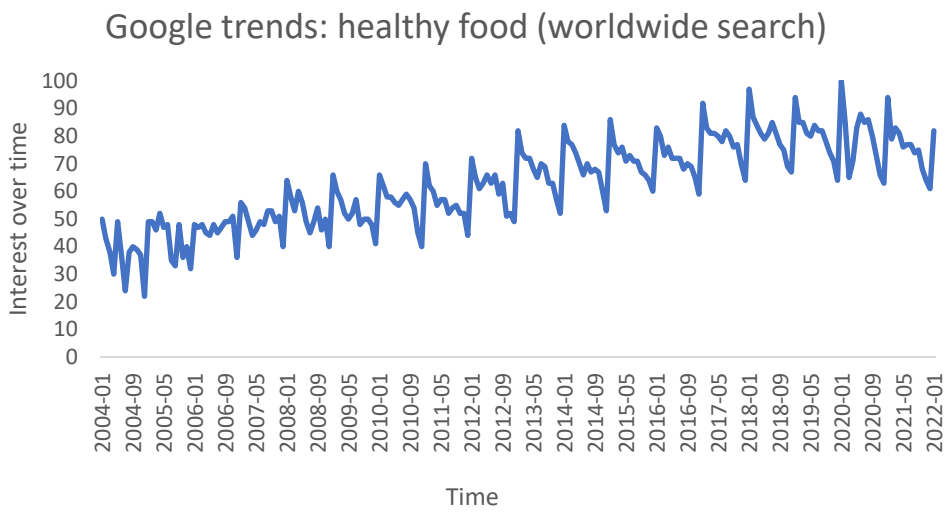

Figure 5.2. Worldwide trends based on healthy food terms by Google Trends. Interest over time: numbers represent search interest relative to the highest point on the chart for the given region and time. A value of 100 is the peak popularity for the term. A value of 50 means that the term is half as popular. A score of 0 means there was not enough data for this term.

Starch digestibility and RS are considered complex traits as many factors can affect that trait. AM is a well-known factor that can reduce the rate and extent of starch digestibility if high amounts are achieved relative to AP in starch (Sissons et al., 2020, Belobrajdic et al., 2019, Corrado et al., 2022a, Schönhofen et al., 2016, Li et al., 2020b). One of the main bottlenecks of adopting the production of high AM wheat is its link to reducing yield performance (Hazard et al., 2015). Acknowledging the above concern, this project focused on discovering different approaches to reduce starch digestibility in wheat. A forward genetic approach provides a possibility to discover genetic information that can reduce starch digestibility and have the potential to affect less yield performance. Several studies have used forward-screen approaches to discover novel genetic information linked to other

health-associated traits (Lovegrove et al., 2020, Kumar et al., 2018, Khokhar et al., 2020). In the case of starch digestibility and RS, few studies have focused on it due to the limited tools available and the labour-intensive work required to screen samples for starch digestibility (Zhang et al., 2020).

To facilitate continued advancements in the identification of genes associated with starch digestibility, more research needs to be conducted on both crops and food processing. This study has successfully demonstrated the impact of thermal processing and matrix effects on starch digestibility. Consequently, for future studies utilizing a forward genetic approach to uncover connections to starch digestibility, it is important to design experiments that incorporate holistic strategies for identifying these links.

5.3 Conclusion

This study screened for the first time a large set of wheat landraces (Watkins collection, 118 lines which capture the majority of the genetic diversity of more than 800 lines) for starch digestibility. Wholemeal flour sample of the Watkins set presented a wide variation in starch digestibility, whereas sieved flour fractions and purified starch from selected lines showed altered starch digestibility profiles compared to wholemeal flour samples. The selected lines were also analysed for flour and starch structure properties, and none of the above factors strongly correlated with starch digestibility data. Therefore, if many interactions of factors are important to achieve low-digestibility profiles, it might not be the most suitable biotechnological approach to target one component but selecting lines based on the outcome of multiple interactions of factors through starch digestibility assays. The Watkins line 777 was the only line with the least effect on starch digestibility when samples were sieved and a stable low-digestibility line when screened for 4 years. For that reason, a population consisting of 777 as one of the parents was used, leading to 5 QTL being detected in the QTL analysis. It is suggested that the low-digestibility observed in the population and selected Watkins lines is likely conferred by matrix properties of flour rather than intrinsic properties of starch granules. Therefore, it is suggested that other genetic factors could contribute to changes in starch digestibility. This forward genetic approach and observed variation can be used to identify more valuable alleles and verify discovered ones to improve future wheat nutrition.

References

AACC 2010. AACC method 46-30.01, Crude protein – combustion

method. In: AACC approved methods of analysis. 11 ed. Minnesota: Cereals & Grains Association.

ADAMSKI, N. M., BORRILL, P., BRINTON, J., HARRINGTON, S. A., MARCHAL, C., BENTLEY, A. R., BOVILL, W. D., CATTIVELLI, L., COCKRAM, J. & CONTRERAS-MOREIRA, B. 2020. A roadmap for gene functional characterisation in crops with large genomes: Lessons from polyploid wheat. *eLife,* 9**,** e55646.

AHMADI, A. & BAKER, D. 2001. The effect of water stress on the activities of key regulatory enzymes of the sucrose to starch pathway in wheat. *Plant Growth Regulation,* 35**,** 81-91.

AL-DHAHER, S. 2015. *Properties of starch from Australian waxy wheat.* Sydney University.

ALOMARI, D. Z., EGGERT, K., VON WIREN, N., ALQUDAH, A. M., POLLEY, A., PLIESKE, J., GANAL, M. W., PILLEN, K. & RÖDER, M. S. 2018. Identifying candidate genes for enhancing grain Zn concentration in wheat. *Frontiers in Plant Science,* 9**,** 1313.

ALSAFFAR, A. A. 2011. Effect of food processing on the resistant starch content of cereals and cereal products – a review. *International Journal of Food Science & Technology,* 46**,** 455-462.

ANDERSON, J. A., CHAO, S. & LIU, S. 2007. Molecular breeding using a major QTL for Fusarium head blight resistance in wheat. *Crop Science,* 47**,** S-112-S-119.

ANDERSSON, A. A. M., ANDERSSON, R., PIIRONEN, V., LAMPI, A.-M., NYSTRÖM, L., BOROS, D., FRAŚ, A., GEBRUERS, K., COURTIN, C. M., DELCOUR, J. A., RAKSZEGI, M., BEDO, Z., WARD, J. L., SHEWRY, P. R. & ÅMAN, P. 2013. Contents of dietary fibre components and their relation to associated bioactive components in whole grain wheat samples from the HEALTHGRAIN diversity screen. *Food Chemistry,* 136**,** 1243-1248.

ANUGERAH, M. P., FARIDAH, D. N., AFANDI, F. A., HUNAEFI, D. & JAYANEGARA, A. 2022. Annealing processing technique divergently affects starch crystallinity characteristic related to resistant starch content: a literature review and meta-analysis. *International Journal of Food Science & Technology*.

ARCILA, J. A. & ROSE, D. J. 2015. Repeated cooking and freezing of whole wheat flour increases resistant starch with beneficial impacts on in vitro fecal fermentation properties. *Journal of Functional Foods,* 12**,** 230-236.

ARENDT, E. & ZANNINI, E. 2013. Wheat and other Triticum grains. Chapter 1 in: Cereal Grains for the Food and Beverage Industries (pp. 1-57). *In:* COX, R. (ed.). Oxford: Woodhead Publishing.

ARORA, S., STEED, A., GODDARD, R., GAURAV, K., O'HARA, T., SCHOEN, A., RAWAT, N., ELKOT, A. F., KOROLEV, A. V. & CHINOY, C. 2023. A wheat kinase and immune receptor form host-specificity barriers against the blast fungus. *Nature Plants,* 9**,** 385-392.

ATWELL, W. A., HOOD, L. F., LINEBACK, D. R., VARRIANO-MARSTON, E. & ZOBEL, H. F. 1988. The terminology and methodology associated with basic starch phenomena. *Cereal Foods World.,* 33**,** 306.

BAHUGUNA, R. N., GUPTA, P., BAGRI, J., SINGH, D., DEWI, A. K., TAO, L., ISLAM, M., SARSU, F., SINGLA-PAREEK, S. L. & PAREEK, A. 2018. Forward and reverse genetics approaches for combined stress tolerance in rice. *Indian Journal of Plant Physiology,* 23**,** 630-646.

BALDWIN, P. M., MELIA, C. D. & DAVIES, M. C. 1997. The Surface Chemistry of Starch Granules Studied by Time-of-Flight Secondary Ion Mass Spectrometry. *Journal of Cereal Science,* 26**,** 329-346.

BALFOURIER, F., ROUSSEL, V., STRELCHENKO, P., EXBRAYAT-VINSON, F., SOURDILLE, P., BOUTET, G., KOENIG, J., RAVEL, C., MITROFANOVA, O. & BECKERT, M. 2007. A worldwide bread wheat core collection arrayed in a 384-well plate. *Theoretical and Applied Genetics,* 114**,** 1265-1275.

BALL, S. G. & MORELL, M. K. 2003. From bacterial glycogen to starch: understanding the biogenesis of the plant starch granule. *Annu Rev Plant Biol,* 54**,** 207-33.

BALLA, M. Y., GORAFI, Y. S. A., KAMAL, N. M., ABDALLA, M. G. A., TAHIR, I. S. A. & TSUJIMOTO, H. 2022. Harnessing the diversity of wild emmer wheat for genetic improvement of durum wheat. *Theoretical and Applied Genetics,* 135**,** 1671-1684.

BANKS, W. & GREENWOOD, C. T. 1975. Starch and its Components. *Edinburgh University Press*.

BANSAL, U. K., ARIEF, V. N., DELACY, I. H. & BARIANA, H. S. 2013. Exploring wheat landraces for rust resistance using a single marker scan. *Euphytica,* 194**,** 219-233.

BANSAL, U. K., FORREST, K. L., HAYDEN, M. J., MIAH, H., SINGH, D. & BARIANA, H. S. 2011. Characterisation of a new stripe rust resistance gene Yr47 and its genetic association with the leaf rust resistance gene Lr52. *Theoretical and Applied Genetics,* 122**,** 1461-1466.

BATES, D., MAECHLER, M., BOLKER, B. & WALKER, S. 2015. Fitting linear mixed-effects models using lme4. Journal of Statistical Software 67: 1–48.

BECHTEL, D. B. & WILSON, J. D. 2003. Amyloplast formation and starch granule development in hard red winter wheat. *Cereal Chemistry,* 80**,** 175-183.

BECHTEL, D. B., ZAYAS, I., KALEIKAU, L. & POMERANZ, Y. 1990. Size-distribution of wheat starch granules during endosperm development. *Cereal Chem.,* 67**,** 59-63.

BELDEROK, B., MESDAG, J., DONNER, D. A. & MESDAG, H. 2000. Developments in bread-making processes: Bread-making quality of wheat: a century of breeding in Europe (pp. 3-85). *In:* DONNER, D. (ed.). Springer Science & Business Media.

BELITZ, H. D., GROSCH, W. & SCHIEBERLE, P. 2009. Food Chemistry: Carbohydrates (pp. 248-339). *In:* GROSCH, W. (ed.). Springer Berlin Heidelberg.

BELOBRAJDIC, D. P., REGINA, A., KLINGNER, B., ZAJAC, I., CHAPRON, S., BERBEZY, P. & BIRD, A. R. 2019. High-amylose wheat lowers the postprandial glycemic response to bread in healthy adults: A randomized controlled crossover trial. *The Journal of Nutrition,* 149**,** 1335-1345.

BEMILLER, J. N. 2011. Pasting, paste, and gel properties of starch–hydrocolloid combinations. *Carbohydrate Polymers,* 86**,** 386-423.

BERRY, C. S. 1986. Resistant starch: Formation and measurement of starch that survives exhaustive digestion with amylolytic enzymes during the determination of dietary fibre. *Journal of Cereal Science,* 4**,** 301-314.

BERTOFT, E. 2004. Lintnerization of Two Amylose-free Starches of A- and B-Crystalline Types, Respectively. *Starch - Stärke,* 56**,** 167-180.

BERTOFT, E. 2017. Understanding Starch Structure: Recent Progress. *Agronomy,* 7**,** 56.

BERTOFT, E., ANNOR, G. A., SHEN, X., RUMPAGAPORN, P., SEETHARAMAN, K. & HAMAKER, B. R. 2016. Small differences in amylopectin fine structure may explain large functional differences of starch. *Carbohydrate Polymers,* 140**,** 113-121.

BHATTARAI, R. R., DHITAL, S. & GIDLEY, M. J. 2016. Interactions among macronutrients in wheat flour determine their enzymic susceptibility. *Food Hydrocolloids,* 61**,** 415-425.

BHATTARAI, R. R., DHITAL, S., MENSE, A., GIDLEY, M. J. & SHI, Y.-C. 2018. Intact cellular structure in cereal endosperm limits starch digestion in vitro. *Food Hydrocolloids,* 81**,** 139-148.

BIFFEN, R. H. 1905. Mendel's laws of inheritance and wheat breeding. *The Journal of Agricultural Science,* 1**,** 4-48.

BLAAK, E. E., ANTOINE, J. M., BENTON, D., BJÖRCK, I., BOZZETTO, L., BROUNS, F., DIAMANT, M., DYE, L., HULSHOF, T., HOLST, J. J., LAMPORT, D. J., LAVILLE, M., LAWTON, C. L., MEHEUST, A., NILSON, A., NORMAND, S., RIVELLESE, A. A., THEIS, S., TOREKOV, S. S. & VINOY, S. 2012. Impact of postprandial glycaemia on health and prevention of disease. *Obes Rev,* 13**,** 923-84.

BLAUTH, S. L., KIM, K. N., KLUCINEC, J., SHANNON, J. C., THOMPSON, D. & GUILTINAN, M. 2002. Identification of Mutator insertional mutants of starch-branching enzyme 1 (sbe1) in Zea mays L. *Plant Molecular Biology,* 48**,** 287-297.

BLAZEK, J., SALMAN, H., RUBIO, A. L., GILBERT, E., HANLEY, T. & COPELAND, L. 2009. Structural characterization of wheat starch granules differing in amylose content and functional characteristics. *Carbohydrate Polymers,* 75**,** 705-711.

BOITA, E. R. F., ORO, T., BRESSIANI, J., SANTETTI, G. S., BERTOLIN, T. E. & GUTKOSKI, L. C. 2016. Rheological properties of wheat flour dough and pan bread with wheat bran. *Journal of Cereal Science,* 71**,** 177-182.

BORLAUG, N. E. 2007. Sixty-two years of fighting hunger: personal recollections. *Euphytica,* 157**,** 287-297.

BORNHORST, G. M. & SINGH, R. P. 2012. Bolus formation and disintegration during digestion of food carbohydrates. *Comprehensive Reviews in Food Science and Food Safety,* 11**,** 101-118.

BORON, W. F. & BOULPAEP, E. L. 2009. Gastric Function: Medical physiology: a cellular and molecular approach. Saunders (pp. 895-980). Elsevier, Philadelphia, PA.

BORON, W. F. & BOULPAEP, E. L. 2012. The Gastrointestinal System: Medical physiology : a cellular and molecular approach (pp. 881-949). *In:* GRADY, E. (ed.). Saunders.

BORRILL, P., HARRINGTON, S. A. & UAUY, C. 2018. Applying the latest advances in genomics and phenomics for trait discovery in polyploid wheat. *The Plant Journal,* 97**,** 56-72.

BOTTICELLA, E., SESTILI, F., SPARLA, F., MOSCATELLO, S., MARRI, L., CUESTA-SEIJO, J. A., FALINI, G., BATTISTELLI, A., TROST, P. & LAFIANDRA, D. 2018. Combining mutations at genes encoding key enzymes involved in starch synthesis affects the amylose content, carbohydrate allocation and hardness in the wheat grain. *Plant Biotechnology Journal,* 16**,** 1723-1734.

BOUIS, H. E. & SALTZMAN, A. 2017. Improving nutrition through biofortification: A review of evidence from HarvestPlus, 2003 through 2016. *Global Food Security,* 12**,** 49-58.
BRIGGS, D. E. 1992. Barley germination: biochemical changes and hormonal control. *Biotechnology in Agriculture*.
BRITANNICA, E. 2019. *Digestion* [Online]. Available: https://www.britannica.com/ [Accessed].
BROMAN, K. W., WU, H., SEN, Ś. & CHURCHILL, G. A. 2003. R/qtl: QTL mapping in experimental crosses. *Bioinformatics,* 19**,** 889-890.
BRUST, H., ORZECHOWSKI, S. & FETTKE, J. 2020. Starch and glycogen analyses: Methods and techniques. *Biomolecules,* 10**,** 1020.
BUCKLER, E. S. T., THORNSBERRY, J. M. & KRESOVICH, S. 2001. Molecular diversity, structure and domestication of grasses. *Genetical Research,* 77**,** 213-218.
BURROS, B. C., YOUNG, L. A. & CARROAD, P. A. 1987. Kinetics of corn meal gelatinization at high temperature and low moisture. *Journal of Food Science,* 52**,** 1372-1376.
BURT, C., GRIFFE, L., RIDOLFINI, A., ORFORD, S., GRIFFITHS, S. & NICHOLSON, P. 2014. Mining the Watkins collection of wheat landraces for novel sources of eyespot resistance. *Plant Pathology,* 63**,** 1241-1250.
BUTTERWORTH, P. J., WARREN, F. J. & ELLIS, P. R. 2011. Human α-amylase and starch digestion: An interesting marriage. *Starch-Stärke,* 63**,** 395-405.
BUTTERWORTH, P. J., WARREN, F. J., GRASSBY, T., PATEL, H. & ELLIS, P. R. 2012. Analysis of starch amylolysis using plots for first-order kinetics. *Carbohydrate Polymers,* 87**,** 2189-2197.
CAI, L. & SHI, Y.-C. 2013. Self-assembly of short linear chains to A-and B-type starch spherulites and their enzymatic digestibility. *Journal of Agricultural and Food Chemistry,* 61**,** 10787-10797.
CALEY, C., DUFFUS, C. & JEFFCOAT, B. 1990. Effects of elevated temperature and reduced water uptake on enzymes of starch synthesis in developing wheat grains. *Functional Plant Biology,* 17**,** 431-439.
CAPRILES, V., COELHO, K., GUERRA-MATIAS, A. & ARÊAS, J. 2008. Effects of processing methods on amaranth starch digestibility and predicted glycemic index. *Journal of Food Science,* 73**,** H160-H164.
CHEN, A. & DUBCOVSKY, J. 2012. Wheat TILLING mutants show that the vernalization gene VRN1 down-regulates the flowering repressor VRN2 in leaves but is not essential for flowering. *PLoS Genetics,* 8**,** e1003134.
CHEN, L., HUANG, L., MIN, D., PHILLIPS, A., WANG, S., MADGWICK, P. J., PARRY, M. A. J. & HU, Y.-G. 2012. Development and characterization of a new TILLING population of common bread wheat (Triticum aestivum L.). *PloS One,* 7**,** e41570-e41570.
CHEN, M.-H., BERGMAN, C. J., MCCLUNG, A. M., EVERETTE, J. D. & TABIEN, R. E. 2017. Resistant starch: Variation among high amylose rice varieties and its relationship with apparent amylose content, pasting properties and cooking methods. *Food Chemistry,* 234**,** 180-189.
CHIA, T., CHIRICO, M., KING, R., RAMIREZ-GONZALEZ, R., SACCOMANNO, B., SEUNG, D., SIMMONDS, J., TRICK, M., UAUY, C. & VERHOEVEN, T. 2020. A carbohydrate-binding protein, B-GRANULE CONTENT 1, influences starch granule size distribution in a dose-dependent manner in polyploid wheat. *Journal of Experimental Botany,* 71**,** 105-115.

CHUNG, H.-J., LIM, H. S. & LIM, S.-T. 2006. Effect of partial gelatinization and retrogradation on the enzymatic digestion of waxy rice starch. *Journal of Cereal Science,* 43**,** 353-359.

COLLARD, B. C., JAHUFER, M., BROUWER, J. & PANG, E. 2005. An introduction to markers, quantitative trait loci (QTL) mapping and marker-assisted selection for crop improvement: the basic concepts. *Euphytica,* 142**,** 169-196.

COPELAND, L., BLAZEK, J., SALMAN, H. & TANG, M. C. 2009. Form and functionality of starch. *Food Hydrocolloids,* 23**,** 1527-1534.

CORGNEAU, M., GAIANI, C., PETIT, J., NIKOLOVA, Y., BANON, S., RITIÉ-PERTUSA, L., LE, D. T. L. & SCHER, J. 2019. Digestibility of common native starches with reference to starch granule size, shape and surface features towards guidelines for starch-containing food products. *International Journal of Food Science & Technology,* 54**,** 2132-2140.

CORRADO, M., AHN-JARVIS, J. H., FAHY, B., SAVVA, G. M., EDWARDS, C. H. & HAZARD, B. A. 2022a. Effect of high-amylose starch branching enzyme II wheat mutants on starch digestibility in bread, product quality, postprandial satiety and glycaemic response. *Food & Function*.

CORRADO, M., CHERTA-MURILLO, A., CHAMBERS, E. S., WOOD, A. J., PLUMMER, A., LOVEGROVE, A., EDWARDS, C. H., FROST, G. S. & HAZARD, B. A. 2020. Effect of semolina pudding prepared from starch branching enzyme IIa and b mutant wheat on glycaemic response in vitro and in vivo: a randomised controlled pilot study. *Food & Function*.

CORRADO, M., ZAFEIRIOU, P., AHN-JARVIS, J. H., SAVVA, G. M., EDWARDS, C. H. & HAZARD, B. A. 2022b. Impact of storage on starch digestibility and texture of a high-amylose wheat bread. *bioRxiv*.

CROFTS, N., ABE, N., OITOME, N. F., MATSUSHIMA, R., HAYASHI, M., TETLOW, I. J., EMES, M. J., NAKAMURA, Y. & FUJITA, N. 2015. Amylopectin biosynthetic enzymes from developing rice seed form enzymatically active protein complexes. *J Exp Bot,* 66**,** 4469-82.

CROWE, T. C., COPELAND, L. & SELIGMAN, S. A. 2000. Inhibition of Enzymic Digestion of Amylose by Free Fatty Acids In Vitro Contributes to Resistant Starch Formation. *The Journal of Nutrition,* 130**,** 2006-2008.

CUMMINGS, J. H. 1984. Microbial digestion of complex carbohydrates in man. *Proc Nutr Soc,* 43**,** 35-44.

CUMMINGS, J. H. 1997. The large intestine in nutrition and disease (pp. 410). *JOURNAL OF THE ROYAL SOCIETY OF MEDICINE,* 90.

CURTIS, T. & HALFORD, N. 2014. Food security: the challenge of increasing wheat yield and the importance of not compromising food safety. *Annals of Applied Biology,* 164**,** 354-372.

DARLINGTON, H., TECSI, L., HARRIS, N., GRIGGS, D., CANTRELL, I. & SHEWRY, P. 2000. Starch granule associated proteins in barley and wheat. *Journal of Cereal Science,* 32**,** 21-29.

DELCOUR, J. A. 2010. Structure of Cereals. Chapter 1 in: Principles of Cereal Science and Technology (pp. 6-80). *In:* HOSENEY, C. (ed.) 3 ed. St. Paul, MN, USA: AACC International.

DENGATE, H., BARUCH, D. & MEREDITH, P. 1978. The density of wheat starch granules: a tracer dilution procedure for determining the density of an immiscible dispersed phase. *Starch-Stärke,* 30**,** 80-84.

DERKX, A. P. & MARES, D. J. 2020. Late-maturity α-amylase expression in wheat is influenced by genotype, temperature and stage of grain development. *Planta,* 251**,** 1-14.
DEVI, A. F., FIBRIANTO, K., TORLEY, P. J. & BHANDARI, B. 2009. Physical properties of cryomilled rice starch. *Journal of Cereal Science,* 49**,** 278-284.
DHITAL, S., BRENNAN, C. & GIDLEY, M. J. 2019. Location and interactions of starches in planta: Effects on food and nutritional functionality. *Trends in Food Science & Technology,* 93**,** 158-166.
DHITAL, S., DOLAN, G., STOKES, J. R. & GIDLEY, M. J. 2014. Enzymatic hydrolysis of starch in the presence of cereal soluble fibre polysaccharides. *Food & Function,* 5**,** 579-586.
DHITAL, S., GIDLEY, M. J. & WARREN, F. J. 2015. Inhibition of α-amylase activity by cellulose: Kinetic analysis and nutritional implications. *Carbohydrate Polymers,* 123**,** 305-312.
DHITAL, S., SHRESTHA, A. K. & GIDLEY, M. J. 2010. Effect of cryo-milling on starches: Functionality and digestibility. *Food Hydrocolloids,* 24**,** 152-163.
DIJK, M., MORLEY, T., RAU, M. L. & SAGHAI, Y. 2021. A meta-analysis of projected global food demand and population at risk of hunger for the period 2010–2050. *Nature Food,* 2**,** 494-501.
DIXON, L. E., GREENWOOD, J. R., BENCIVENGA, S., ZHANG, P., COCKRAM, J., MELLERS, G., RAMM, K., CAVANAGH, C., SWAIN, S. M. & BODEN, S. A. 2018. TEOSINTE BRANCHED1 regulates inflorescence architecture and development in bread wheat (Triticum aestivum). *The Plant Cell,* 30**,** 563-581.
DOEBLEY, J. F., GAUT, B. S. & SMITH, B. D. 2006. The Molecular Genetics of Crop Domestication. *Cell,* 127**,** 1309-1321.
DONA, A. C., PAGES, G., GILBERT, R. G. & KUCHEL, P. W. 2010. Digestion of starch: In vivo and in vitro kinetic models used to characterise oligosaccharide or glucose release. *Carbohydrate Polymers,* 80**,** 599-617.
DONALD, A. M. 2001. Plasticization and Self Assembly in the Starch Granule. *Cereal Chemistry,* 78**,** 307-314.
DONG, C. D. M., VINCENT, J. & KATE SHARP, P. 2009. A modified TILLING method for wheat breeding. *The Plant Genome,* 2.
DREHER, K., KHAIRALLAH, M., RIBAUT, J.-M. & MORRIS, M. 2003. Money matters (I): costs of field and laboratory procedures associated with conventional and marker-assisted maize breeding at CIMMYT. *Molecular Breeding,* 11**,** 221-234.
DREISIGACKER, S., KISHII, M., LAGE, J. & WARBURTON, M. 2008. Use of synthetic hexaploid wheat to increase diversity for CIMMYT bread wheat improvement. *Australian Journal of Agricultural Research,* 59**,** 413-420.
DUBCOVSKY, J. & DVORAK, J. 2007. Genome plasticity a key factor in the success of polyploid wheat under domestication. *Science,* 316.
DVORAK, J., LUO, M.-C., YANG, Z.-L. & ZHANG, H.-B. 1998. The structure of the Aegilops tauschii genepool and the evolution of hexaploid wheat. *Theoretical and Applied Genetics,* 97**,** 657-670.
DYCK, P. & JEDEL, P. 1989. Genetics of resistance to leaf rust in two accessions of common wheat. *Canadian Journal of Plant Science,* 69**,** 531-534.
EDWARDS, C. H., COCHETEL, N., SETTERFIELD, L., PEREZ-MORAL, N. & WARREN, F. J. 2019. A single-enzyme system for starch digestibility screening and its relevance to understanding and predicting the glycaemic index of food products. *Food & Function,* 10**,** 4751-4760.

EDWARDS, C. H., GRUNDY, M. M., GRASSBY, T., VASILOPOULOU, D., FROST, G. S., BUTTERWORTH, P. J., BERRY, S. E., SANDERSON, J. & ELLIS, P. R. 2015. Manipulation of starch bioaccessibility in wheat endosperm to regulate starch digestion, postprandial glycemia, insulinemia, and gut hormone responses: a randomized controlled trial in healthy ileostomy participants. *The American Journal of Clinical Nutrition,* 102**,** 791-800.

EDWARDS, C. H., MAILLOT, M., PARKER, R. & WARREN, F. J. 2018. A comparison of the kinetics of in vitro starch digestion in smooth and wrinkled peas by porcine pancreatic alpha-amylase. *Food Chemistry,* 244**,** 386-393.

EDWARDS, C. H., RYDEN, P., MANDALARI, G., BUTTERWORTH, P. J. & ELLIS, P. R. 2021. Structure–function studies of chickpea and durum wheat uncover mechanisms by which cell wall properties influence starch bioaccessibility. *Nature Food,* 2**,** 118-126.

EDWARDS, C. H., WARREN, F. J., MILLIGAN, P. J., BUTTERWORTH, P. J. & ELLIS, P. R. 2014. A novel method for classifying starch digestion by modelling the amylolysis of plant foods using first-order enzyme kinetic principles. *Food & Function,* 5**,** 2751-2758.

ENGLYST, H. N. & CUMMINGS, J. H. 1985. Digestion of the polysaccharides of some cereal foods in the human small intestine. *American Journal of Clinical Nutrition,* 42**,** 778-787.

ENGLYST, H. N., KINGMAN, S. M. & CUMMINGS, J. H. 1992. Classification and measurement of nutritionally important starch fractions. *European Journal of Clinical Nutrition,* 46 Suppl 2**,** S33-50.

ENGLYST, H. N., VEENSTRA, J. & HUDSON, G. J. 1996. Measurement of rapidly available glucose (RAG) in plant foods: a potential in vitro predictor of the glycaemic response. *British Journal of Nutrition,* 75**,** 327-337.

ENGLYST, K. N., ENGLYST, H. N., HUDSON, G. J., COLE, T. J. & CUMMINGS, J. H. 1999. Rapidly available glucose in foods: an in vitro measurement that reflects the glycemic response. *The American Journal of Clinical Nutrition,* 69**,** 448-454.

ESPOSITO, S., BOWSHER, C. G., EMES, M. J. & TETLOW, I. J. 1999. Phosphoglucomutase activity during development of wheat grains. *Journal of Plant Physiology,* 154**,** 24-29.

EVENSON, R. E. & GOLLIN, D. 2003. Assessing the impact of the Green Revolution, 1960 to 2000. *Science,* 300**,** 758-762.

EVERS, T. & MILLAR, S. 2002. Cereal Grain Structure and Development: Some Implications for Quality. *Journal of Cereal Science,* 36**,** 261-284.

FAHY, B., GONZALEZ, O., SAVVA, G. M., AHN-JARVIS, J. H., WARREN, F. J., DUNN, J., LOVEGROVE, A. & HAZARD, B. A. 2022. Loss of starch synthase IIIa changes starch molecular structure and granule morphology in grains of hexaploid bread wheat. *Scientific Reports,* 12**,** 1-14.

FAHY, B., SIDDIQUI, H., DAVID, L. C., POWERS, S. J., BORRILL, P., UAUY, C. & SMITH, A. M. 2018. Final grain weight is not limited by the activity of key starch-synthesising enzymes during grain filling in wheat. *Journal of Experimental Botany,* 69**,** 5461-5475.

FAO 2018. Food Security and Nutrition Around the World in 2018. Chapter 1 in: The state of food security and nutrition in the world 2018: building climate resilience for food security and nutrition (pp. 1-26). *In:* CANTILLO, M. (ed.). Food & Agriculture Org.

FERNANDES, J., VOGT, J. & WOLEVER, T. M. 2014. Kinetic model of acetate metabolism in healthy and hyperinsulinaemic humans. *Eur J Clin Nutr,* 68**,** 1067-71.

FOX, G. 2018. Starch in Brewing Applications. Chapter 16 in: Starch in Food (Second Edition): Structure, Function and Applications. Woodhead Publishing Series in Food Science, Technology and Nutrition.

FRENCH, D. 1972. Fine structure of starch and its relationship to the organization of starch granules. *Journal of the Japanese Society of Starch Science,* 19**,** 8-25.

FUJITA, N., SATOH, R., HAYASHI, A., KODAMA, M., ITOH, R., AIHARA, S. & NAKAMURA, Y. 2011. Starch biosynthesis in rice endosperm requires the presence of either starch synthase I or IIIa. *Journal of Experimental Botany,* 62**,** 4819-4831.

GALLANT, D. J., BOUCHET, B. & BALDWIN, P. M. J. C. P. 1997. Microscopy of starch: evidence of a new level of granule organization. *Carbohydrate Polymers,* 32**,** 177-191.

GANAL, M. W., PLIESKE, J., HOHMEYER, A., POLLEY, A. & RÖDER, M. S. 2019. High-throughput genotyping for cereal research and breeding. Chapter 1 in: Applications of Genetic and Genomic Research in Cereals. (pp. 3-17). *In:* MIEDANER, T. (ed.). Woodhead Publishing.

GATES, D. J., RUNCIE, D., JANZEN, G. M., NAVARRO, A. R., WILLCOX, M., SONDER, K., SNODGRASS, S. J., RODRÍGUEZ-ZAPATA, F., SAWERS, R. J. & RELLÁN-ÁLVAREZ, R. 2019. Single-gene resolution of locally adaptive genetic variation in Mexican maize. *BioRxiv***,** 706739.

GAUT, B. S., SEYMOUR, D. K., LIU, Q. & ZHOU, Y. 2018. Demography and its effects on genomic variation in crop domestication. *Nature Plants,* 4**,** 512-520.

GAUTIER, M.-F., COSSON, P., GUIRAO, A., ALARY, R. & JOUDRIER, P. 2000. Puroindoline genes are highly conserved in diploid ancestor wheats and related species but absent in tetraploid Triticum species. *Plant Science,* 153**,** 81-91.

GEBRUERS, K., DORNEZ, E., BOROS, D., FRAŚ, A., DYNKOWSKA, W., BEDŐ, Z., RAKSZEGI, M., DELCOUR, J. A. & COURTIN, C. M. 2008. Variation in the Content of Dietary Fiber and Components Thereof in Wheats in the HEALTHGRAIN Diversity Screen. *Journal of Agricultural and Food Chemistry,* 56**,** 9740-9749.

GIDLEY, M. J. & BULPIN, P. V. 1989. Aggregation of amylose in aqueous systems: the effect of chain length on phase behavior and aggregation kinetics. *Macromolecules,* 22**,** 341-346.

GOODE, D. L., ULMER, H. M. & ARENDT, E. K. 2005. Model studies to understand the effects of amylase additions and pH adjustment on the rheological behaviour of simulated brewery mashes. *Journal of the Institute of Brewing,* 111**,** 153-164.

GRASSINI, P., ESKRIDGE, K. M. & CASSMAN, K. G. 2013. Distinguishing between yield advances and yield plateaus in historical crop production trends. *Nature Communications,* 4**,** 2918-2918.

GREENWELL, P. 1986. A starch granule protein associated with endosperm softness in wheat. *Cereal Chem.,* 63**,** 379-380.

GRIFFITHS, S., SIMMONDS, J., LEVERINGTON, M., WANG, Y., FISH, L., SAYERS, L., ALIBERT, L., ORFORD, S., WINGEN, L. & SNAPE, J. 2012. Meta-QTL analysis of the genetic control of crop height in elite European winter wheat germplasm. *Molecular Breeding,* 29**,** 159-171.

GRIME, K. & BRIGGS, D. 1996. The release of bound β-amylase by macromolecules. *Journal of the Institute of Brewing,* 102**,** 261-270.
GUAN, H. P. & PREISS, J. 1993. Differentiation of the properties of the branching isozymes from maize (Zea mays). *Plant Physiology,* 102**,** 1269-1273.
GUERRA, A., ETIENNE-MESMIN, L., LIVRELLI, V., DENIS, S., BLANQUET-DIOT, S. & ALRIC, M. 2012. Relevance and challenges in modeling human gastric and small intestinal digestion. *Trends in Biotechnology,* 30**,** 591-600.
GUO, Y., QIAO, D., ZHAO, S., ZHANG, B. & XIE, F. 2021. Starch-based materials encapsulating food ingredients: Recent advances in fabrication methods and applications. *Carbohydrate Polymers,* 270**,** 118358.
GURAYA, H. S., KADAN, R. S. & CHAMPAGNE, E. T. 1997. Effect of rice starch-lipid complexes on in vitro digestibility, complexing index, and viscosity. *Cereal Chemistry,* 74**,** 561-565.
HADNAĐEV, M. S., HADNAĐEV-DAPČEVIĆ, T., POJIĆ, M. M., ŠARIĆ, B. M., MIŠAN, A. Č., JOVANOV, P. T. & SAKAČ, M. B. 2017. Progress in vegetable proteins isolation techniques: A review. *Food and Feed Research,* 44**,** 11-21.
HAGUE, A., MANNING, A. M., HANLON, K. A., HUSCHTSCHA, L. I., HART, D. & PARASKEVA, C. 1993. Sodium butyrate induces apoptosis in human colonic tumour cell lines in a p53-independent pathway: implications for the possible role of dietary fibre in the prevention of large-bowel cancer. *Int J Cancer,* 55**,** 498-505.
HALLORAN, G., OGBONNAYA, F. & LAGUDAH, E. 2008. Triticum (Aegilops) tauschii in the natural and artificial synthesis of hexaploid wheat. *Australian Journal of Agricultural Research,* 59**,** 475-490.
HAN, X.-Z. & HAMAKER, B. R. 2001. Amylopectin fine structure and rice starch paste breakdown. *Journal of Cereal Science,* 34**,** 279-284.
HARDY, K., BUCKLEY, S., COLLINS, M. J., ESTALRRICH, A., BROTHWELL, D., COPELAND, L., GARCÍA-TABERNERO, A., GARCÍA-VARGAS, S., DE LA RASILLA, M. & LALUEZA-FOX, C. 2012. Neanderthal medics? Evidence for food, cooking, and medicinal plants entrapped in dental calculus. *Naturwissenschaften,* 99**,** 617-626.
HARDY, K., RADINI, A., BUCKLEY, S., BLASCO, R., COPELAND, L., BURJACHS, F., GIRBAL, J., YLL, R., CARBONELL, E. & BERMÚDEZ DE CASTRO, J. M. 2017. Diet and environment 1.2 million years ago revealed through analysis of dental calculus from Europe's oldest hominin at Sima del Elefante, Spain. *The Science of Nature,* 104**,** 1-5.
HASJIM, J., AI, Y. & JANE, J. L. 2013. Novel applications of amylose-lipid complex as resistant starch type 5. *Resistant Starch: Sources, Applications and Health Benefits***,** 79-94.
HAUDRY, A., CENCI, A., RAVEL, C., BATAILLON, T., BRUNEL, D., PONCET, C., HOCHU, I., POIRIER, S., SANTONI, S. & GLÉMIN, S. 2007. Grinding up wheat: a massive loss of nucleotide diversity since domestication. *Molecular Biology and Evolution,* 24**,** 1506-1517.
HAWKINS, E., CHEN, J., WATSON-LAZOWSKI, A., AHN-JARVIS, J., BARCLAY, J. E., FAHY, B., HARTLEY, M., WARREN, F. J. & SEUNG, D. 2021. STARCH SYNTHASE 4 is required for normal starch granule initiation in amyloplasts of wheat endosperm. *BioRxiv*.
HAWORTH, W. N., PEAT, S. & BOURNE, E. J. 1944. Synthesis of amylopectin. *Nature,* 154**,** 236.

HAZARD, B., TRAFFORD, K., LOVEGROVE, A., GRIFFITHS, S., UAUY, C. & SHEWRY, P. 2020. Strategies to improve wheat for human health. *Nature Food,* 1**,** 475-480.

HAZARD, B., ZHANG, X., COLASUONNO, P., UAUY, C., BECKLES, D. M. & DUBCOVSKY, J. 2012. Induced mutations in the starch branching enzyme II (SBEII) genes increase amylose and resistant starch content in durum wheat. *Crop Science,* 52**,** 1754-1766.

HAZARD, B., ZHANG, X., NAEMEH, M. & DUBCOVSKY, J. 2014. Registration of Durum Wheat Germplasm Lines with Combined Mutations in SBEII a and SBEIIb Genes Conferring Increased Amylose and Resistant Starch. *Journal of Plant Registrations,* 8**,** 334-338.

HAZARD, B., ZHANG, X., NAEMEH, M., HAMILTON, M. K., RUST, B., RAYBOULD, H. E., NEWMAN, J. W., MARTIN, R. & DUBCOVSKY, J. 2015. Mutations in durum wheat SBEII genes affect grain yield components, quality, and fermentation responses in rats. *Crop science,* 55**,** 2813-2825.

HE, C., HOLME, J. & ANTHONY, J. 2014. SNP genotyping: the KASP assay. *Crop Breeding: Methods and Protocols***,** 75-86.

HEERDT, B. G., HOUSTON, M. A. & AUGENLICHT, L. H. 1994. Potentiation by specific short-chain fatty acids of differentiation and apoptosis in human colonic carcinoma cell lines. *Cancer Res,* 54**,** 3288-93.

HERNANDEZ, M. V., CROSSA, J., SINGH, P. K., BAINS, N. S., SINGH, K. & SHARMA, I. 2012. Multi-trait and multi-environment QTL analyses for resistance to wheat diseases. *PLoS One,* 7**,** e38008.

HIZUKURI, S., TAKEDA, Y., MARUTA, N. & JULIANO, B. O. 1989. Molecular structures of rice starch. *Carbohydrate Research,* 189**,** 227-235.

HIZUKURI, S., TAKEDA, Y., YASUDA, M. & SUZUKI, A. 1981. Multi-branched nature of amylose and the action of debranching enzymes. *Carbohydrate Research,* 94**,** 205-213.

HOGG, A. C., GAUSE, K., HOFER, P., MARTIN, J. M., GRAYBOSCH, R. A., HANSEN, L. E. & GIROUX, M. J. 2013. Creation of a high-amylose durum wheat through mutagenesis of starch synthase II (SSIIa). *Journal of Cereal Science,* 57**,** 377-383.

HOGG, A. C., MARTIN, J. M. & GIROUX, M. J. 2017. Novel ssIIa alleles produce specific seed amylose levels in hexaploid wheat. *Cereal Chemistry,* 94**,** 1008-1015.

HOLM, J., BJÖRCK, I., OSTROWSKA, S., ELIASSON, A.-C., ASP, N.-G., LARSSON, K. & LUNDQUIST, I. 1983. Digestibility of Amylose-Lipid Complexes in-vitro and in-vivo. *Starch - Stärke,* 35**,** 294-297.

HOLM, J., LUNDQUIST, I., BJÖRCK, I., ELIASSON, A.-C. & ASP, N.-G. 1988. Degree of starch gelatinization, digestion rate of starch in vitro, and metabolic response in rats. *The American Journal of Clinical Nutrition,* 47**,** 1010-1016.

HOLME, I. B., GREGERSEN, P. L. & BRINCH-PEDERSEN, H. 2019. Induced genetic variation in crop plants by random or targeted mutagenesis: convergence and differences. *Frontiers in Plant Science,* 10.

HOU, J., DENG, H., WANG, Y., LIU, C., GENG, S., LI, W., QIN, M., DAI, Z., SHI, X. & YANG, P. 2022. Starch Bio-Synthetic Pathway Genes Contribute to Resistant Starch Content Differentiation in Bread Wheat. *Agronomy,* 12**,** 2967.

HU, P., ZHAO, H., DUAN, Z., LINLIN, Z. & WU, D. 2004. Starch digestibility and the estimated glycemic score of different types of rice differing in amylose contents. *Journal of Cereal Science,* 40**,** 231-237.

HUANG, B. E., GEORGE, A. W., FORREST, K. L., KILIAN, A., HAYDEN, M. J., MORELL, M. K. & CAVANAGH, C. R. 2012. A multiparent advanced generation inter-cross population for genetic analysis in wheat. *Plant Biotechnology Journal,* 10**,** 826-839.

HUANG, X., BÖRNER, A., RÖDER, M. & GANAL, M. 2002. Assessing genetic diversity of wheat (Triticum aestivum L.) germplasm using microsatellite markers. *Theoretical and Applied Genetics,* 105**,** 699-707.

HUCL, P. & CHIBBAR, R. N. 1996. Variation for starch concentration in spring wheat and its repeatability relative to protein concentration. *Cereal Chemistry,* 73**,** 756-758.

HUGHES, R. L., HORN, W. H., FINNEGAN, P., NEWMAN, J. W., MARCO, M. L., KEIM, N. L. & KABLE, M. E. 2021. Resistant Starch Type 2 from Wheat Reduces Postprandial Glycemic Response with Concurrent Alterations in Gut Microbiota Composition. *Nutrients,* 13.

IMBERTY, A., BULÉON, A., TRAN, V. & PÉEREZ, S. 1991. Recent Advances in Knowledge of Starch Structure. *Starch - Stärke,* 43**,** 375-384.

IMBERTY, A. & PÉREZ, S. 1989. Conformational analysis and molecular modelling of the branching point of amylopectin. *International Journal of Biological Macromolecules,* 11**,** 177-185.

JAMES, R. A., BLAKE, C., BYRT, C. S. & MUNNS, R. 2011. Major genes for Na+ exclusion, Nax1 and Nax2 (wheat HKT1; 4 and HKT1; 5), decrease Na+ accumulation in bread wheat leaves under saline and waterlogged conditions. *Journal of Experimental Botany,* 62**,** 2939-2947.

JANE, J. & ROBYT, J. F. 1984. Structure studies of amylose-V complexes and retrograded amylose by action of alpha amylases, and a new method for preparing amylodextrins. *Carbohydr Res,* 132**,** 105-18.

JENKINS, D. J., KENDALL, C. W., AUGUSTIN, L. S., FRANCESCHI, S., HAMIDI, M., MARCHIE, A., JENKINS, A. L. & AXELSEN, M. 2002. Glycemic index: overview of implications in health and disease. *The American Journal of Clinical Nutrition,* 76**,** 266S-273S.

JENKINS, P. & DONALD, A. J. I. J. O. B. M. 1995. The influence of amylose on starch granule structure. *International Journal of Biological Macromolecules,* 17**,** 315-321.

JENKINS, P. J., CAMERON, R. E. & DONALD, A. M. 1993. A Universal Feature in the Structure of Starch Granules from Different Botanical Sources. *Starch - Stärke,* 45**,** 417-420.

JENNER, C., UGALDE, T. & ASPINALL, D. 1991. The physiology of starch and protein deposition in the endosperm of wheat. *Functional Plant Biology,* 18**,** 211-226.

JESWANI, H. K., BURKINSHAW, R. & AZAPAGIC, A. 2015. Environmental sustainability issues in the food–energy–water nexus: Breakfast cereals and snacks. *Sustainable Production and Consumption,* 2**,** 17-28.

JI, N., LIU, C., LI, M., SUN, Q. & XIONG, L. 2018. Interaction of cellulose nanocrystals and amylase: Its influence on enzyme activity and resistant starch content. *Food Chemistry,* 245**,** 481-487.

JONES, R. G., PURE, I. U. O., DIVISION, A. C. P. & WILKS, E. S. 2009. Compendium of polymer terminology and nomenclature: Terminology. IUPAC recommendations, (pp. 56-63). *In:* JONES, R. (ed.). RSC Pub.

JORDAN, K. W., WANG, S., HE, F., CHAO, S., LUN, Y., PAUX, E., SOURDILLE, P., SHERMAN, J., AKHUNOVA, A. & BLAKE, N. K. 2018. The genetic architecture of genome-wide recombination rate variation in allopolyploid wheat revealed by nested association mapping. *The Plant Journal,* 95**,** 1039-1054.

JOYE, I. J., LAGRAIN, B. & DELCOUR, J. A. 2009. Endogenous redox agents and enzymes that affect protein network formation during breadmaking–A review. *Journal of Cereal Science,* 50**,** 1-10.

JUHLIN-DANNFELT, A. 1977. Ethanol effects of substrate utilization by the human brain. *Scand J Clin Lab Invest,* 37**,** 443-9.

KAN, L., OLIVIERO, T., VERKERK, R., FOGLIANO, V. & CAPUANO, E. 2020. Interaction of bread and berry polyphenols affects starch digestibility and polyphenols bio-accessibility. *Journal of Functional Foods,* 68**,** 103924.

KAUFMAN, R. C., WILSON, J. D., BEAN, S. R., HERALD, T. J. & SHI, Y. C. 2015. Development of a 96-well plate iodine binding assay for amylose content determination. *Carbohydrate Polymers,* 115**,** 444-447.

KAUR, B., MAVI, G., GILL, M. S. & SAINI, D. K. 2020. Utilization of KASP technology for wheat improvement. *Cereal Research Communications,* 48**,** 409-421.

KAWAI, K., TAKATO, S., SASAKI, T. & KAJIWARA, K. 2012. Complex formation, thermal properties, and in-vitro digestibility of gelatinized potato starch–fatty acid mixtures. *Food Hydrocolloids,* 27**,** 228-234.

KEELING, P. L., BANISADR, R., BARONE, L., WASSERMAN, B. & SINGLETARY, G. 1994. Effect of temperature on enzymes in the pathway of starch biosynthesis in developing wheat and maize grain. *Functional Plant Biology,* 21**,** 807-827.

KHOKHAR, J. S., KING, J., KING, I. P., YOUNG, S. D., FOULKES, M. J., DE SILVA, J., WEERASINGHE, M., MOSSA, A., GRIFFITHS, S. & RICHE, A. B. 2020. Novel sources of variation in grain Zinc (Zn) concentration in bread wheat germplasm derived from Watkins landraces. *PLoS One,* 15**,** e0229107.

KIANFAR, E. 2021. Protein nanoparticles in drug delivery: animal protein, plant proteins and protein cages, albumin nanoparticles. *Journal of Nanobiotechnology,* 19**,** 159.

KIM, H.-S., HAN, M.-R., KIM, A.-J. & KIM, M.-H. 2011. Physicochemical property changes in wheat starch by ultra-fine pulverization. *Food Science and Biotechnology,* 20**,** 137-142.

KIM, W. K., CHUNG, M. K., KANG, N. E., KIM, M. H. & PARK, O. J. 2003. Effect of resistant starch from corn or rice on glucose control, colonic events, and blood lipid concentrations in streptozotocin-induced diabetic rats. *Journal of Nutritional Biochemistry,* 14**,** 166-172.

KING, R., NOAKES, M., BIRD, A., MORELL, M. & TOPPING, D. 2008. An extruded breakfast cereal made from a high amylose barley cultivar has a low glycemic index and lower plasma insulin response than one made from a standard barley. *Journal of Cereal Science,* 48**,** 526-530.

KLEIN, S., COHN, S. & ALPERS, D. 1998. The alimentary tract in nutrition. *Modern Nutrition in Health and Disease,* 9**,** 605-629.

KNUTSON, C. 1986. A simplified colorimetric procedure for determination of amylose in maize starches. *Cereal Chem,* 63**,** 89-92.

KNUTSON, C. & GROVE, M. 1994. Rapid method for estimation of amylose in maize starches. *Cereal Chemistry,* 71**,** 469-471.

KOEV, T. T., MUÑOZ-GARCÍA, J. C., IUGA, D., KHIMYAK, Y. Z. & WARREN, F. J. 2020. Structural heterogeneities in starch hydrogels. *Carbohydrate Polymers,* 249**,** 116834.

KOHYAMA, N., CHONO, M., NAKAGAWA, H., MATSUO, Y., ONO, H. & MATSUNAKA, H. 2017. Flavonoid compounds related to seed coat color of wheat. *Bioscience, Biotechnology and Biochemistry,* 81**,** 2112-2118.

KOROMPOKIS, K., DE BRIER, N. & DELCOUR, J. A. 2019. Differences in endosperm cell wall integrity in wheat (Triticum aestivum L.) milling fractions impact on the way starch responds to gelatinization and pasting treatments and its subsequent enzymatic in vitro digestibility. *Food & Function,* 10**,** 4674-4684.

KOROTEEVA, D. A., KISELEVA, V. I., KRIVANDIN, A. V., SHATALOVA, O. V., BŁASZCZAK, W., BERTOFT, E., PIYACHOMKWAN, K. & YURYEV, V. P. 2007. Structural and thermodynamic properties of rice starches with different genetic background: Part 2. Defectiveness of different supramolecular structures in starch granules. *International Journal of Biological Macromolecules,* 41**,** 534-547.

KOZLOV, S. S., NODA, T., BERTOFT, E. & YURYEV, V. P. 2006. Structure of starches extracted from near isogenic wheat lines: Part I. Effect of different GBSS I combinations. *Journal of Thermal Analysis and Calorimetry,* 86**,** 291-301.

KRASILEVA, K. V., VASQUEZ-GROSS, H. A., HOWELL, T., BAILEY, P., PARAISO, F., CLISSOLD, L., SIMMONDS, J., RAMIREZ-GONZALEZ, R. H., WANG, X. & BORRILL, P. 2017. Uncovering hidden variation in polyploid wheat. *Proceedings of the National Academy of Sciences,* 114**,** E913-E921.

KUMAR, J., JAISWAL, V., KUMAR, A., KUMAR, N., MIR, R., KUMAR, S., DHARIWAL, R., TYAGI, S., KHANDELWAL, M. & PRABHU, K. 2011. Introgression of a major gene for high grain protein content in some Indian bread wheat cultivars. *Field Crops Research,* 123**,** 226-233.

KUMAR, J., MIR, R., KUMAR, N., KUMAR, A., MOHAN, A., PRABHU, K., BALYAN, H. & GUPTA, P. 2010a. Marker-assisted selection for pre-harvest sprouting tolerance and leaf rust resistance in bread wheat. *Plant Breeding,* 129**,** 617-621.

KUMAR, J., SARIPALLI, G., GAHLAUT, V., GOEL, N., MEHER, P. K., MISHRA, K. K., MISHRA, P. C., SEHGAL, D., VIKRAM, P. & SANSALONI, C. 2018. Genetics of Fe, Zn, β-carotene, GPC and yield traits in bread wheat (Triticum aestivum L.) using multi-locus and multi-traits GWAS. *Euphytica,* 214**,** 1-17.

KUMAR, V., SINHA, A. K., MAKKAR, H. P. S. & BECKER, K. 2010b. Dietary roles of phytate and phytase in human nutrition: A review. *Food Chemistry,* 120**,** 945-959.

KUNZETSOVA, A., BROCKHOFF, P. & CHRISTENSEN, R. 2017. lmerTest package: tests in linear mixed effect models. *J Stat Softw,* 82**,** 1-26.

KURIKI, T., STEWART, D. C. & PREISS, J. 1997. Construction of chimetic enzymes out of maize endosperm branching enzymes I and II: Activity and properties. *Journal of Biological Chemistry,* 272**,** 28999-29004.

KUSUMAH, S., ANDOYO, R. & RIALITA, T. Protein isolation techniques of beans using different methods: A review. IOP Conference Series: Earth and Environmental Science, 2020. IOP Publishing, 012053.

LABUDA, J., BOWATER, R. P., FOJTA, M., GAUGLITZ, G., GLATZ, Z., HAPALA, I., HAVLIŠ, J., KILAR, F., KILAR, A. & MALINOVSKÁ, L. 2018. Terminology of bioanalytical methods (IUPAC Recommendations 2018). *Pure and Applied Chemistry,* 90**,** 1121-1198.

LADDOMADA, B., CARETTO, S. & MITA, G. 2015. Wheat bran phenolic acids: Bioavailability and stability in whole wheat-based foods. *Molecules,* 20**,** 15666-15685.
LAFIANDRA, D., SESTILI, F., D'OVIDIO, R., JANNI, M., BOTTICELLA, E., FERRAZZANO, G., SILVESTRI, M., RANIERI, R. & DEAMBROGIO, E. 2010. Approaches for modification of starch composition in durum wheat. *Cereal Chemistry,* 87**,** 28-34.
LANGEVELD, S. M., VAN WIJK, R., STUURMAN, N., KIJNE, J. W. & DE PATER, S. 2000. B-type granule containing protrusions and interconnections between amyloplasts in developing wheat endosperm revealed by transmission electron microscopy and GFP expression. *Journal of Experimental Botany,* 51**,** 1357-1361.
LATEEF, D. D. 2015. DNA marker technologies in plants and applications for crop improvements. *Journal of Biosciences and Medicines,* 3**,** 7.
LEEMAN, A. M., KARLSSON, M. E., ELIASSON, A.-C. & BJÖRCK, I. M. 2006. Resistant starch formation in temperature treated potato starches varying in amylose/amylopectin ratio. *Carbohydrate Polymers,* 65**,** 306-313.
LEITAO, J. 2011. Plant mutation breeding and biotechnology. *Chemical Mutagenesis***,** 135-158.
LELIEVRE, J. 1974. Starch gelatinization. *Journal of Applied Polymer Science,* 18**,** 293-296.
LENG, G. & HALL, J. 2019. Crop yield sensitivity of global major agricultural countries to droughts and the projected changes in the future. *Science of The Total Environment,* 654**,** 811-821.
LEVER, M. 1972. A new reaction for colorimetric determination of carbohydrates. *Analytical Biochemistry,* 47**,** 273-279.
LI, C., DHITAL, S., GILBERT, R. G. & GIDLEY, M. J. 2020a. High-amylose wheat starch: Structural basis for water absorption and pasting properties. *Carbohydrate Polymers,* 245**,** 116557.
LI, C., WU, A. C., GO, R. M., MALOUF, J., TURNER, M. S., MALDE, A. K., MARK, A. E. & GILBERT, R. G. 2015. The characterization of modified starch branching enzymes: toward the control of starch chain-length distributions. *PLoS One,* 10**,** e0125507.
LI, H.-T., SARTIKA, R. S., KERR, E. D., SCHULZ, B. L., GIDLEY, M. J. & DHITAL, S. 2020b. Starch granular protein of high-amylose wheat gives innate resistance to amylolysis. *Food Chemistry,* 330**,** 127328.
LI, H., DHITAL, S., SLADE, A. J., YU, W., GILBERT, R. G. & GIDLEY, M. J. 2019. Altering starch branching enzymes in wheat generates high-amylose starch with novel molecular structure and functional properties. *Food Hydrocolloids*.
LI, H., GIDLEY, M. J. & DHITAL, S. 2019. High-Amylose Starches to Bridge the "Fiber Gap": Development, Structure, and Nutritional Functionality. *Comprehensive Reviews in Food Science and Food Safety*.
LIM, M. H., WU, H. & REID, D. S. 2000. The effect of starch gelatinization and solute concentrations on T g' of starch model system. *Journal of the Science of Food and Agriculture,* 80**,** 1757-1762.
LIN, A. H.-M., HAMAKER, B. R. & NICHOLS JR, B. L. 2012. Direct starch digestion by sucrase-isomaltase and maltase-glucoamylase. *Journal of Pediatric Gastroenterology and Nutrition,* 55**,** S43-S45.
LIN, A. H., LEE, B. H., NICHOLS, B. L., QUEZADA-CALVILLO, R., ROSE, D. R., NAIM, H. Y. & HAMAKER, B. R. 2012. Starch source influences dietary glucose

generation at the mucosal alpha-glucosidase level. *J Biol Chem,* 287**,** 36917-21.
LINDEBOOM, N., CHANG, P. R. & TYLER, R. T. 2004. Analytical, Biochemical and Physicochemical Aspects of Starch Granule Size, with Emphasis on Small Granule Starches: A Review. *Starch - Stärke,* 56**,** 89-99.
LINDENEG, O., MELLEMGA, K., FABRICIU, J. & LUNDQUIS, F. 1964. MYOCARDIAL UTILIZATION OF ACETATE LACTATE AND FREE FATTY ACIDS AFTER INGESTION OF ETHANOL. *Clinical Science,* 27**,** 427-&.
LIU, H. S., XIE, F. W., YU, L., CHEN, L. & LI, L. 2009. Thermal processing of starch-based polymers. *Progress in Polymer Science,* 34**,** 1348-1368.
LIU, P., GUO, W., JIANG, Z., PU, H., FENG, C., ZHU, X., PENG, Y., KUANG, A. & LITTLE, C. 2011. Effects of high temperature after anthesis on starch granules in grains of wheat (Triticum aestivum L.). *The Journal of Agricultural Science,* 149**,** 159-169.
LIU, Q., GU, Z., DONNER, E., TETLOW, I. & EMES, M. 2007. Investigation of digestibility in vitro and physicochemical properties of A- and B-type starch from soft and hard wheat flour. *Cereal Chemistry,* 84**,** 15-21.
LIU, W., MACCAFERRI, M., BULLI, P., RYNEARSON, S., TUBEROSA, R., CHEN, X. & PUMPHREY, M. 2017. Genome-wide association mapping for seedling and field resistance to Puccinia striiformis f. sp. tritici in elite durum wheat. *Theoretical and Applied Genetics,* 130**,** 649-667.
LÓPEZ-BARÓN, N., GU, Y., VASANTHAN, T. & HOOVER, R. 2017. Plant proteins mitigate in vitro wheat starch digestibility. *Food Hydrocolloids,* 69**,** 19-27.
LOVEGROVE, A., WINGEN, L. U., PLUMMER, A., WOOD, A., PASSMORE, D., KOSIK, O., FREEMAN, J., MITCHELL, R. A. C., HASSALL, K., ULKER, M., TREMMEL-BEDE, K., RAKSZEGI, M., BEDŐ, Z., PERRETANT, M.-R., CHARMET, G., PONT, C., SALSE, J., WAITE, M. L., ORFORD, S., BURRIDGE, A., PELLNY, T. K., SHEWRY, P. R. & GRIFFITHS, S. 2020. Identification of a major QTL and associated molecular marker for high arabinoxylan fibre in white wheat flour. *PLOS ONE,* 15**,** e0227826.
LU, H., HU, Y., WANG, C., LIU, W., MA, G., HAN, Q. & MA, D. 2019. Effects of high temperature and drought stress on the expression of gene encoding enzymes and the activity of key enzymes involved in starch biosynthesis in wheat grains. *Frontiers in Plant Science,* 10**,** 1414.
LU, H., WANG, C., GUO, T., XIE, Y., FENG, W. & LI, S. 2014. Starch composition and its granules distribution in wheat grains in relation to post-anthesis high temperature and drought stress treatments. *Starch-Stärke,* 66**,** 419-428.
LUENGWILAI, K., BECKLES, D. M. J. J. O. A. & CHEMISTRY, F. 2008. Structural investigations and morphology of tomato fruit starch. *Journal of Agricultural and Food Chemistry,* 57**,** 282-291.
LUKASZEWSKI, A. J., ALBERTI, A., SHARPE, A., KILIAN, A., STANCA, A. M., KELLER, B., CLAVIJO, B. J., FRIEBE, B., GILL, B. & WULFF, B. 2014. A chromosome-based draft sequence of the hexaploid bread wheat (Triticum aestivum) genome. *Science,* 345**,** 1251788.
LUNDQUIST, F., SESTOFT, L., DAMGAARD, S. E., CLAUSEN, J. P. & TRAP-JENSEN, J. 1973. Utilization of acetate in the human forearm during exercise after ethanol ingestion. *J Clin Invest,* 52**,** 3231-5.
LUPTON, F. 1987. History of wheat breeding. Chapter 3 in: Wheat Breeding. (pp. 51-52). *In:* LUPTON, H. (ed.). Springer.
LUPTON, J. R. 2004. Microbial Degradation Products Influence Colon Cancer Risk: the Butyrate Controversy. *The Journal of Nutrition,* 134**,** 479-482.

MA, J., LIU, Y., ZHANG, P., CHEN, T., TIAN, T., WANG, P., CHE, Z., SHAHINNIA, F. & YANG, D. 2022. Identification of quantitative trait loci (QTL) and meta-QTL analysis for kernel size-related traits in wheat (Triticum aestivum L.). *BMC Plant Biology,* 22**,** 1-18.

MACKAY, I. J., BANSEPT-BASLER, P., BARBER, T., BENTLEY, A. R., COCKRAM, J., GOSMAN, N., GREENLAND, A. J., HORSNELL, R., HOWELLS, R. & O'SULLIVAN, D. M. 2014. An eight-parent multiparent advanced generation inter-cross population for winter-sown wheat: creation, properties, and validation. *G3: Genes, Genomes, Genetics,* 4**,** 1603-1610.

MAMMADOV, J., AGGARWAL, R., BUYYARAPU, R. & KUMPATLA, S. 2012. SNP markers and their impact on plant breeding. *International Journal of Plant Genomics,* 2012.

MATHER, A. & POLLOCK, C. 2011. Glucose handling by the kidney. *Kidney International,* 79**,** S1-S6.

MBA, C., AFZA, R. & SHU, Q. 2012. Mutagenic radiations: X-rays, ionizing particles and ultraviolet. *Plant Mutation Breeding and Biotechnology***,** 83-90.

MCCLEARY, B. V., MCNALLY, M., MONAGHAN, D. & MUGFORD, D. C. 2002. Measurement of α-amylase activity in white wheat flour, milled malt, and microbial enzyme preparations, using the Ceralpha assay: collaborative study. *Journal of AOAC international,* 85**,** 1096-1102.

MENCZEL, J. D. & PRIME, R. B. 2009. Differential Scanning Calorimetry (DSC): Thermal Analysis of Polymers: Fundamentals and Applications (pp. 7-58). *In:* MENCZEL, J. D. (ed.). John Wiley & Sons.

MIEDANER, T. & KORZUN, V. 2012. Marker-assisted selection for disease resistance in wheat and barley breeding. *Phytopathology,* 102**,** 560-566.

MIŁEK, J. 2021. Determination of activation energies and the optimum temperatures of hydrolysis of starch by α-amylase from porcine pancreas. *Molecules,* 26**,** 4117.

MILNER, S. G., MACCAFERRI, M., HUANG, B. E., MANTOVANI, P., MASSI, A., FRASCAROLI, E., TUBEROSA, R. & SALVI, S. 2016. A multiparental cross population for mapping QTL for agronomic traits in durum wheat (T riticum turgidum ssp. durum). *Plant Biotechnology Journal,* 14**,** 735-748.

MINEKUS, M., ALMINGER, M., ALVITO, P., BALLANCE, S., BOHN, T., BOURLIEU, C., CARRIÈRE, F., BOUTROU, R., CORREDIG, M. & DUPONT, D. 2014. A standardised static in vitro digestion method suitable for food–an international consensus. *Food & Function,* 5**,** 1113-1124.

MIR, R. R., REYNOLDS, M., PINTO, F., KHAN, M. A. & BHAT, M. A. 2019. High-throughput phenotyping for crop improvement in the genomics era. *Plant Science,* 282**,** 60-72.

MISHRA, A., SINGH, A., SHARMA, M., KUMAR, P. & ROY, J. 2016. Development of EMS-induced mutation population for amylose and resistant starch variation in bread wheat (Triticum aestivum) and identification of candidate genes responsible for amylose variation. *BMC Plant Biology,* 16**,** 1-15.

MOHAMED, A. A. & RAYAS-DUARTE, P. 2003. The effect of mixing and wheat protein/gluten on the gelatinization of wheat starch. *Food Chemistry,* 81**,** 533-545.

MORELL, M. K., BLENNOW, A., KOSAR-HASHEMI, B. & SAMUEL, M. S. 1997. Differential expression and properties of starch branching enzyme isoforms in developing wheat endosperm. *Plant Physiology,* 113**,** 201-208.

MORRIS, C. F. 2002. Puroindolines: the molecular genetic basis of wheat grain hardness. *Plant Molecular Biology,* 48**,** 633-647.
MORRISON, W., MILLIGAN, T. & AZUDIN, M. 1984. A relationship between the amylose and lipid contents of starches from diploid cereals. *Journal of Cereal Science,* 2**,** 257-271.
MORRISON, W., TESTER, R. & GIDLEY, M. 1994a. Properties of damaged starch granules. II. Crystallinity, molecular order and gelatinisation of ball-milled starches. *Journal of Cereal Science,* 19**,** 209-217.
MORRISON, W. R. 1988. Lipids in cereal starches: A review. *Journal of Cereal Science,* 8**,** 1-15.
MORRISON, W. R., TESTER, R. F. & GIDLEY, M. J. 1994b. Properties of Damaged Starch Granules. II. Crystallinity, Molecular Order and Gelatinisation of Ball-milled Starches. *Journal of Cereal Science,* 19**,** 209-217.
MULLER, R. 2000. A mathematical model of the formation of fermentable sugars from starch hydrolysis during high-temperature mashing. *Enzyme and Microbial Technology,* 27**,** 337-344.
MULLIS, K., FALOONA, F., SCHARF, S., SAIKI, R., HORN, G. & ERLICH, H. Specific enzymatic amplification of DNA in vitro: the polymerase chain reaction (pp. 263-273). Cold Spring Harbor symposia on quantitative biology, 1986. Cold Spring Harbor Laboratory Press.
NAKAMURA, S., SATOH, H. & OHTSUBO, K. I. 2015. Development of formulae for estimating amylose content, amylopectin chain length distribution, and resistant starch content based on the iodine absorption curve of rice starch. *Bioscience, Biotechnology, and Biochemistry,* 79**,** 443-455.
NAKAMURA, Y., UTSUMI, Y., SAWADA, T., AIHARA, S., UTSUMI, C., YOSHIDA, M. & KITAMURA, S. 2010. Characterization of the reactions of starch branching enzymes from rice endosperm. *Plant and Cell Physiology,* 51**,** 776-794.
NARDUCCI, V., FINOTTI, E., GALLI, V. & CARCEA, M. 2019. Lipids and fatty acids in Italian durum wheat (Triticum durum Desf.) cultivars. *Foods,* 8**,** 223.
NESBITT, M. 1996. From staple crop to extinction? The archaeology and history of hulled wheat: Hulled Wheat: Promoting the Conservation and Use of Underutilized and Neglected Crops. (pp. 41-100). *In:* PADULOSI, S. (ed.). IPGRI.
NEWBERRY, M., ZWART, A. B., WHAN, A., MIEOG, J. C., SUN, M., LEYNE, E., PRITCHARD, J., DANERI-CASTRO, S. N., IBRAHIM, K. & DIEPEVEEN, D. 2018. Does late maturity alpha-amylase impact wheat baking quality? *Frontiers in Plant Science,* 9**,** 1356.
NEWEY, H. 1967. Absorption of carbohydrates. *British Medical Bulletin,* 23**,** 236-240.
NHAN, M. T. & COPELAND, L. 2014. Effects of growing environment on properties of starch from five Australian wheat varieties. *Cereal Chemistry,* 91**,** 587-594.
NILSSON-EHLE, H. 1910. Arbetena med hvete och havre vid Svalof under ar 1909. *Sv Utsädesf Tidskr,* 20**,** 332-53.
NILSSON, A., ÖSTMAN, E., PRESTON, T. & BJÖRCK, I. 2008. Effects of GI vs content of cereal fibre of the evening meal on glucose tolerance at a subsequent standardized breakfast. *European Journal of Clinical Nutrition,* 62**,** 712.
OBADI, M., LI, C., LI, Q., LI, X., QI, Y. & XU, B. 2020. Relationship between starch fine molecular structures and cooked wheat starch digestibility. *Journal of Cereal Science,* 95**,** 103047.

OKUMUS, B. N., TACER-CABA, Z., KAHRAMAN, K. & NILUFER-ERDIL, D. 2018. Resistant starch type V formation in brown lentil (Lens culinaris Medikus) starch with different lipids/fatty acids. *Food Chemistry,* 240**,** 550-558.

OLKKU, J. & RHA, C. 1978. Gelatinisation of starch and wheat flour starch—A review. *Food Chemistry,* 3**,** 293-317.

OUELLETTE, L. A., REID, R. W., BLANCHARD, S. G. & BROUWER, C. R. 2018. LinkageMapView—rendering high-resolution linkage and QTL maps. *Bioinformatics,* 34**,** 306-307.

PANDURANGAN, S., WORKMAN, C., NILSEN, K. & KUMAR, S. 2021. Introduction to marker-assisted selection in wheat breeding: Accelerated breeding of cereal crops. (pp. 77-117). *In:* BILICHAK, A. & LAURIE, J. (eds.). Springer.

PARADA, J. & AGUILERA, J. M. 2009. In vitro digestibility and glycemic response of potato starch is related to granule size and degree of gelatinization. *Journal of Food Science,* 74**,** E34-E38.

PASHA, I., ANJUM, F. & MORRIS, C. 2010. Grain hardness: a major determinant of wheat quality. *Food Science and Technology International,* 16**,** 511-522.

PATEL, H., DAY, R., BUTTERWORTH, P. J. & ELLIS, P. R. 2014. A mechanistic approach to studies of the possible digestion of retrograded starch by α-amylase revealed using a log of slope (LOS) plot. *Carbohydrate Polymers,* 113**,** 182-188.

PATIL, A. R., MURRAY, S. M., FAHEY, G. C., JR., MERCHEN, N. R., WOLF, B. W., LAI, C.-S. & GARLEB, K. A. 1998. Apparent Digestibility of a Debranched Amylopectin-Lipid Complex and Resistant Starch Incorporated into Enteral Formulas Fed to Ileal-Cannulated Dogs. *The Journal of Nutrition,* 128**,** 2032-2035.

PATRON, N. J., SMITH, A. M., FAHY, B. F., HYLTON, C. M., NALDRETT, M. J., ROSSNAGEL, B. G. & DENYER, K. 2002. The Altered Pattern of Amylose Accumulation in the Endosperm of Low-Amylose Barley Cultivars Is Attributable to a Single Mutant Allele of Granule-Bound Starch Synthase I with a Deletion in the 5'-Non-Coding Region. *Plant Physiology,* 130**,** 190-198.

PENG, M., GAO, M., ABDEL-AAL, E. S. M., HUCL, P. & CHIBBAR, R. N. 1999. Separation and characterization of A- and B-type starch granules in wheat endosperm. *Cereal Chemistry,* 76**,** 375-379.

PEREZ-MORAL, N., PLANKEELE, J.-M., DOMONEY, C. & WARREN, F. J. 2018. Ultra-high performance liquid chromatography-size exclusion chromatography (UPLC-SEC) as an efficient tool for the rapid and highly informative characterisation of biopolymers. *Carbohydrate Polymers,* 196**,** 422-426.

PÉREZ, S. & BERTOFT, E. J. S. S. 2010. The molecular structures of starch components and their contribution to the architecture of starch granules: A comprehensive review. *Starch-Stärke,* 62**,** 389-420.

PETERSEN, G., SEBERG, O., YDE, M. & BERTHELSEN, K. 2006. Phylogenetic relationships of Triticum and Aegilops and evidence for the origin of the A, B, and D genomes of common wheat (Triticum aestivum). *Molecular Phylogenetics and Evolution,* 39**,** 70-82.

PETROPOULOU, K., SALT, L. J., EDWARDS, C. H., WARREN, F. J., GARCIA-PEREZ, I., CHAMBERS, E. S., ALSHAALAN, R., KHATIB, M., PEREZ-MORAL, N. & CROSS, K. L. 2020. A natural mutation in Pisum sativum L.(pea) alters starch assembly and improves glucose homeostasis in humans. *Nature Food,* 1**,** 693-704.

PFISTER, B. & ZEEMAN, S. C. 2016. Formation of starch in plant cells. *Cellular and Molecular Life Sciences,* 73**,** 2781-2807.
PHILIPPE, S., SAULNIER, L. & GUILLON, F. 2006. Arabinoxylan and (1→ 3),(1→ 4)-β-glucan deposition in cell walls during wheat endosperm development. *Planta,* 224**,** 449-461.
PHILLIPS, J., MUIR, J. G., BIRKETT, A., LU, Z. X., JONES, G. P., O'DEA, K. & YOUNG, G. P. 1995. Effect of resistant starch on fecal bulk and fermentation-dependent events in humans. *The American Journal Of Clinical Nutrition,* 62**,** 121-130.
PINGALI, P. L. 2012. Green revolution: impacts, limits, and the path ahead. *Proceedings of the National Academy of Sciences,* 109**,** 12302-12308.
PINHEIRO, J., BATES, D., DEBROY, S. & SARKAR, D. 2022. R Core Team. 2021. nlme: linear and nonlinear mixed effects models. R package version 3.1-153. *Availble at: https://cran. r-project. org/web/packages/nlme/index. html (Accessed March 31, 2022)*.
PLANCHOT, V., COLONNA, P. & BULEON, A. 1997. Enzymatic hydrolysis of α-glucan crystallites. *Carbohydrate Research,* 298**,** 319-326.
POURKHEIRANDISH, M., GOLICZ, A. A., BHALLA, P. L. & SINGH, M. B. 2020. Global role of crop genomics in the face of climate change. *Frontiers in Plant Science,* 11**,** 922.
PULIGUNDLA, P., SMOGROVICOVA, D., MOK, C. & OBULAM, V. S. R. 2020. Recent developments in high gravity beer-brewing. *Innovative Food Science & Emerging Technologies,* 64**,** 102399.
QI, K., YI, X. & LI, C. 2022. Effects of endogenous macronutrients and processing conditions on starch digestibility in wheat bread. *Carbohydrate Polymers***,** 119874.
RAEKER, M. Ö., GAINES, C. S., FINNEY, P. L. & DONELSON, T. 1998. Granule size distribution and chemical composition of starches from 12 soft wheat cultivars. *Cereal Chemistry,* 75**,** 721-728.
RAHIM, M. S., KUMAR, V. & ROY, J. 2022. Genetic dissection of quantitative traits loci identifies new genes for gelatinization parameters of starch and amylose-lipid complex (Resistant starch 5) in bread wheat. *Plant Science,* 325**,** 111452.
RAHMAN, S., ISLAM, S., YU, Z., SHE, M., NEVO, E. & MA, W. 2020. Current progress in understanding and recovering the wheat genes lost in evolution and domestication. *International Journal of Molecular Sciences,* 21**,** 5836.
RAIGOND, P., EZEKIEL, R. & RAIGOND, B. 2015. Resistant starch in food: a review. *Journal of the Science of Food and Agriculture,* 95**,** 1968-1978.
RAMADOSS, B. R., GANGOLA, M. P., AGASIMANI, S., JAISWAL, S., VENKATESAN, T., SUNDARAM, G. R. & CHIBBAR, R. N. 2019. Starch granule size and amylopectin chain length influence starch in vitro enzymatic digestibility in selected rice mutants with similar amylose concentration. *Journal of Food Science and Technology,* 56**,** 391-400.
RAMIREZ-GONZALEZ, R. H., UAUY, C. & CACCAMO, M. 2015. PolyMarker: a fast polyploid primer design pipeline. *Bioinformatics,* 31**,** 2038-2039.
RANDHAWA, M. S., BARIANA, H. S., MAGO, R. & BANSAL, U. K. 2015. Mapping of a new stripe rust resistance locus Yr57 on chromosome 3BS of wheat. *Molecular Breeding,* 35.
RATNAYAKE, W. S. & JACKSON, D. S. 2008. Starch gelatinization. *Advances in Food and Nutrition Research,* 55**,** 221-268.

RAY, D. K., MUELLER, N. D., WEST, P. C. & FOLEY, J. A. 2013. Yield trends are insufficient to double global crop production by 2050. *PloS One,* 8**,** e66428.

REGINA, A., BERBEZY, P., KOSAR-HASHEMI, B., LI, S., CMIEL, M., LARROQUE, O., BIRD, A. R., SWAIN, S. M., CAVANAGH, C., JOBLING, S. A., LI, Z. & MORELL, M. 2015. A genetic strategy generating wheat with very high amylose content. *Plant Biotechnology Journal,* 13**,** 1276-1286.

REGINA, A., BIRD, A., TOPPING, D., BOWDEN, S., FREEMAN, J., BARSBY, T., KOSAR-HASHEMI, B., LI, Z., RAHMAN, S. & MORELL, M. 2006. High-amylose wheat generated by RNA interference improves indices of large-bowel health in rats. *Proceedings of the National Academy of Sciences of the United States of America,* 103**,** 3546-3551.

REIF, J. C., ZHANG, P., DREISIGACKER, S., WARBURTON, M. L., VAN GINKEL, M., HOISINGTON, D., BOHN, M. & MELCHINGER, A. E. 2005. Wheat genetic diversity trends during domestication and breeding. *Theoretical and Applied Genetics,* 110**,** 859-864.

REPELLIN, A., BÅGA, M. & CHIBBAR, R. N. 2008. In vitro pullulanase activity of wheat (Triticum aestivum L.) limit-dextrinase type starch debranching enzyme is modulated by redox conditions. *Journal of Cereal Science,* 47**,** 302-309.

RING, S. G., COLONNA, P., I'ANSON, K. J., KALICHEVSKY, M. T., MILES, M. J., MORRIS, V. J. & ORFORD, P. D. 1987. The gelation and crystallisation of amylopectin. *Carbohydrate Research,* 162**,** 277-293.

ROEDIGER, W. E. 1982. Utilization of nutrients by isolated epithelial cells of the rat colon. *Gastroenterology,* 83**,** 424-9.

ROMAN, L. & MARTINEZ, M. M. 2019. Structural basis of resistant starch (RS) in bread: Natural and commercial alternatives. *Foods,* 8**,** 267.

ROUSSEL, V., LEISOVA, L., EXBRAYAT, F., STEHNO, Z. & BALFOURIER, F. 2005. SSR allelic diversity changes in 480 European bread wheat varieties released from 1840 to 2000. *Theoretical and Applied Genetics,* 111**,** 162-170.

RYDBERG, U., ANDERSSON, L., ANDERSSON, R., ÅMAN, P. & LARSSON, H. 2001. Comparison of starch branching enzyme I and II from potato. *European Journal of Biochemistry,* 268**,** 6140-6145.

SACCOMANNO, B., BERBEZY, P., FINDLAY, K., SHOESMITH, J., UAUY, C., VIALLIS, B. & TRAFFORD, K. 2022. Characterization of wheat lacking B-type starch granules. *Journal of Cereal Science,* 104**,** 103398.

SAHU, P. K., SAO, R., MONDAL, S., VISHWAKARMA, G., GUPTA, S. K., KUMAR, V., SINGH, S., SHARMA, D. & DAS, B. K. 2020. Next generation sequencing based forward genetic approaches for identification and mapping of causal mutations in crop plants: A comprehensive review. *Plants,* 9**,** 1355.

SAINTENAC, C., LEE, W.-S., CAMBON, F., RUDD, J. J., KING, R. C., MARANDE, W., POWERS, S. J., BERGÈS, H., PHILLIPS, A. L. & UAUY, C. 2018. Wheat receptor-kinase-like protein Stb6 controls gene-for-gene resistance to fungal pathogen Zymoseptoria tritici. *Nature Genetics,* 50**,** 368.

SAJILATA, M. G., SINGHAL, R. S. & KULKARNI, P. R. 2006. Resistant starch–a review. *Comprehensive Reviews in Food Science and Food Safety,* 5**,** 1-17.

SALMAN, H., BLAZEK, J., LOPEZ-RUBIO, A., GILBERT, E. P., HANLEY, T. & COPELAND, L. 2009. Structure–function relationships in A and B granules from wheat starches of similar amylose content. *Carbohydrate Polymers,* 75**,** 420-427.

SANDERSON, J. S., DANIELS, R. D., DONALD, A. M., BLENNOW, A. & ENGELSEN, S. B. 2006. Exploratory SAXS and HPAEC-PAD studies of starches from diverse plant genotypes. *Carbohydrate Polymers,* 64**,** 433-443.

SCHLEUSSNER, C.-F., LISSNER, T. K., FISCHER, E. M., WOHLAND, J., PERRETTE, M., GOLLY, A., ROGELJ, J., CHILDERS, K., SCHEWE, J. & FRIELER, K. 2016. Differential climate impacts for policy-relevant limits to global warming: the case of 1.5 C and 2 C. *Earth system dynamics,* 7**,** 327-351.

SCHOEN, A., JOSHI, A., TIWARI, V., GILL, B. S. & RAWAT, N. 2021. Triple null mutations in starch synthase SSIIa gene homoeologs lead to high amylose and resistant starch in hexaploid wheat. *BMC Plant Biology,* 21**,** 1-11.

SCHÖNHOFEN, A., HAZARD, B., ZHANG, X. & DUBCOVSKY, J. 2016. Registration of common wheat germplasm with mutations in SBEII genes conferring increased grain amylose and resistant starch content. *Journal of Plant Registrations,* 10**,** 200-205.

SCHONHOFEN, A., ZHANG, X. Q. & DUBCOVSKY, J. 2017. Combined mutations in five wheat STARCH BRANCHING ENZYME II genes improve resistant starch but affect grain yield and bread-making quality. *Journal of Cereal Science,* 75**,** 165-174.

SCHUR, F. 1980. Malt analysis and starch degradation in wort production. *Brauwissenschaft.* VERLAG HANS CARL ANDERNACHER STR 33 A, D-90411 NURNBERG, GERMANY.

SEUNG, D. & SMITH, A. M. 2019. Starch granule initiation and morphogenesis—progress in Arabidopsis and cereals. *Journal of Experimental Botany,* 70**,** 771-784.

SHAAF, S., SHARMA, R., BALOCH, F. S., BADAEVA, E. D., KNÜPFFER, H., KILIAN, B. & ÖZKAN, H. 2016. The grain Hardness locus characterized in a diverse wheat panel (Triticum aestivum L.) adapted to the central part of the Fertile Crescent: genetic diversity, haplotype structure, and phylogeny. *Molecular Genetics and Genomics,* 291**,** 1259-1275.

SHARMA, A., YADAV, B. S. & RITIKA, A. 2008. Resistant Starch: Physiological Roles and Food Applications. *Food Reviews International,* 24**,** 193-234.

SHEWRY, P. 2023. Wheat grain proteins: Past, present, and future. *Cereal Chemistry,* 100**,** 9-22.

SHEWRY, P. & LOVEGROVE, A. 2014. Exploiting natural variation to improve the content and composition of dietary fibre in wheat grain: A review. *Acta Alimentaria,* 43**,** 357-372.

SHEWRY, P., REYNOLDS, S., PELLNY, T., FREEMAN, J., WILKINSON, M., KOSIK, O., ULKER, M., WINGEN, L., ORFORD, S. & GRIFFITHS, S. 2015. Improving wheat as a source of dietary fibre for human health. *Proceedings of the Nutrition Society,* 74.

SHEWRY, P. R., HAWKESFORD, M. J., PIIRONEN, V., LAMPI, A.-M., GEBRUERS, K., BOROS, D., ANDERSSON, A. A., ÅMAN, P., RAKSZEGI, M. & BEDO, Z. 2013. Natural variation in grain composition of wheat and related cereals. *Journal of Agricultural and Food Chemistry,* 61**,** 8295-8303.

SHINDE, S. V., NELSON, J. E. & HUBER, K. C. 2003. Soft wheat starch pasting behavior in relation to A- and B-type granule content and composition. *Cereal Chemistry,* 80**,** 91-98.

SHU, X., JIA, L., YE, H., LI, C. & WU, D. 2009. Slow digestion properties of rice different in resistant starch. *Journal of Agricultural and Food Chemistry,* 57**,** 7552-7559.

SIEVERT, D. & POMERANZ, Y. 1989. Enzyme-resistant starch. I. Characterization and evaluation by enzymatic, thermoanalytical, and microscopic methods. *Cereal Chem,* 66**,** 342-347.
SINGH, N., SINGH, J., KAUR, L., SINGH SODHI, N. & SINGH GILL, B. 2003. Morphological, thermal and rheological properties of starches from different botanical sources. *Food Chemistry,* 81**,** 219-231.
SINGH, S., SINGH, G., SINGH, P. & SINGH, N. 2008. Effect of water stress at different stages of grain development on the characteristics of starch and protein of different wheat varieties. *Food Chemistry,* 108**,** 130-139.
SINGH, V. J., BHOWMICK, P. K., VINOD, K. K., KRISHNAN, S. G., NANDAKUMAR, S., KUMAR, A., KUMAR, M., SHEKHAWAT, S., DIXIT, B. K. & MALIK, A. 2022. Population Structure of a Worldwide Collection of Tropical Japonica Rice Indicates Limited Geographic Differentiation and Shows Promising Genetic Variability Associated with New Plant Type. *Genes,* 13**,** 484.
SISSONS, M., CUTILLO, S., MARCOTULI, I. & GADALETA, A. 2021. Impact of durum wheat protein content on spaghetti in vitro starch digestion and technological properties. *Journal of Cereal Science,* 98**,** 103156.
SISSONS, M., SESTILI, F., BOTTICELLA, E., MASCI, S. & LAFIANDRA, D. 2020. Can Manipulation of Durum Wheat Amylose Content Reduce the Glycaemic Index of Spaghetti? *Foods,* 9**,** 693.
SKUTCHES, C. L., HOLROYDE, C. P., MYERS, R. N., PAUL, P. & REICHARD, G. A. 1979. Plasma acetate turnover and oxidation. *J Clin Invest,* 64**,** 708-13.
SLADE, A. J., MCGUIRE, C., LOEFFLER, D., MULLENBERG, J., SKINNER, W., FAZIO, G., HOLM, A., BRANDT, K. M., STEINE, M. N., GOODSTAL, J. F. & KNAUF, V. C. 2012. Development of high amylose wheat through TILLING. *BMC Plant Biology,* 12**,** 69.
SLAVIN, J. 2013. Fiber and Prebiotics: Mechanisms and Health Benefits. *Nutrients,* 5**,** 1417-1435.
SMITH, A. M., DENYER, K. & MARTIN, C. 1997. The synthesis of the starch granule. *Annual Review of Plant Biology,* 48**,** 67-87.
SMITH, C. M. 2004. Metabolic Fuels and Dietary Components. Chapter 1 in: Marks' basic medical biochemistry: a clinical approach (pp. 3-19). Lippincott Williams & Wilkins.
SOULAKA, A. B. & MORRISON, W. R. 1985. The amylose and lipid contents, dimensions, and gelatinisation characteristics of some wheat starches and their A- and B-granule fractions. *Journal of the Science of Food and Agriculture,* 36**,** 709-718.
ŠRAMKOVÁ, Z., GREGOVÁ, E. & ŠTURDÍK, E. 2009. Chemical composition and nutritional quality of wheat grain. *Acta Chimica Slovaca,* 2**,** 115-138.
SRICHUWONG, S., ISONO, N., MISHIMA, T. & HISAMATSU, M. 2005. Structure of lintnerized starch is related to X-ray diffraction pattern and susceptibility to acid and enzyme hydrolysis of starch granules. *International Journal of Biological Macromolecules,* 37**,** 115-121.
STEPHEN, A. M., CHAMP, M. M.-J., CLORAN, S. J., FLEITH, M., VAN LIESHOUT, L., MEJBORN, H. & BURLEY, V. J. 2017. Dietary fibre in Europe: current state of knowledge on definitions, sources, recommendations, intakes and relationships to health. *Nutrition Research Reviews,* 30**,** 149-190.
SU, H., TU, J., ZHENG, M., DENG, K., MIAO, S., ZENG, S., ZHENG, B. & LU, X. 2020. Effects of oligosaccharides on particle structure, pasting and thermal properties of wheat starch granules under different freezing temperatures. *Food Chemistry,* 315**,** 126209.

SUKUMARAN, S., DREISIGACKER, S., LOPES, M., CHAVEZ, P. & REYNOLDS, M. P. 2015. Genome-wide association study for grain yield and related traits in an elite spring wheat population grown in temperate irrigated environments. *Theoretical and Applied Genetics,* 128**,** 353-363.

SVIHUS, B., UHLEN, A. K. & HARSTAD, O. M. 2005. Effect of starch granule structure, associated components and processing on nutritive value of cereal starch: A review. *Animal Feed Science and Technology,* 122**,** 303-320.

SZAREJKO, I., SZURMAN-ZUBRZYCKA, M., NAWROT, M., MARZEC, M., GRUSZKA, D., KUROWSKA, M., CHMIELEWSKA, B., ZBIESZCZYK, J., JELONEK, J. & MALUSZYNSKI, M. 2017. Creation of a TILLING population in barley after chemical mutagenesis with sodium azide and MNU: Biotechnologies for Plant Mutation Breeding. (pp. 91-111). *In:* JANKOWICZ-CIESLAK, J. (ed.). Springer, Cham.

TAGLIERI, I., MACALUSO, M., BIANCHI, A., SANMARTIN, C., QUARTACCI, M. F., ZINNAI, A. & VENTURI, F. 2021. Overcoming bread quality decay concerns: main issues for bread shelf life as a function of biological leavening agents and different extra ingredients used in formulation. A review. *Journal of the Science of Food and Agriculture,* 101**,** 1732-1743.

TAKATO, S., UEDA, M., OHNISHI, N., VIRIYARATTANASAK, C. & KAJIWARA, K. 2017. Effects of fatty acid and emulsifier on the complex formation and in vitro digestibility of gelatinized potato starch AU - Kawai, Kiyoshi. *International Journal of Food Properties,* 20**,** 1500-1510.

TAKEDA, Y., GUAN, H. P. & PREISS, J. 1993. Branching of amylose by the branching isoenzymes of maize endosperm. *Carbohydrate Research,* 240**,** 253-263.

TAKEDA, Y., HIZUKURI, S., TAKEDA, C. & SUZUKI, A. 1987. Structures of branched molecules of amyloses of various origins, and molar fractions of branched and unbranched molecules. *Carbohydrate Research,* 165**,** 139-145.

TANKSLEY, S. D. 1993. Mapping polygenes. *Annual review of genetics,* 27**,** 205-233.

TAYLOR, J. & BUTLER, D. 2017. R package ASMap: efficient genetic linkage map construction and diagnosis. *arXiv preprint arXiv:1705.06916*.

TESTER, R. & SOMMERVILLE, M. 2001. Swelling and enzymatic hydrolysis of starch in low water systems. *Journal of Cereal Science,* 33**,** 193-203.

TESTER, R. F., KARKALAS, J. & QI, X. 2004. Starch - Composition, fine structure and architecture. *Journal of Cereal Science,* 39**,** 151-165.

TESTER, R. F., KARKALAS, J. & QI, X. 2007. Starch structure and digestibility Enzyme-Substrate relationship. *World's Poultry Science Journal,* 60**,** 186-195.

TETLOW, I. J. & EMES, M. J. 2014. A review of starch-branching enzymes and their role in amylopectin biosynthesis. *IUBMB Life,* 66**,** 546-558.

THACHUK, C., CROSSA, J., FRANCO, J., DREISIGACKER, S., WARBURTON, M. & DAVENPORT, G. F. 2009. Core Hunter: an algorithm for sampling genetic resources based on multiple genetic measures. *BMC Bioinformatics,* 10**,** 1-13.

THITISAKSAKUL, M., JIMÉNEZ, R. C., ARIAS, M. C. & BECKLES, D. M. 2012. Effects of environmental factors on cereal starch biosynthesis and composition. *Journal of Cereal Science,* 56**,** 67-80.

THOMPSON, L. U. & YOON, J. H. 1984. Starch Digestibility as Affected by Polyphenols and Phytic Acid. *Journal of Food Science,* 49**,** 1228-1229.

TIAN, S. & SUN, Y. 2020. Influencing factor of resistant starch formation and application in cereal products: A review. *International Journal of Biological Macromolecules,* 149**,** 424-431.

TIAN, Y., LI, Y., JIN, Z. & XU, X. 2009. A novel molecular simulation method for evaluating the endothermic transition of amylose recrystallite. *European Food Research and Technology,* 229**,** 853-858.

TOOR, A. K., BANSAL, U. K., BHARDWAJ, S., BADEBO, A. & BARIANA, H. S. 2013. Characterization of stem rust resistance in old tetraploid wheat landraces from the Watkins collection. *Genetic Resources and Crop Evolution,* 60**,** 2081-2089.

TOPPING, D. L., BAJKA, B. H., BIRD, A. R., CLARKE, J. M., COBIAC, L., CONLON, M. A., MORELL, M. K. & TODEN, S. 2008. Resistant starches as a vehicle for delivering health benefits to the human large bowel. *Microbial Ecology in Health and Disease,* 20**,** 103-108.

TOPPING, D. L. & CLIFTON, P. M. 2001. Short-chain fatty acids and human colonic function: roles of resistant starch and nonstarch polysaccharides. *Physiological reviews,* 81**,** 1031-1064.

TOUTOUNJI, M. R., BUTARDO, V. M., ZOU, W., FARAHNAKY, A., PALLAS, L., OLI, P. & BLANCHARD, C. L. 2019. A High-Throughput In Vitro Assay for Screening Rice Starch Digestibility. *Foods,* 8**,** 601.

UAUY, C., PARAISO, F., COLASUONNO, P., TRAN, R. K., TSAI, H., BERARDI, S., COMAI, L. & DUBCOVSKY, J. 2009. A modified TILLING approach to detect induced mutations in tetraploid and hexaploid wheat. *BMC Plant Biol,* 9.

VAMADEVAN, V. & BERTOFT, E. 2015. Structure-function relationships of starch components. *Starch - Stärke,* 67**,** 55-68.

VARSHNEY, R. K., NAYAK, S. N., MAY, G. D. & JACKSON, S. A. 2009. Next-generation sequencing technologies and their implications for crop genetics and breeding. *Trends in Biotechnology,* 27**,** 522-530.

VENSKE, E., DOS SANTOS, R. S., BUSANELLO, C., GUSTAFSON, P. & COSTA DE OLIVEIRA, A. 2019. Bread wheat: a role model for plant domestication and breeding. *Hereditas,* 156**,** 1-11.

VIKRAM, P., FRANCO, J., BURGUEÑO-FERREIRA, J., LI, H., SEHGAL, D., SAINT PIERRE, C., ORTIZ, C., SNELLER, C., TATTARIS, M. & GUZMAN, C. 2016. Unlocking the genetic diversity of Creole wheats. *Scientific Reports,* 6**,** 23092.

VRINTEN, P. L. & NAKAMURA, T. 2000. Wheat Granule-Bound Starch Synthase I and II Are Encoded by Separate Genes That Are Expressed in Different Tissues. *Plant Physiology,* 122**,** 255-264.

WANG, J., SUN, J., LIU, D., YANG, W., WANG, D., TONG, Y. & ZHANG, A. 2008. Analysis of Pina and Pinb alleles in the micro-core collections of Chinese wheat germplasm by Ecotilling and identification of a novel Pinb allele. *Journal of Cereal Science,* 48**,** 836-842.

WANG, R., CHEN, Y., REN, J. & GUO, S. 2014. Aroma stability of millet powder during storage and effects of cooking methods and antioxidant treatment. *Cereal Chemistry,* 91**,** 262-269.

WANG, S., BLAZEK, J., GILBERT, E. & COPELAND, L. 2012. New insights on the mechanism of acid degradation of pea starch. *Carbohydrate Polymers,* 87**,** 1941-1949.

WANG, S. & COPELAND, L. 2013. Molecular disassembly of starch granules during gelatinization and its effect on starch digestibility: a review. *Food & Function,* 4**,** 1564-1580.

WANG, S. & COPELAND, L. 2015. Effect of Acid Hydrolysis on Starch Structure and Functionality: A Review. *Critical Reviews in Food Science and Nutrition,* 55**,** 1081-1097.
WANG, S., LI, C., COPELAND, L., NIU, Q. & WANG, S. 2015. Starch retrogradation: A comprehensive review. *Comprehensive Reviews in Food Science and Food Safety,* 14**,** 568-585.
WANG, S., SHARP, P. & COPELAND, L. J. F. C. 2011. Structural and functional properties of starches from field peas. *Food Chemistry,* 126**,** 1546-1552.
WANG, S., WANG, S., GUO, P., LIU, L. & WANG, S. 2017. Multiscale Structural Changes of Wheat and Yam Starches during Cooking and Their Effect on in Vitro Enzymatic Digestibility. *Journal of Agricultural and Food Chemistry,* 65**,** 156-166.
WANG, S., YU, J. & YU, J. J. C. P. 2008. The semi-crystalline growth rings of C-type pea starch granule revealed by SEM and HR-TEM during acid hydrolysis. *Carbohydrate Polymers,* 74**,** 731-739.
WANG, S. S., CHIANG, W. C., ZHAO, B., ZHENG, X. G. & KIM, I. H. 1991. EXPERIMENTAL-ANALYSIS AND COMPUTER-SIMULATION OF STARCH-WATER INTERACTIONS DURING PHASE-TRANSITION. *Journal of Food Science,* 56**,** 121-124.
WANG, Y., KANSOU, K., PRITCHARD, J., ZWART, A. B., SAULNIER, L. & RAL, J.-P. 2022. Beyond amylose content, selecting starch traits impacting in vitro α-amylase degradability in a wheat MAGIC population. *Carbohydrate Polymers***,** 119652.
WARD, J. L., POUTANEN, K., GEBRUERS, K., PIIRONEN, V., LAMPI, A.-M., NYSTRÖM, L., ANDERSSON, A. A., BOROS, D., RAKSZEGI, M. & BEDŐ, Z. 2008. The HEALTHGRAIN cereal diversity screen: concept, results, and prospects. *Journal of Agricultural and Food Chemistry,* 56**,** 9699-9709.
WEN, L., RODIS, P. & WASSERMAN, B. 1990. Starch fragmentation and protein insolubilization during twin-screw extrusion of corn meal. *Cereal Chemistry*.
WHITCOMB, D. C. & LOWE, M. E. 2007. Human pancreatic digestive enzymes. *Digestive Diseases and Sciences,* 52**,** 1-17.
WHITE, J., LAW, J. R., MACKAY, I., CHALMERS, K. J., SMITH, J. S. C., KILIAN, A. & POWELL, W. 2008. The genetic diversity of UK, US and Australian cultivars of Triticum aestivum measured by DArT markers and considered by genome. *Theoretical and Applied Genetics,* 116**,** 439-453.
WHITNEY, K. & SIMSEK, S. 2017. Reduced gelatinization, hydrolysis, and digestibility in whole wheat bread in comparison to white bread. *Cereal Chemistry,* 94**,** 991-1000.
WICKHAM, H. 2016. Data analysis. *ggplot2.* Springer.
WILLIAMSON, G., BELSHAW, N. J., SELF, D. J., NOEL, T. R., RING, S. G., CAIRNS, P., MORRIS, V. J., CLARK, S. A. & PARKER, M. L. 1992. Hydrolysis of A-and B-type crystalline polymorphs of starch by α-amylase, β-amylase and glucoamylase 1. *Carbohydrate Polymers,* 18**,** 179-187.
WINFIELD, M. O., ALLEN, A. M., WILKINSON, P. A., BURRIDGE, A. J., BARKER, G. L. A., COGHILL, J., WATERFALL, C., WINGEN, L. U., GRIFFITHS, S. & EDWARDS, K. J. 2018. High-density genotyping of the A.E. Watkins Collection of hexaploid landraces identifies a large molecular diversity compared to elite bread wheat. *Plant Biotechnology Journal,* 16**,** 165-175.
WINGEN, L. U., ORFORD, S., GORAM, R., LEVERINGTON-WAITE, M., BILHAM, L., PATSIOU, T. S., AMBROSE, M., DICKS, J. & GRIFFITHS, S. 2014. Establishing

the A. E. Watkins landrace cultivar collection as a resource for systematic gene discovery in bread wheat. *Theoretical and Applied Genetics,* 127**,** 1831-1842.

WINGEN, L. U., WEST, C., LEVERINGTON-WAITE, M., COLLIER, S., ORFORD, S., GORAM, R., YANG, C. Y., KING, J., ALLEN, A. M., BURRIDGE, A., EDWARDS, K. J. & GRIFFITHS, S. 2017. Wheat Landrace Genome Diversity. *Genetics,* 205**,** 1657-1676.

WINTER, P. & KAHL, G. 1995. Molecular marker technologies for plant improvement. *World Journal of Microbiology and Biotechnology,* 11**,** 438-448.

WOLEVER, T. M. & MEHLING, C. 2002. High-carbohydrate–low-glycaemic index dietary advice improves glucose disposition index in subjects with impaired glucose tolerance. *British Journal of Nutrition,* 87**,** 477-487.

WOLF, M., MELVIN, E., GARCIA, W., DIMLER, R., KWOLEK, W., KAMETANI, T., HIBINO, S., TAKANO, S. & KERSHAW, K. 1970. Amylose determination in dimethyl sulfoxide extracts of maize. *Cereal Chemistry,* 47**,** 437-446.

WONG, J. M. W., DE SOUZA, R., KENDALL, C. W. C., EMAM, A. & JENKINS, D. J. A. 2006. Colonic Health: Fermentation and Short Chain Fatty Acids. *Journal of Clinical Gastroenterology,* 40**,** 235-243.

WRIGHT, E. M. 1993. The Intestinal Na+/Glucose Cotransporter. *Annual Review of Physiology,* 55**,** 575-589.

WRIGHT, E. M., LOO, D. D., HIRAYAMA, B. A. & TURK, E. 2004. Surprising versatility of Na+-glucose cotransporters: SLC5. *Physiology,* 19**,** 370-376.

WRIGLEY, C. W., CORKE, H., SEETHARAMAN, K. & FAUBION, J. 2015. The Cereal Grains: Encyclopedia of Food Grains. (pp. 73-117). *In:* WRIGLEY, C. (ed.). Elsevier Science.

WU, A. C., LI, E. & GILBERT, R. G. 2014. Exploring extraction/dissolution procedures for analysis of starch chain-length distributions. *Carbohydrate Polymers,* 114**,** 36-42.

XIA, H., YANDEAU-NELSON, M., THOMPSON, D. B. & GUILTINAN, M. J. 2011. Deficiency of maize starch-branching enzyme i results in altered starch fine structure, decreased digestibility and reduced coleoptile growth during germination. *BMC Plant Biology,* 11.

YAMAMORI, M., KATO, M., YUI, M. & KAWASAKI, M. 2006. Resistant starch and starch pasting properties of a starch synthase IIa-deficient wheat with apparent high amylose. *Australian Journal of Agricultural Research,* 57**,** 531-535.

YANG, C., SHU, X., ZHANG, L., WANG, X., ZHAO, H. J., MA, C. & WU, D. 2006. Starch properties of mutant rice high in resistant starch. *Journal of Agricultural and Food Chemistry,* 54**,** 523-528.

YIRGU, M., KEBEDE, M., FEYISSA, T., LAKEW, B., WOLDEYOHANNES, A. B. & FIKERE, M. 2023. Single nucleotide polymorphism (SNP) markers for genetic diversity and population structure study in Ethiopian barley (Hordeum vulgare L.) germplasm. *BMC Genomic Data,* 24**,** 1-13.

YOUNG, N. 1996. QTL mapping and quantitative disease resistance in plants. *Annual Review of Phytopathology,* 34**,** 479-501.

YOUNG, N. D. 1999. A cautiously optimistic vision for marker-assisted breeding. *Molecular Breeding,* 5**,** 505-510.

YU, J., WANG, S., WANG, J., LI, C., XIN, Q., HUANG, W., ZHANG, Y., HE, Z. & WANG, S. 2015. Effect of laboratory milling on properties of starches isolated

from different flour millstreams of hard and soft wheat. *Food Chemistry,* 172**,** 504-514.

ZAFEIRIOU, P., SAVVA, G. M., AHN-JARVIS, J. H., WARREN, F. J., PASQUARIELLO, M., GRIFFITHS, S., SEUNG, D. & HAZARD, B. A. 2023. Mining the AE Watkins Wheat Landrace Collection for Variation in Starch Digestibility Using a New High-Throughput Assay. *Foods,* 12**,** 266.

ZEEMAN, S. C., KOSSMANN, J. & SMITH, A. M. 2010. Starch: Its metabolism, evolution, and biotechnological modification in plants. *Annual Review of Plant Biology*.

ZEVEN, A. C. 1999. The traditional inexplicable replacement of seed and seed ware of landraces and cultivars: a review. *Euphytica,* 110**,** 181-191.

ZHANG, C., JIANG, D., LIU, F., CAI, J., DAI, T. & CAO, W. 2010. Starch granules size distribution in superior and inferior grains of wheat is related to enzyme activities and their gene expressions during grain filling. *Journal of Cereal Science,* 51**,** 226-233.

ZHANG, G., CHENG, Z., ZHANG, X., GUO, X., SU, N., JIANG, L., MAO, L. & WAN, J. 2011. Double repression of soluble starch synthase genes SSIIa and SSIIIa in rice (Oryza sativa L.) uncovers interactive effects on the physicochemical properties of starch. *Genome,* 54**,** 448-59.

ZHANG, N., WANG, M., FU, J., SHEN, Y., DING, Y., WU, D., SHU, X. & SONG, W. 2020. Identifying genes for resistant starch, slowly digestible starch, and rapidly digestible starch in rice using genome-wide association studies. *Genes & Genomics,* 42**,** 1227-1238.

ZHAO, H., DAI, T., JIANG, D. & CAO, W. 2008. Effects of high temperature on key enzymes involved in starch and protein formation in grains of two wheat cultivars. *Journal of Agronomy and Crop Science,* 194**,** 47-54.

ZHONG, F., YOKOYAMA, W., WANG, Q. & SHOEMAKER, C. F. 2006. Rice starch, amylopectin, and amylose: molecular weight and solubility in dimethyl sulfoxide-based solvents. *Journal of Agricultural and Food Chemistry,* 54**,** 2320-2326.

ZHOU, X. & LIM, S.-T. 2012. Pasting viscosity and in vitro digestibility of retrograded waxy and normal corn starch powders. *Carbohydrate Polymers,* 87**,** 235-239.

Supplemental data

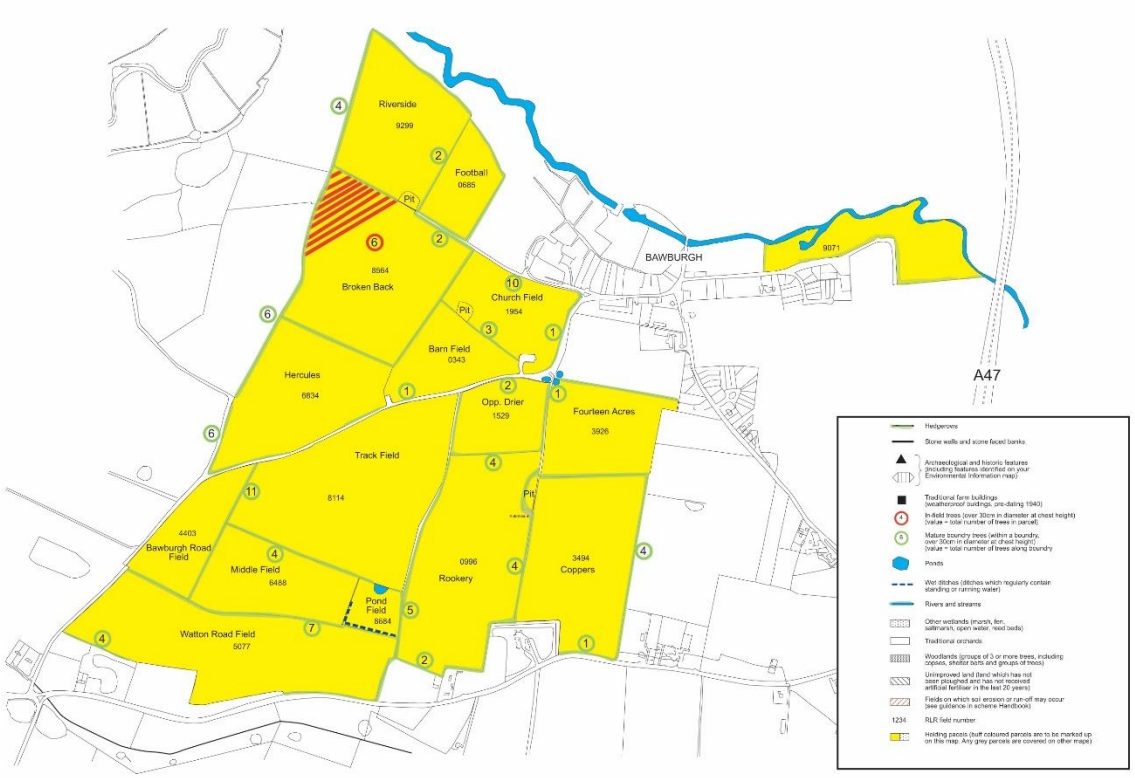

Supplemental Figure 2.1. Map Fields at Church farm, Norwich, Norfolk, UK.

Supplemental Table 2.1. Field trials of selected Watkins lines.

GRU Store Code	ID	Year	m^2 plots	Location
1190007	7	2010	1	Barn Field, Norfolk, UK
1190042	42	2010	1	Barn Field, Norfolk, UK
1190092	92	2010	1	Barn Field, Norfolk, UK
1190103	103	2010	1	Barn Field, Norfolk, UK
1190141	141	2010	1	Barn Field, Norfolk, UK
1190145	145	2010	1	Barn Field, Norfolk, UK
1190231	231	2010	1	Barn Field, Norfolk, UK
1190281	281	2010	1	Barn Field, Norfolk, UK
1190444	444	2010	1	Barn Field, Norfolk, UK

GRU Store Code	ID	Year	m^2 plots	Location
1190471	471	2010	1	Barn Field, Norfolk, UK
1190475	475	2010	1	Barn Field, Norfolk, UK
1190551	551	2010	1	Barn Field, Norfolk, UK
1190627	627	2010	1	Barn Field, Norfolk, UK
1190629	629	2010	1	Barn Field, Norfolk, UK
1190639	639	2010	1	Barn Field, Norfolk, UK
1190671	671	2010	1	Barn Field, Norfolk, UK
1190680	680	2010	1	Barn Field, Norfolk, UK
1190694	694	2010	1	Barn Field, Norfolk, UK
1190704	704	2010	1	Barn Field, Norfolk, UK
1190705	705	2010	1	Barn Field, Norfolk, UK
1190746	746	2010	1	Barn Field, Norfolk, UK
1190747	747	2010	1	Barn Field, Norfolk, UK
1190777	777	2010	1	Barn Field, Norfolk, UK
1190788	788	2010	1	Barn Field, Norfolk, UK
1190789	789	2010	1	Barn Field, Norfolk, UK
1190816	816	2010	1	Barn Field, Norfolk, UK
1190007	7	2012	6	Coopers Field, Norfolk, UK
1190042	42	2012	6	Coopers Field, Norfolk, UK
1190092	92	2012	6	Coopers Field, Norfolk, UK
1190103	103	2012	6	Coopers Field, Norfolk, UK
1190141	141	2012	6	Coopers Field, Norfolk, UK
1190145	145	2012	6	Coopers Field, Norfolk, UK
1190231	231	2012	6	Coopers Field, Norfolk, UK
1190281	281	2012	6	Coopers Field, Norfolk, UK
1190291	291	2012	6	Coopers Field, Norfolk, UK

GRU Store Code	ID	Year	m^2 plots	Location
1190444	444	2012	6	Coopers Field, Norfolk, UK
1190471	471	2012	6	Coopers Field, Norfolk, UK
1190475	475	2012	6	Coopers Field, Norfolk, UK
1190551	551	2012	6	Coopers Field, Norfolk, UK
1190560	560	2012	6	Coopers Field, Norfolk, UK
1190627	627	2012	6	Coopers Field, Norfolk, UK
1190629	629	2012	6	Coopers Field, Norfolk, UK
1190639	639	2012	6	Coopers Field, Norfolk, UK
1190671	671	2012	6	Coopers Field, Norfolk, UK
1190680	680	2012	6	Coopers Field, Norfolk, UK
1190694	694	2012	6	Coopers Field, Norfolk, UK
1190704	704	2012	6	Coopers Field, Norfolk, UK
1190705	705	2012	6	Coopers Field, Norfolk, UK
1190746	746	2012	6	Coopers Field, Norfolk, UK
1190747	747	2012	6	Coopers Field, Norfolk, UK
1190777	777	2012	6	Coopers Field, Norfolk, UK
1190788	788	2012	6	Coopers Field, Norfolk, UK
1190789	789	2012	6	Coopers Field, Norfolk, UK
1190816	816	2012	6	Coopers Field, Norfolk, UK
1190007	7	2013	1	Bylands, Yorkshire, UK
1190042	42	2013	1	Bylands, Yorkshire, UK
1190092	92	2013	1	Bylands, Yorkshire, UK
1190103	103	2013	1	Bylands, Yorkshire, UK
1190141	141	2013	1	Bylands, Yorkshire, UK
1190145	145	2013	1	Bylands, Yorkshire, UK
1190231	231	2013	1	Bylands, Yorkshire, UK

GRU Store Code	ID	Year	m^2 plots	Location
1190281	281	2013	1	Bylands, Yorkshire, UK
1190291	291	2013	1	Bylands, Yorkshire, UK
1190444	444	2013	1	Bylands, Yorkshire, UK
1190471	471	2013	1	Bylands, Yorkshire, UK
1190475	475	2013	1	Bylands, Yorkshire, UK
1190551	551	2013	1	Bylands, Yorkshire, UK
1190560	560	2013	1	Bylands, Yorkshire, UK
1190627	627	2013	1	Bylands, Yorkshire, UK
1190629	629	2013	1	Bylands, Yorkshire, UK
1190639	639	2013	1	Bylands, Yorkshire, UK
1190671	671	2013	1	Bylands, Yorkshire, UK
1190680	680	2013	1	Bylands, Yorkshire, UK
1190694	694	2013	1	Bylands, Yorkshire, UK
1190704	704	2013	1	Bylands, Yorkshire, UK
1190705	705	2013	1	Bylands, Yorkshire, UK
1190746	746	2013	1	Bylands, Yorkshire, UK
1190747	747	2013	1	Bylands, Yorkshire, UK
1190777	777	2013	1	Bylands, Yorkshire, UK
1190788	788	2013	1	Bylands, Yorkshire, UK
1190789	789	2013	1	Bylands, Yorkshire, UK
1190816	816	2013	1	Bylands, Yorkshire, UK
1190007	7	2014	1	Coopers Field, Norfolk, UK
1190042	42	2014	1	Coopers Field, Norfolk, UK
1190092	92	2014	1	Coopers Field, Norfolk, UK
1190103	103	2014	1	Coopers Field, Norfolk, UK
1190141	141	2014	1	Coopers Field, Norfolk, UK

GRU Store Code	ID	Year	m^2 plots	Location
1190281	281	2014	1	Coopers Field, Norfolk, UK
1190291	291	2014	1	Coopers Field, Norfolk, UK
1190444	444	2014	1	Coopers Field, Norfolk, UK
1190475	475	2014	1	Coopers Field, Norfolk, UK
1190551	551	2014	1	Coopers Field, Norfolk, UK
1190560	560	2014	1	Coopers Field, Norfolk, UK
1190627	627	2014	1	Coopers Field, Norfolk, UK
1190629	629	2014	1	Coopers Field, Norfolk, UK
1190671	671	2014	1	Coopers Field, Norfolk, UK
1190694	694	2014	1	Coopers Field, Norfolk, UK
1190705	705	2014	1	Coopers Field, Norfolk, UK
1190747	747	2014	1	Coopers Field, Norfolk, UK
1190777	777	2014	1	Coopers Field, Norfolk, UK
1190788	788	2014	1	Coopers Field, Norfolk, UK
1190789	789	2014	1	Coopers Field, Norfolk, UK
1190816	816	2014	1	Coopers Field, Norfolk, UK

	698	349
	694	324
	694	313
	690	Soison
	690	313
	685	308
	Soison	305
	685	300
	683	299
	680	292
	671	291
	670	352
	662	273
	652	264
	639	254
	637	325
	629	246
	627	239
	627	238
	Soison	Soison
912	624	231
827	605	224
827	591	Soison
827	591	223
816	580	219
816	Soison	218
814	579	216
811	568	Soison
Soison	568	209
811	566	209
789	562	Soison
788	560	199
784	551	199
777	546	181
771	507	160
753	496	149
750	483	145
749	481	141
747	475	139
Soison	Soison	Soison
746	474	127
742	471	Soison
742	471	126
740	468	110
651	Soison	103
732	468	92
731	460	81
Soison	451	79
731	444	Soison
729	440	45
729	433	44
722	420	42
707	406	40
705	398	34
705	397	34
704	396	32
700	387	23
700	360	7
698	355	4
Soison	Soison	Soison

Supplemental Table 2.2. Field trial (1 m^2 plots at Church Farm, Norfolk UK (52°37'49.2"N 1°10'40.2"E)) of Watkins. Numbers represent the lines, and Soison was used as a standard for the field trial validation.

Supplemental Table 2.3. AM content (%) of different starch types. This data has been adopted from (Fahy et al., 2022, Corrado et al., 2022a, Koev et al., 2020)

Starch type	AM Content (%)
Waxy maize	1.1 (± 0.6)
Normal maize	23.1 (± 0.4)
High AM maize	69.7 (± 0.7)
High AM (*ssIIIa*) wheat	35.1 (± 0.56)
High AM (*sbeII*) wheat	39 (± 1.1)

Supplemental Table 2.4. Starch digested (%) for Watkins and elite varieties. Values represent mean (± SE) of n ≥ 3 replicates.

Lines	0 min	6 min	12 min	18 min	24 min	40 min	90 min
4	0.43 (0.4)	24.66 (2.92)	27.67 (3.79)	27.44 (3.21)	28.15 (3.77)	28.09 (3.04)	31.3 (2.4)
7	0.55 (0.15)	19.19 (0.7)	24.71 (0.68)	26.05 (0.76)	27.18 (1.01)	28.12 (0.65)	30.37 (1.1)
23	0.81 (0.21)	17.25 (2.5)	22.19 (2.96)	23.67 (2.35)	23.44 (1.8)	24.79 (1.56)	27.83 (1.23)
32	0.27 (0.33)	17.72 (3.84)	24.25 (3.83)	26.53 (3.52)	25.81 (1.94)	27 (2.47)	29.78 (2.29)
34	0.97 (0.5)	12.97 (0.26)	17.44 (0.25)	19.68 (0.21)	20.24 (1.33)	22.69 (0.93)	26.03 (0.5)
40	0.79 (0.52)	14.69 (3.83)	18.82 (3.74)	20.49 (3.59)	20.87 (2.91)	23.09 (2.38)	24.9 (0.38)
42	0.48 (0.13)	23.83 (0.51)	28.01 (0.74)	29.16 (0.72)	29.02 (1.06)	30.75 (1.85)	32.04 (0.8)
44	1.16 (0.38)	13.78 (2.25)	19.27 (1.71)	21.43 (1.99)	22.9 (1.29)	25.36 (1.84)	28.18 (1.85)
45	0.24 (0.19)	24.34 (1.65)	29.01 (1.19)	29.59 (1.12)	30.99 (1.21)	31.6 (2.15)	34.33 (1.89)
79	0.65 (0.54)	22.61 (3.52)	27.02 (3.59)	28.96 (3.43)	28.03 (3.02)	29.87 (3.79)	32.86 (4.27)
81	1.42 (0.32)	15.1 (4.16)	19.86 (4.61)	22.3 (4.63)	23.3 (3.86)	25.42 (3.83)	28.92 (3)
92	1.04 (0.18)	15.64 (1.48)	20.88 (1.5)	22.45 (0.66)	23.54 (0.81)	24.88 (0.61)	27.33 (1.32)
103	0.55 (0.39)	17.35 (2.45)	22.44 (2.34)	24.78 (1.88)	25.51 (1.84)	26.64 (1.62)	29.22 (1.24)
110	0.07 (0.32)	23.2 (0.68)	26.21 (0.8)	26.31 (1.15)	25.9 (1.64)	26.64 (1.54)	28.81 (2.03)
126	1.23 (0.21)	21.58 (0.9)	26.26 (1.87)	25.44 (3.58)	28.54 (1.8)	30.8 (2.06)	32.65 (1.1)
127	0.38 (0.15)	22.84 (1.51)	26.67 (1.77)	28.45 (2)	29.76 (1.78)	31.8 (1.48)	31.34 (1.1)
139	0.76 (0.39)	16.42 (3.65)	21.9 (4.18)	24.92 (3.56)	26.04 (3.28)	27.85 (2.96)	29.48 (2.47)
141	1.28 (0.35)	18.54 (1.35)	24.53 (0.95)	26.71 (0.97)	26.85 (1.18)	27.96 (1.18)	29.93 (0.74)
145	0.94 (0.23)	14.97 (2.93)	19.41 (3.52)	21.09 (3.67)	22.82 (3.4)	24.74 (2.77)	26.32 (2.04)
149	0.35 (0.33)	22.97 (2.2)	26 (2.41)	26.79 (1.66)	26.39 (1.28)	26.8 (1.87)	29.9 (1.15)
160	0.78 (0.1)	28.75 (1.44)	31.61 (1.67)	33.92 (2.67)	33.43 (3.06)	34.86 (3.56)	37.18 (3.26)
181	0.58 (0.37)	25.77 (1.15)	28.22 (1.17)	28.81 (0.94)	28.4 (1.03)	28.58 (1.14)	31.47 (1.48)

Lines	0 min	6 min	12 min	18 min	24 min	40 min	90 min
199	1.01 (0.47)	20.69 (3.52)	27.13 (3.47)	30.31 (3.87)	29.29 (3.57)	29.39 (2.74)	32.36 (2.71)
209	0.9 (0.41)	25.62 (4.28)	31.68 (3.74)	32.75 (2.24)	33.03 (2.25)	34.22 (2.15)	35.48 (1.89)
216	1.23 (0.29)	10.51 (2.5)	15.27 (3.71)	17.58 (3.63)	18.76 (3.33)	20.25 (3.18)	23.86 (3.28)
218	0.27 (0.13)	13.05 (1.87)	18.54 (1.95)	21.78 (2.6)	23.03 (2.31)	25.04 (2.54)	27.2 (2.98)
219	0.61 (0.15)	18.22 (1.66)	22.34 (1.43)	22.31 (2.33)	23.12 (2.17)	24.06 (2.44)	27.39 (2.47)
223	1.44 (0.17)	24.96 (5.14)	30.46 (4.35)	32.35 (3.08)	32.95 (3.85)	34.13 (3.21)	36.68 (3.01)
224	0.6 (0.38)	20.53 (1.78)	24.08 (1.45)	24.63 (1.83)	25.38 (1.26)	23.5 (4.33)	28.58 (2.21)
231	0.42 (0.31)	15.4 (1.04)	21.33 (1.21)	23.23 (0.82)	23.72 (1.31)	25.77 (1.38)	28.1 (0.39)
238	0.15 (0.33)	16.15 (2.32)	23.32 (3.04)	25.13 (2.84)	26.63 (2.73)	28.53 (2.86)	32.25 (2.77)
239	0.33 (0.13)	24.34 (2.18)	28.29 (2.63)	29.68 (2.73)	31.04 (2.12)	32.8 (2.19)	33.75 (1.86)
246	1.27 (0.09)	18.11 (2.63)	23.99 (1.86)	25.19 (1.35)	27.21 (1.25)	27.75 (0.43)	30.43 (1.66)
254	1.13 (0.54)	18.2 (4.41)	22.72 (4.71)	24.58 (3.6)	24.8 (2.75)	26.77 (2.21)	29.7 (1.93)
264	-0.17 (0.61)	18.81 (3.11)	24.43 (3.08)	27.79 (2.15)	27.69 (1.52)	28.95 (0.77)	31.91 (0.46)
273	0.97 (0.82)	13.66 (4.63)	18.15 (6.04)	19.99 (5.5)	20.57 (5.09)	21.81 (4.41)	26.74 (5.28)
291	0.18 (0.25)	18.99 (1.62)	24.55 (1.88)	25.45 (1.58)	26.48 (1.6)	28.06 (1.42)	30.65 (0.44)
292	0.92 (0.51)	15.85 (2.23)	21.58 (2.55)	23.45 (1.77)	24 (1.25)	24.9 (0.8)	28.84 (1)
299	0.94 (0.49)	23.12 (2.59)	26.09 (2.24)	26.75 (1.62)	25.85 (1.24)	25.24 (0.84)	27.51 (1.34)
300	-0.08 (0.56)	11.06 (2.14)	15.28 (2.73)	17.83 (3.41)	18.65 (2.78)	20.24 (2.47)	24.4 (2.45)
305	1.03 (0.81)	18.28 (2.85)	23.43 (2.42)	24.95 (2.03)	26.12 (2.08)	27.47 (1.37)	29.57 (1.45)
308	1.92 (0.29)	26.68 (3.23)	33.01 (2.66)	35.31 (2.14)	35.79 (2.37)	36.14 (1.21)	37.57 (1.41)
313	0.91 (0.52)	11.54 (0.49)	16.97 (0.4)	19.57 (0.25)	21.84 (0.43)	24.19 (0.9)	27.96 (0.84)
324	0 (0.46)	24.56 (5.91)	29.03 (6.55)	32.37 (6.19)	30.81 (5.93)	31.96 (5.23)	35.67 (5.58)
325	1.06 (0.07)	31.61 (5.92)	33.77 (5.13)	34.35 (4.69)	34.37 (4.01)	34.39 (2.96)	36.66 (4.57)
349	1.25 (0.37)	25.85 (3.56)	30.15 (3.66)	30.92 (3.31)	30.49 (3.45)	30.93 (5.25)	32.38 (5.26)
352	0.85 (0.42)	18.57 (3.26)	22.72 (2.38)	23.99 (1.73)	24.35 (2.29)	25.27 (2.48)	29.33 (1.28)
355	1.19 (0.49)	17.84 (3.31)	23.04 (4.08)	24.42 (4.2)	24.01 (3.46)	24.7 (2.73)	28.27 (3.06)
360	0.7 (0.38)	14.97 (2.46)	20.13 (3.19)	22.77 (2.91)	23.49 (2.52)	24.62 (3.18)	28.88 (3.21)
387	0.45 (0.07)	16.51 (1.41)	22.72 (1.96)	24.58 (1.74)	24.92 (2.06)	26.86 (2.66)	27.5 (2.12)
396	0.78 (0.23)	20.77 (4.43)	25.82 (4.64)	27.34 (3.89)	28.23 (3.53)	28.62 (2.57)	28.28 (3.32)
397	1 (0.35)	27.43 (8.63)	33.04 (9.08)	34.63 (7.56)	34.51 (6.22)	35.67 (5.87)	37.19 (5.67)
398	0.39 (0.42)	20.21 (4.6)	25.72 (4.37)	26.84 (3.55)	27.26 (2.87)	27.71 (2.75)	31.26 (2.33)
406	1.12 (0.61)	17.94 (2.08)	23.62 (1.73)	24.5 (1.59)	23.79 (1.47)	23.74 (1.31)	27.8 (1.18)
420	1.33 (0.26)	11.2 (2.86)	14.35 (3.45)	16.84 (3.67)	17.71 (3.14)	20.75 (2.33)	24.03 (1.98)
433	0.74 (0.54)	14.97 (3.91)	20.31 (3.98)	23.07 (3.39)	23.76 (2.97)	25.07 (2.48)	28.65 (2.81)
440	0.04 (0.39)	21.35 (4.24)	27.26 (3.59)	28.83 (3.34)	28.7 (3.31)	30.05 (3.43)	32.08 (3.63)
444	1.18 (0.25)	22.24 (3.52)	27.49 (3.2)	29.24 (2.49)	28.53 (2.61)	28 (2.22)	32.41 (2.97)
451	0.58 (0.28)	16.91 (1.86)	22.34 (1.89)	23.54 (2.37)	24.33 (2.43)	25.96 (2.48)	27.58 (2.51)
460	1.19 (0.45)	19.66 (5.7)	23.5 (6.14)	24.9 (5.1)	24.97 (4.9)	26.83 (3.32)	30.73 (4.26)

Lines	0 min	6 min	12 min	18 min	24 min	40 min	90 min
468	1.25 (0.47)	22.34 (0.24)	26.48 (0.5)	28.04 (0.42)	27.76 (0.4)	29.25 (0.64)	32.68 (1.04)
471	1.06 (0.43)	21.22 (4.19)	26.41 (3.6)	27.68 (3.1)	28.25 (2.99)	29.01 (2.21)	33.34 (3.73)
474	0.4 (0.06)	25.73 (1.94)	29.73 (2)	31.16 (1.79)	31.14 (2.29)	32.24 (2.85)	33.17 (2.36)
475	1.47 (0.41)	27.15 (5.64)	33.53 (4.69)	34.11 (3.24)	34.86 (4.06)	35.05 (3.7)	36.82 (2.94)
481	0.74 (0.6)	20.03 (3.46)	26.96 (3.7)	28.83 (3.53)	28.15 (4.02)	30.67 (3.34)	34.42 (3.51)
483	0.56 (0.41)	22.22 (4.35)	27.47 (3.95)	30.15 (3.53)	30.36 (3.07)	32.12 (1.71)	32.81 (2.52)
496	0.39 (0.22)	19.89 (2.16)	25.88 (2.73)	29.01 (2.68)	28.88 (2.43)	30.62 (2.31)	32.33 (1.47)
507	0.63 (0.24)	24.54 (3.9)	28.68 (4.06)	29.86 (4.47)	30.98 (4.73)	33.74 (4.83)	35.23 (4.44)
546	0.57 (0.44)	28.17 (2.06)	32.67 (1.51)	33.79 (1.58)	32.71 (1.68)	34.31 (2.18)	37.87 (1.42)
551	0.33 (0.34)	12.37 (0.52)	18.95 (0.57)	21.06 (1.57)	22.34 (1.02)	23.12 (1.03)	26.58 (0.82)
560	0.56 (0.23)	19.28 (1.68)	24.73 (1.63)	25.72 (2.14)	25.93 (2.65)	27.43 (2.96)	28.6 (3.7)
562	1.09 (0.35)	21.84 (1.42)	27.6 (1.21)	28.82 (0.92)	29.35 (1.49)	30.24 (2.39)	33 (1.95)
566	1.41 (0.49)	20.92 (2.87)	25.24 (2.22)	29.06 (2.38)	29.82 (2.05)	31.69 (1.46)	31.81 (1.89)
568	0.28 (0.4)	17.58 (3.75)	24.57 (3.4)	27.55 (3.27)	27.32 (2.82)	28.95 (3.77)	31.27 (2.66)
579	1.12 (0.54)	21.57 (1.7)	27.27 (0.56)	29.01 (0.86)	28.75 (0.14)	30.13 (0.36)	33.45 (0.7)
580	0.76 (0.52)	16.87 (3.25)	21.8 (3.13)	23.54 (2.25)	24.01 (1.78)	25.27 (2.03)	25.62 (1.69)
591	0.09 (0.47)	21.29 (4.16)	26.1 (3.27)	26.29 (2.39)	25.73 (2.03)	26.87 (1.32)	30.76 (0.21)
605	0.33 (0.27)	15.91 (4.3)	19.68 (4.72)	21.09 (3.97)	21.39 (3.89)	22.86 (2.61)	26.45 (2.53)
624	0.7 (0.73)	14.61 (4.06)	17.33 (4.55)	19.51 (4.64)	19.88 (4.54)	22.11 (4.3)	24.97 (3.81)
627	0.76 (0.48)	17.36 (3.13)	23.13 (3.29)	25.26 (2.8)	25.32 (2.21)	26.3 (1.4)	29.14 (0.63)
629	1.1 (0.51)	23.11 (2.26)	26.37 (1.58)	26.91 (1.28)	26.38 (0.95)	28.63 (1.86)	31.82 (2.35)
637	0.78 (0.28)	22.77 (2.78)	27.73 (2.16)	28.53 (1.84)	27.55 (1.79)	27.89 (1.9)	30.67 (2.56)
639	1.01 (0.47)	9.76 (1.34)	14.06 (1.41)	17.2 (1.84)	18.83 (1.66)	21.64 (1.73)	24.27 (1.51)
651	1.07 (0.65)	13.83 (0.22)	19.45 (0.8)	23.56 (1.59)	25.09 (1.84)	28.54 (2.3)	32.45 (1.76)
652	0.76 (0.15)	20.2 (2.03)	25.99 (2.28)	28.39 (2.1)	27.64 (0.72)	29.4 (1.44)	31.63 (0.99)
662	1.36 (0.52)	23.59 (2.14)	27.46 (1.9)	27.17 (1.63)	25.92 (1.06)	26.67 (1.82)	30.66 (2.59)
670	0.69 (0.1)	25.39 (2.42)	30.26 (2.25)	32.09 (2.7)	32.93 (1.87)	34.03 (1.97)	37.58 (2.13)
671	1.32 (0.74)	17.06 (3.26)	22.02 (2.86)	24.75 (2.11)	25.26 (2.41)	27.02 (1.91)	29.71 (1.43)
680	0.09 (0.71)	21.81 (3.07)	27.57 (2.79)	29.42 (2.63)	30.22 (2.81)	33.32 (3.31)	36.83 (2.47)
683	0.43 (0.65)	27.11 (2.8)	31.44 (2.17)	33.85 (2.47)	32.37 (2.16)	33.5 (2.52)	35.11 (1.95)
685	-0.1 (0.23)	28.82 (0.72)	32.02 (0.98)	32.78 (0.89)	32.73 (0.15)	34.27 (0.79)	34.25 (0.79)
690	0.35 (0.46)	18.13 (5.91)	22.23 (5.73)	24.89 (5.45)	26.22 (5.72)	26.88 (5.07)	29.36 (4.75)
694	1.59 (0.3)	25.31 (2.88)	30.54 (2.54)	31.04 (2.4)	31.17 (1.55)	32.78 (1.83)	34.64 (2.72)
698	0.66 (0.39)	26.28 (1.2)	32.68 (1.19)	33.46 (1.31)	34.22 (0.81)	35.8 (0.81)	38.16 (1.04)
700	0.08 (0.4)	10.92 (1.36)	16 (2.13)	19.52 (1.7)	20.45 (2.17)	22.06 (2.35)	24.11 (1.58)
704	0.95 (0.28)	24.11 (3.63)	28.07 (3.34)	29.09 (2.88)	28.08 (3.87)	28.38 (4.1)	32.73 (4.36)
707	0.36 (0.29)	21.69 (4.14)	26.05 (3.26)	27.4 (2.42)	27.42 (2.52)	28.79 (1.83)	32.7 (1.25)
722	1.06 (0.62)	19.24 (2.36)	23.93 (2.75)	26.03 (2.41)	26.01 (2.43)	28.6 (3.07)	31.33 (1.76)

Lines	0 min	6 min	12 min	18 min	24 min	40 min	90 min
729	0.21 (0.4)	16.31 (2.15)	21.81 (2.57)	23.73 (2.11)	23.41 (2.18)	23.9 (2.57)	27.03 (2.74)
731	0.65 (0.46)	20.23 (1.07)	26.08 (0.84)	28.62 (1.03)	27.84 (1.17)	29.17 (0.49)	32.22 (0.51)
732	3.02 (0.13)	25.23 (2.69)	29.75 (2.04)	31.31 (2.05)	31.14 (1.49)	32.43 (1.32)	34.44 (1.38)
740	0.75 (0.1)	29.3 (2.44)	32.71 (2.91)	34.05 (2.97)	31.9 (2.12)	33.15 (2.42)	36.54 (2)
742	0.76 (0.42)	17.71 (4.66)	24.3 (5.42)	27.05 (5.04)	27.19 (3.51)	28.94 (2.52)	30.93 (3.12)
746	0.69 (0.13)	28.62 (4.64)	34.37 (4.91)	36.03 (5.12)	35.16 (4.3)	34.58 (4.12)	37.06 (3.95)
747	1.69 (0.33)	26.5 (4.01)	31.23 (2.89)	32.38 (1.7)	33.28 (1.99)	33.92 (1.11)	36.05 (1.66)
749	0.82 (0.42)	28.73 (2.52)	34.99 (2.17)	36.91 (1.94)	36.07 (1.15)	37.79 (1.99)	39.89 (1.88)
750	1.07 (0.33)	19.3 (1.05)	24.04 (1.12)	25.65 (1.02)	25.72 (1.25)	25.37 (1.5)	29.32 (1.16)
753	0.75 (0.05)	19.41 (1.21)	23.91 (1.59)	26.34 (1.52)	26.34 (1.55)	27.8 (1.42)	28.31 (1.24)
771	1.07 (0.05)	18.44 (4.61)	22.56 (4.11)	23.48 (3.21)	23.73 (2.92)	24.14 (2.42)	25.93 (1.28)
777	1.58 (0.7)	9.69 (0.61)	13.19 (0.87)	14.81 (0.86)	16.15 (1.07)	18.98 (1.08)	23.54 (1.46)
784	0.62 (0.64)	14.68 (2.07)	20.21 (1.59)	22.71 (1.63)	23.24 (1.81)	24.15 (2.42)	27.63 (2.35)
788	0.95 (0.45)	21.67 (2.77)	26.11 (2.31)	26.32 (2.32)	26.3 (3.14)	26.77 (2.61)	28.02 (2.29)
789	1.12 (0.34)	20.35 (3.77)	25.12 (3.12)	26.33 (3.81)	25.89 (3.21)	27.44 (3.9)	29.77 (3.66)
811	0.43 (0.45)	18.16 (3.65)	24.04 (3.94)	25.32 (1.91)	25.62 (2.05)	27.57 (2.05)	30.14 (3.26)
814	0.87 (0.29)	20.46 (3.69)	25.37 (3.93)	26.79 (3.73)	25.91 (3.54)	27.24 (3.58)	29.72 (4.71)
816	1.18 (0.34)	30.08 (1.27)	34.03 (1.48)	37.23 (2.15)	35.31 (0.79)	36.78 (1.16)	39.2 (1.58)
827	-0.05 (0.73)	20.28 (3.08)	25.19 (2.63)	26.73 (1.11)	26.9 (1.1)	28.85 (1.37)	30.93 (0.85)
912	0.64 (0.4)	21.15 (4.87)	25.71 (4.59)	28.02 (3.96)	27.63 (3.32)	29.01 (3.49)	32.63 (3.02)
Cougar	0.81 (0.49)	36.43 (2.85)	40.43 (1.74)	43.81 (0.08)	43.41 (1.41)	43.39 (1.08)	43.45 (2.23)
Crusoe	1.9 (0.18)	28.62 (3.81)	32.3 (2.89)	33.57 (2.84)	33.37 (2.6)	31.33 (2.19)	35 (3.86)
Dickens	1.87 (0.39)	31.82 (2.69)	34.84 (2.45)	34.63 (2.48)	35.25 (2.3)	35.9 (2.12)	37.56 (2.64)
Diego	1.15 (0.24)	26.77 (1.41)	29.41 (1.08)	30.64 (1.62)	30.02 (1.08)	31.84 (1.18)	31.19 (1.25)
Myriad	0.62 (0.25)	34.79 (2.27)	38.13 (2.62)	38.71 (2.84)	37.59 (2.51)	39.01 (2.56)	41.58 (1.07)
Paragon	0.86 (0.16)	29.24 (1.35)	33.17 (1.15)	34.55 (1.39)	34.37 (1.54)	34.93 (2.38)	38.01 (1.18)
Santiago	1.82 (0.49)	28.67 (2.28)	32.36 (2.5)	32.57 (2.79)	32.37 (2.85)	33.48 (2.9)	36.82 (2.96)
Skyfall	1.11 (0.37)	28.95 (2.14)	32.83 (2.1)	33.18 (3.09)	32.13 (2.77)	32.98 (2.37)	35.13 (1.45)

Supplemental Table 2.5. TS content (g/100 flour) of the Watkins lines and selected elite varieties measured by HK assay (Megazyme), ordered from lowest to highest. Values represent mean ± (SE) of n = 4 replicates.

Lines	TS content g/100 flour
651	42.8 (3.3)
680	45.0 (4.7)
292	45.4 (2.4)
Cougar	45.5 (3.6)
420	46.2 (1.3)
34	47.4 (2.7)
440	47.4 (1)
722	47.7 (2.4)
313	48.1 (3.5)
481	48.2 (1.6)
671	48.3 (1.3)
216	48.4 (3.2)
324	48.6 (2.3)
690	48.6 (1)
731	48.7 (2.7)
700	48.9 (2.4)
460	49.1 (1.1)
360	49.1 (1.8)
308	49.1 (2.8)
300	49.1 (0.7)
Myriad	49.8 (4.9)
496	50.0 (3.9)

Lines	TS content g/100 flour
305	50.0 (0.9)
568	50.2 (0.9)
551	50.3 (0.6)
149	50.4 (1.2)
729	50.5 (0.6)
139	50.6 (3.2)
273	50.9 (2.3)
562	51.2 (0.9)
199	51.2 (1.7)
246	51.3 (1.7)
355	51.4 (1.6)
591	51.5 (4.7)
742	51.5 (0.9)
698	51.5 (2.4)
44	51.6 (2)
92	51.7 (2.2)
777	51.7 (1.6)
475	51.7 (1.5)
264	51.9 (2)
141	52.1 (1.7)
238	52.1 (1.6)
483	52.1 (1.3)
639	52.1 (2)
444	52.2 (2.2)
398	52.3 (1.5)
254	52.4 (1.2)

Lines	TS content g/100 flour
126	52.4 (3.5)
627	52.4 (0.8)
784	52.6 (1.7)
471	52.7 (1.9)
40	52.8 (2.8)
749	52.9 (1.8)
218	52.9 (0.6)
811	53.0 (1.7)
81	53.0 (1.1)
468	53.1 (0.6)
827	53.1 (2.1)
670	53.1 (3.8)
629	53.2 (1.5)
352	53.2 (1.3)
566	53.3 (2.6)
223	53.4 (1.6)
694	53.4 (1)
579	53.4 (1.9)
605	53.4 (1.2)
145	53.5 (1.3)
816	53.6 (1.7)
79	53.8 (1.1)
7	53.9 (1.9)
732	53.9 (1.1)
789	53.9 (2.3)
291	54.0 (4.7)

Lines	TS content g/100 flour
580	54.1 (1.4)
397	54.2 (1.1)
219	54.2 (1.5)
433	54.4 (2.1)
683	54.5 (1.7)
788	54.6 (1.2)
231	55.1 (1.2)
624	55.1 (1.5)
750	55.2 (0.9)
707	55.4 (2.3)
747	55.5 (0.9)
912	55.6 (0.9)
Crusoe	55.6 (0.7)
560	55.7 (1.6)
652	55.9 (1.5)
103	56.0 (1.9)
546	56.0 (1.7)
299	56.1 (0.6)
Skyfall	56.2 (1.8)
209	56.2 (1)
325	56.2 ()1.9
451	56.3 (1.5)
740	56.3 (1.2)
771	56.4 (3.8)
406	56.5 (1.7)
224	56.6 (0.4)

Lines	TS content g/100 flour
637	56.8 (1)
507	56.8 (0.6)
Paragon	56.8 (1.3)
746	56.8 (1.7)
160	56.9 (1.6)
Santiago	56.9 (2)
23	56.9 (1.6)
814	57.1 (0.8)
387	57.2 (1.1)
474	57.2 (1)
4	57.3 (1.6)
349	57.4 (0.5)
685	57.4 (1)
127	57.6 (1.1)
662	58.0 (0.6)
753	58.0 (1.7)
45	58.2 (0.7)
704	58.3 (1.6)
396	59.0 (1.5)
181	59.5 (1.4)
110	60.1 (1.2)
32	60.4 (1.2)
239	60.4 (1)
Dickens	60.5 (1)
42	60.9 (2.4)
Diego	61.3 (0.9)

Supplemental Table 2.6. NIR parameters of the Watkins and elite line grains. Values represent the mean of n = 3 technical replicates.

Lines	**Moisture %, NIR**	**Protein Dry basis %, NIR**	**Starch Dry basis %, NIR**	**Ash Dry basis %, NIR**	**NDF Dry basis %, NIR**
4	11.7	15.3	73.5	1.78	18.29
7	11.8	15.5	73	1.79	18.17
23	12.2	13.6	74.8	1.72	18.08
32	12.2	12.9	75.4	1.74	18.33
34	11.9	17.5	71.1	1.83	16.43
40	11.6	11.9	75.5	1.69	17.13
42	12.4	13.5	74.7	1.71	16.97
44	12.3	13.4	76	1.74	17.82
45	12.1	14.8	74.1	1.76	16.23
79	12	16.8	72.4	1.78	18.26
81	11.8	15.6	72.8	1.74	16.45
92	12.1	13.9	74.5	1.75	16.59
103	12.3	16.8	72.8	1.79	18.68
110	12	15.9	72.1	1.78	17.77
126	11.4	17.9	70.7	1.82	20.16
127	11.6	16.6	72.4	1.8	17.91
139	12.1	17.4	72.8	1.82	18.69
141	11.7	16.2	72.2	1.81	18.42
145	11.8	17.4	70.4	1.82	20.34
149	11.4	15.9	71.8	1.78	19.03
160	12.3	15.2	73.3	1.73	17.99
181	12.2	15.7	73	1.78	19.15

Lines	Moisture %, NIR	Protein Dry basis %, NIR	Starch Dry basis %, NIR	Ash Dry basis %, NIR	NDF Dry basis %, NIR
199	12.2	15	74	1.74	19.59
209	12.6	14.8	73.5	1.71	17.95
216	12.2	18.4	69.7	1.84	20.04
218	12.1	17.5	69	1.82	19.43
219	12.2	15.5	72.7	1.78	17.94
223	12.4	17	70.1	1.8	19.29
224	12.7	16.3	72.9	1.78	18.3
231	12.7	14	72.6	1.75	19.57
238	11.9	16.6	71.9	1.81	21.41
239	12.5	14.5	74.3	1.74	18.53
246	12.2	20.8	68.1	1.88	19.62
254	12.2	14.7	73.4	1.75	19.34
264	11.8	15.1	73.4	1.76	18.87
273	12.9	14.4	75.1	1.77	19.44
291	12.1	14.7	73	1.77	19.92
292	12.2	16.6	72.7	1.81	21.12
299	12.7	15.2	72.6	1.8	20.35
300	12	16.2	72.5	1.8	20.19
305	11.7	16	73	1.8	19.03
308	11.4	14.6	72.4	1.74	20.44
313	11.2	16.5	72.2	1.8	18.79
324	12.4	17.3	71.6	1.8	20.07
325	11.3	15.5	72.5	1.75	18.3
349	12.8	15.8	73.6	1.79	19.02
352	11.3	17.3	71.7	1.79	19.47
355	11.2	18.3	70	1.82	19.81

Lines	Moisture %, NIR	Protein Dry basis %, NIR	Starch Dry basis %, NIR	Ash Dry basis %, NIR	NDF Dry basis %, NIR
360	11.7	15.5	73.8	1.76	18.85
387	11.2	14.7	73.7	1.78	20.47
396	12.2	14.3	73.3	1.72	20.64
397	11.6	16.5	72.7	1.78	19.52
398	11.4	19.4	69.7	1.84	20.57
406	11.3	16	72.8	1.78	20.36
420	12.2	17.3	72.7	1.81	18.3
433	11.3	16.1	72.1	1.8	20.74
440	12.2	16.8	70.7	1.84	20.9
444	11.4	15.9	74.4	1.72	18.36
451	11.5	17	71.8	1.79	17.78
460	11.3	16.1	71.9	1.8	20.57
468	12.1	21.1	69.2	1.89	17.81
471	11.4	18.2	70	1.84	21.88
474	12.7	17.2	72.6	1.83	20.34
475	12.1	15	73.3	1.76	19.61
481	12.3	16.4	72.2	1.8	16.96
483	12	18.3	70.1	1.83	19.48
496	12.3	16.7	70.9	1.8	18.49
507	12.1	16.9	70.9	1.81	17.98
546	12.4	17.5	71.1	1.8	20.66
551	12.3	17.1	71.8	1.82	18.14
560	11.9	16.4	71.9	1.79	19.34
562	12.7	18.3	70.3	1.87	19.92
566	12	18	71.4	1.83	21.15
568	12.9	18.6	70.1	1.86	20.9

Lines	Moisture %, NIR	Protein Dry basis %, NIR	Starch Dry basis %, NIR	Ash Dry basis %, NIR	NDF Dry basis %, NIR
579	12.5	16.6	73.3	1.79	18.16
580	11.9	16.2	71.1	1.79	20.09
591	12.3	20.3	68.5	1.88	18.96
605	12.5	16.9	71.6	1.81	20.07
624	12.5	13.7	75.7	1.75	19.37
627	12.1	15.6	72.6	1.79	20.99
629	12.6	16.5	71.7	1.8	21.54
637	12.5	16.2	71.8	1.78	19.19
639	12.5	15.2	74.3	1.77	18.7
651	11.4	15.6	73.6	1.78	19.59
652	12.8	15.7	72.6	1.8	20.86
662	12.1	15.4	72.4	1.76	19.78
670	11.8	15.2	73.8	1.76	20.72
671	11.7	17.8	70.4	1.83	21.94
680	12.1	17.5	71.2	1.83	20.28
683	12.2	17.7	71.7	1.82	19.28
685	11.4	17.4	70.5	1.8	18.81
690	12.1	17.3	72	1.8	20.14
694	11.7	19.4	69.1	1.85	19.44
698	12	18.4	68.9	1.81	17.96
700	11.9	21.1	66.7	1.9	19.24
704	12.1	13.9	74.8	1.77	18.78
705	12	17.1	72.6	1.81	17.9
707	12.5	16.9	72.5	1.79	18.5
722	12	14.9	73	1.74	17.91
729	11.8	20.4	68.3	1.88	20.55

Lines	Moisture %, NIR	Protein Dry basis %, NIR	Starch Dry basis %, NIR	Ash Dry basis %, NIR	NDF Dry basis %, NIR
731	11.5	16.8	71.2	1.82	20.81
732	11.7	15.1	73.5	1.76	19.53
740	11.9	14.8	73.4	1.74	17.95
742	12.3	18.1	70.4	1.81	19.81
746	12	14.1	74.5	1.72	19.57
747	12.7	14.1	74.8	1.71	19.62
749	12.4	16.3	72.8	1.76	20.17
750	12.9	16.3	71.9	1.77	16.87
753	12.9	13.5	75.5	1.71	18.39
771	12.3	14.7	73.4	1.74	18.95
777	12.6	14.8	73.9	1.76	18.78
784	12.6	15.1	73.2	1.76	19.69
788	12	16.6	71	1.77	21.19
789	12.7	14.5	73.1	1.75	20.99
811	13.1	15.8	72.7	1.79	19.97
814	12.8	15.3	73.9	1.77	18.89
816	12.9	17.5	70.1	1.81	22.24
827	12.3	16.8	71.1	1.8	19.77
912	12.3	15.1	73.3	1.77	17.91
Cougar	12	11.4	76.6	1.71	19.6
Crusoe	10.7	12.1	76.8	1.64	18.92
Dickens	11	10.9	77.9	1.65	19.38
Diego	11.2	11.1	77.8	1.67	17.47
Myriad	12.4	11.6	76.6	1.67	19.78
Paragon	10.1	14	74.5	1.71	19.25
Santiago	11.1	11.3	76	1.68	19.14

Lines	Moisture %, NIR	Protein Dry basis %, NIR	Starch Dry basis %, NIR	Ash Dry basis %, NIR	NDF Dry basis %, NIR
Skyfall	10.9	11.3	77	1.64	16.64

Supplemental Table 2.7. Hardness of Watkins from 2010 obtained by SKCS, provided by Dr Alison Lovegrove (Rothamsted Research). Hardness distribution and classification code refers to % soft kernels - % semi-soft kernels - % semi-hard kernels - % hard kernels.

Lines	kernel hardness index (mean)	Hardness distribution and classification code	class index
4	34.4	57-21-16-06-04	4
7	46.3	18-25-41-16-03	3
23	69.7	00-05-25-70-01	1
32	14.3	84-13-03-00-05	5
40	16.1	90-07-02-01-05	5
42	17.2	90-09-01-00-05	5
44	46.3	16-30-33-21-03	3
79	47.5	11-37-34-18-03	3
81	80.5	00-01-10-89-01	1
92	36.2	44-30-19-07-04	4
103	17.0	94-04-01-01-05	5
110	47.6	11-35-43-11-03	3
126	84.6	00-00-06-94-01	1
127	88.5	00-00-05-95-01	1
139	20.0	86-10-03-01-05	5
141	39.2	31-47-18-04-05	5
145	70.4	02-05-15-78-01	1
149	29.4	61-27-08-04-05	5
160	30.5	53-39-07-01-05	5
181	42.3	24-36-32-08-04	4
209	64.7	04-16-23-57-01	1
216	28.8	61-30-08-01-05	5
218	24.9	74-20-05-01-05	5
219	22.7	79-14-07-00-05	5
223	35.9	44-35-14-07-04	4
224	70.5	00-01-17-82-01	1
231	29.8	62-28-07-03-05	5
238	30.4	59-29-10-02-05	5

Lines	kernel hardness index (mean)	Hardness distribution and classification code	class index
239	19.3	85-12-03-00-05	5
246	73.9	04-03-09-84-01	1
254	31.7	57-32-07-04-05	5
264	28.8	65-22-08-05-05	5
273	20.3	84-13-03-00-05	5
291	34.1	49-31-17-03-05	5
292	31.4	60-28-09-03-05	5
299	28.6	62-26-08-04-05	5
300	31.9	54-26-17-03-05	5
305	36.7	41-36-16-07-04	4
308	104.8	00-00-00-100-01	1
313	44.4	18-36-32-14-03	3
324	32.9	47-40-10-03-05	5
325	37.3	35-44-17-04-05	5
349	66.1	03-03-22-72-01	1
352	86.5	00-01-00-99-01	1
355	69.7	01-00-22-77-01	1
360	16.2	92-07-00-01-05	5
387	48.3	19-31-24-26-03	3
396	50.9	07-26-44-23-01	1
397	35.6	47-38-13-02-05	5
398	30.5	62-30-07-01-05	5
406	44.8	20-37-27-16-03	3
420	18.0	93-06-01-00-05	5
433	80.9	00-00-06-94-01	1
440	46.9	22-25-30-23-03	3
444	82.0	00-00-05-95-01	1
451	41.8	22-40-34-04-05	5
468	63.4	00-09-28-63-01	1
471	70.6	00-02-21-77-01	1
481	39.5	27-50-19-04-05	5
483	27.6	69-19-11-01-05	5
496	33.4	49-35-14-02-05	5
507	63.0	01-11-23-65-01	1
546	37.1	31-51-16-02-05	5
551	7.2	98-01-00-01-05	5
562	73.4	00-03-06-91-01	1
565	49.1	09-35-36-20-01	1
568	61.4	13-15-22-50-03	3
579	78.8	06-02-05-87-03	3
580	83.0	00-01-03-96-01	1
591	39.4	43-24-21-12-03	3
605	79.9	00-00-08-92-01	1

Lines	kernel hardness index (mean)	Hardness distribution and classification code	class index
624	29.5	64-24-09-03-05	5
627	37.5	44-31-13-12-03	3
629	37.7	40-33-14-13-03	3
637	67.1	01-05-19-75-01	1
639	38.1	36-38-20-06-04	4
651	46.5	14-35-34-17-03	3
652	38.8	35-40-15-10-04	4
662	75.7	00-01-07-92-01	1
670	36.1	49-24-21-06-04	4
671	36.8	39-36-20-05-05	5
680	18.2	89-10-01-00-05	5
683	63.7	01-11-31-57-01	1
685	31.9	57-28-09-06-04	4
694	78.0	01-02-05-92-01	1
698	82.9	01-01-06-92-01	1
700	46.1	18-29-38-15-03	3
704	71.2	00-05-13-82-01	1
707	63.5	06-12-24-58-01	1
722	42.8	15-48-32-05-05	5
731	32.0	57-24-13-06-04	4
732	96.6	00-00-02-98-01	1
740	66.4	11-11-16-62-03	3
742	27.3	70-26-04-00-05	5
746	77.9	00-02-09-89-01	1
747	79.5	00-00-05-95-01	1
749	79.8	00-00-05-95-01	1
750	77.7	00-03-06-91-01	1
753	57.1	10-25-23-42-01	1
771	79.8	00-03-05-92-01	1
777	78.5	01-00-07-92-01	1
784	19.8	85-13-00-02-05	5
788	73.9	00-07-12-81-01	1
789	100.4	00-00-01-99-01	1
811	45.7	19-32-33-16-03	3
814	29.8	60-23-13-04-05	5
816	39.9	44-25-17-14-03	3
912	46.7	12-40-30-18-03	3

Supplemental Table 3.1. Grain and starch characteristics on selected Watkins lines and elite varieties. Protein content of wholemeal flour was measured on a fresh weight basis. Coulter counter analysis, granule size distribution described as the relative volume of B-type granules (%), B-type granule diameter (µm) and A-type granule diameter (µm). CLD was determined by SEC, AP long to short chains (ratio of 37<x<100 to <37 DP), AM long/short chains (ratio of and >1000 to >100-1000 DP), AM/AP (ratio of >100 to <100). Endogenous α-amylase was determined as Ceralpha Units/g of flour. Values represent mean ± SE. Statistically significant value p shows the difference between low digestibility and high digestibility group.

	Lines	Protein content (g/100 flour)	B granule (%)	B-type granule diameter (µm)	A-type granule diameter (µm)	AP long/short chains	AM long/short chains	AM/AP ratio	Endogenous α-amylase Ceralpha Units/g flour
p-value		p < 0.001	ns	p < 0.01	p < 0.001	p < 0.001	p < 0.005	ns	p < 0.05
Low Digestibility	639	15.1 (0.17)	37.1 (1.9)	6.4 (0.2)	18.2 (0.1)	0.23 (0.01)	0.94 (0.06)	0.32 (0.01)	0.06 (0.01)
	777	14.2 (0.16)	34 (2)	6 (0.1)	18.2 (0.2)	0.24 (0.01)	0.93 (0.05)	0.30	0.07 (0.01)
	216	18.4 (0.05)	28.6 (1.6)	8.4 (0.2)	20.1 (0.2)	0.26	1.10 (0.04)	0.29 (0.01)	0.15 (0.01)
High Digestibility	308	14.9 (0.18)	35.3 (1.7)	6.2 (0.1)	17.7	0.21 (0.01)	1.06 (0.06)	0.26 (0.02)	0.13 (0.01)
	Myriad	11.1 (0.22)	34.2 (2.4)	6.7 (0.1)	19.2 (0.5)	0.25	0.84 (0.13)	0.29 (0.02)	0.06 (0.01)
	816	17.4 (0.19)	34.8 (0.7)	6.9 (0.4)	19 (0.5)	0.20 (0.01)	0.65 (0.05)	0.27 (0.03)	0.09 (0.01)
	Paragon	13.5 (0.24)	30.9 (1)	6.6 (0.1)	20.1 (0.2)	0.21	1.16 (0.14)	0.29 (0.01)	0.05 (0.01)
	Dickens	10.6 (0.15)	29 (3.3)	6.3 (0.2)	19.2 (0.3)	0.22	1.09 (0.04)	0.28	0.05 (0.01)

Supplemental Table 3.2. Pearson correlation of starch digestibility % (90 min) and flour and starch structure parameters.

Parameters	r	p value
Onset T (1st cycle)	0.37	ns
Peak T (1st cycle)	0.5	ns
Enthalpy (2nd cycle)	0.56	ns
Onset T (2nd cycle)	**-0.77**	**<0.05**
Peak T (2nd cycle)	-0.65	ns
Enthalpy (2nd cycle)	**-0.73**	**<0.05**
Particle size	-0.14	ns
Protein content	-0.47	ns
En α-amylase	-0.66	ns
B granule (%)	-0.01	ns
A-granule diameter (µm)	-0.23	ns
B-granule diameter (µm)	0.12	ns
AM/AP	-0.66	ns
AM c. (long/short)	-0.19	ns
AP c. (long/short)	-0.53	ns

Supplemental Table 3.3. DSC parameters measured for wholemeal flour samples of low- and high-digestibility lines. Values represent mean (SE) of n = 3 replicates.

	1st Cycle				**2nd Cycle**		
	Lines	**Onset Temp** (°C)	**Peak Temp** (°C)s	**Enthalpy** (J/g)	**Onset Temp** (°C)	**Peak Temp** (°C)	**Enthalpy** (J/g)
p - value		p < 0.001	p < 0.001	p < 0.001	p < 0.05	p < 0.001	p < 0.001
Low Digestibility	639	54.5 (0)	62.1 (0.1)	9.2 (0.1)	80.5 (0.3)	92.2 (0)	10.2 (0.7)
	777	58.2 (0)	65.2 (0.1)	9.4 (0.2)	79.5 (0.3)	92.5 (0.1)	10.1 (0.7)
	216	55.6 (0.1)	63.3 (0.1)	9.2 (0.2)	81.3 (2)	93 (0.2)	10.1 (0.3)
High Digestibility	308	56.9 (0)	65.1 (0)	10 (0.2)	79.6 (0.3)	92.5 (0)	9.8 (0.4)
	Myriad	58.4 (0.1)	65.6 (0.2)	11.5 (0.5)	76.4 (0.8)	91.7 (0)	8.4 (0.1)
	816	58.3 (0)	65.4 (0)	10.5 (0.1)	78.9 (0.3)	92.5 (0)	7.8 (0.7)
	Paragon	54.6 (0)	62.8 (0.1)	9 (0.1)	78.5 (0.2)	91.9 (0)	7.6 (0.1)
	Dickens	57.5 (0)	64.9 (0.1)	9.1 (0.1)	78.7 (0.4)	91.8 (0.2)	6.3 (0.3)

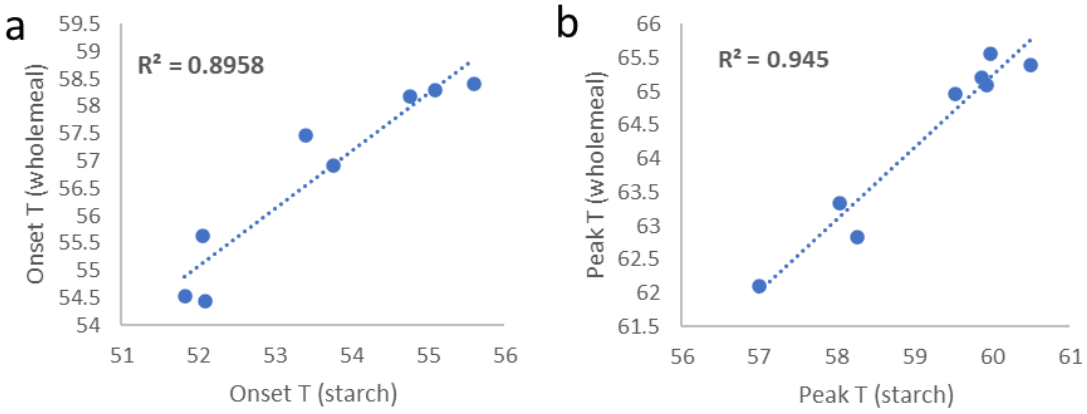

*Supplemental Figure 3.1. Scatter plot for the 1st heating cycle (DSC) (heating 10-80°C at 2°C/min, 80°C for 15 min). The **(a)** graph represents the onset temperature of starch and wholemeal samples. The **(b)** graph represents the peak temperature of starch and wholemeal samples.*

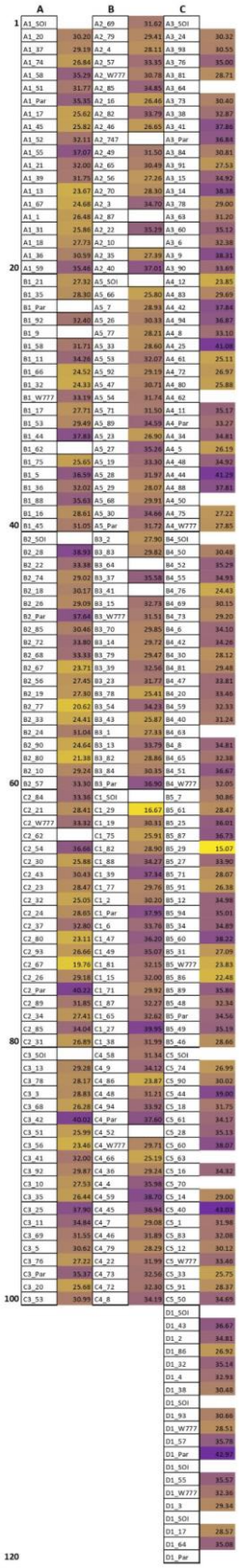

Supplemental Figure 4.1. Paragon x 777 field experimental design and starch digestibility (90 min timepoint).

Supplemental Table 4.1. Starch digested (%) of white flour of the Watkins lines. Values represent mean (± SE).

Lines	0 min	6 min	12 min	18 min	24 min	40 min	90 min	Year
7	0.6 (0)	5.7 (0.5)	7.8 (0.5)	11.4 (1.4)	13.5 (1.7)	17 (1.4)	23.9 (1.7)	2010
42	0.4 (0.3)	12.2 (1)	19 (1.4)	23.1 (1.4)	24.8 (0.8)	28.3 (0.4)	33.4 (0.2)	2010
92	0.3 (0.1)	7.3 (0.9)	12.7 (1.2)	16.2 (1.5)	18.9 (1.9)	22.6 (1.2)	28.5 (0.7)	2010
103	0.2 (0.2)	7.2 (0.9)	11.4 (1.4)	14.7 (1.8)	17.2 (2.1)	20.6 (3)	29.2 (1.9)	2010
141	0.4 (0.2)	7.5 (1.7)	12.4 (1.4)	15.9 (2.5)	18.6 (1.7)	21 (1.4)	28.9 (1.4)	2010
145	0.7 (0.1)	5.5 (1.8)	10.5 (1.3)	13.7 (1.4)	16.1 (1.6)	22.1 (0.7)	30.3 (3.2)	2010
231	0.4 (0)	10 (1.1)	15.9 (1.8)	19.4 (2)	21.5 (2)	24.3 (1.6)	30.4 (2)	2010
281	0.6 (0.1)	7.5 (0.6)	10.9 (1.3)	14.7 (1.4)	17.9 (1.6)	21.4 (0.5)	27.4 (0.5)	2010
444	1.4 (0.8)	16.3 (1.7)	25.9 (4.6)	31.1 (2.1)	33.4 (1.4)	37.1 (1.8)	39.8 (1.9)	2010
471	0.6 (0.1)	10.9 (0.9)	17.4 (1.4)	20.9 (1.9)	22.7 (1)	26 (0.7)	30.2 (0.5)	2010
475	0.9 (0)	15.4 (0.2)	23 (0.2)	25.7 (0.3)	27.9 (0.7)	30 (1.1)	33 (0.5)	2010
551	0.1 (0)	8.2 (0.1)	11.7 (0.9)	15.7 (1.2)	17.8 (1.3)	21.3 (1.3)	26.8 (1.4)	2010
627	0.7 (0.1)	12.2 (0.7)	18 (1.4)	21.3 (1)	23.1 (0.9)	26.2 (0.7)	31.4 (0.9)	2010
629	0.5 (0)	8.6 (1)	13.8 (1.5)	17 (1.6)	19.4 (1.9)	22.7 (1.2)	28.4 (0.6)	2010
639	0.3 (0)	10.2 (0.4)	15.9 (0.7)	19.2 (0.4)	22 (0.9)	25.2 (0.6)	30.3 (0.4)	2010
671	1.1 (0)	16.8 (0.5)	22.9 (0.4)	25.7 (0.3)	27.1 (0.2)	29.1 (1.1)	32 (1.1)	2010
680	0.3 (0.3)	5.4 (0.7)	9 (1.9)	11.9 (1.9)	14.3 (2.1)	19.6 (2)	27.4 (0.4)	2010
694	0.7 (0)	5.8 (0.6)	9.9 (1.1)	13.6 (1.5)	16.5 (1.9)	21.3 (1.4)	27.6 (1.1)	2010
704	0.6 (0)	10.1 (0.5)	15.5 (0.9)	18.9 (0.9)	20.3 (1)	23.3 (1)	28.9 (0.6)	2010
705	0.6 (0)	12.9 (1.4)	19.7 (2.1)	22.6 (1.6)	24.5 (1.7)	27.1 (1.6)	31.5 (1.5)	2010
746	0.1 (0)	6.2 (0.8)	10.1 (1.7)	13.1 (2.1)	15.3 (2.3)	19.5 (1.9)	25.5 (1.4)	2010
747	0.5 (0.2)	11.5 (1.3)	17.5 (2.1)	21.2 (2.1)	23.1 (1.8)	25.8 (3.1)	32.2 (1.6)	2010
777	0.7 (0)	6.7 (0.6)	10 (1)	12.7 (1.4)	14.8 (1.6)	19 (1.5)	24 (1)	2010
788	0.5 (0.1)	13.8 (0.4)	22.1 (0.7)	25.1 (0.4)	27 (0.4)	30.9 (0.4)	34.8 (0.7)	2010
789	0.7 (0)	11.3 (0.6)	18.7 (0.1)	20.9 (0.3)	23.2 (0.1)	25.7 (1)	30.3 (1.2)	2010
816	0.3 (0)	7.3 (0.4)	11.7 (0.7)	14.8 (0.9)	17.2 (0.9)	21.8 (0.9)	28.5 (1)	2010
7	0.5 (0.1)	15.7 (0.7)	22.8 (1)	25.4 (0.6)	28 (0.4)	29.2 (0.4)	34.4 (0.4)	2012
42	0.3 (0.2)	18.1 (1.1)	25.7 (1.1)	28.3 (0.2)	30.3 (1.1)	31.9 (0.6)	36.9 (1.1)	2012
92	0 (0)	17.2 (1)	25.2 (1.2)	27.5 (1.3)	28.6 (0.7)	31.9 (0.6)	35.9 (1.2)	2012
103	0.3 (0.1)	15.7 (0.4)	23 (0.8)	25.6 (1.1)	27.4 (0.8)	29.5 (0.8)	32.7 (0.7)	2012
141	0.5 (0.2)	16.3 (1.1)	23.9 (1.3)	26.5 (0.6)	28.2 (0.5)	29.6 (0.8)	34.5 (1.2)	2012
145	0.8 (0.2)	10.8 (1)	15.6 (1.3)	18.6 (1.6)	20.3 (1.4)	23.3 (2.1)	27.9 (1.2)	2012
231	0.6 (0.2)	17 (0.3)	24.7 (0.1)	27.3 (0.3)	28.8 (0.9)	31.2 (1.3)	34.5 (1.3)	2012
281	0.5 (0.2)	17.7 (1.5)	25.9 (2)	29 (1.4)	31.1 (1.7)	32.3 (1.8)	37.4 (1.2)	2012
291	0.6 (0.2)	20.7 (0.6)	29.6 (0.8)	32.8 (1.5)	34.7 (1.1)	36.9 (1.6)	40.2 (1.5)	2012

Lines	0 min	6 min	12 min	18 min	24 min	40 min	90 min	Year
444	0.9 (0.2)	18.9 (1)	27 (0.5)	29.8 (1.1)	31.2 (1.2)	34.4 (2.3)	38 (1.6)	2012
471	1 (0.1)	17.3 (2.5)	24.4 (2.3)	27.7 (1.9)	29.1 (1.7)	31.2 (0.7)	35.2 (0.9)	2012
475	1.1 (0.1)	20.4 (1)	29.2 (0.9)	31.5 (0.6)	34 (1.1)	36.5 (0.7)	40.8 (0.5)	2012
551	0.2 (0.1)	16.1 (1)	22.9 (0.6)	26.3 (0.2)	28.7 (0.4)	29.6 (0.7)	36.3 (0.5)	2012
560	0.4 (0.2)	12.9 (0.9)	19.1 (1.1)	22.2 (0.7)	23.9 (0.4)	26.5 (1)	31.4 (1.2)	2012
627	0.7 (0.2)	18.8 (1.6)	26 (1.7)	28.6 (1.9)	29 (1.5)	32.7 (2)	36 (1.1)	2012
629	1.3 (0.3)	20.2 (0.9)	26.6 (1)	28.6 (0.9)	30.2 (0.4)	31.1 (0.9)	35.1 (1.1)	2012
639	0.8 (0.2)	20.7 (0.2)	28.2 (1.1)	30.3 (1.4)	31.7 (1.7)	33.6 (2.9)	37.6 (1.3)	2012
671	2.6 (0.7)	23.7 (1.6)	30.2 (1.2)	32.1 (1)	33.1 (1.1)	34.6 (1)	37.8 (1)	2012
680	0.4 (0.3)	10.8 (0.5)	17.5 (0.7)	20.5 (0.3)	22.6 (1)	25.9 (0.4)	31.3 (0.4)	2012
694	0.9 (0.2)	15.6 (1.5)	21.9 (1)	25 (1)	27.2 (0.8)	28.5 (0.1)	34.1 (1.2)	2012
704	0.5 (0.2)	16.4 (1.2)	24.8 (0.8)	25.6 (1.2)	27 (0.5)	29.5 (1.3)	33.4 (0.7)	2012
705	0.5 (0.1)	16.8 (0.6)	24.7 (0.5)	27 (0.2)	28.8 (0.6)	31.1 (0.9)	35.3 (0.7)	2012
746	0.6 (0.2)	13 (0.6)	19.4 (0.3)	23.3 (0.3)	25.6 (0.2)	27.8 (0.9)	33.8 (0.8)	2012
747	0.5 (0.1)	17.7 (0.7)	25.6 (0.4)	27.4 (0.4)	28.9 (1.1)	30.7 (1.4)	35.1 (0.8)	2012
777	0.3 (0.1)	11 (2.2)	16.3 (3.1)	18.5 (3.3)	20.2 (3.1)	23.8 (1.8)	28.8 (1.3)	2012
788	0.3 (0.2)	17.9 (0.9)	25.5 (1)	28 (0.6)	30.4 (1.2)	30.9 (0.2)	36.9 (0.8)	2012
789	0.4 (0.1)	13.2 (1.8)	20.1 (1.9)	22.8 (1.8)	24.9 (1.4)	28.6 (1)	32.3 (0.8)	2012
816	0.4 (0.1)	13.7 (0.8)	21.2 (1)	24.2 (0.7)	26.9 (1.2)	28.5 (0.4)	34.3 (0.8)	2012
7	0.9 (0.1)	9.4 (0.3)	14.4 (0.4)	18.1 (0.2)	20.8 (0)	24.6 (0.9)	30.2 (0.7)	2013
42	0.7 (0.2)	10.5 (0.3)	16.8 (0.3)	20.9 (0.6)	23.8 (0.6)	28.1 (1.1)	33.6 (1.3)	2013
92	0.8 (0.1)	9.8 (0.5)	15.2 (0.9)	19.2 (0.8)	21.4 (0.7)	25.2 (1.1)	31.3 (1.2)	2013
103	0.7 (0.1)	10.4 (0.7)	15.6 (1.1)	19.3 (1)	21.2 (1)	24.8 (0.8)	30.4 (1.2)	2013
141	1 (0.1)	12.3 (0.5)	19.3 (1.5)	24 (1.6)	26.1 (1.9)	30.9 (1.8)	34.9 (1.8)	2013
145	1 (0.2)	9 (0.6)	13.7 (0.9)	17.2 (1.3)	19.3 (0.9)	22.5 (1.2)	29 (1.5)	2013
231	1.3 (0.2)	16.1 (0.8)	24.7 (1.1)	28.7 (1.1)	30.9 (1.1)	33.9 (0.8)	38.5 (1.2)	2013
281	1 (0.1)	13.1 (1.2)	19.8 (1.9)	23.4 (1.9)	25.3 (1.6)	29.2 (1.8)	35.1 (2)	2013
291	1 (0.2)	14.2 (0.7)	21.6 (1.2)	25.2 (1.6)	28 (0.9)	30.6 (1.5)	36 (1)	2013
444	1.6 (0.2)	16.2 (1.3)	26.2 (2.1)	30.4 (2)	33 (1.1)	35 (1.5)	39.6 (1.1)	2013
471	1.4 (0.1)	13.6 (0.3)	21 (1)	25.4 (1)	27.7 (0)	31 (1.3)	34.9 (1.9)	2013
475	1.1 (0.2)	13.2 (0.2)	20.5 (0.5)	24.2 (0.1)	25.9 (0.6)	29.2 (0.9)	33.5 (1)	2013
551	0.9 (0.3)	6.1 (2.1)	12.8 (0.4)	16.3 (1)	19 (0.7)	23.7 (1.4)	30.7 (1.2)	2013
560	0.8 (0.2)	12.3 (0.7)	19.1 (1.2)	22.3 (1.6)	24.7 (0.9)	27.7 (1.3)	34.5 (1.8)	2013
627	1 (0)	11.1 (0.7)	16.8 (1.2)	21.1 (1.4)	23.7 (1.4)	27.1 (1.5)	32.3 (1.7)	2013
629	0.7 (0.2)	11.2 (0.9)	17.9 (1.3)	20.7 (1.8)	22.6 (1.3)	25.3 (2)	30.4 (2.1)	2013
639	0.8 (0.1)	11.8 (0.9)	19.3 (1.4)	23.4 (1.5)	25.9 (1.3)	30.1 (2)	35.6 (2)	2013
671	0.9 (0.2)	10.7 (0.5)	17.2 (1.2)	21 (1.5)	23.5 (1.3)	26.7 (1.1)	34.3 (1.9)	2013
680	0.8 (0.1)	11 (1.1)	17.7 (1.9)	22.5 (2.1)	24.7 (2.1)	28.8 (1.9)	34.2 (1.9)	2013
690	1.2 (0.5)	10.9 (0.5)	16.4 (0.8)	19.9 (0.8)	21.6 (0.4)	24.7 (1)	29.4 (0.6)	2013
694	1.2 (0.2)	10.8 (0.2)	17.6 (0.6)	22.5 (0.8)	24.4 (0.7)	28.5 (1.2)	33.4 (0.6)	2013
704	1 (0.1)	9.9 (0.8)	15.1 (1.3)	18.7 (1.2)	20.7 (1.3)	24.9 (1.4)	29.7 (1.1)	2013

Lines	0 min	6 min	12 min	18 min	24 min	40 min	90 min	Year
705	0.8 (0.1)	10.8 (0.4)	17 (1.2)	20.5 (1.4)	22.4 (1.2)	26.5 (1.5)	32.4 (1.9)	2013
746	0.9 (0.1)	9.4 (1)	14.7 (1.7)	18.5 (1.9)	20.9 (2)	25.1 (2.3)	30.8 (2.1)	2013
747	1.5 (0.1)	14.2 (0.8)	21.8 (1.5)	26.4 (1.5)	28.4 (1.6)	32 (2.2)	36.6 (2)	2013
777	1.5 (0.2)	12.7 (0.7)	19.1 (1.7)	23.4 (1.9)	25.6 (1.9)	29.5 (1.4)	33.8 (1.8)	2013
788	1.1 (0.1)	15.3 (1.1)	23.9 (1.3)	28.3 (1.4)	30 (1.5)	33.5 (1.9)	37.7 (1.8)	2013
789	0.7 (0.1)	15.2 (1)	22.9 (1.6)	26.5 (2)	27.9 (2.4)	31 (1.9)	35.3 (1.6)	2013
816	0.9 (0.2)	10.4 (0.6)	17.4 (0.9)	21 (1.5)	23.7 (1.3)	27.4 (1.4)	33.4 (1.5)	2013
7	0.8 (0.2)	11.2 (0.7)	17.7 (1.1)	20.4 (1.3)	22.7 (1.7)	27 (1.2)	31.1 (1.7)	2014
42	0.8 (0.1)	13.9 (0.9)	21.8 (1.2)	25.9 (1.5)	26.5 (2.1)	30.9 (1.6)	36.1 (1.7)	2014
92	0.8 (0.1)	14.5 (1.2)	22.3 (1.8)	27.1 (2)	28.5 (2)	31.5 (1.8)	35.9 (2.5)	2014
103	0.6 (0.1)	12.7 (2.7)	21.5 (1.4)	25.2 (1.6)	26.6 (1.6)	29.4 (1.2)	32.8 (1.9)	2014
141	0.8 (0.2)	13.3 (1.2)	19.9 (1.7)	23.2 (1.6)	25.5 (1.8)	28 (1.7)	32.6 (1.6)	2014
281	0.7 (0)	10.5 (0.7)	16.3 (1.4)	20.5 (1.4)	23 (1.6)	26.7 (1.6)	31.3 (1.7)	2014
291	0.7 (0.2)	15.8 (1.1)	24.5 (1.4)	27.5 (1.4)	30.2 (1.6)	34 (1.4)	38.4 (1.9)	2014
444	1.1 (0.1)	11.2 (1)	18.7 (1.8)	22 (1.6)	24.7 (2.1)	27.7 (1.6)	33 (1.7)	2014
475	1.1 (0.1)	18.7 (1)	28.1 (2.1)	31.7 (1.3)	32.6 (1.5)	35.7 (1)	39.6 (1.7)	2014
551	0.6 (0)	10.3 (1.7)	17.3 (2)	21.1 (2.1)	23.1 (2)	26 (2)	31.2 (1.8)	2014
560	0.7 (0.1)	10.8 (1.1)	16.6 (2)	20.4 (2.2)	22.6 (2.2)	26.7 (2.5)	31.7 (1.9)	2014
627	0.9 (0.3)	11.9 (0.4)	18.4 (0.8)	22 (0.7)	24.3 (1.1)	27.1 (0.9)	33.2 (0.9)	2014
629	1 (0.1)	9.9 (1.4)	16.1 (2)	19.4 (2.1)	21.5 (1.9)	24.6 (1.4)	30 (1.6)	2014
671	0.9 (0.2)	14.8 (0.5)	23.2 (1.2)	26.2 (1.2)	28.9 (1.2)	33.2 (1.2)	37.6 (1.8)	2014
690	0.8 (0.1)	12.3 (0.9)	19.4 (1.7)	20.1 (1.8)	25.2 (1.9)	27.8 (1.7)	33.3 (2)	2014
694	0.9 (0.3)	10.2 (1.3)	17.3 (2)	20.9 (1.9)	23.7 (1.9)	27.4 (1.8)	33.1 (1.7)	2014
705	0.7 (0.2)	17 (0.4)	24.8 (0.6)	27.7 (0.4)	28.8 (0.5)	33.1 (0.1)	35.5 (1.1)	2014
747	0.8 (0.1)	14.8 (1)	21.7 (1.5)	25.5 (1.9)	27.1 (1.8)	30.2 (1.8)	33.7 (2.2)	2014
777	0.9 (0.1)	11.1 (0.5)	16.9 (1.4)	20 (1.5)	21.9 (1.8)	25 (1.5)	29.8 (2)	2014
788	0.7 (0.1)	14.3 (0.3)	20.2 (0.6)	23.4 (0.5)	24.6 (0.7)	27.3 (1.1)	30.8 (0.3)	2014
789	0.8 (0.2)	11.8 (0.6)	18.8 (1.3)	22.3 (1.3)	23.9 (2.2)	27.4 (1.6)	32.8 (1.6)	2014
816	0.9 (0.1)	8 (2)	15.4 (0.9)	19.1 (1.1)	21.5 (1.4)	25.4 (1.2)	31.6 (1.1)	2014

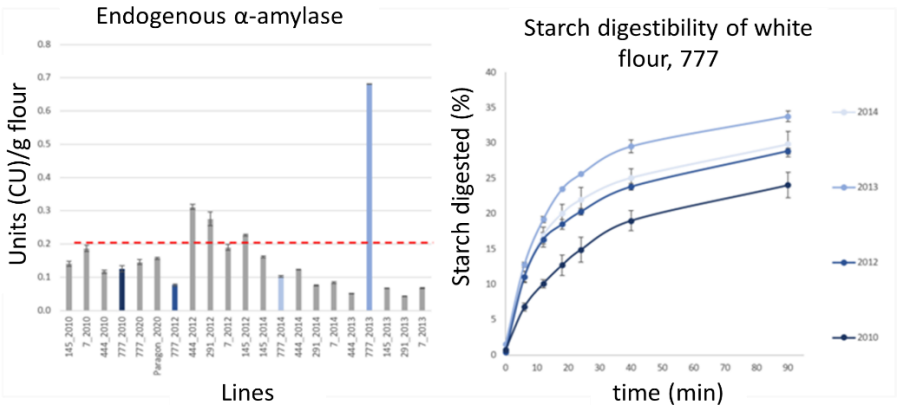

Supplemental Figure 4.2. Endogenous α-amylase of selected Watkins lines and Paragon.

Supplemental Table 4.2. TS content (g/100 flour) of white flour of the Watkins lines measured by HK assay (Megazyme). Values represent mean (± SE).

Lines	TS content g/100 flour	Year
7	60.1 (3)	2010
42	61.6 (1.5)	2010
92	63.5 (1.4)	2010
103	60.3 (0.6)	2010
141	64.4 (1.7)	2010
145	59.4 (3)	2010
231	60.4 (1.7)	2010
281	60.7 (3)	2010
444	56 (3.1)	2010
471	62.3 (1)	2010
475	66 (1.3)	2010
551	67.2 (0.5)	2010

Lines	TS content g/100 flour	Year
627	60.5 (3.5)	2010
629	64.3 (2.8)	2010
639	62.8 (2.7)	2010
671	63.4 (1.4)	2010
680	62.8 (4.2)	2010
694	55.5 (2.5)	2010
704	65.4 (0.6)	2010
705	65.3 (0.4)	2010
746	60.7 (1.2)	2010
747	62 (1.3)	2010
777	64.9 (2.9)	2010
788	60 (2.9)	2010
789	61.8 (2.2)	2010
816	63.1 (3.4)	2010
7	62.5 (1.5)	2012
42	65.4 (3.2)	2012
92	66.4 (0.9)	2012
103	65.9 (0.9)	2012
141	63.1 (0.7)	2012
145	61.9 (1.7)	2012
231	63.4 (0.9)	2012
281	64.4 (1.2)	2012
291	63.1 (0.9)	2012
444	59.4 (2.7)	2012

Lines	TS content g/100 flour	Year
471	60.8 (2)	2012
475	60.8 (1.5)	2012
551	61.8 (2.7)	2012
560	66.2 (1.6)	2012
627	62.2 (0.2)	2012
629	63.6 (0.8)	2012
639	65.2 (0.8)	2012
671	61.1 (0.4)	2012
680	60.9 (0.3)	2012
690	64.4 (0.7)	2012
694	56.9 (0.4)	2012
704	63.8 (0.9)	2012
705	65 (0.4)	2012
746	60.2 (0.8)	2012
747	64.7 (1.7)	2012
777	63.4 (0.9)	2012
788	62.1 (0.8)	2012
789	62.5 (1.6)	2012
816	62.6 (1.5)	2012
7	65.5 (1)	2013
42	64.4 (1)	2013
92	66.8 (0.6)	2013
103	64.8 (2.1)	2013
141	62.9 (0.6)	2013

Lines	TS content g/100 flour	Year
145	64.1 (2.2)	2013
231	64.8 (1.4)	2013
281	63.9 (0.7)	2013
291	63.3 (1.4)	2013
444	66.1 (0.7)	2013
471	62.7 (0.8)	2013
475	65.7 (0.8)	2013
551	62.7 (0.7)	2013
560	61.7 (1)	2013
627	63.5 (1.1)	2013
629	68.1 (0.4)	2013
639	64.2 (1.3)	2013
671	64.6 (0.5)	2013
680	58.6 (3.1)	2013
690	65.8 (0.2)	2013
694	62.7 (1.4)	2013
704	64.4 (1.4)	2013
705	65.9 (0.7)	2013
746	62.1 (2)	2013
747	63 (2.9)	2013
777	63.1 (0.7)	2013
788	63.8 (2.7)	2013
789	65.6 (0.3)	2013
816	63.7 (2.1)	2013

Lines	TS content g/100 flour	Year
7	65.5 (1)	2014
42	63 (1.2)	2014
92	61.7 (1.7)	2014
103	65 (1.1)	2014
141	66.1 (2)	2014
145	59.6 (0.8)	2014
231	59.9 (0.9)	2014
281	57.2 (2.5)	2014
291	62.8 (0.8)	2014
444	61.1 (2.1)	2014
475	60.1 (0.8)	2014
551	61.7 (0.9)	2014
560	61.1 (0.6)	2014
627	59.7 (3.6)	2014
629	66.7 (0.3)	2014
671	61 (2)	2014
690	63.5 (1.8)	2014
694	59.4 (2.5)	2014
705	66.6 (0.5)	2014
747	64.8 (1.2)	2014
777	64.4 (0.9)	2014
788	65.4 (1.1)	2014
789	62 (0.5)	2014
816	63.6 (2.9)	2014

Supplemental Table 4.3. TS content (g/100 flour) and starch digestibility (%) of wholemeal flour of the Paragon x 777 population. Values represent mean (± SE).

Lines	**TS content g/100 flour**	0 min (SE)	4 min (SE)	6 min (SE)	12 min (SE)	16 min (SE)	40 min (SE)	90 min (SE)
1	57.5 (1.3)	1.2 (0)	8.2 (0.4)	13.3 (1.1)	17.8 (2)	19.6 (2.1)	23.8 (1.6)	28.5 (1.7)
2	56.8 (1.9)	1.4 (0)	10.3 (0.8)	16.1 (0.7)	20.8 (0.5)	21.6 (0.7)	26.1 (0.8)	30.9 (2)
3	58.1 (1.6)	1.3 (0.1)	12.6 (1.4)	19.4 (1.9)	23.7 (2.1)	24 (2.1)	29.1 (1.6)	30.9 (1.8)
4	59.3 (1.4)	1 (0)	12.6 (2.1)	20 (3)	23.5 (2.5)	25.1 (2)	27.9 (1.6)	32.3 (2.2)
5	58.1 (1.3)	1.3 (0.2)	10.7 (2.3)	18.2 (2.6)	20.7 (3.4)	21.8 (3.5)	26.1 (3)	31.1 (3)
6	56.9 (0.9)	1.7 (0.2)	13.9 (1)	21.2 (1.1)	24.6 (0.8)	25.9 (1.3)	29.5 (0.9)	33.4 (0.5)
7	59.9 (1.5)		8.1 (0.4)	12.8 (0.6)	17.3 (0.6)	19.2 (0.4)	24.9 (0.4)	29.6 (0.6)
8	58.8 (0.8)	1.1 (0.3)	12.7 (0.2)	19.7 (0.8)	24.3 (0.5)	26.1 (0.2)	31.4 (1.1)	34 (0.4)
9	57.5 (2.7)		15.6 (0.3)	22 (1.8)	27.5 (1.7)	27.2 (1.5)	32.2 (1.6)	36.2 (2)
10	56.4 (1.4)	0.7 (0.2)	6.7 (0.3)	10.8 (0.7)	14.3 (0.9)	16.6 (1.2)	23.6 (0.8)	28.3 (0.8)
11	58.8 (2.3)	1.3 (0.1)	12.2 (0.8)	20.1 (0.9)	24.4 (0.7)	25.9 (0.6)	30.5 (0.2)	34.7 (0.2)
12	58.4 (0.1)	1.4 (0.1)	7.7 (2)	12.7 (3.2)	15.2 (4.2)	17.3 (4.5)	25.2 (4.1)	29.6 (3.2)
13	57.5 (1.2)	1.3 (0.3)	6.9 (1.7)	13.6 (2.4)	14.6 (3.5)	17 (4)	24.2 (3)	28.9 (2.9)
14	57.7 (1.5)	1.2 (0.2)	9.3 (2.9)	14.8 (4.5)	18.3 (4.7)	20.4 (4.5)	27.6 (3.5)	32.3 (3)
15	58.2 (2)	1.3 (0.2)	8.8 (1.3)	16.4 (2.1)	18.9 (2.2)	22.5 (2)	28.5 (0.8)	33.2 (0.8)
16	59.3 (1)	1 (0.3)	7.6 (1)	14.3 (0.1)	16.5 (2)	19.5 (2.2)	26.6 (1.7)	29.7 (2.3)
17	57.1 (1.5)	1.4 (0.2)	6.2 (0.2)	9.7 (0.5)	12.5 (0.7)	15.3 (0.1)	22.5 (0.3)	27.2 (0.8)
18	58 (0.5)	1.7 (0)	7.7 (0.7)	12.2 (1)	16.7 (1.3)	18.5 (1.3)	24.1 (1.1)	29.8 (1.1)
19	60.2 (1)	1.1 (0.1)	9.5 (0.8)	15.9 (1.2)	19.5 (0.6)	20.7 (1)	26.3 (1.6)	30.3 (1.7)
20	58.2 (0.2)	1.1 (0)	8.8 (0.9)	13.9 (1.5)	17.4 (1.7)	20.2 (2.3)	25.8 (2)	29.7 (2.2)
21	58.1 (1.2)	0.9 (0)	9.2 (1.9)	15 (2.8)	18.5 (2.8)	20.6 (2.1)	26 (1.5)	29.2 (1.4)
22	57.7 (0.5)	1.7 (0)	10.7 (0.2)	16.8 (0.1)	20.7 (1)	24.2 (1.3)	28.9 (1.5)	33.5 (0.9)
23	57.5 (0.9)	1.7 (0)	7.8 (0.3)	12.8 (0.6)	16.9 (0.8)	18 (1.5)	24.3 (1.3)	29 (1.4)
24	56.4 (0.6)	1.7 (0.1)	9.6 (0.1)	14 (0.7)	17.2 (1.2)	19.2 (0)	25 (0)	30 (0.7)
25	56.4 (1.4)	1.2 (0)	11.8 (0.8)	18.5 (1.2)	23.2 (1.1)	25.9 (1.9)	31.2 (1.7)	38.3 (1.4)
26	56.8 (0.6)	1 (0.1)	6.3 (0.3)	10.2 (0.3)	12.8 (0.6)	14.9 (0.4)	22.6 (0.6)	29.5 (0.4)
27	55 (0.7)	1.1 (0.1)	10.4 (2.6)	17 (4)	22.8 (3.1)	24.8 (2.5)	32.1 (1.7)	36.3 (1.8)
28	58.7 (0.8)	0.9 (0.1)	10.3 (1.1)	16.6 (1.5)	21.3 (1.6)	23.8 (1.4)	27.7 (0.7)	35.3 (2)
29	58 (0.9)	0.5 (0)	5 (0.7)	8.3 (1.2)	11 (1.7)	12.5 (2.2)	17.3 (3.4)	19.9 (4)
30	59.6 (1)	0.7 (0.2)	8.9 (1.1)	14.7 (1.7)	19.1 (2.3)	20.7 (1.8)	26.6 (2.4)	29.5 (2.6)

Lines	**TS content g/100 flour**	0 min (SE)	4 min (SE)	6 min (SE)	12 min (SE)	16 min (SE)	40 min (SE)	90 min (SE)
31	58.7 (0.6)	1 (0)	8.2 (0.3)	13.1 (0.6)	16.3 (0.5)	18.4 (0.7)	22.6 (0.6)	26.6 (0.3)
32	58.7 (1.2)	0.9 (0.2)	8.3 (1.1)	12.2 (3.8)	16.8 (2.5)	19.4 (2.5)	25.7 (2.6)	28.1 (3.4)
33	57.3 (1.4)	1.1 (0.1)	6.3 (0.8)	9.1 (1.2)	12 (1.5)	14.2 (1.7)	20.8 (1.5)	26.2 (1.2)
34	59.9 (1.1)	1.1 (0)	8.5 (1.3)	14.3 (2.1)	18 (2.2)	21.4 (3)	26.5 (2)	32.3 (2.4)
35	59.7 (0.9)	1 (0.1)	7.1 (0.7)	11.7 (1.2)	14.7 (2.4)	17.2 (1.3)	23.3 (1.2)	27.3 (0.5)
36	60.5 (0.4)	0.9 (0.2)	9.8 (0.7)	16.4 (2.1)	20 (1.2)	22.6 (1.1)	27.3 (0.7)	30.6 (0.8)
37	58.8 (1.6)	1 (0)	14.4 (1.4)	21.4 (1.5)	24.1 (1.4)	26 (1.5)	30.4 (2.5)	32.5 (1.8)
38	57.3 (0.6)	0.8 (0)	10.3 (1.1)	16.3 (1.2)	20 (0.8)	22.7 (0.7)	28.5 (0.8)	31.7 (0.6)
39	56.5 (1)	0.7 (0)	10.9 (0.1)	18.1 (0.5)	21.6 (0.3)	23.9 (1.1)	30.4 (1.1)	33.8 (1.7)
40	57.5 (1.1)	0.9 (0.2)	12.5 (2.3)	21 (3.5)	24.3 (2.6)	27.3 (3.9)	32.3 (3.8)	37 (3.4)
41	55.1 (2.1)	0.7 (0.3)	11.8 (2.3)	19.9 (3)	24.4 (4.4)	26.3 (2.7)	30.2 (2.1)	34.9 (2.9)
42	57.5 (2.3)	1.1 (0.2)	12.9 (0.3)	21.5 (1.8)	24 (1.2)	26.9 (1.3)	33 (1.1)	37.3 (1.6)
43	57.6 (0.9)	0.8 (0.2)	7.8 (2.3)	13.4 (3.4)	17.5 (4.3)	19.1 (4.3)	25.8 (3.8)	30.9 (3.1)
44	56 (1.6)	1.2 (0.2)	14.9 (1.1)	26 (2.5)	29.6 (1.5)	31.1 (1.6)	36.2 (1.6)	39.3 (1)
45	59.5 (1.7)	1.2 (0.3)	8.4 (1.3)	13.2 (2.3)	17.7 (3.7)	19.6 (3)	26.4 (2.1)	31.2 (3.2)
46	57.7 (0.6)	0.7 (0.1)	7.6 (1)	13.3 (0.9)	16.6 (1.7)	17.7 (1.1)	23.5 (0.5)	29 (1.5)
47	58.9 (1.3)	1 (0.1)	11.2 (0.8)	18.7 (1.4)	22.5 (1.8)	26.1 (1.9)	29.8 (1.3)	33.5 (1.5)
48	56.9 (0.7)	0.8 (0.2)	10 (1.4)	15.6 (2)	19.7 (1.8)	22.2 (1.3)	28.7 (1)	32.8 (1)
49	56.8 (1.3)	1.1 (0)	12 (1.2)	20.6 (3.2)	23.4 (2)	25.6 (1.6)	30 (1.2)	33.9 (1.2)
50	53.9 (0.3)	1.2 (0.2)	8.7 (1.8)	17.2 (3)	18 (3.7)	20.2 (3.7)	26.6 (2.3)	31.4 (1.6)
51	61.8 (1.6)	1 (0)	10.3 (1.6)	17.3 (2)	20.1 (2.6)	21.5 (3.1)	25.5 (2.2)	31.4 (3)
52	58.2 (1.5)	1.1 (0)	11.1 (1.4)	18.5 (2.1)	21.8 (2.7)	23.3 (2.1)	28 (1)	32.9 (1.2)
53	58.2 (1.4)	1.3 (0.1)	8.1 (0.3)	12.9 (0.1)	17.3 (0.4)	19.6 (0.4)	25.5 (0.5)	30.8 (0.7)
54	57 (0.8)	1.5 (0.4)	10.9 (1.5)	18.3 (2.7)	21.5 (2.8)	24.1 (2.1)	29.3 (1.6)	34.2 (1.4)
55	55.8 (0.6)	1.7 (0)	11.9 (1)	21.4 (1.3)	24 (1.7)	26 (1.3)	31.6 (1.3)	35.8 (0.6)
56	59.2 (0.8)	1.1 (0.1)	5.4 (0.9)	8.2 (1.3)	10.5 (1.6)	12.4 (1.6)	21.1 (2.1)	26 (1.3)
57	57.2 (0.3)	1.2 (0.1)	9.7 (1.5)	16.8 (2.6)	21.5 (2)	23.5 (1.7)	29.4 (0.8)	34.1 (0.8)
58	55.9 (0.9)	1.9 (0.5)	8.8 (1.4)	14.5 (2.8)	18.7 (2.6)	21.8 (2.3)	28.9 (2)	33.4 (1.7)

Lines	**TS content g/100 flour**	0 min (SE)	4 min (SE)	6 min (SE)	12 min (SE)	16 min (SE)	40 min (SE)	90 min (SE)
59	54.9 (1)	1.1 (0)	10.3 (1.1)	17.1 (1.5)	21.9 (1.6)	24.5 (1.6)	30.2 (2.2)	35.4 (1.8)
60	57.9 (0.3)	1.3 (0)	9.8 (0.7)	17.5 (1.2)	22.8 (1.3)	25.9 (1.5)	31.5 (0.9)	37.1 (1)
61	60.1 (1.4)	1.1 (0.1)	6.3 (1.7)	10.4 (3.2)	13.2 (3.6)	16.1 (3.9)	24.3 (3.1)	29.2 (2.6)
65	57.8 (0.2)	0.7 (0)	10.7 (0.5)	14.9 (0.8)	21.8 (1.2)	21.9 (0.8)	26.6 (0.5)	31.8 (0.6)
66	57 (2)	0.7 (0.1)	5.1 (0.8)	7.7 (0)	9.9 (1.5)	11.1 (1.1)	19 (1)	25.1 (0.3)
67	58.8 (0.3)	1.3 (0.2)	3.9 (0.7)	6 (1.8)		9.3 (2.4)	16.2 (2.1)	22.7 (1.5)
68	59 (2.6)	1.2 (0.1)	8 (0.7)	12.4 (0.6)	17.3 (1.2)	19.7 (1.2)	26.3 (1.3)	29.8 (2)
69	58.2 (0.7)	1.1 (0.1)	9.4 (0.7)	15.5 (0.8)	20.3 (1.3)	23.5 (0.7)	29.1 (1.2)	31.1 (0.4)
70	59.9 (1.6)	1.5 (0.3)	7.8 (1.5)	12 (1.8)	15.5 (1.4)	17.9 (1.3)	24.7 (0.3)	29 (0.7)
71	59 (0.7)	1.7 (0.1)	8.8 (0.9)	14 (1.5)	17.5 (1.6)	20 (1.5)	25.1 (0.8)	29.8 (0.9)
72	58.6 (0.4)	1.6 (0.2)	9 (1.3)	14.7 (2.1)	18.5 (2.6)	20.9 (2.5)	25.5 (2.1)	31 (2)
73	53.2 (1.3)	1.4 (0.4)	6.4 (0.7)	10.6 (1.3)	14 (1.8)	17.4 (1.8)	25.2 (1.4)	30.7 (0.9)
74	53.1 (0.9)	1.2 (0.1)	6.8 (0.5)	10.4 (0.6)	13.4 (0.8)	16.3 (0.4)	22.4 (0.3)	27.6 (0.7)
75	57.4 (1.8)	1.3 (0.1)	6.4 (0.3)	10 (0.7)			21.9 (0.9)	26.2 (0.4)
76	59 (2.1)	1.5 (0.1)	8.3 (1.3)	12.8 (2.3)			24.7 (2.9)	28.8 (3.1)
77	57.6 (1.6)	1.5 (0.1)	5.9 (0.5)	8.8 (1.1)	12.3 (2.2)	14.1 (2.1)	21 (2.4)	26.1 (2.8)
78	56.3 (1.5)	1.3 (0)	6 (0.9)	9.1 (1.9)			22.3 (1.3)	27.5 (1)
79	56.8 (1.5)	1.6 (0.1)	6.1 (0.1)	9.6 (0.3)	13 (0.2)	15.7 (0.5)	23.7 (0.6)	29 (0.3)
80	60.6 (2.1)	1.4 (0.1)	4.7 (0.7)	7.7 (2.2)	10 (2.7)	11.5 (3.1)	17.5 (1.8)	23.4 (1.3)
81	56.9 (0.2)	1.7 (0)	6.2 (0.4)	10.2 (1)	13.5 (1.2)	16.1 (1)	24.8 (1.1)	30.1 (1)
82	56.4 (0.1)	0.7 (0)	9.9 (1.8)	14 (3)	18.5 (3.1)	20.8 (3)	26.9 (2.3)	30.5 (1.6)
83	56 (1)	1 (0.2)	13.1 (0.8)	17.9 (1.5)	22.5 (1.8)	22.9 (1.2)	28 (1.5)	30.5 (0.7)
84	57.7 (1.3)	1.3 (0.3)	10.2 (0.3)	14.8 (0.7)	19.1 (0.5)	20.6 (0.6)	26.4 (0.5)	31.5 (0.9)
85	58 (0.9)	1.3 (0)	8.9 (1)	13.8 (1.6)	18 (1.7)	20.6 (1.8)	27.1 (1.4)	33.1 (1.3)
86	57.6 (0.5)	1.2 (0.1)	3.9 (0.9)	6 (1.4)	7.8 (2.1)	9.1 (2.3)	16.7 (2)	24.4 (1.3)
87	57.2 (1)	1.4 (0.1)	8.2 (1)	11.8 (2.7)	17.2 (2.3)	19.6 (2.6)	26.5 (2.8)	32.7 (2.1)
88	55 (0.4)	1.2 (0)	9.2 (0.6)	15.3 (0.9)	19.9 (1.3)	22.7 (1.3)	29.9 (1)	35.9 (1)
89	56.9 (0.6)	1 (0)	9.7 (0.8)	15.9 (1.6)	19.9 (1.7)	22.1 (1.5)	28 (1.1)	34 (1.1)

Lines	**TS content g/100 flour**	0 min (SE)	4 min (SE)	6 min (SE)	12 min (SE)	16 min (SE)	40 min (SE)	90 min (SE)
90	55.7 (1.2)	1.2 (0)	7.7 (2.2)	11.8 (3.5)	14.8 (4.1)	17.1 (4.3)	23.9 (3)	29.4 (2.6)
91	56.6 (1.4)	1.3 (0.1)	6.5 (0.4)	11 (0.9)	14.3 (0.9)	16.5 (0.9)	24.1 (0.3)	27.4 (0.5)
92	56.4 (0.2)	1.3 (0.1)	7.6 (0.8)	12.5 (1.7)	16.4 (2.2)	18.5 (2)	25.3 (1.2)	30.4 (0.9)
93	56.7 (1.3)	1.1 (0)	7.3 (0.2)	11.8 (0.6)	15.1 (0.7)	18 (0.9)	24.3 (1.2)	29.2 (1.3)
94	52.7 (0.7)	1.8 (0.1)	8.8 (0.2)	14.5 (0.4)	18.9 (0.5)	21.1 (0.3)	28.7 (0.1)	35.2 (0.8)
777	56.8 (0.8)	1.1 (0.1)	9.2 (0.6)	14.4 (1)	18 (1)	19.7 (0.9)	25.6 (0.7)	30.1 (0.8)
Paragon	60.6 (1)	1.3 (0.1)	13.8 (0.3)	22.1 (0.6)	26.6 (0.6)	27.7 (0.5)	32.7 (0.7)	36.6 (0.8)

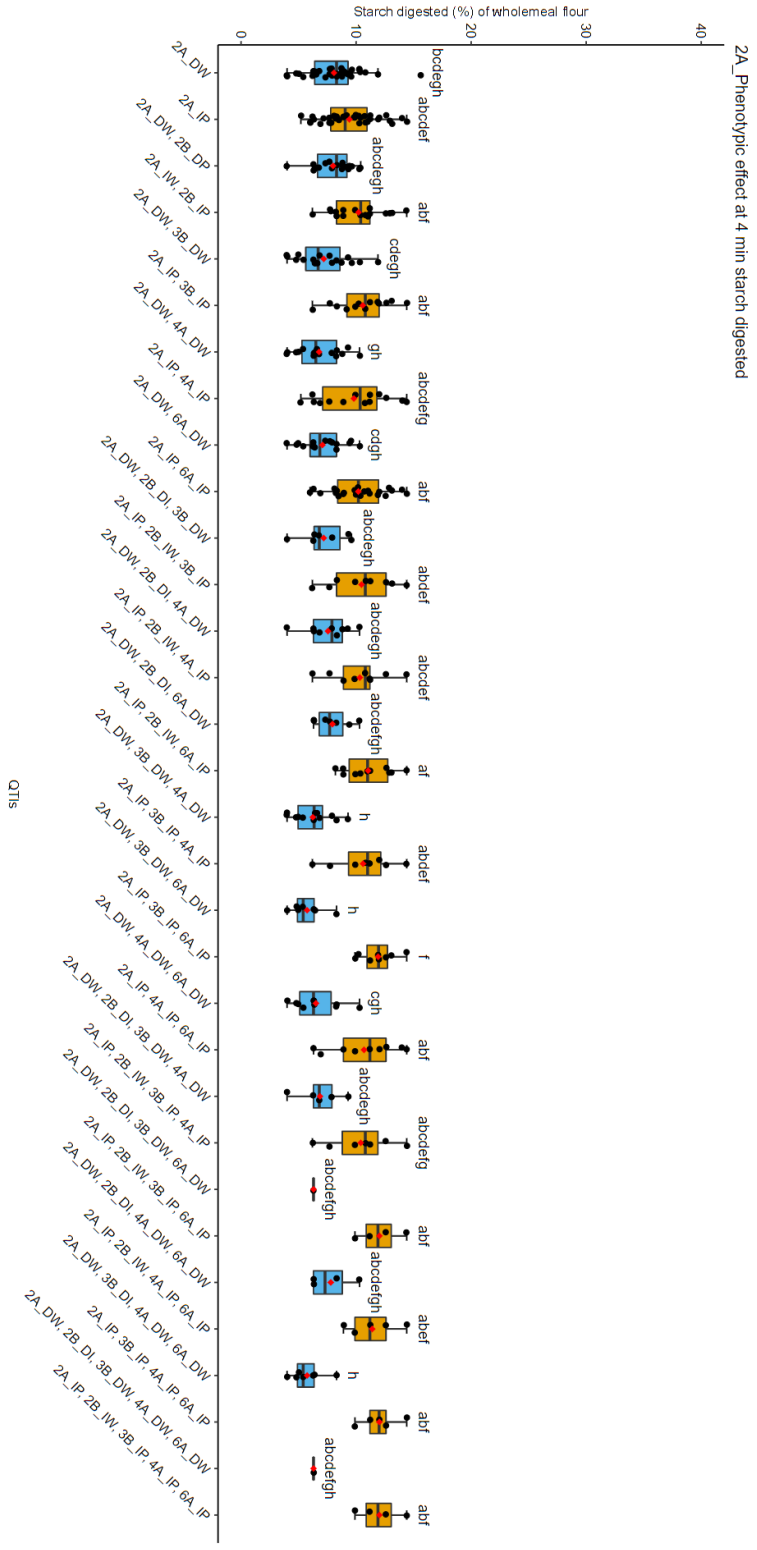

Supplemental Figure 4.3. 2A Phenotypic effect at 4 min starch digested. DW refers to the decreasing allele of Watkins 777, while DP represents the decreasing allele of Paragon. Similarly, IW stands for the increasing allele of Watkins 777, and IP stands for the increasing allele of Paragon.

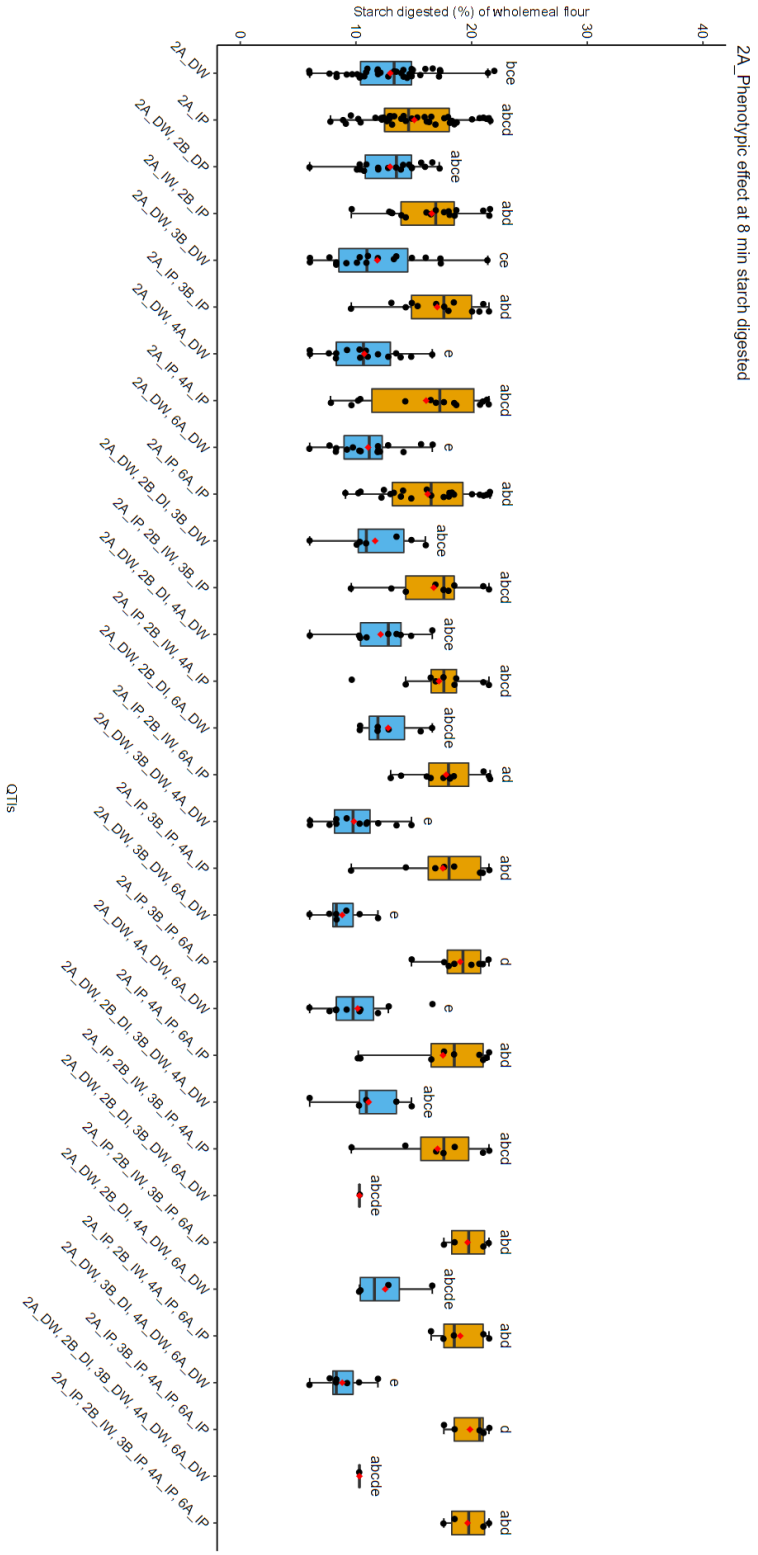

Supplemental Figure 4.4. 2A Phenotypic effect at 8 min starch digested. DW refers to the decreasing allele of Watkins 777, while DP represents the decreasing allele of Paragon. Similarly, IW stands for the increasing allele of Watkins 777, and IP stands for the increasing allele of Paragon.

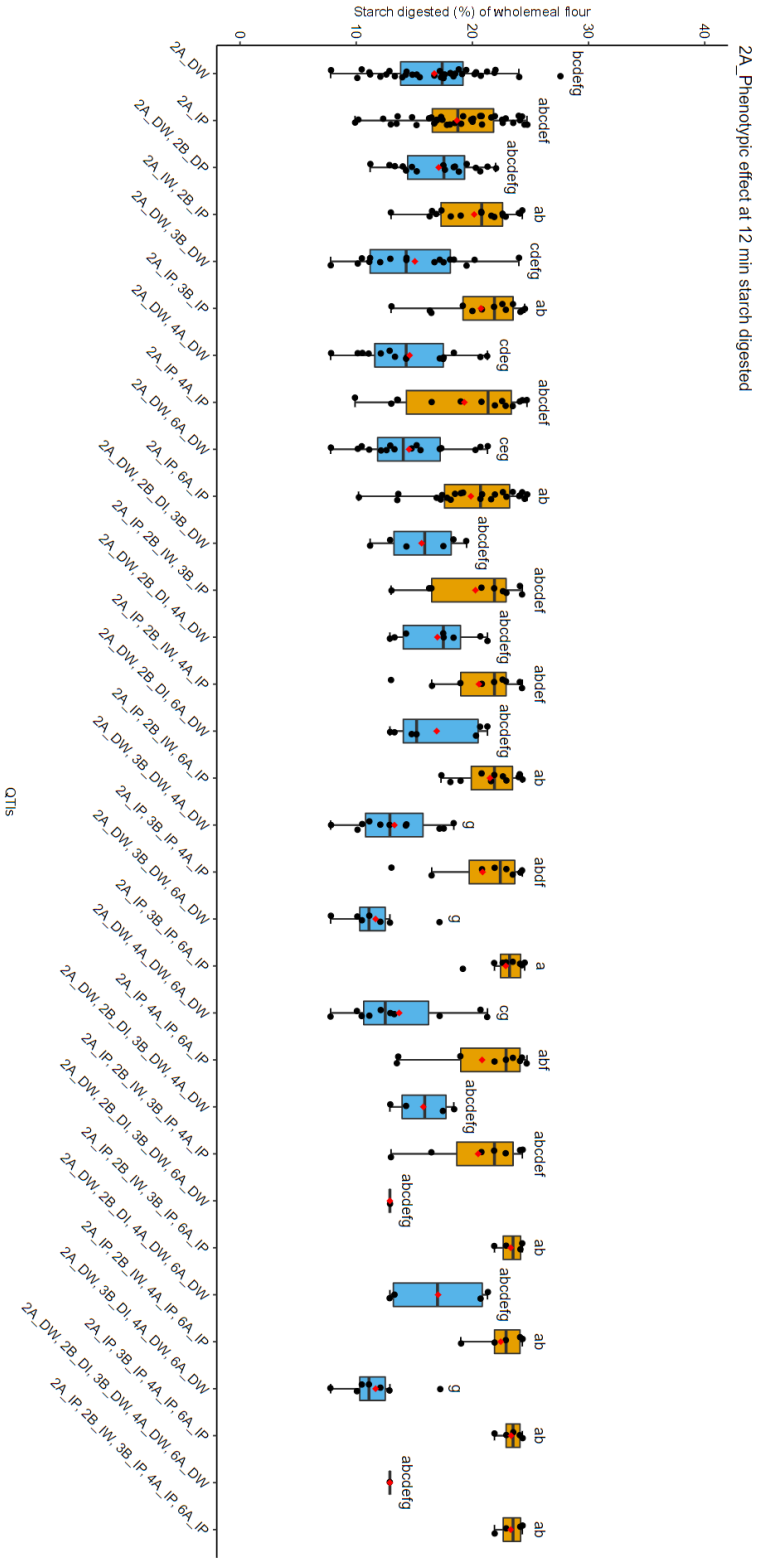

Supplemental Figure 4.5. 2A Phenotypic effect at 12 min starch digested. DW refers to the decreasing allele of Watkins 777, while DP represents the decreasing allele of Paragon. Similarly, IW stands for the increasing allele of Watkins 777, and IP stands for the increasing allele of Paragon.

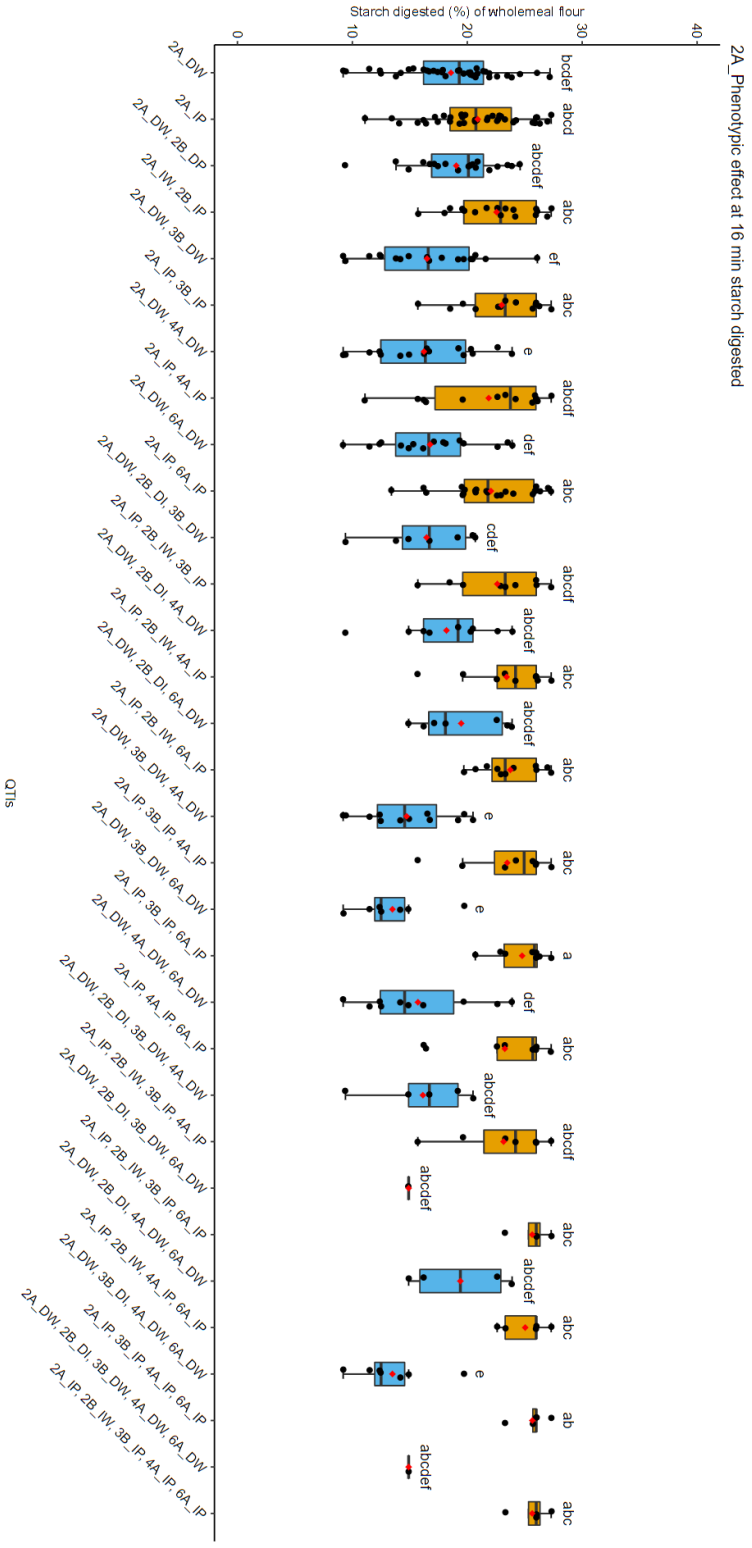

Supplemental Figure 4.6. 2A Phenotypic effect at 16 min starch digested. DW refers to the decreasing allele of Watkins 777, while DP represents the decreasing allele of Paragon. Similarly, IW stands for the increasing allele of Watkins 777, and IP stands for the increasing allele of Paragon.

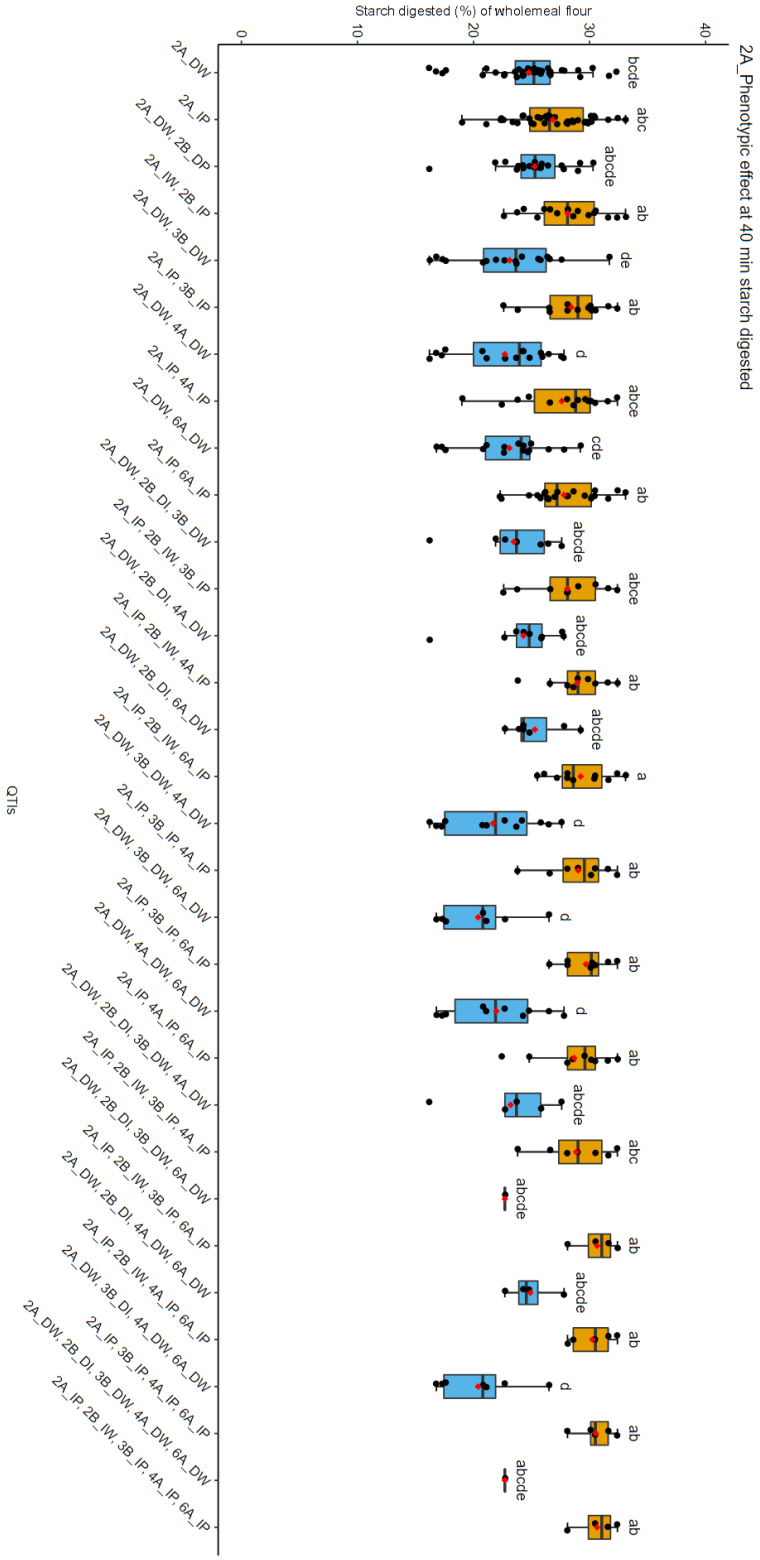

Supplemental Figure 4.7. 2A Phenotypic effect at 40 min starch digested. DW refers to the decreasing allele of Watkins 777, while DP represents the decreasing allele of Paragon. Similarly, IW stands for the increasing allele of Watkins 777, and IP stands for the increasing allele of Paragon.

Supplemental Figure 4.8. 2A Phenotypic effect at 90 min starch digested. DW refers to the decreasing allele of Watkins 777, while DP represents the decreasing allele of Paragon. Similarly, IW stands for the increasing allele of Watkins 777, and IP stands for the increasing allele of Paragon.

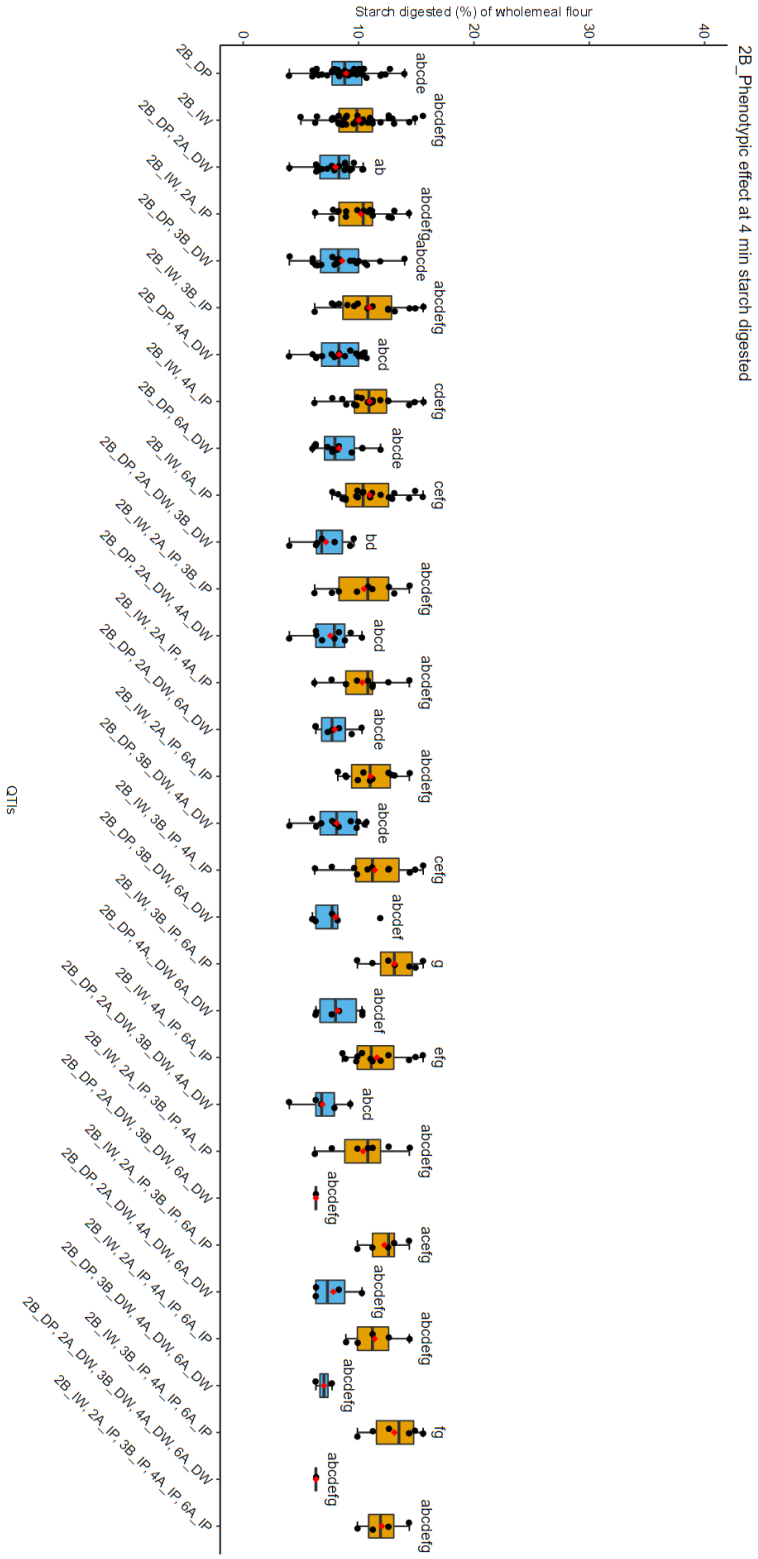

Supplemental Figure 4.9. 2B Phenotypic effect at 4 min starch digested. DW refers to the decreasing allele of Watkins 777, while DP represents the decreasing allele of Paragon. Similarly, IW stands for the increasing allele of Watkins 777, and IP stands for the increasing allele of Paragon.

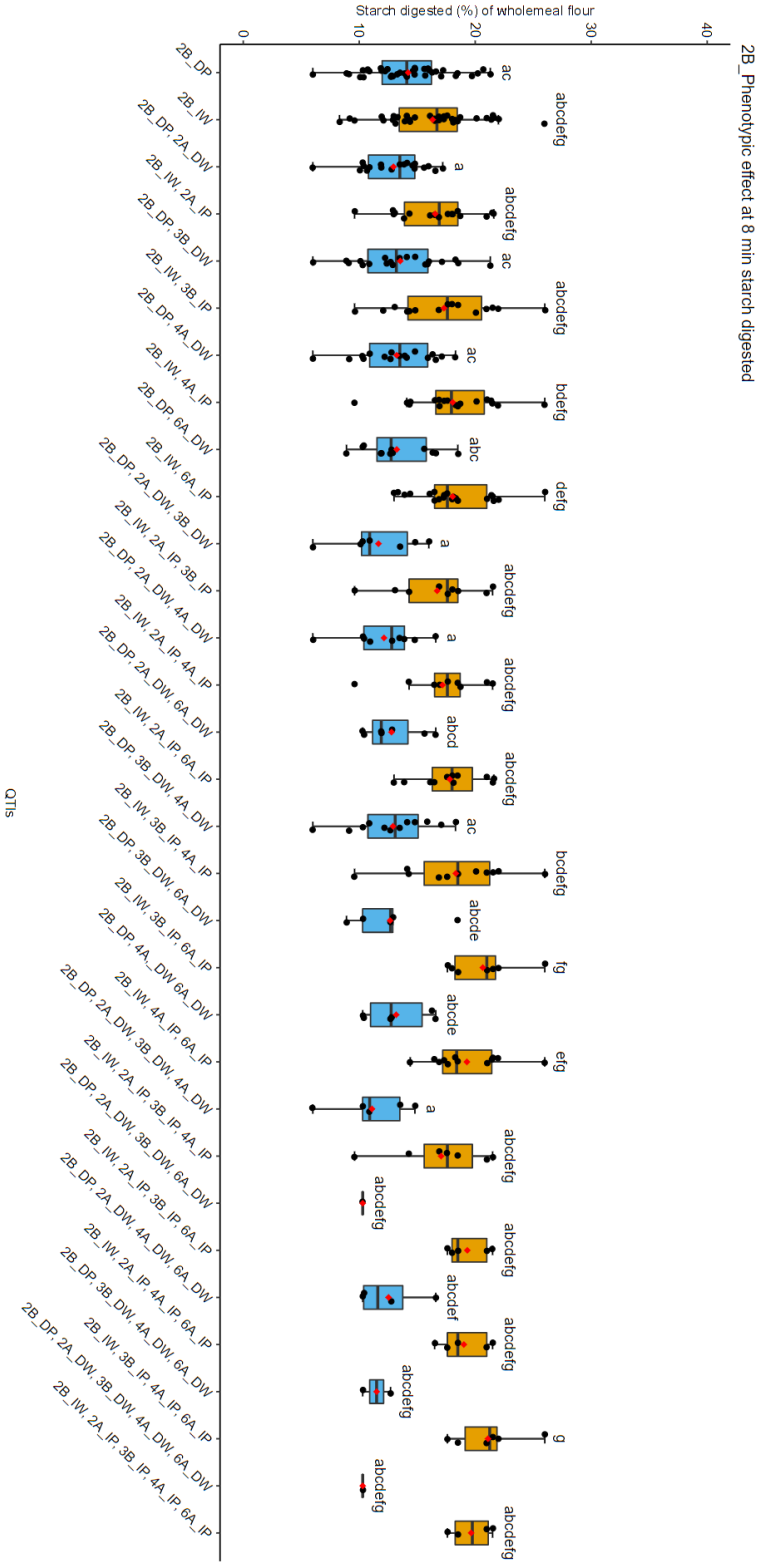

Supplemental Figure 4.10. 2B Phenotypic effect at 8 min starch digested. DW refers to the decreasing allele of Watkins 777, while DP represents the decreasing allele of Paragon. Similarly, IW stands for the increasing allele of Watkins 777, and IP stands for the increasing allele of Paragon.

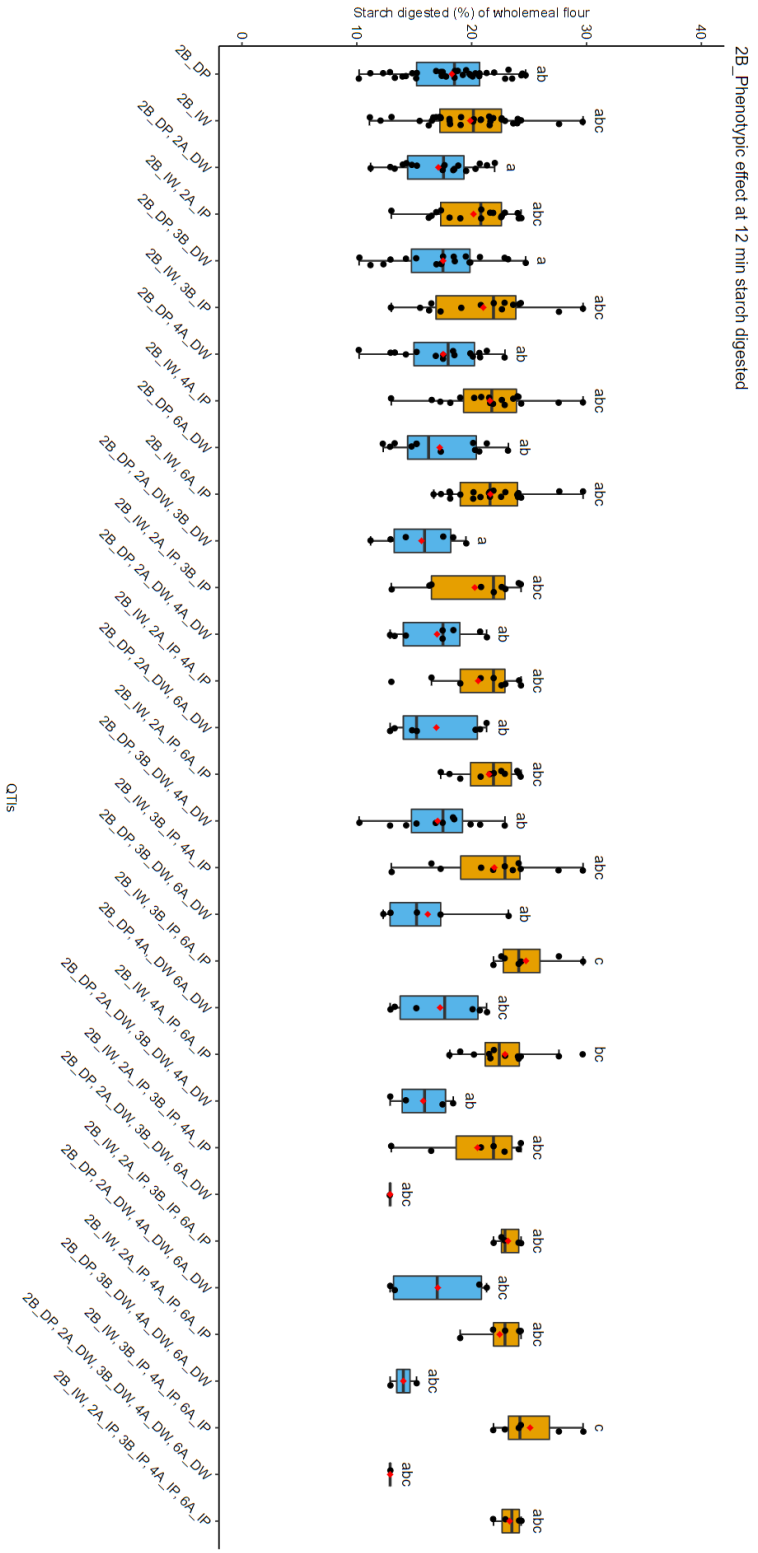

Supplemental Figure 4.11. 2B Phenotypic effect at 12 min starch digested. DW refers to the decreasing allele of Watkins 777, while DP represents the decreasing allele of Paragon. Similarly, IW stands for the increasing allele of Watkins 777, and IP stands for the increasing allele of Paragon.

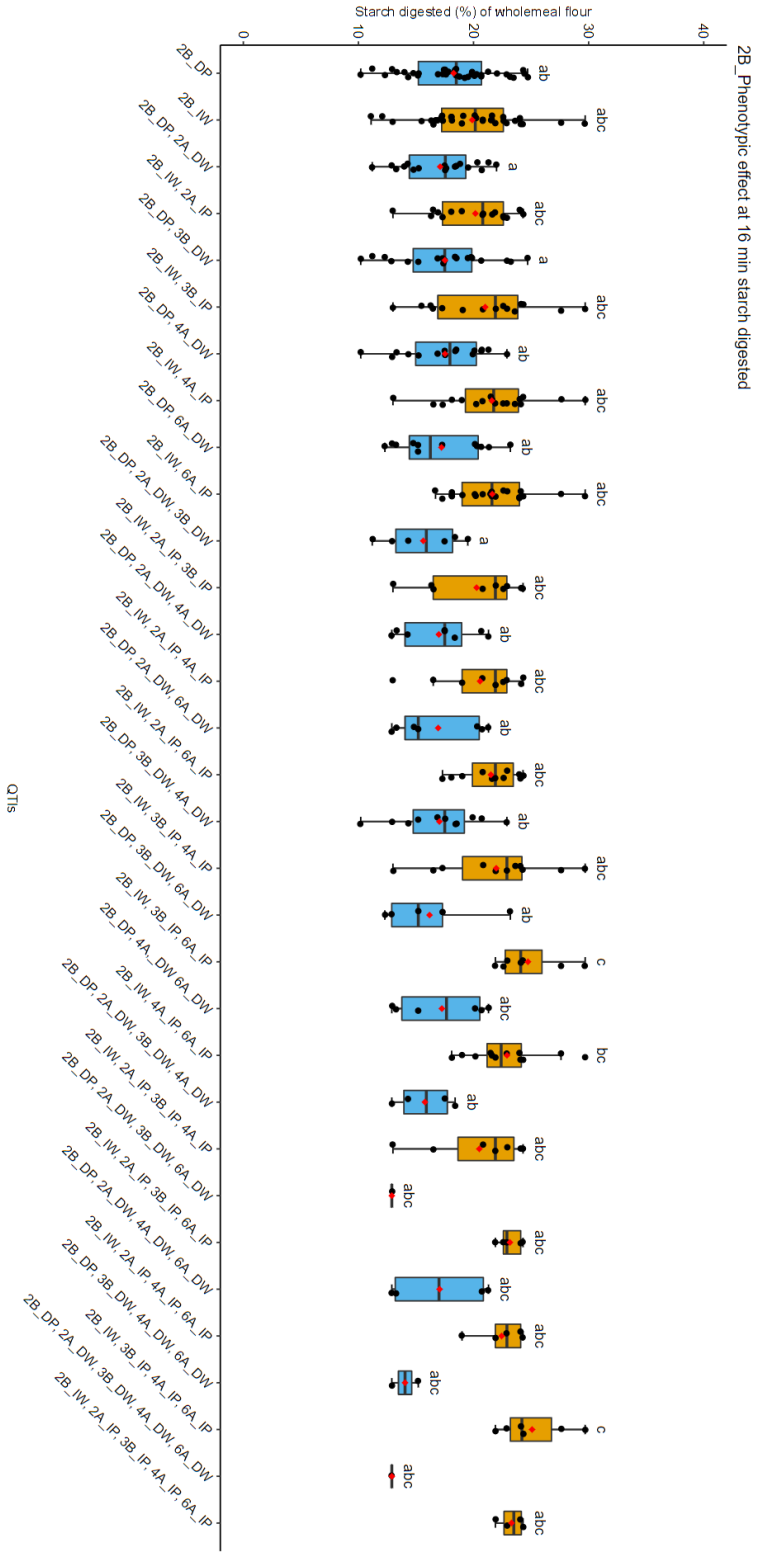

Supplemental Figure 4.12. 2B Phenotypic effect at 16 min starch digested. DW refers to the decreasing allele of Watkins 777, while DP represents the decreasing allele of Paragon. Similarly, IW stands for the increasing allele of Watkins 777, and IP stands for the increasing allele of Paragon.

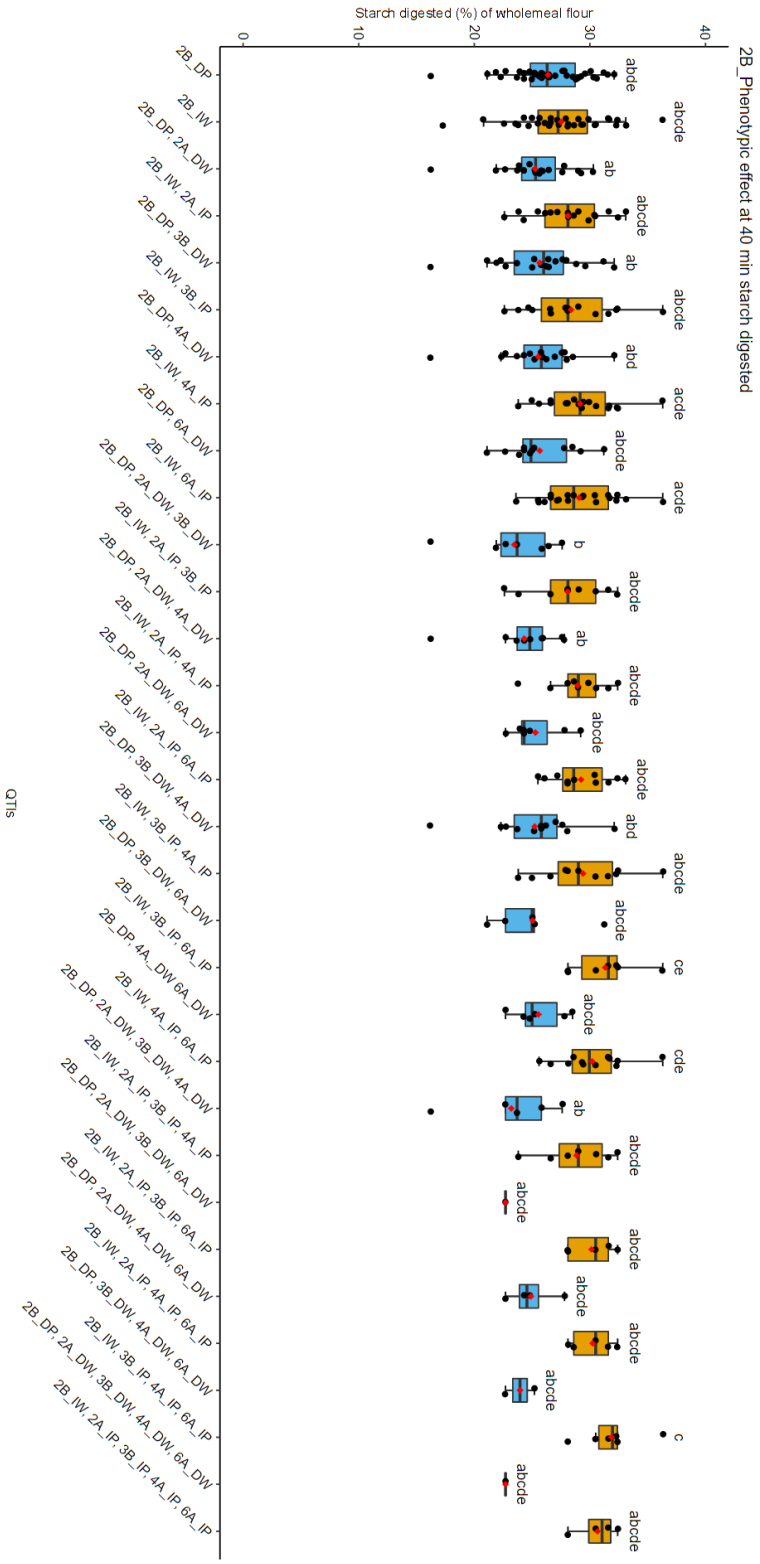

Supplemental Figure 4.13. 2B Phenotypic effect at 40 min starch digested. DW refers to the decreasing allele of Watkins 777, while DP represents the decreasing allele of Paragon. Similarly, IW stands for the increasing allele of Watkins 777, and IP stands for the increasing allele of Paragon.

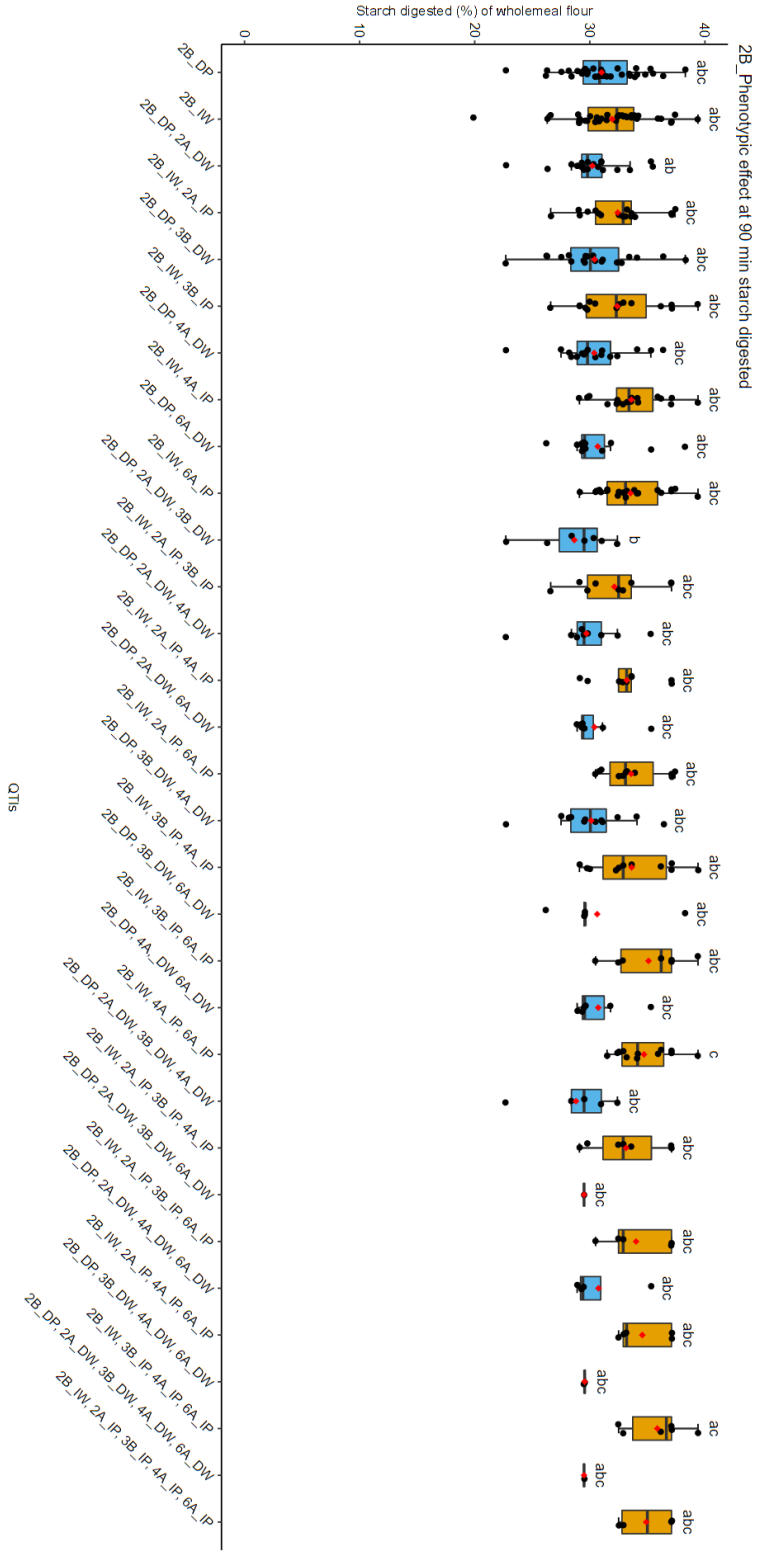

Supplemental Figure 4.14. 2B Phenotypic effect at 90 min starch digested. DW refers to the decreasing allele of Watkins 777, while DP represents the decreasing allele of Paragon. Similarly, IW stands for the increasing allele of Watkins 777, and IP stands for the increasing allele of Paragon.

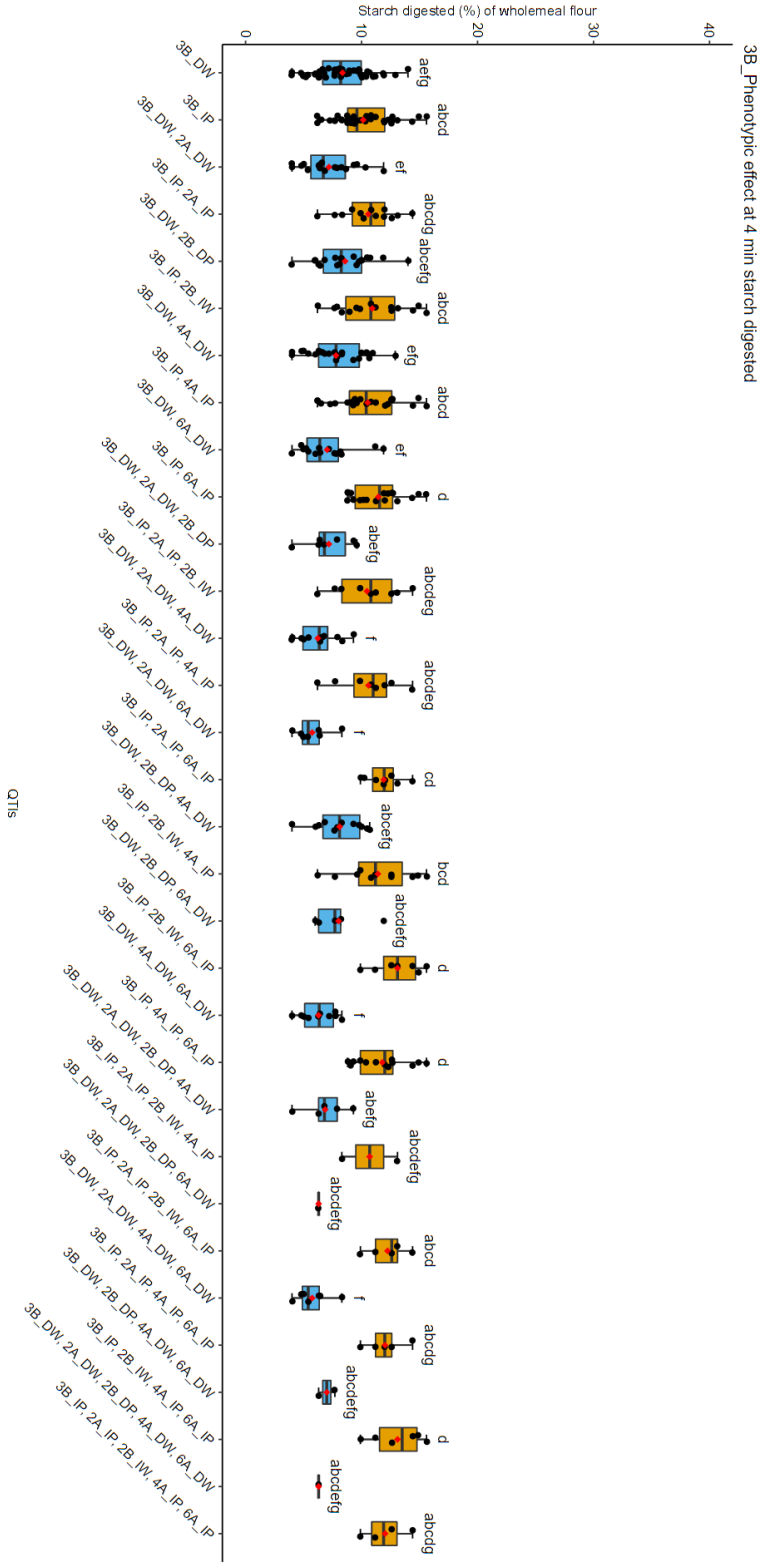

Supplemental Figure 4.15. 3B Phenotypic effect at 4 min starch digested. DW refers to the decreasing allele of Watkins 777, while DP represents the decreasing allele of Paragon. Similarly, IW stands for the increasing allele of Watkins 777, and IP stands for the increasing allele of Paragon.

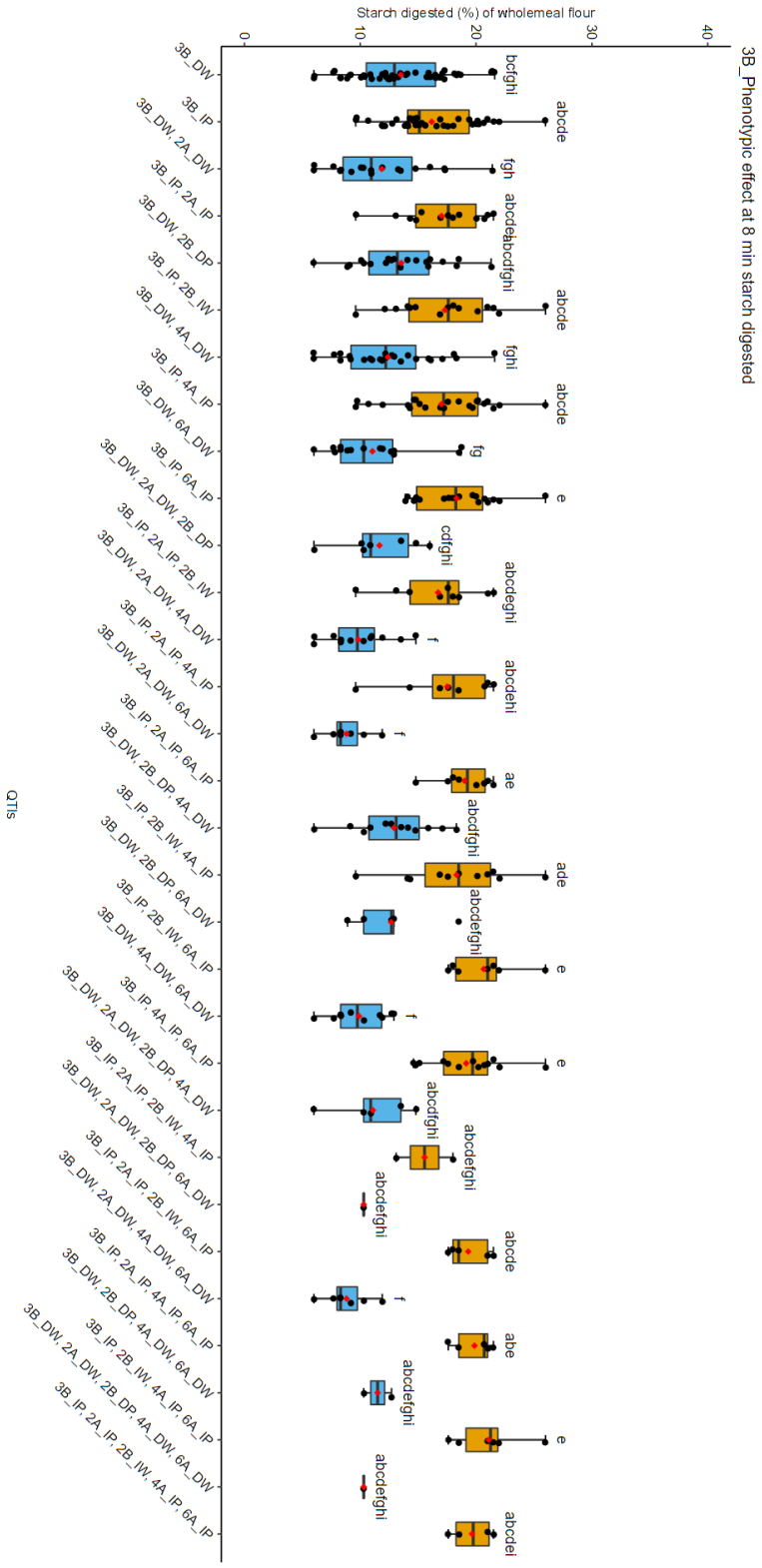

Supplemental Figure 4.16. 3B Phenotypic effect at 8 min starch digested. DW refers to the decreasing allele of Watkins 777, while DP represents the decreasing allele of Paragon. Similarly, IW stands for the increasing allele of Watkins 777, and IP stands for the increasing allele of Paragon.

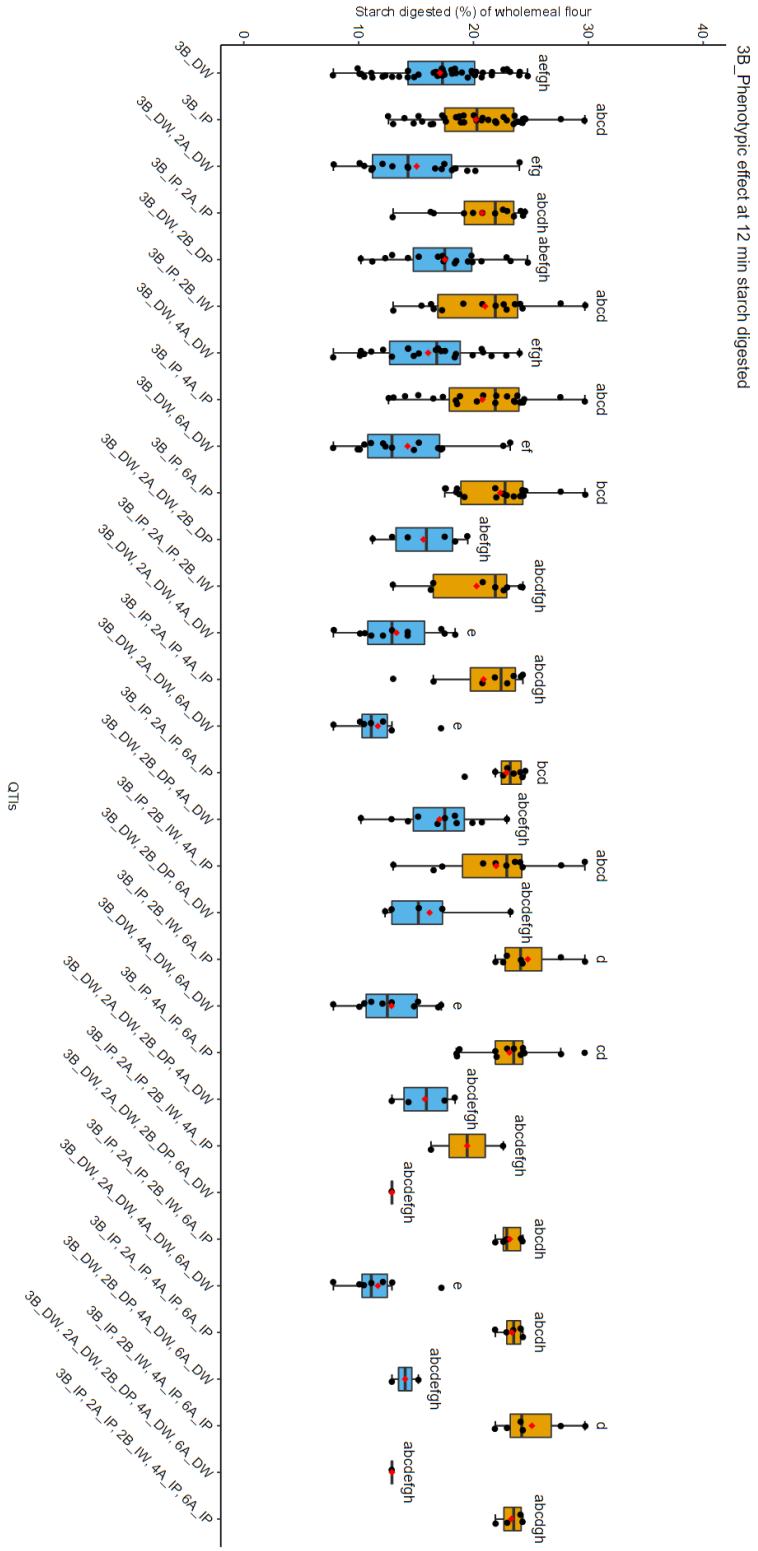

Supplemental Figure 4.17. 3B Phenotypic effect at 12 min starch digested. DW refers to the decreasing allele of Watkins 777, while DP represents the decreasing allele of Paragon. Similarly, IW stands for the increasing allele of Watkins 777, and IP stands for the increasing allele of Paragon.

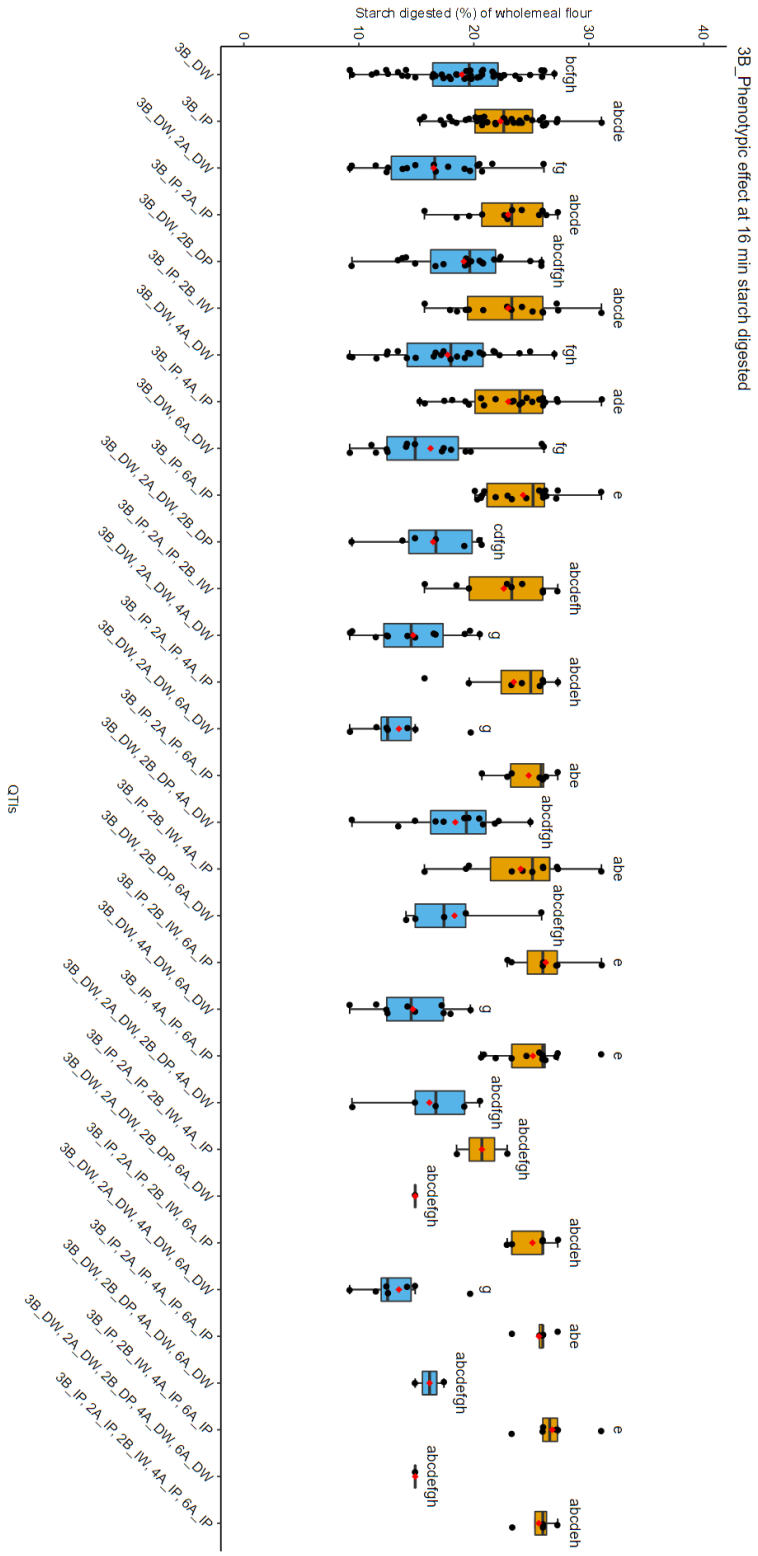

Supplemental Figure 4.18. 3B Phenotypic effect at 16 min starch digested. DW refers to the decreasing allele of Watkins 777, while DP represents the decreasing allele of Paragon. Similarly, IW stands for the increasing allele of Watkins 777, and IP stands for the increasing allele of Paragon.

Supplemental Figure 4.19. 3B Phenotypic effect at 40 min starch digested. DW refers to the decreasing allele of Watkins 777, while DP represents the decreasing allele of Paragon. Similarly, IW stands for the increasing allele of Watkins 777, and IP stands for the increasing allele of Paragon.

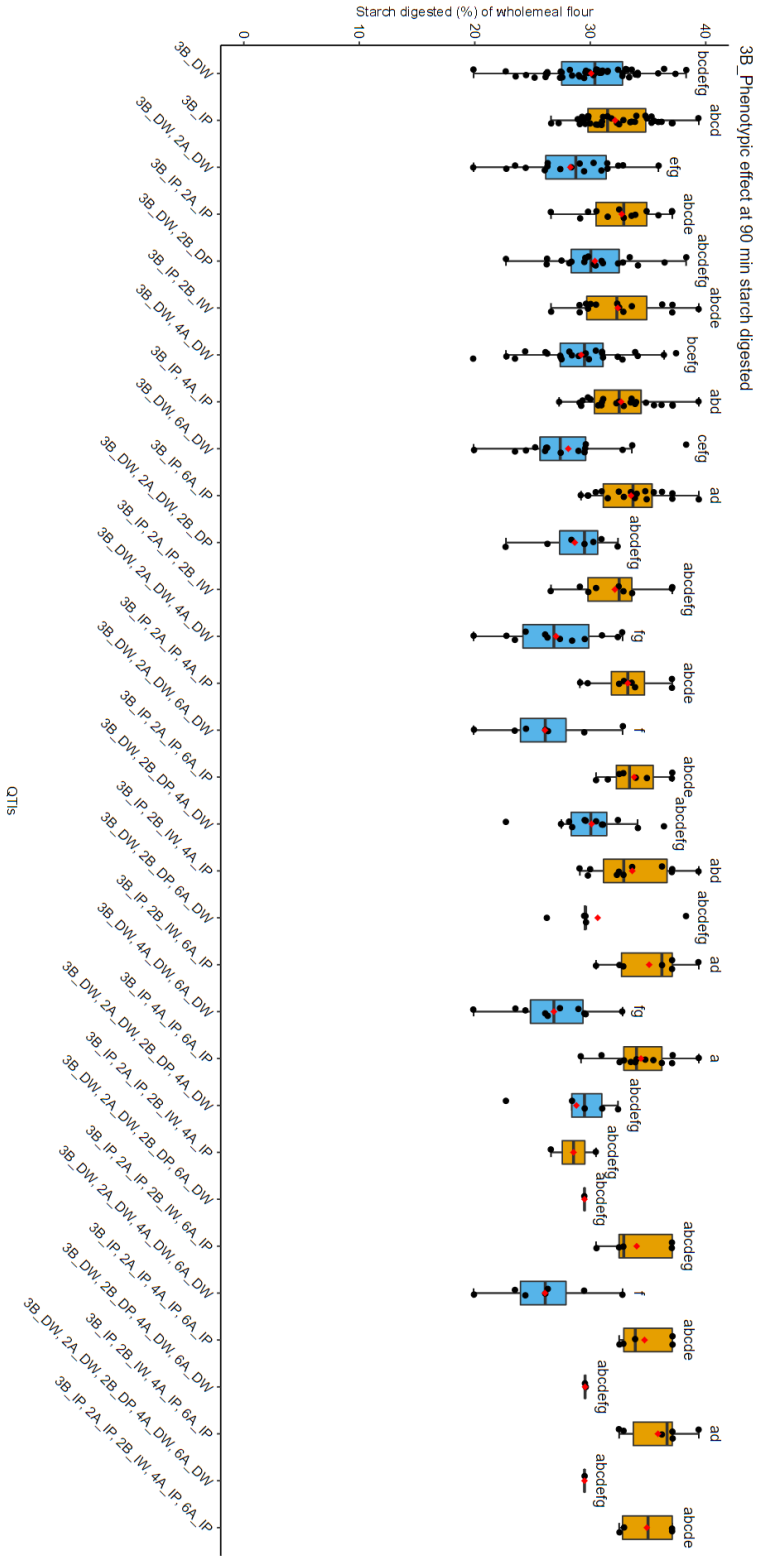

Supplemental Figure 4.20. 3B Phenotypic effect at 90 min starch digested. DW refers to the decreasing allele of Watkins 777, while DP represents the decreasing allele of Paragon. Similarly, IW stands for the increasing allele of Watkins 777, and IP stands for the increasing allele of Paragon.

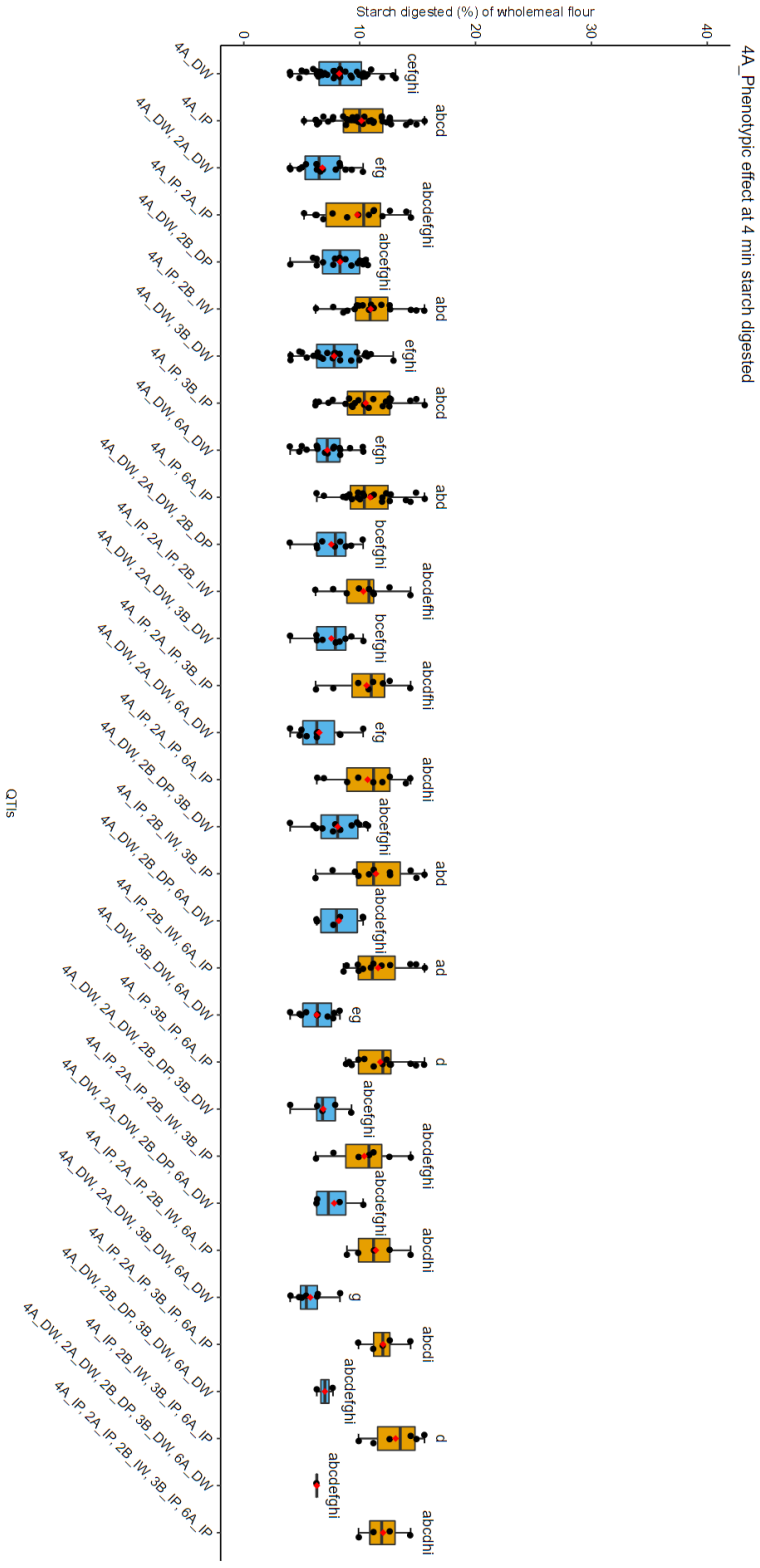

Supplemental Figure 4.21. 4A Phenotypic effect at 4 min starch digested. DW refers to the decreasing allele of Watkins 777, while DP represents the decreasing allele of Paragon. Similarly, IW stands for the increasing allele of Watkins 777, and IP stands for the increasing allele of Paragon.

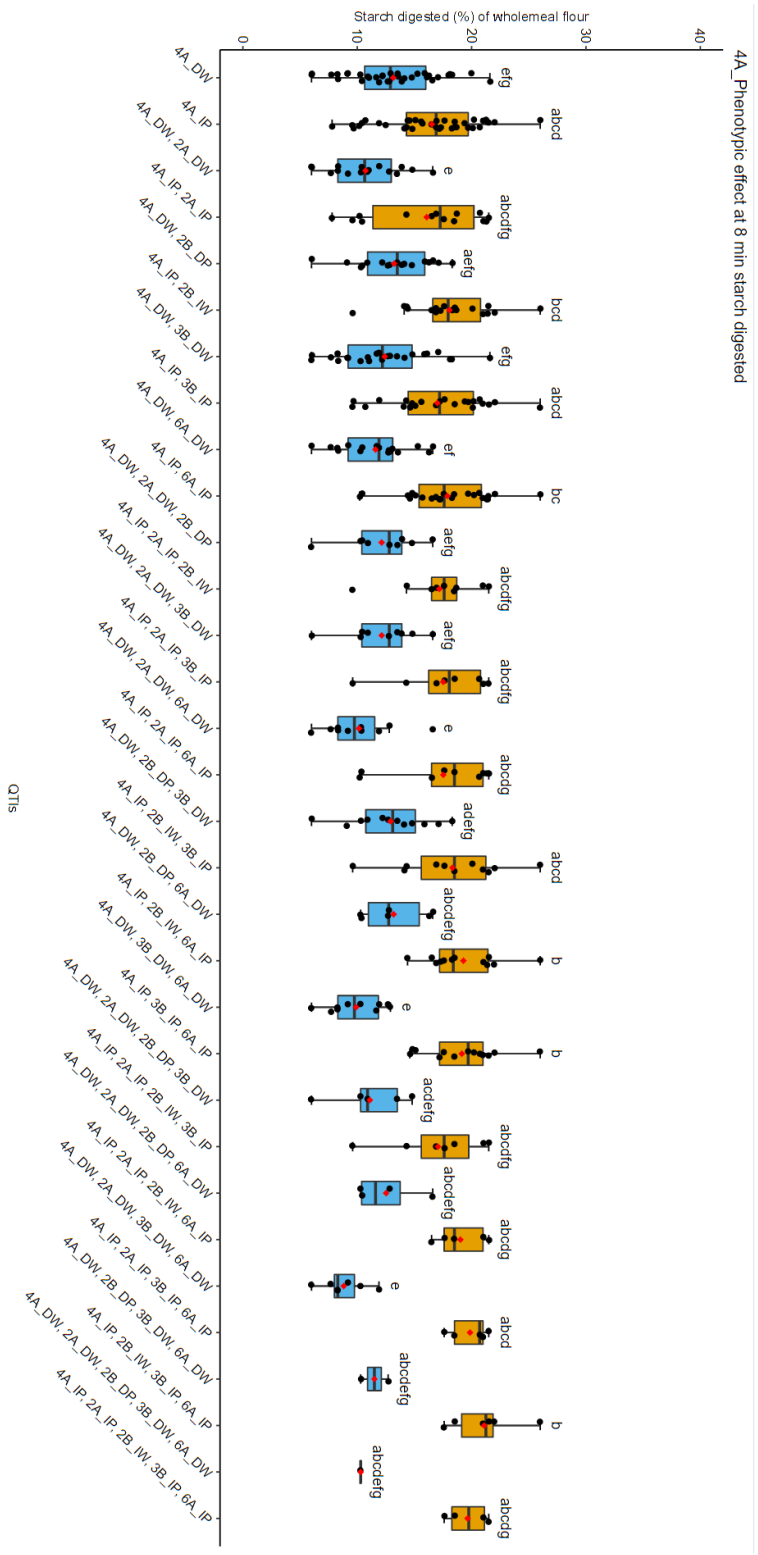

Supplemental Figure 4.22. 4A Phenotypic effect at 8 min starch digested. DW refers to the decreasing allele of Watkins 777, while DP represents the decreasing allele of Paragon. Similarly, IW stands for the increasing allele of Watkins 777, and IP stands for the increasing allele of Paragon.

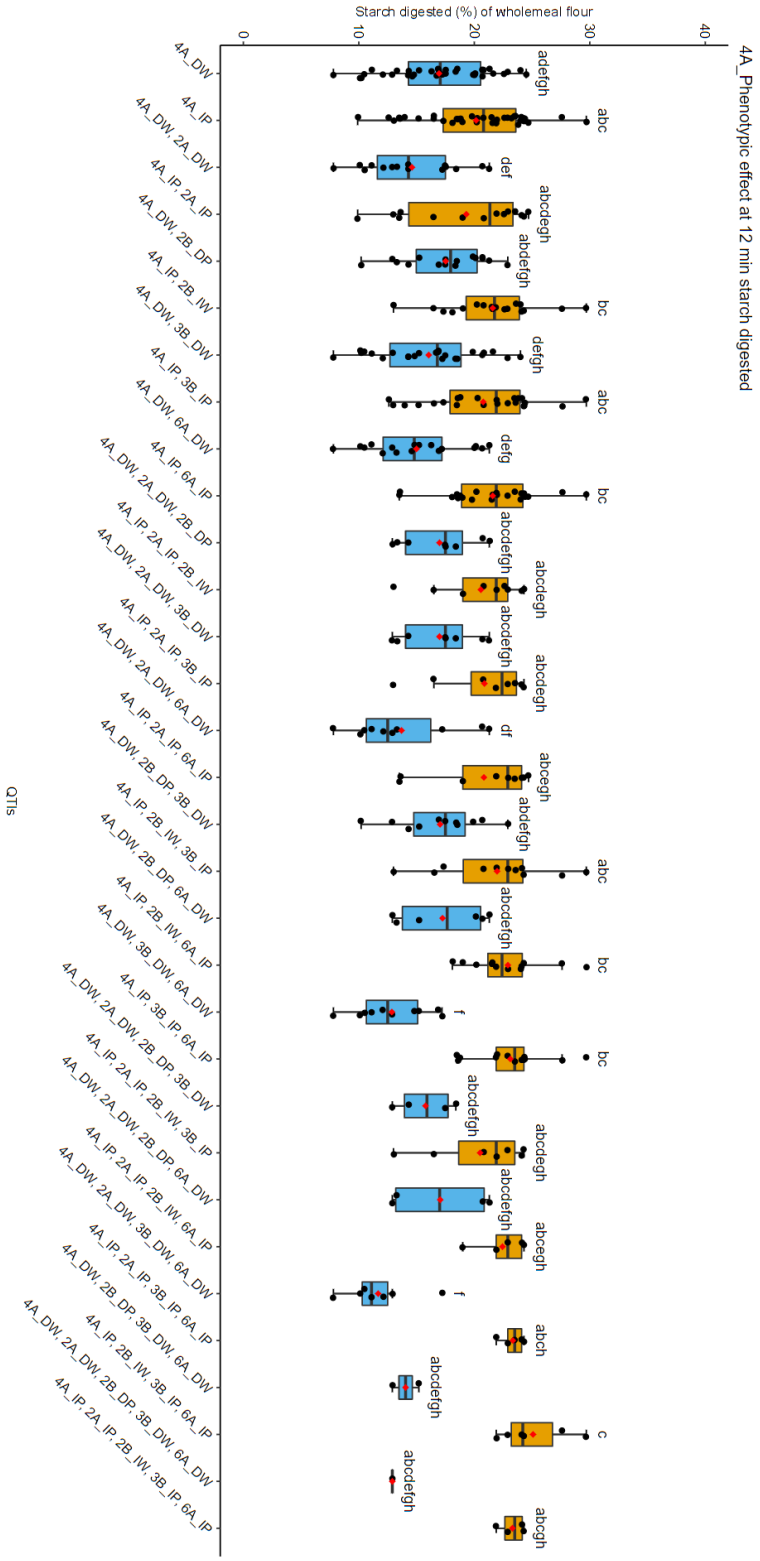

Supplemental Figure 4.23. 4A Phenotypic effect at 12 min starch digested. DW refers to the decreasing allele of Watkins 777, while DP represents the decreasing allele of Paragon. Similarly, IW stands for the increasing allele of Watkins 777, and IP stands for the increasing allele of Paragon.

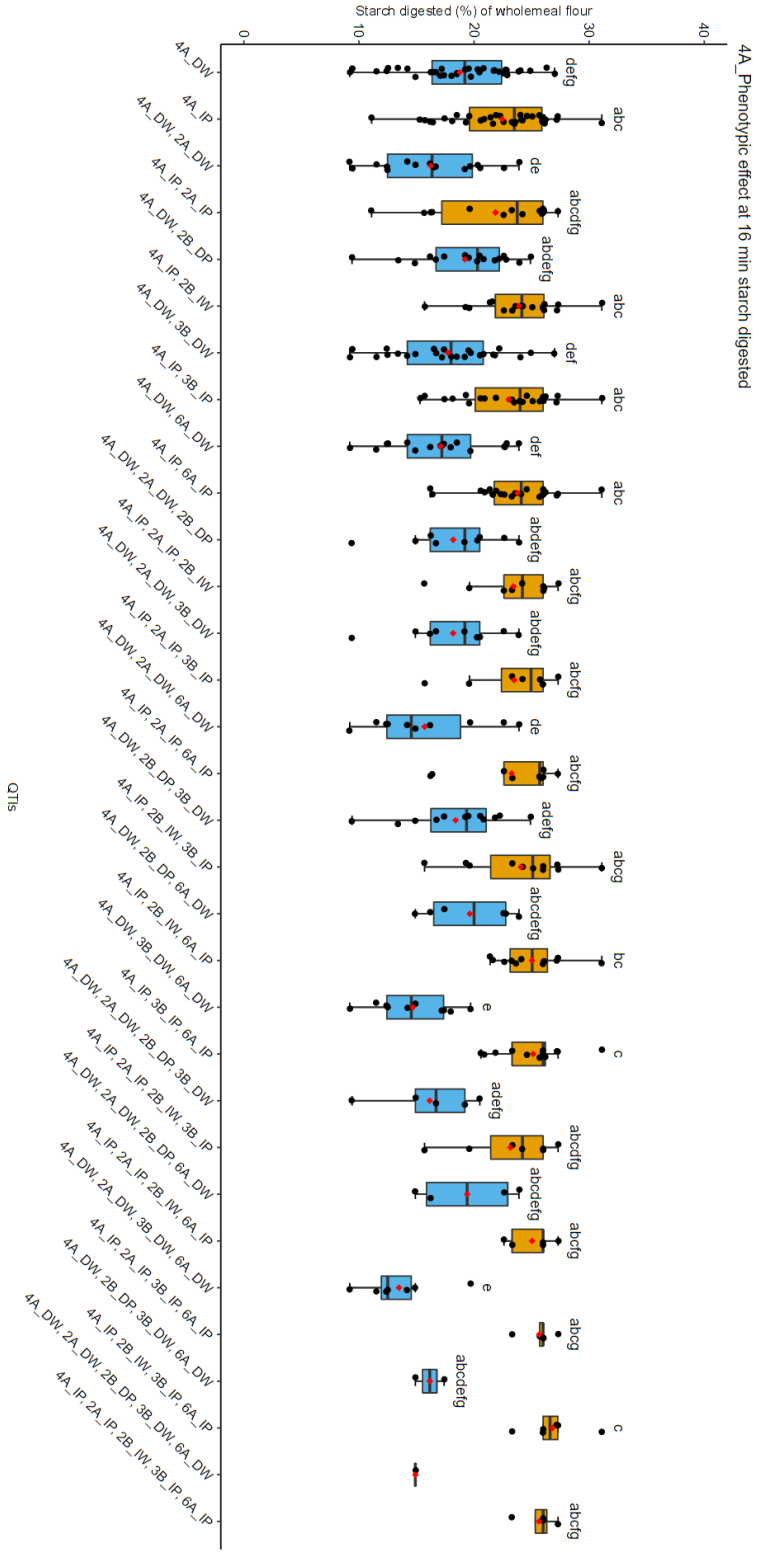

Supplemental Figure 4.24. 4A Phenotypic effect at 16 min starch digested. DW refers to the decreasing allele of Watkins 777, while DP represents the decreasing allele of Paragon. Similarly, IW stands for the increasing allele of Watkins 777, and IP stands for the increasing allele of Paragon.

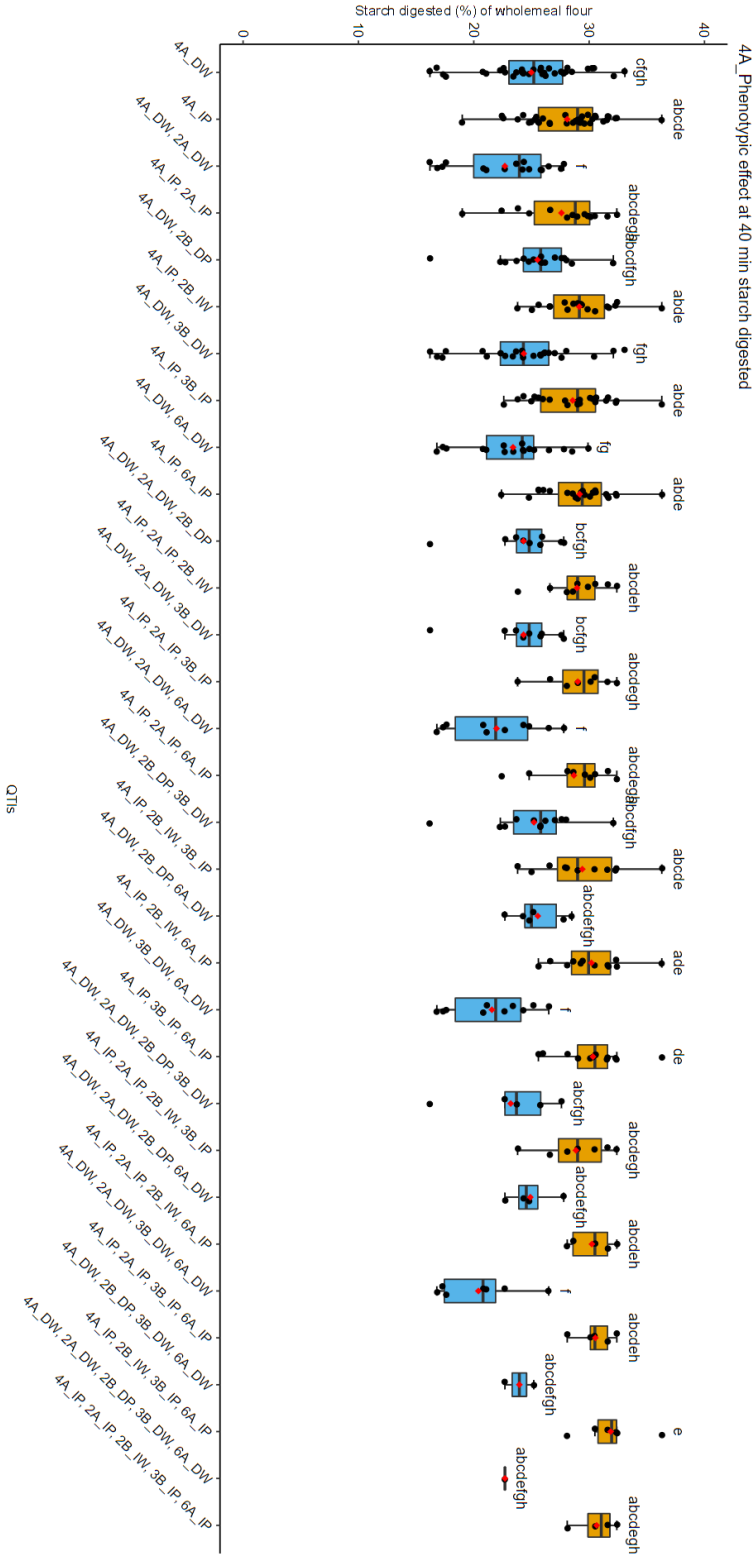

Supplemental Figure 4.25. 4A Phenotypic effect at 40 min starch digested. DW refers to the decreasing allele of Watkins 777, while DP represents the decreasing allele of Paragon. Similarly, IW stands for the increasing allele of Watkins 777, and IP stands for the increasing allele of Paragon.

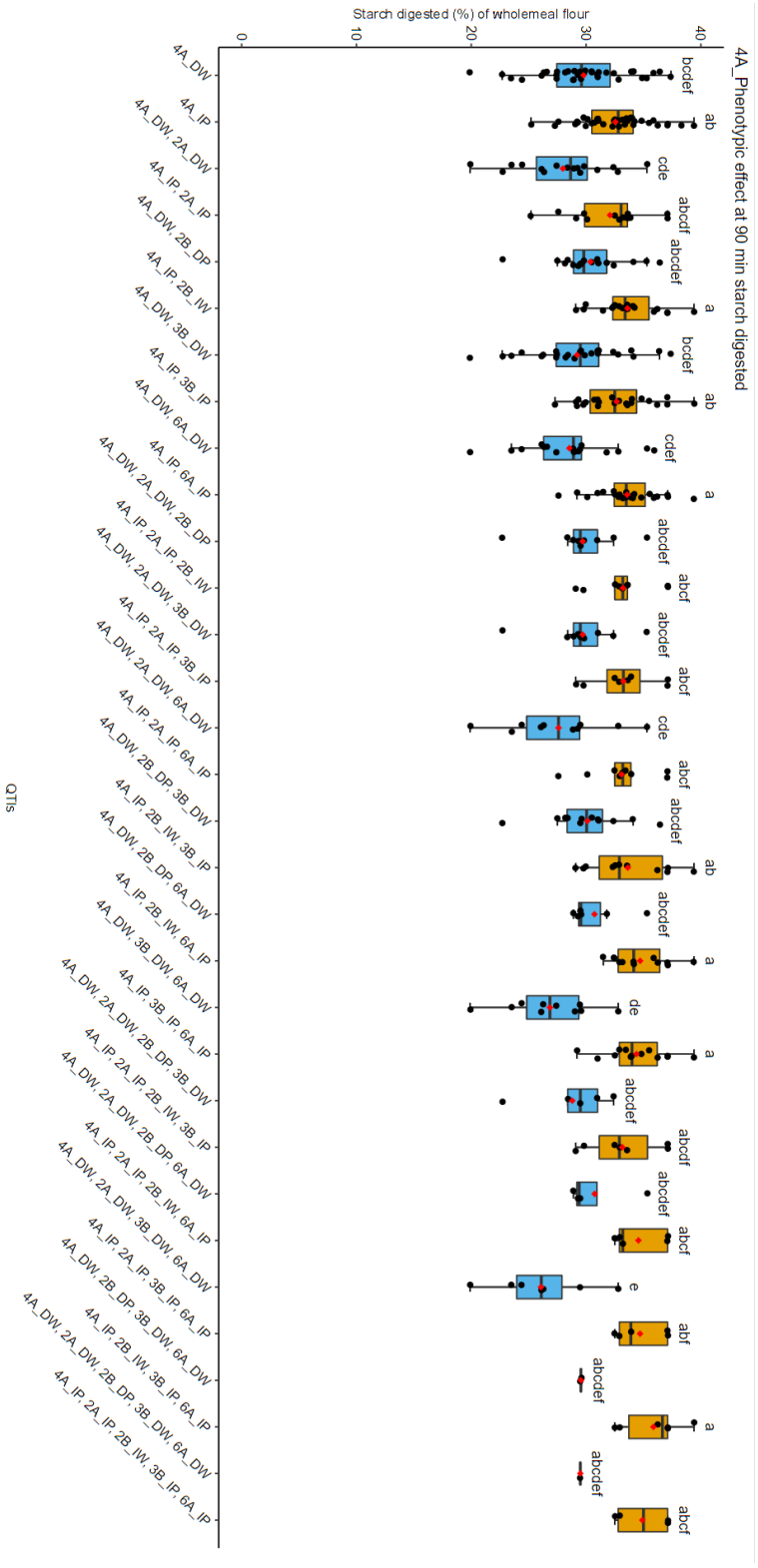

Supplemental Figure 4.26. 4A Phenotypic effect at 90 min starch digested. DW refers to the decreasing allele of Watkins 777, while DP represents the decreasing allele of Paragon. Similarly, IW stands for the increasing allele of Watkins 777, and IP stands for the increasing allele of Paragon.

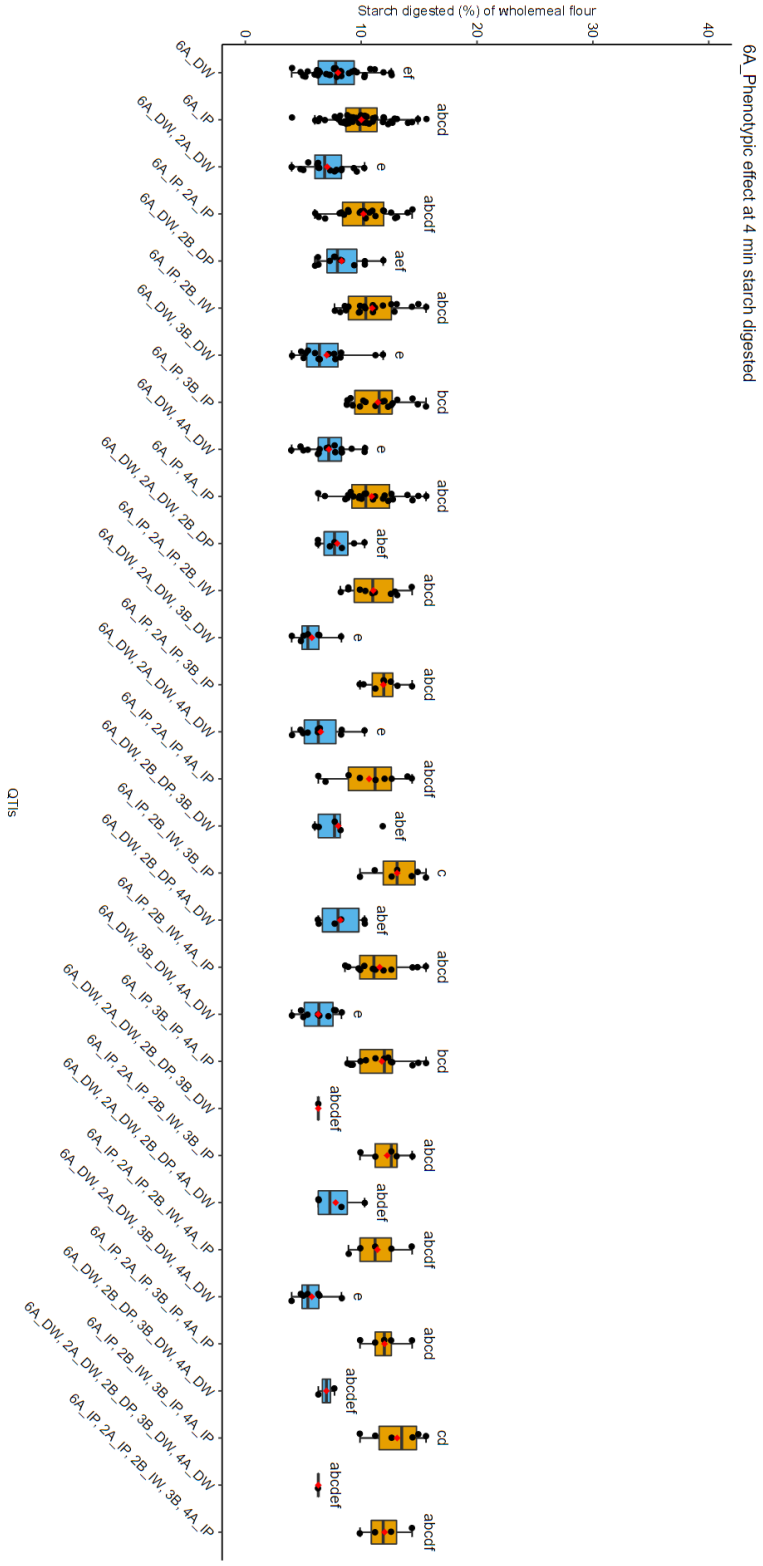

Supplemental Figure 4.27. 6A Phenotypic effect at 4 min starch digested. DW refers to the decreasing allele of Watkins 777, while DP represents the decreasing allele of Paragon. Similarly, IW stands for the increasing allele of Watkins 777, and IP stands for the increasing allele of Paragon.

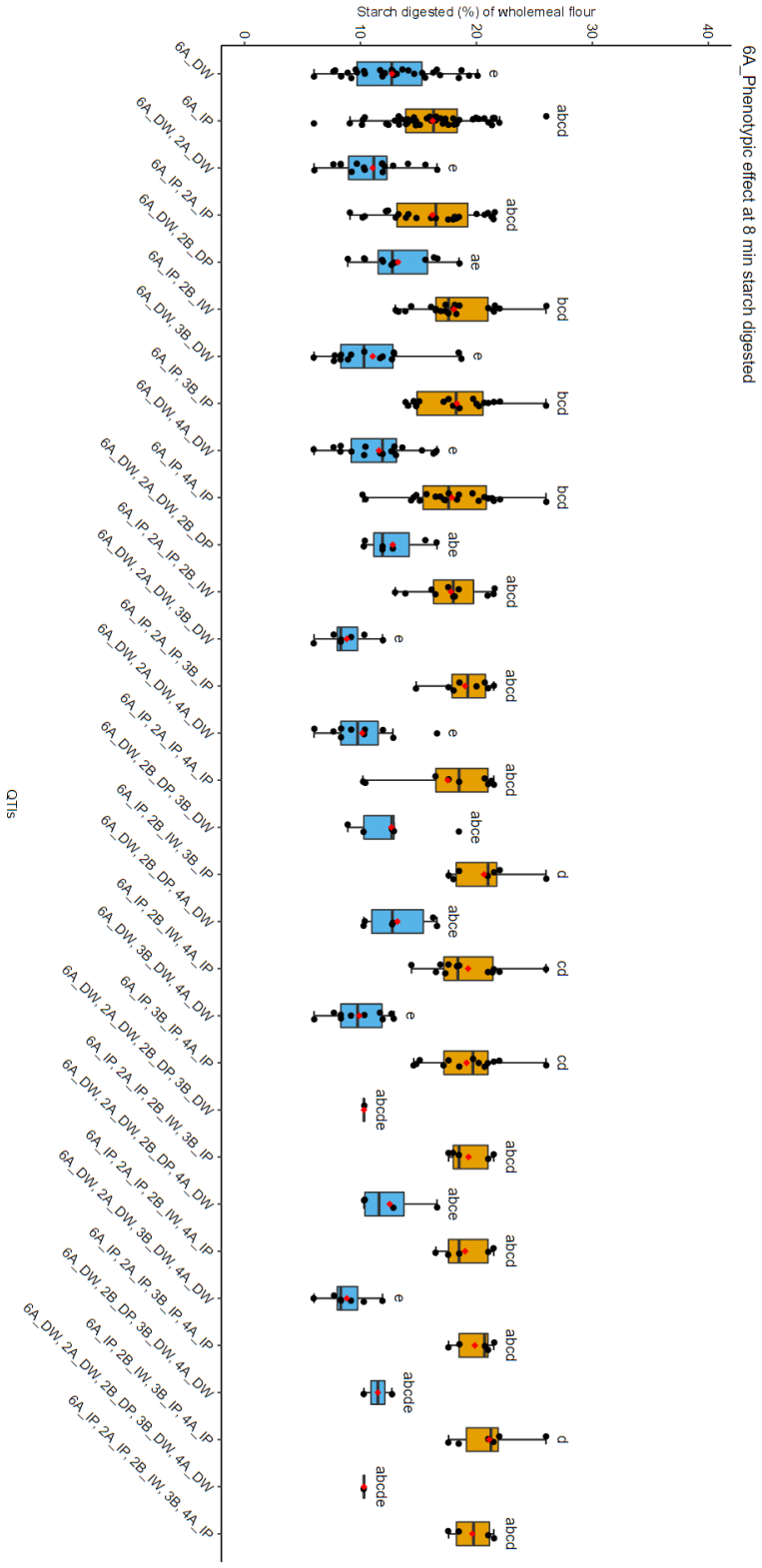

Supplemental Figure 4.28. 6A Phenotypic effect at 8 min starch digested. DW refers to the decreasing allele of Watkins 777, while DP represents the decreasing allele of Paragon. Similarly, IW stands for the increasing allele of Watkins 777, and IP stands for the increasing allele of Paragon.

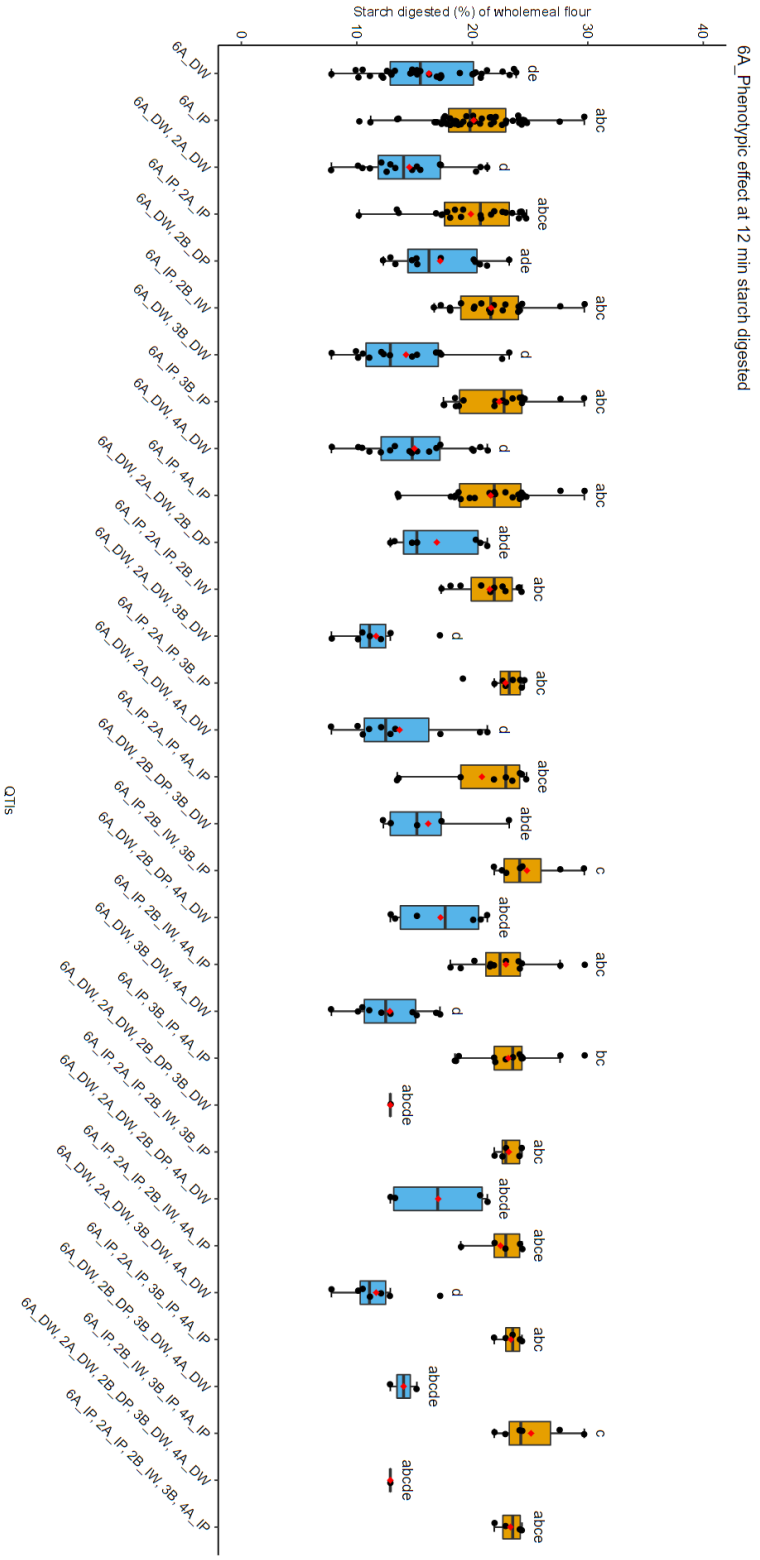

Supplemental Figure 4.29. 6A Phenotypic effect at 12 min starch digested. DW refers to the decreasing allele of Watkins 777, while DP represents the decreasing allele of Paragon. Similarly, IW stands for the increasing allele of Watkins 777, and IP stands for the increasing allele of Paragon.

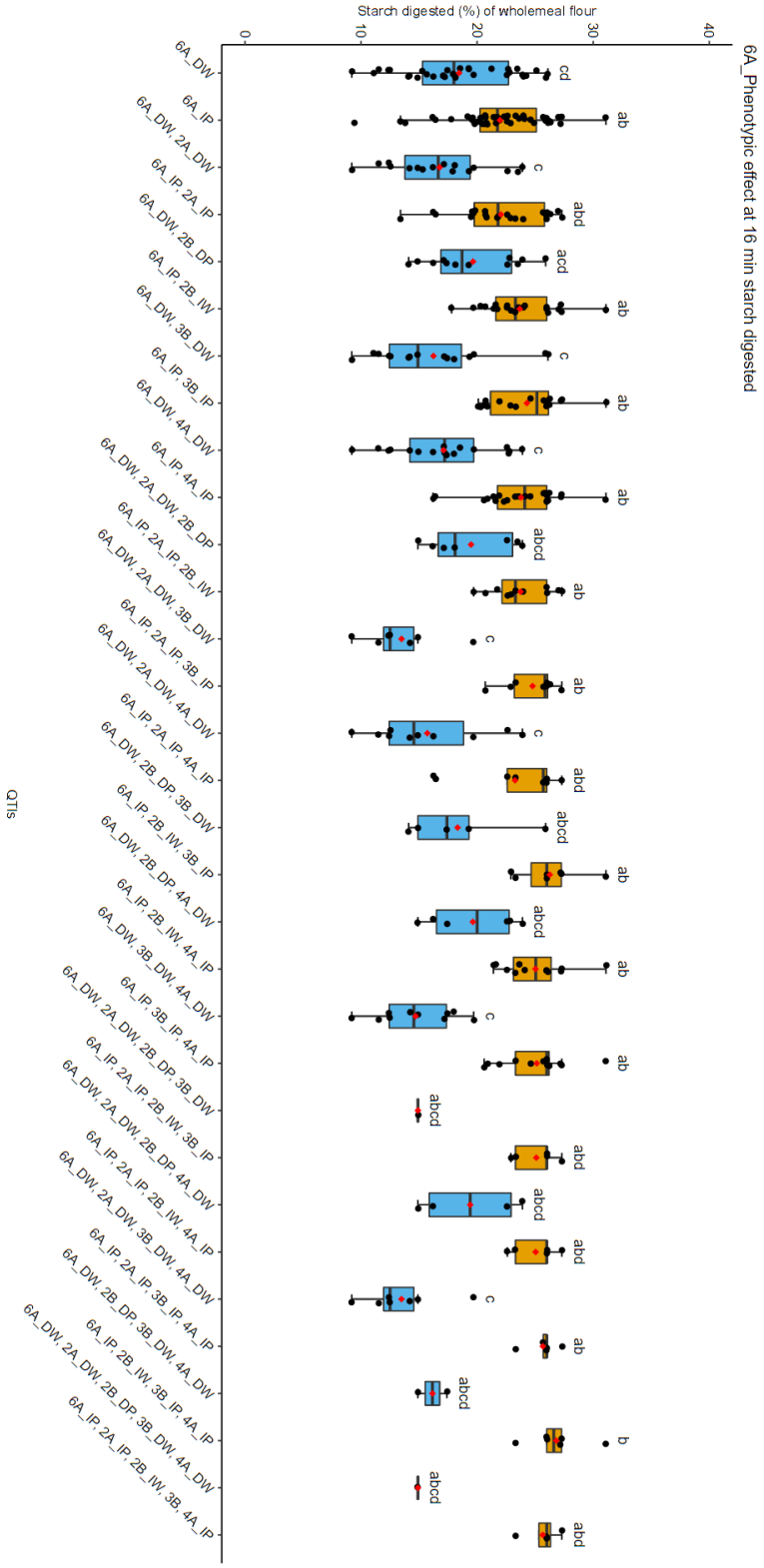

Supplemental Figure 4.30. 6A Phenotypic effect at 16 min starch digested. DW refers to the decreasing allele of Watkins 777, while DP represents the decreasing allele of Paragon. Similarly, IW stands for the increasing allele of Watkins 777, and IP stands for the increasing allele of Paragon.

Supplemental Figure 4.31. 6A Phenotypic effect at 40 min starch digested. DW refers to the decreasing allele of Watkins 777, while DP represents the decreasing allele of Paragon. Similarly, IW stands for the increasing allele of Watkins 777, and IP stands for the increasing allele of Paragon.

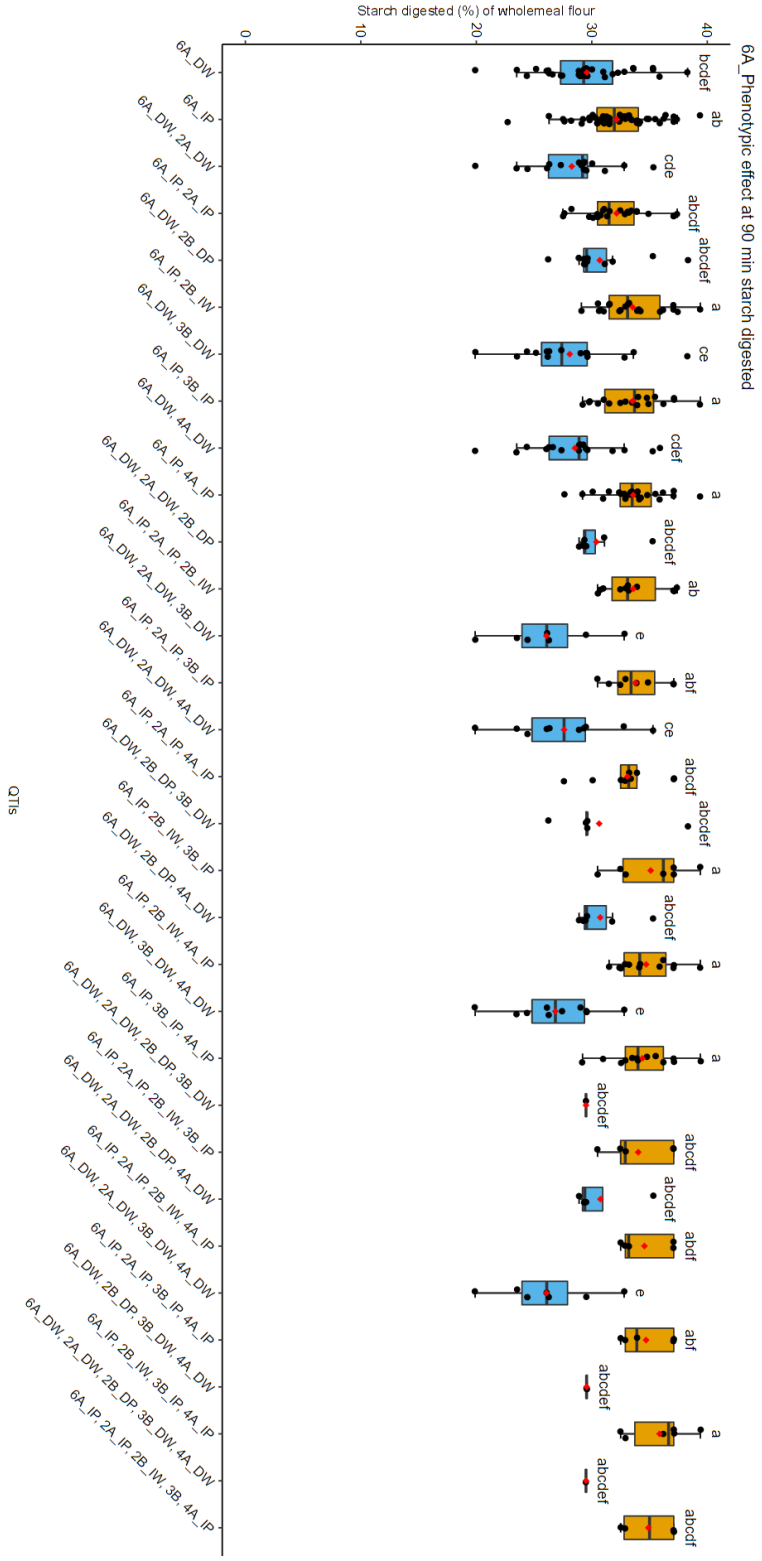

Supplemental Figure 4.32. 6A Phenotypic effect at 90 min starch digested. DW refers to the decreasing allele of Watkins 777, while DP represents the decreasing allele of Paragon. Similarly, IW stands for the increasing allele of Watkins 777, and IP stands for the increasing allele of Paragon.

Supplemental publication. Zafeiriou, P., Savva, G.M., Ahn-Jarvis, J.H., Warren, F.J., Pasquariello, M., Griffiths, S., Seung, D. and Hazard, B.A., 2023. Mining the AE Watkins Wheat Landrace Collection for Variation in Starch Digestibility Using a New High-Throughput Assay. Foods, 12(2), p.266.

foods

MDPI

Article

Mining the A.E. Watkins Wheat Landrace Collection for Variation in Starch Digestibility Using a New High-Throughput Assay

Petros Zafeiriou [1], George M. Savva [1], Jennifer H. Ahn-Jarvis [1], Frederick J. Warren [1], Marianna Pasquariello [2], Simon Griffiths [2], David Seung [2] and Brittany A. Hazard [1,*]

[1] Quadram Institute Bioscience, Norwich NR4 7UQ, UK
[2] John Innes Centre, Norwich NR4 7UH, UK
* Correspondence: brittany.hazard@quadram.ac.uk; Tel.: +44-(0)1603-255000

Abstract: Breeding for less digestible starch in wheat can improve the health impact of bread and other wheat foods. The application of forward genetic approaches has lately opened opportunities for the discovery of new genes that influence the digestibility of starch, without the burden of detrimental effects on yield or on pasta and bread-making quality. In this study we developed a high-throughput in vitro starch digestibility assay (HTA) for use in forward genetic approaches to screen wheat germplasm. The HTA was validated using standard maize and wheat starches. Using the HTA we measured starch digestibility in hydrothermally processed flour samples and found wide variation among 118 wheat landraces from the A. E. Watkins collection and among eight elite UK varieties (23.5 to 39.9% and 31.2 to 43.5% starch digested after 90 min, respectively). We further investigated starch digestibility in fractions of sieved wholemeal flour and purified starch in a subset of the Watkins lines and elite varieties and found that the matrix properties of flour rather than the intrinsic properties of starch granules conferred lower starch digestibility.

Keywords: wheat; landrace; starch digestibility; natural variation; high-throughput; retrograded starch; starch structure; screening tool; pipetting tool; breeding

Citation: Zafeiriou, P.; Savva, G.M.; Ahn-Jarvis, J.H.; Warren, F.J.; Pasquariello, M.; Griffiths, S.; Seung, D.; Hazard, B.A. Mining the A.E. Watkins Wheat Landrace Collection for Variation in Starch Digestibility Using a New High-Throughput Assay. *Foods* **2023**, *12*, 266. https://doi.org/10.3390/foods12020266

Academic Editor: Wenhao Li

Received: 16 November 2022
Revised: 20 December 2022
Accepted: 22 December 2022
Published: 6 January 2023

1. Introduction

Starchy foods are a main source of carbohydrate in our diet and an important source of energy. Reducing the rate and extent of starch digestibility in foods can help to maintain healthy blood glucose levels, which is important for the prevention and management of obesity and chronic diseases like type II diabetes [1]. Furthermore, there is substantial evidence that consumption of resistant starch, that is the starch that escapes digestion in the small intestine and reaches the colon, can reduce blood glucose and help to maintain a healthy gut [2–4]. Wheat (*Triticum aestivum* L.) is one of the most widely consumed crops worldwide and provides up to 50% of the calories in the human diet, mainly in the form of starch, so improving its nutritional quality could deliver health benefits to a large number of people [5,6]. Thus, breeding for wheat with less digestible starch is an important strategy to develop healthier foods to reduce dietary risk factors of chronic diseases.

A mature wheat grain contains predominately starch, 60–70% (w/w), which is the greatest contributor to calories, and also 10–15% (w/w) protein and 11–15% (w/w) dietary fiber [7,8]. Starch is produced in the endosperm of wheat during grain filling and is composed of two distinct α-glucan polymers, amylose (linear α-1,4-linked chains) and amylopectin (α-1,4-linked chains with α-1,6-linked branches). In their native state, starch polymers exist as partially crystalline granules, which are difficult for humans to digest; thus starch-based foods are typically cooked prior to consumption. Heating starch in the presence of water leads to starch gelatinization making starch polymers more digestible [9–11]. Subsequent cooling leads to retrogradation in which starch polymers form crystalline structures that are less digestible [12,13]. Moreover, there are several other factors which

contribute to differences in starch digestibility such as starch molecular structure [14–16] and properties of wheat flour (particle size and protein content) [17,18].

To date, reverse genetic studies in wheat have demonstrated potential for increasing resistant starch levels using induced mutations in starch biosynthesis genes [14,19–21]. However, initial analyses of some mutants have shown detrimental effects on yield and on pasta and bread-making quality, so identifying additional sources of genetic variation for starch digestibility could support the development of improved traits for commercial breeding applications [14,20]. Wheat landraces, locally adapted lines that have not been modified through modern breeding techniques, present reservoirs of genetic diversity that can be introduced into modern varieties. Of special note is the A.E. Watkins bread wheat landrace collection, encompassing 826 bread wheat landraces collected in the 1920s and 1930s from a global geographic distribution. This collection showed a greater level of genetic diversity compared to modern elite European bread wheat varieties and has been used to identify resistance genes for a variety of diseases [22–26]. The Watkins lines have been purified by single-seed descent from which many genomic and genetic resources have been developed. A core set of 118 accessions (c.Watkins) capturing most of the genetic diversity in the Watkins collection was presented by Wingen et al. [22], and used to generate nested association mapping populations, all of which were genotyped, have genetic maps available, and are free to access (http://wisplandracepillar.jic.ac.uk/) (accessed on 16 November 2022). Thus, a key aim of this study was to determine the extent of natural variation in starch digestibility of the c.Watkins lines and in modern elite UK varieties (bread, biscuit, and animal feed varieties recommended on the UK Agriculture and Horticulture Development Board Recommended List, AHDB).

Despite the availability of diverse wheat germplasm resources like the c.Watkins collection, forward screening approaches for starch digestibility have been limited due to the lack of informative, accurate, and efficient phenotyping methods. Screening based on amylose content, which has a positive association with resistant starch content, can identify lines with high levels of resistant starch but cannot identify factors beyond amylose content that may cause resistance to digestion [27,28]. Only a few studies have developed methods to directly screen large populations for starch digestibility and these have focused on analyzing purified starch [29]. However, other components of the wheat flour matrix and processing (e.g., starch retrogradation) could potentially impact starch digestibility [30–32]. To our knowledge, no previous studies have screened flour samples of wheat germplasm collections.

To facilitate rapid assessment of starch digestibility in the c.Watkins wheat landraces, an in vitro single-enzyme system was utilized (Figure 1, study workflow) [30,33,34]. This system has proved useful for measuring starch digestibility in mechanistic studies and early-stage food product development and produces results which are well correlated with human glycaemic responses to foods [33,35]. Moreover, compared to other in vitro digestion methods, the single-enzyme system has advantages such as fewer steps, low consumables, and non-specialized equipment which support its adaptation to a high-throughput assay (HTA). Here, we describe the development of a HTA for measuring starch digestibility based on the single-enzyme system [33], which utilizes a 96-sample format for simultaneous starch digestion analysis over a 90 min period. The HTA allows smaller amounts of flour to be analyzed in a standardised 96 well-format using only a thermomixer compared to a cabinet incubator, tube rotator and water bath. These modifications were made to tailor the method for screening large wheat germplasm collections accurately and efficiently. Using standard samples of wheat and maize starch, we validated the assay by comparing starch digestibility profiles to those produced by the single-enzyme system protocol reported in Edwards et al., 2019 [33]. The HTA was then used to screen for the first time processed flour samples of the entire c.Watkins collection [22] as well as elite UK varieties (representing commercial wheat lines for bread, biscuit, and animal feed), which revealed natural phenotypic variation for starch digestibility.

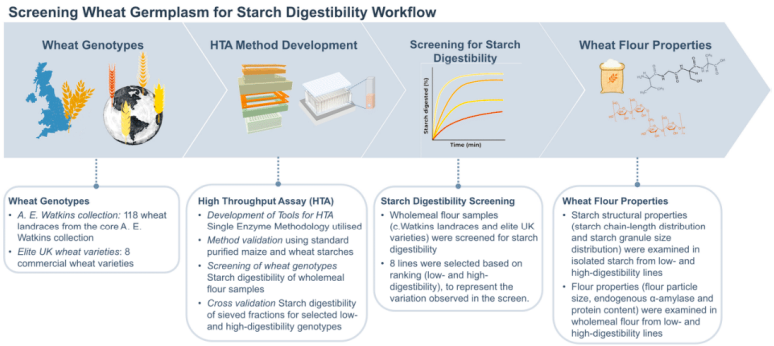

Figure 1. Study workflow for screening starch digestibility of wheat germplasm.

2. Materials and Methods

2.1. Chemicals

Chemicals used in this study: PercollTM (17-0891-01, GE Healthcare), 4-Hydroxybenzh ydrazide (PAHBAH) (5351-23-5), TRIS (77-86-1), EDTA (60-00-4), SDS (151-21-3), DTT (3483-12-3), Phosphate buffered saline (PBS) (P4417-100), Sodium Carbonate (497-19-8), DMSO (67-68-5), maltose (6363-53-7), sodium hydroxide (1310-73-2) and α-amylase (DFP Treated, Type I-A, saline suspension, 647-015-00-4) were purchased from Sigma-Aldrich Company Ltd., Poole, UK.

2.2. High-Throughput Starch Digestibility Assay

A graphical scheme of the HTA assay is presented in Figure 2. Starch digestion assays were carried out on samples that were gelatinized and cooled to accelerate retrogradation following a protocol by Edwards [33], modified for screening a large number of samples. Wholemeal flour samples were weighed (6 mg) and transferred into a deep well plate (96/1000 µL, Eppendorf, Stevenage, UK). Phosphate buffered saline (600 µL, PBS, pH 7.4) was added to each sample with a 1 mm glass ball to improve mixing. The deep well plate was sealed and secured with a Cap-mat (96-well, 7 mm, Round Plug, Silicone/PTFE) and added to a preheated thermal mixer (80 °C) with a 96 SmartBlock™ DWP 1000 n attachment (Thermomixer C, Eppendorf Ltd., Stevenage, UK) for 15 min at 1500 rpm to gelatinize the starch, then cooled at 4 °C for 21 h to accelerate retrogradation. The plate was then briefly spun (100 g for 1 min) to collect condensed liquid on the Cap-mat and placed on the thermal mixer for 30 min at 37 °C, 1600 rpm. Time zero samples (50 µL) were collected using a 12-multichannel pipette and transferred into a 2 mL deep well plate containing 1.95 mL of stop solution (17 mM $NaCO_3$). Digestion was started by adding pancreatic α-amylase suspended in PBS targeting 2 U/mL activity into the samples. Enzyme activity was determined by applying the starch digestibility assay on gelatinized potato starch and obtaining the linear rate of maltose release every 3 min (mg/mL). Aliquots (50 µL) were then taken after 6, 12, 18, 24, 40, and 90 min from the onset of digestion and transferred to the stop solution.

The stopped reactions were then centrifuged at 4000× *g* for 5 min to avoid transferring any starch remnants, and 50 µL of the supernatant was transferred to a new deep well plate; 50 µL of maltose standards (5–1000 µM) were also added to the plate. The PAHBAH reducing end assay was used to quantify the reducing ends released [36]. Briefly, 0.5 mL of freshly prepared reagent (2 g of p-hydroxybenzoic acid hydrazide dissolved in 38 mL of 0.5 M HCl and 360 mL of 0.5 M NaOH) was added to each sample. The deep-well plate was held at 100 °C for 7 min and then placed in an ice bath for 10 min. Samples were then transferred to a microplate, and absorbance was measured at 405 nm using a microplate reader (Bio-Rad Benchmark Plus, Waukegan, IL, USA). Reducing sugars were expressed as

maltose equivalents, using a standard curve of maltose standards (5–1000 µM) from each sample plate. Starch digestibility (%) was expressed according to the single-enzyme system; each timepoint's maltose equivalents were corrected by subtracting the baseline maltose (time zero) and then divided by the maltose equivalent of total starch. Four technical replicates were used, each carried out on a different day.

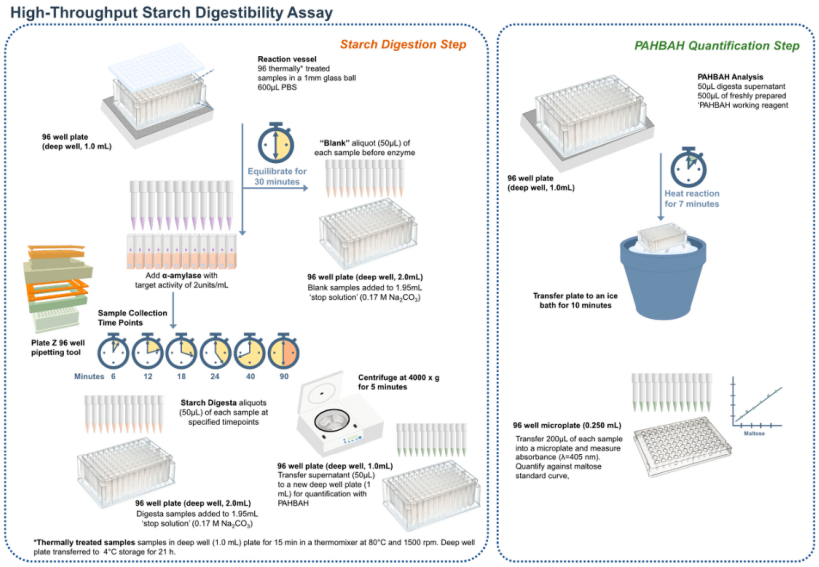

Figure 2. Principle of the high-throughput in vitro starch digestibility assay using a single enzyme system. For amylolysis, a known enzyme-substrate ratio is used, and starch is hydrolysed by porcine pancreatic α-amylase to produce reducing sugars. During amylolysis, aliquots are transferred to a 'stop solution' at predetermined time points to inactivate amylase activity. The reducing sugar concentration is quantified using a colorimetric p-hydroxybenzoic acid hydrazide (PAHBAH) assay and maltose standards [36]. The portion of starch digested for each timepoint is calculated based on reducing sugars and is then displayed against time.

2.3. Validation of the High-Throughput Starch Digestibility Assay

Starch digestion profiles from the HTA and the single-enzyme system were compared using standards of purified starch from standard maize, waxy maize, and high-amylose maize (purchased from Merck, formerly Sigma-Aldrich, Darmstadt, Germany), standard wheat starch (purchased from Merck, formerly Sigma-Aldrich, Darmstadt, Germany), and two high-amylose starches: sbeII and ssIIIa, previously characterized, respectively, by Corrado et al. and Fahy et al. [2,21]. Starch samples were aliquoted to make 5.4 mg of starch/mL of PBS, and α-amylase activity was adjusted at 2 U/mL. The thermal treatment procedure was followed as described above for the starch digestibility HTA. Three runs were obtained for both protocols over different days. For each run, six replicates per starch sample were placed randomly in the 96-well plate for the HTA, and two replicates were used for the standard protocol. For each run, starch samples and enzyme solution were prepared in stock and aliquoted for use in both the HTA and single-enzyme system.

2.4. Field Trial Design

Grains for the c.Watkins lines were ordered from the Germplasm Resources Unit (John Innes Centre in Norwich, UK) using the publicly accessible SeedStor system https://www.seedstor.ac.uk/, (accessed on 16 November 2022); permission to use the materials

for research purposes was obtained. The 118 c.Watkins lines were grown in Autumn 2018 in 1 m^2 plots (one plot per line, except for the low yield lines) at Church Farm, Norfolk UK (52°37′49.2″ N 1°10′40.2″ E) using standard agronomic practices (Supplemental Figure S1). Based on yield data from previous years, lines with a lower yield performance were grown in duplicate or triplicate (to ensure production of sufficient grains), and grains were pooled for analysis (Supplemental Figure S2). Seeds from elite varieties of bread, biscuit, and animal feed commercial groups of the UK AHDB Recommended List (Cougar, Crusoe, Dickens, Diego, Myriad, Paragon, Santiago, Skyfall) were kindly provided by Brendan Fahy [37] (ahdb.org.uk) (accessed on 16 November 2022). Elite varieties were grown in 2013 in plots (one per genotype) of 1.5 m^2 at Morley Farm, Norfolk, UK (52°33′15.57″ N 1°10′58.956″ E).

2.5. Milling and Sieving

Grains from the c.Watkins and elite varieties were coarsely milled in a cyclone mill fitted with a 0.5 mm screen (UDY Corporation). Milled samples were passed through a 0.3 mm sieve (Endecotts Limited, London, UK) to produce 'wholemeal' flour samples, and selected lines were passed through a 0.053 mm sieve to produce 'sieved' flour samples. The flour samples were kept in a vacuum desiccator for five days before analysis.

2.6. Starch Isolation

Starch was isolated using an adapted method reported in Hawkins, et al. [38]. Wheat flour samples were resuspended with water and filtered through a 100 µm cell strainer (BD Falcon #352360). Samples were then centrifuged at 3000× *g* for 5 min, and the pellets were resuspended in 2 mL of water. The starch suspensions were then overlayed into a Percoll solution (90% *v*/*v*) and centrifuged at 2500× *g* for 15 min to remove cell walls and proteins. The recovered starch pellets were washed with 1 mL buffer (50 mM Tris-HCl, pH 6.8; 10 mM EDTA; 4% SDS; and 10 mM DTT), transferred into a 2 mL tube and left to incubate for 5 min. The starch suspension was then centrifuged at 4000× *g* for 1 min. The pellets were recovered, and the washing procedure was repeated once more. The pellets were then washed three times with 1 mL of water, then once with 100% ethanol. Samples were then kept one day in the fume hood, followed by five days in a desiccator containing silicon dioxide prior to analysis.

2.7. Total Starch Assay

Wholemeal flour samples were weighed (~8 mg) and transferred into a deep well plate (96/1000 µL, Eppendorf), each well containing 20 µL of DMSO and a 3 mm glass ball to improve mixing. The plate was mixed for 5 min at 1600 rpm to disperse the samples before adding 500 µL of a thermostable α-amylase to each sample. The thermostable α-amylase was solubilized at 1:30 (*v*/*v*) in 100 mM sodium acetate buffer, pH 5.0 (Total Starch hexokinase kit, AOAC Method 996.1 1; Megazyme, Bray, IE). The deep well plate was sealed and secured with a Cap-mat (96-well, 7 mm, Round Plug, Silicone/PTFE). Samples were heated at 90 °C for 10 min at 1600 rpm using a thermal mixer with a 96 SmartBlock™ DWP 1000 n attachment (Thermomixer C, Eppendorf Ltd., Stevenage, UK). Total starch content was determined using a Total Starch HK kit (Total Starch hexokinase kit, AOAC Method 996.1 1; Megazyme, Bray, IE, Wicklow, Ireland) following manufacturer instructions, except volumes of reagents were scaled down by a factor of 10.

2.8. In Depth Analysis of Selected High- and Low-Digestibility Lines

Methods for particle size analysis of flour and starch, size exclusion chromatography, protein content and endogenous α-amylase are available in Supplementary Materials.

2.9. Tools

During optimization of the HTA, a low-cost 3D-printed pipetting tool was developed, which allowed for manageable weighing and transferring of samples into 96-sample deep

well plates and improved speed and control of pipette aspiration (Plate Z). The PLZ 3D design is available to download and print for free (https://www.hackster.io/386082/high-throughput-pipetting-plate-z-bde2c7) (accessed on 16 November 2022).

2.10. Data Analysis

Statistical analyses and graphs were produced using RStudio (R version 4.2.1, Posit Software, Boston, MA, USA). Datasets of the validation of the in vitro starch digestibility HTA were analysed using the packages lme4 (v 1.1-30) and lmerTest (v 3.1-3) for a mixed model fit [39–41]. Plots were made using the ggplot2 package (v 3.3.6) [42].

For validation of the HTA, the methods were compared by plotting the estimated starch digestion profiles from the HTA and the single-enzyme system (protocol from Edwards et al., 2019 [33]) and by comparing the estimated starch digested at 90 min. The bias (difference in estimates between methods for the same material) and variation between runs (technical variation) in starch digested at 90 min was estimated using linear mixed models, including the type of starch as a fixed effect and sample batch as a random effect. The variances were estimated using separate models for each method, so that the variability of each method could be compared, while the bias was estimated using a single joint model including all data points, with 'method' corresponding to an additional fixed effect.

A linear mixed model including line as a fixed effect and experimental run as a random effect was used for analysis of in vitro starch digestibility of the c.Watkins lines and elite varieties. Marginal means with standard errors (calculated using a pooled standard deviation) are plotted for each line.

The correlation between starch digestibility and total starch was estimated using linear regression. All values reported represent the mean, and the number of replicates and variance metrics are specified in the description of the corresponding figure and Supplementary Datasets.

For complete details of analyses, all data and analysis code is available as Supplementary Materials.

3. Results and Discussion

3.1. Screening of c.Watkins Landraces and Elite Varieties

3.1.1. In Vitro Starch Digestibility

The aim of this experiment was to determine the extent of natural variation in starch digestibility of the c.Watkins collection and compare it with elite UK varieties representing each commercial group (qualities of bread, biscuit and animal feed).

Results of the HTA revealed a wide range of variation in starch digestibility among c.Watkins landraces; starch digestibility profiles formed a gradient of low- to high- digestibility rather than two distinct groups, as expected from complex traits (Figure 3A shows the individual trajectories of starch digested over time, Figure 3B compares the starch digested for each line at 90 min). For the c.Watkins lines, the levels of starch digested at 90 min ranged between 9.7–31.6% (at 6 min), 13.2–35% (at 12 min), 14.8–37.2% (at 18 min), 16.2–36.1% (at 24 min), 19–37.8% (at 40 min), and 23.5–39.9% (Figure 3B). The residual variance from the mixed effect model, measuring the variability between technical replicates from the same sample in the same run, was 3.7 percentage points. There was no statistical evidence for a relationship between the plot location in the field and the starch digestibility at 90 min, as no trend was observed between field rows and columns (Supplemental Figure S3).

Elite UK varieties showed less variation and greater starch digestibility compared to most c.Watkins lines, although a direct comparison is confounded by the different growing conditions between the two groups (Figure 3A). For example, the levels of starch digested for the elite varieties ranged between 26.8–36.4% (at 6 min), 29.4–40.4% (at 12 min), 30.6–43.8% (at 18 min), 30–43.4% (at 24 min), 31.3–43.4% (at 40 min) and 31.2–43.5% (at 90 min) (Figure 3B).

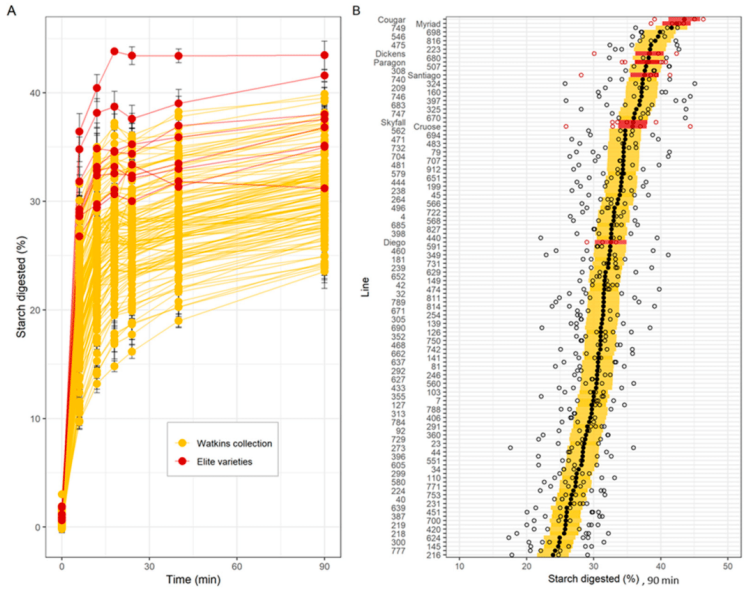

Figure 3. Starch digestibility and total starch of c.Watkins landraces (yellow) and elite varieties (red) of wholemeal flour. (**A**). Starch digested (%) for c.Watkins (yellow) and elite varieties (red). Points and lines represent the mean and standard error from between 3 and 6 technical replicates per line. (**B**). Starch digested (%) at 90 min. Individual data points from technical replicates are shown in white dots, and marginal mean values from a mixed effects model with line as a fixed effect and experimental run as a random effect are shown in black (c.Watkins) and red dots (elite). The standard error estimated from the model is displayed as yellow (c.Watkins) and red (elite) bars. Values represent mean ± SE of $n \geq 3$ replicates.

Our results demonstrate that natural phenotypic variation for starch digestibility exists in the c.Watkins collection (representing the genetic diversity of the entire Watkins collection, 826 lines) as well as in elite varieties representing commercial groups of bread, biscuit and animal feed groups, and so there is potential for identifying underlying genetic diversity. The variation observed among the c.Watkins lines was greater than among the elite varieties screened, which is consistent with the higher levels of genetic diversity previously reported for the c.Watkins collection compared to modern European bread wheat varieties, as well as increased phenotypic variation for agronomically desirable traits, such as stripe, leaf, and stem rust resistance, as well as grain surface area and grain width [22–26]. It is important to note that a limitation of our study was that the grain samples of c.Watkins lines and elite varieties were not produced in the same field trial, and each a single plot per line, so it is possible that environmental conditions between and within fields could influence the average starch digestibility levels and the variation observed; this will be important to consider in future trials. With the availability of structured germplasm panels (nested association mapping populations) and genotypic data [43], there is now potential for use of the HTA to investigate the genetic factors underlying the variation in starch digestibility observed through approaches like QTL analysis which will aid in identification of underlying candidate genes and development of tools for marker assisted-selection. Furthermore, once lines are identified, digestion of starch and other nutrients in wheat foods can be explored using more extensive in vitro

models of digestion in the upper gastrointestinal track such as the standardized INFOGEST protocol, based on an international consensus by COST INFOGEST network [44].

3.1.2. Total Starch

Total starch (TS) content of wholemeal flour varied significantly for c.Watkins landraces (43 ± 3.3 g/100 flour to 61 ± 2.4 g/100 flour, mean ± SE, $p \leq 0.001$), and the elite varieties (46 ± 3.6 g/100 flour to 61 ± 0.9 g/100 flour, mean ± SE, $p \leq 0.05$). The elite variety Diego had the highest TS content (61 ± 0.9 g/100 flour, mean ± SE), and the c.Watkins line 651 had the lowest (43 ± 3.3 g/100 flour, mean ± SE). Most of the samples had a TS content between 47 to 57 g/100 flour. Linear regression analysis showed that total starch content only weakly correlated ($R^2 = 0.0108$) with starch digested at 90 min which suggests that the differences in total starch content do not explain the variation observed for starch digestibility (Supplemental Figure S4).

3.1.3. Analysis of Low- and High-Digestibility Lines

To gain further insight into factors influencing the difference in starch digestibility a subset of c.Watkins lines and elite varieties were selected, based on their starch digestibility profiles (high- vs. low-digestibility) to measure starch digestibility in sieved flour (to obtain smaller particle size fractions) and purified starch.

Three low-digestibility lines: 777 (WATDE0111), 216 (WATDE0025), and 639 (WATDE0083); and five high-digestibility lines: including two c.Watkins landraces 816 (WATDE0117), 308 (WATDE0042) and the three UK elite varieties Myriad, Dickens, and Paragon were selected for further analysis. The selection was based on the starch digestibility HTA results, specifically the ranking (low to high), to represent the variation observed in the screen.

Results presented in Figure 4 show that starch digestibility profiles differed considerably for wholemeal flour, sieved flour, and purified starch, suggesting that other flour components besides starch likely may contribute to the variation in starch digestibility observed. For wholemeal flour (<0.3 mm), starch digestibility profiles of selected 'low-'and 'high-digestibility' lines grouped separately where the high-digestibility samples varied between 37.6–41.6% and low-digestibility samples varied between 23.5–24.3% (at 90 min) (Figure 4A). For sieved flour (<0.05 mm), the digestibility of two low digestibility-lines (216 and 639) increased significantly ($p < 0.05$) compared to the corresponding wholemeal samples, and while the third low-line (777) remained low (Figure 4B). Purified starch samples showed a greater extent of starch digested at 90 min compared to wholemeal and sieved flour fractions (Figure 4C). Moreover, there were no differences between the high- and low-digestibility groups in purified starch samples. For example, high-digestibility lines differed between 46.9–52.3% and low-digestibility lines varied between 47.6–49.2% (at 90 min).

Finally, these selected lines were also analyzed for starch structural properties (starch chain-length distribution and starch granule size distribution) and flour properties (flour particle size, endogenous α-amylase and protein content). These results are described below. In summary, while differences between the lines themselves were evident for many properties, none of these factors significantly correlated with starch digestibility in this sample (Supplemental Table S1 and Supplemental Figures S5–S7).

Starch molecular structure and composition have been shown to influence its digestibility; thus, starch fine molecular structure and starch granule size-distribution was examined in the selected low- and high-digestibility lines. Starch chain-length distributions showed significant differences between lines in the proportion of long and short chains of amylopectin (AP) and amylose (AM) ($p < 0.001$) (Supplemental Figure S5 and Table S1). However, the overall AM:AP ratio was not significant. Starch granule size distribution of purified starch using a Coulter counter revealed significant variation among starch granule diameter ($p < 0.001$), whereas minor differences were observed for the overall volume of A and B granules (Supplemental Table S1). Low-digestibility lines showed the greatest variation in B-granule diameter, with 6 ± 0.1 µm SE for line 777 to 8.4 ± 0.2 µm SE for line

216 (40% greater). The diameter of B-granules in high-digestibility lines varied less; 816 had the highest (6.9 ± 0.4 µm SE), and 308 had the lowest (6.2 ± 0.1 µm SE). In general, similar trends were also observed for A-granule diameter, except that low-digestibility line 216 had significantly larger A-granules. The diameter of A-granules from low digestibility lines ranged from 18.2 ± 0.2 µm SE (lines 777 and 639) to 20.1 ± 0.2 µm SE (line 216). There was also significant variation in A-granule diameter among high-digestibility lines; 308 had the smallest (17.7 ± 0.04 µm SE) and Paragon the largest (20.1, ± 0.2 µm SE). Overall, we observed differences in chain-length distribution profiles and starch granule size distribution of the selected lines but the there was no correlation of either factor to starch digestibility of the wholemeal flour.

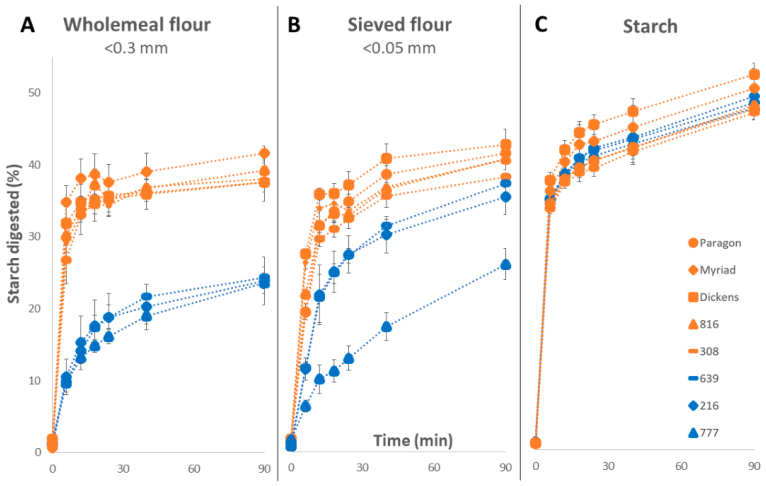

Figure 4. Starch digestibility of selected low- and high-digestibility lines measured in wholemeal flour (**A**), sieved flour (**B**) and purified starch (**C**) using the HTA. Samples in blue represent the low-digestibility lines, and samples in orange represent the high-digestibility lines. Values represent mean ± SE of $n = 3$ replicates.

Starch digestibility has also been shown to be affected by the particle size of wheat flour [17]. Particle size analysis of wholemeal flour from selected low- and high-digestibility lines showed no major variation (Supplemental Figure S6). There was a statistically significant difference ($p < 0.003$) in the particle size of wholemeal flour; line 639 had more particles in the range of 14–20 µm whereas Paragon showed a slightly smaller number of particles in that range. Micrographs of wholemeal flour (produced using scanning electron microscopy) showed aggregate formations ≥ 120µm in all lines apart from the low-digestibility line 639, which only had particles smaller than 120µm (Supplemental Figure S7). This data suggests that the milling efficiency was similar in all lines apart from 639.

Elevated amounts of endogenous α-amylase in cereals could trigger early starch amylolysis in the endosperm and thus significantly affect starch digestibility [45,46]. The activity of endogenous α-amylase in low- and high-digestibility lines differed significantly ($p < 0.05$), (Supplemental Table S1), however values were within a normal range (<0.2 Ceralpha Units/g) according to prior studies (McCleary et al., 2002, Derkx and Mares, 2020). The activity of endogenous α-amylase in low-digestibility lines ranged from 0.06 ± 0.01 to 0.15 ± 0.01 Ceralpha Units/g of flour, mean ± SD, with the lowest in line 639 and the highest line 216. High-digestibility lines varied from 0.05 ± 0.01 to

0.13 ± 0.01 Ceralpha Units/g of flour, mean ± SD, Paragon being the lowest and line 308 the highest.

Grain hardness can impact starch digestibility and is mainly affected by the protein content and composition in the endosperm [47]. Thus, protein content of wholemeal flour was analysed in the selected lines. Results showed that protein content varied significantly ($p < 0.001$) (Supplemental Table S1); low-digestibility lines ranged from 14.2–18.4 g/100 flour, mean and high-digestibility lines ranged from 10.6–17.4 g/100 g flour, mean.

The different digestibility profiles observed across purification steps (wholemeal flour to sieved flour to purified starch) suggest that multiple mechanisms in the selected lines could be affecting starch digestibility and that different factors in each line could have a distinct effect. This is consistent with prior studies which have shown effects of flour characteristics and starch structure on starch digestibility in cooked wheat samples including particle size of wholemeal flour, protein content, and chain-length distribution of starch polymers [31,48,49]. An important limitation of this aspect of the study was the small number of lines selected for this analysis severely limiting the power to detect correlations of phenotypes between lines; prior work by Wang et al. [29] identified starch properties influencing starch digestibility in a screen of 224 wheat starches. Nevertheless, our study suggests that a combination and interaction of many factors are required to achieve low starch digestibility profiles in flour, so using a starch digestibility HTA for screening or selection approaches may be more efficient and informative than selection based solely on underlying factors such as starch molecular structure.

3.2. Establishment and Validation of a High-Throughput Starch Digestibility Assay

The aim of this experiment was to validate and assess the reliability of the 96-sample format starch digestibility assay using established starch standards of maize and wheat by comparing the HTA with the single-enzyme system protocol presented in Edwards et al., 2019 [33].

The HTA (detailed in the Section 2) was scaled from a 6-tube format to a 96-well plate format which required optimizations for maintaining even heat distribution during starch digestions and PAHBAH assays, for the mixing ability of samples, and for recovering adequate sample volumes for analysis. We also developed new tools to allow faster sample handling for sample preparation and pipetting (Plate Z, available free to download from hackster.io, (accessed on 16 November 2022). A graphical scheme is presented in the Supplemental Materials highlighting the changes made to develop the HTA (Supplementary Figure S8).

Digestion profiles of maize and wheat starch standards were comparable to profiles generated using the single-enzyme system protocol in Edwards et al., 2019 [33] (Figure 5A). For example, the difference in the average estimates at 90 min (Figure 5B) from the two methods was −0.72 percentage points (not statistically significant), and the technical variation observed at 90 min within the runs was 2.1 percentage points in the HTA and 2.2 percentage points in the single-enzyme system protocol, suggesting that the HTA is not biased and is no less reliable.

There were no significant differences in the percent of starch digested at all the time points measured between the single-enzyme system protocol and the HTA. Thus, the HTA provided comparisons between samples that were accurate and reproducible, and the reliability of the assay was sufficient for use as a screening tool to aid in the selection of low- and high-digestibility samples.

The variance using wholemeal flour (in the c.Watkins screen, Section 3.1.1) was higher than the variance using starch standards in the validation experiment which could be due to the higher variability in wholemeal flour composition compared to purified starch samples. The number of technical replicates needed to estimate starch digestibility to a given precision can be calculated from residual variance.

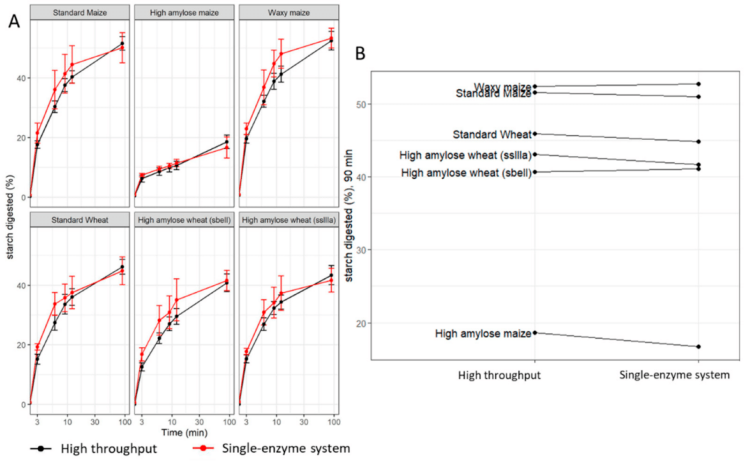

Figure 5. Comparison of the HTA to the single-enzyme system protocol reported in Edwards et al., 2019. (**A**) Digestibility profiles of purified maize and wheat starch produced by the HTA (black) and the single-enzyme system (red). (**B**) Starch digested (%) at 90 min, ranking comparison of the HTA (left) to the single-enzyme system (right). Values represent the mean ± SD of $n = 18$ replicates for the HTA and $n = 6$ for the single-enzyme system.

Recent studies have reported improved methods to increase the throughput of starch digestibility assays. Wang et al. [29] developed a 96-sample format assay to screen starch from a wheat MAGIC population and used a multifactorial analysis to identify the most influential factors for starch digestibility (starch granule size distribution, amylopectin chain length distribution, amylose content and endogenous α-amylase activity). Other studies have also aimed to increase the throughput of starch characterization techniques however, the starch properties analyzed may or may not have a direct impact on starch digestibility [50,51]. It is important to consider that other components of wheat flour and factors like processing are likely to have a major impact on starch digestibility thus, determining starch digestibility on processed flour samples may better represent what people may consume in wheat-based foods [29,30,33,53]. Some progress has been made for other crops like rice; Toutounji et al. [52] developed a 15-sample format assay for screening starch digestibility of cooked rice grains with potential to allow analysis of 60 samples per day (if 15 samples are prepared every two hours). In this method, samples were handled individually with a single pipette, which was a limiting factor for the number of samples that could be processed simultaneously. Furthermore, the assay was performed using a set of 8 samples and this assay still needs to be validated on a larger sample set. The HTA assay described here addresses some of these key limitations presented by prior assays namely the type of sample analyzed (hydrothermally processed flour) and sample size (96-sample format). For future work, it will be important to consider improving the efficiency of upstream steps, including milling, sieving, and weighing samples which present additional bottlenecks.

4. Conclusions

In this study we identified wide variation in starch digestibility among the c.Watkins lines which could be used to recover valuable alleles that were lost during modern breeding with the aim of improving wheat nutritional quality. Starch digestibility profiles of sieved flour and purified starch from selected lines suggested that the differences observed in starch digestibility are likely due to multiple factors in the flour matrix and are not limited

to starch structural properties. Previously, strategies to reduce starch digestibility in wheat have mainly focused on reverse genetic approaches, but with new tools like the HTA there is potential to discover other useful sources of variation to support development of wheat varieties with improved health benefits. Furthermore, future work to determine starch digestibility in white flour samples will be useful for identifying sources of reduced starch digestibility for applications in foods made with refined flour.

Supplementary Materials: The following supporting information can be downloaded at: https://www.mdpi.com/article/10.3390/foods12020266/s1, Supplemental.docx, data sets of starch digestibility and total starch, and all statistical analysis code. Additional references cited in Supplementary Materials: [53,54].

Author Contributions: P.Z.: Conceptualization, investigation, methodology, project administration, data curation, and formal analysis, writing—original draft preparation, writing—review and editing, G.M.S.: methodology, data curation, visualization, formal analysis, writing—review and editing, J.H.A.-J.: investigation, methodology, writing—review and editing, F.J.W.: conceptualization, methodology, supervision, writing—review and editing, M.P.: investigation, methodology, writing—review and editing, S.G.: conceptualization, methodology, supervision, writing—review and editing, D.S.: conceptualization, investigation, methodology, supervision, writing—review and editing, B.A.H.: conceptualization, funding acquisition, methodology, supervision, writing—review and editing. All authors have read and agreed to the published version of the manuscript.

Funding: This research was funded by the UKRI Biotechnology and Biological Sciences Research Council Norwich Research Park Biosciences Doctoral Training Partnership [grant number BB/M011216/1] (PZ) and the UKRI Biotechnology and Biological Sciences Research Council (BBSRC) Institute Strategic Programme 'Food Innovation and Health' (grant number BB/R012512/1) and its constituent projects BBS/E/F/000PR10343 (Theme 1, Food Innovation) and BBS/E/F/000PR10345 (Theme 2, Digestion in the Upper GI Tract) and the BBSRC Core Capability Grant BB/CCG1860/1 awarded to Quadram Institute Bioscience; the BBSRC Institute Strategic Programme Grants 'Molecules from Nature'—Crop Quality BBS/E/J/000PR9799 awarded to the John Innes Centre and 'Designing Future Wheat' BB/P016855/1 awarded to the John Innes Centre.

Data Availability Statement: Data sets of starch digestibility and total starch and all statistical analysis code are included as Supplementary Materials.

Conflicts of Interest: The authors declare no conflict of interest. The funders had no role in the design of the study; in the collection, analyses, or interpretation of data; in the writing of the manuscript; or in the decision to publish the results.

References

1. Blaak, E.E.; Antoine, J.M.; Benton, D.; Björck, I.; Bozzetto, L.; Brouns, F.; Diamant, M.; Dye, L.; Hulshof, T.; Holst, J.J.; et al. Impact of postprandial glycaemia on health and prevention of disease. *Obes. Rev.* **2012**, *13*, 923–984. [CrossRef] [PubMed]
2. Corrado, M.; Ahn-Jarvis, J.H.; Fahy, B.; Savva, G.M.; Edwards, C.H.; Hazard, B.A. Effect of high-amylose starch branching enzyme II wheat mutants on starch digestibility in bread, product quality, postprandial satiety and glycaemic response. *Food Funct.* **2022**, *13*, 1617–1627. [CrossRef] [PubMed]
3. Belobrajdic, D.P.; Regina, A.; Klingner, B.; Zajac, I.; Chapron, S.; Berbezy, P.; Bird, A.R. High-amylose wheat lowers the postprandial glycemic response to bread in healthy adults: A randomized controlled crossover trial. *J. Nutr.* **2019**, *149*, 1335–1345. [CrossRef] [PubMed]
4. Hughes, R.L.; Horn, W.H.; Finnegan, P.; Newman, J.W.; Marco, M.L.; Keim, N.L.; Kable, M.E. Resistant Starch Type 2 from Wheat Reduces Postprandial Glycemic Response with Concurrent Alterations in Gut Microbiota Composition. *Nutrients* **2021**, *13*, 645. [CrossRef] [PubMed]
5. Shewry, P.R.; Hey, S.J. The contribution of wheat to human diet and health. *Food Energy Secur.* **2015**, *4*, 178–202. [CrossRef] [PubMed]
6. Hazard, B.; Trafford, K.; Lovegrove, A.; Griffiths, S.; Uauy, C.; Shewry, P. Strategies to improve wheat for human health. *Nat. Food* **2020**, *1*, 475–480. [CrossRef]
7. Shewry, P.R.; Hawkesford, M.J.; Piironen, V.; Lampi, A.-M.; Gebruers, K.; Boros, D.; Andersson, A.A.; Åman, P.; Rakszegi, M.; Bedo, Z. Natural variation in grain composition of wheat and related cereals. *J. Agric. Food Chem.* **2013**, *61*, 8295–8303. [CrossRef]
8. Delcour, J.A.; Hoseney, R.C. *Principles of Cereal Science and Technology*, 3rd ed.; AACC International: St. Paul, MN, USA, 2010.
9. Wang, S.; Copeland, L. Molecular disassembly of starch granules during gelatinization and its effect on starch digestibility: A review. *Food Funct.* **2013**, *4*, 1564–1580. [CrossRef]

10. Chung, H.-J.; Lim, H.S.; Lim, S.-T. Effect of partial gelatinization and retrogradation on the enzymatic digestion of waxy rice starch. *J. Cereal Sci.* **2006**, *43*, 353–359. [CrossRef]
11. Parada, J.; Aguilera, J.M. In vitro digestibility and glycemic response of potato starch is related to granule size and degree of gelatinization. *J. Food Sci.* **2009**, *74*, E34–E38. [CrossRef]
12. Wang, S.; Li, C.; Copeland, L.; Niu, Q.; Wang, S. Starch retrogradation: A comprehensive review. *Compr. Rev. Food Sci. Food Saf.* **2015**, *14*, 568–585. [CrossRef]
13. Corrado, M.; Cherta-Murillo, A.; Chambers, E.S.; Wood, A.J.; Plummer, A.; Lovegrove, A.; Edwards, C.H.; Frost, G.S.; Hazard, B.A. Effect of semolina pudding prepared from starch branching enzyme IIa and b mutant wheat on glycaemic response in vitro and in vivo: A randomised controlled pilot study. *Food Funct.* **2020**, *11*, 617–627. [CrossRef] [PubMed]
14. Hazard, B.; Zhang, X.; Naemeh, M.; Hamilton, M.K.; Rust, B.; Raybould, H.E.; Newman, J.W.; Martin, R.; Dubcovsky, J. Mutations in durum wheat SBEII genes affect grain yield components, quality, and fermentation responses in rats. *Crop Sci.* **2015**, *55*, 2813–2825. [CrossRef] [PubMed]
15. Schönhofen, A.; Hazard, B.; Zhang, X.; Dubcovsky, J. Registration of common wheat germplasm with mutations in SBEII genes conferring increased grain amylose and resistant starch content. *J. Plant Regist.* **2016**, *10*, 200–205. [CrossRef] [PubMed]
16. Anugerah, M.P.; Faridah, D.N.; Afandi, F.A.; Hunaefi, D.; Jayanegara, A. Annealing processing technique divergently affects starch crystallinity characteristic related to resistant starch content: A literature review and meta-analysis. *Int. J. Food Sci. Technol.* **2022**, *57*, 2535–2544. [CrossRef]
17. Edwards, C.H.; Grundy, M.M.; Grassby, T.; Vasilopoulou, D.; Frost, G.S.; Butterworth, P.J.; Berry, S.E.; Sanderson, J.; Ellis, P.R. Manipulation of starch bioaccessibility in wheat endosperm to regulate starch digestion, postprandial glycemia, insulinemia, and gut hormone responses: A randomized controlled trial in healthy ileostomy participants. *Am. J. Clin. Nutr.* **2015**, *102*, 791–800. [CrossRef]
18. López-Barón, N.; Gu, Y.; Vasanthan, T.; Hoover, R. Plant proteins mitigate in vitro wheat starch digestibility. *Food Hydrocoll.* **2017**, *69*, 19–27. [CrossRef]
19. Botticella, E.; Sestili, F.; Sparla, F.; Moscatello, S.; Marri, L.; Cuesta-Seijo, J.A.; Falini, G.; Battistelli, A.; Trost, P.; Lafiandra, D. Combining mutations at genes encoding key enzymes involved in starch synthesis affects the amylose content, carbohydrate allocation and hardness in the wheat grain. *Plant Biotechnol. J.* **2018**, *16*, 1723–1734. [CrossRef]
20. Schonhofen, A.; Zhang, X.Q.; Dubcovsky, J. Combined mutations in five wheat STARCH BRANCHING ENZYME II genes improve resistant starch but affect grain yield and bread-making quality. *J. Cereal Sci.* **2017**, *75*, 165–174. [CrossRef]
21. Fahy, B.; Gonzalez, O.; Savva, G.M.; Ahn-Jarvis, J.H.; Warren, F.J.; Dunn, J.; Lovegrove, A.; Hazard, B.A. Loss of starch synthase IIIa changes starch molecular structure and granule morphology in grains of hexaploid bread wheat. *Sci. Rep.* **2022**, *12*, 1–14. [CrossRef]
22. Wingen, L.U.; Orford, S.; Goram, R.; Leverington-Waite, M.; Bilham, L.; Patsiou, T.S.; Ambrose, M.; Dicks, J.; Griffiths, S. Establishing the A. E. Watkins landrace cultivar collection as a resource for systematic gene discovery in bread wheat. *Theor. Appl. Genet.* **2014**, *127*, 1831–1842. [CrossRef] [PubMed]
23. Bansal, U.K.; Forrest, K.L.; Hayden, M.J.; Miah, H.; Singh, D.; Bariana, H.S. Characterisation of a new stripe rust resistance gene Yr47 and its genetic association with the leaf rust resistance gene Lr52. *Theor. Appl. Genet.* **2011**, *122*, 1461–1466. [CrossRef]
24. Bansal, U.K.; Arief, V.N.; DeLacy, I.H.; Bariana, H.S. Exploring wheat landraces for rust resistance using a single marker scan. *Euphytica* **2013**, *194*, 219–233. [CrossRef]
25. Randhawa, M.S.; Bariana, H.S.; Mago, R.; Bansal, U.K. Mapping of a new stripe rust resistance locus Yr57 on chromosome 3BS of wheat. *Mol. Breed.* **2015**, *35*, 65. [CrossRef]
26. Toor, A.K.; Bansal, U.K.; Bhardwaj, S.; Badebo, A.; Bariana, H.S. Characterization of stem rust resistance in old tetraploid wheat landraces from the Watkins collection. *Genet. Resour. Crop Evol.* **2013**, *60*, 2081–2089. [CrossRef]
27. Chen, M.-H.; Bergman, C.J.; McClung, A.M.; Everette, J.D.; Tabien, R.E. Resistant starch: Variation among high amylose rice varieties and its relationship with apparent amylose content, pasting properties and cooking methods. *Food Chem.* **2017**, *234*, 180–189. [CrossRef] [PubMed]
28. Mishra, A.; Singh, A.; Sharma, M.; Kumar, P.; Roy, J. Development of EMS-induced mutation population for amylose and resistant starch variation in bread wheat (Triticum aestivum) and identification of candidate genes responsible for amylose variation. *BMC Plant Biol.* **2016**, *16*, 1–15. [CrossRef] [PubMed]
29. Wang, Y.; Kansou, K.; Pritchard, J.; Zwart, A.B.; Saulnier, L.; Ral, J.-P. Beyond amylose content, selecting starch traits impacting in vitro α-amylase degradability in a wheat MAGIC population. *Carbohydr. Polym.* **2022**, *291*, 119652. [CrossRef]
30. Edwards, C.H.; Warren, F.J.; Milligan, P.J.; Butterworth, P.J.; Ellis, P.R. A novel method for classifying starch digestion by modelling the amylolysis of plant foods using first-order enzyme kinetic principles. *Food Funct.* **2014**, *5*, 2751–2758. [CrossRef] [PubMed]
31. Sissons, M.; Cutillo, S.; Marcotuli, I.; Gadaleta, A. Impact of durum wheat protein content on spaghetti in vitro starch digestion and technological properties. *J. Cereal Sci.* **2021**, *98*, 103156. [CrossRef]
32. Qi, K.; Yi, X.; Li, C. Effects of endogenous macronutrients and processing conditions on starch digestibility in wheat bread. *Carbohydr. Polym.* **2022**, *295*, 119874. [CrossRef] [PubMed]
33. Edwards, C.H.; Cochetel, N.; Setterfield, L.; Perez-Moral, N.; Warren, F.J. A single-enzyme system for starch digestibility screening and its relevance to understanding and predicting the glycaemic index of food products. *Food Funct.* **2019**, *10*, 4751–4760. [CrossRef] [PubMed]

34. Butterworth, P.J.; Warren, F.J.; Grassby, T.; Patel, H.; Ellis, P.R. Analysis of starch amylolysis using plots for first-order kinetics. *Carbohydr. Polym.* **2012**, *87*, 2189–2197. [CrossRef]
35. Goñi, I.; Garcia-Alonso, A.; Saura-Calixto, F. A starch hydrolysis procedure to estimate glycemic index. *Nutr. Res.* **1997**, *17*, 427–437. [CrossRef]
36. Lever, M. A new reaction for colorimetric determination of carbohydrates. *Anal. Biochem.* **1972**, *47*, 273–279. [CrossRef]
37. Fahy, B.; Siddiqui, H.; David, L.C.; Powers, S.J.; Borrill, P.; Uauy, C.; Smith, A.M. Final grain weight is not limited by the activity of key starch-synthesising enzymes during grain filling in wheat. *J. Exp. Bot.* **2018**, *69*, 5461–5475. [CrossRef]
38. Hawkins, E.; Chen, J.; Watson-Lazowski, A.; Ahn-Jarvis, J.; Barclay, J.E.; Fahy, B.; Hartley, M.; Warren, F.J.; Seung, D. STARCH SYNTHASE 4 is required for normal starch granule initiation in amyloplasts of wheat endosperm. *BioRxiv* **2021**, *230*, 2371–2386. [CrossRef]
39. Kunzetsova, A.; Brockhoff, P.; Christensen, R. lmerTest package: Tests in linear mixed effect models. *J. Stat. Softw.* **2017**, *82*, 1–26.
40. Bates, D.; Maechler, M.; Bolker, B.; Walker, S. Fitting linear mixed-effects models using lme4. *arXiv* **2014**, arXiv:1406.5823.
41. Pinheiro, J.; Bates, D.; DebRoy, S.; Sarkar, D. R Core Team. 2021. Nlme: Linear and Nonlinear Mixed Effects Models. R Package Version 3.1-153. Available online: https://cran.r-project.org/web/packages/nlme/index.html (accessed on 31 March 2022).
42. Wickham, H. Data Analysis. In *ggplot2: Elegant Graphics for Data Analysis*; Springer International Publishing: Cham, Switzerland, 2016; pp. 189–201.
43. Wingen, L.U.; West, C.; Leverington-Waite, M.; Collier, S.; Orford, S.; Goram, R.; Yang, C.Y.; King, J.; Allen, A.M.; Burridge, A.; et al. Wheat Landrace Genome Diversity. *Genetics* **2017**, *205*, 1657–1676. [CrossRef]
44. Brodkorb, A.; Egger, L.; Alminger, M.; Alvito, P.; Assunção, R.; Ballance, S.; Bohn, T.; Bourlieu-Lacanal, C.; Boutrou, R.; Carrière, F.; et al. INFOGEST static in vitro simulation of gastrointestinal food digestion. *Nat. Protoc.* **2019**, *14*, 991–1014. [CrossRef] [PubMed]
45. Newberry, M.; Zwart, A.B.; Whan, A.; Mieog, J.C.; Sun, M.; Leyne, E.; Pritchard, J.; Daneri-Castro, S.N.; Ibrahim, K.; Diepeveen, D.; et al. Does Late Maturity Alpha-Amylase Impact Wheat Baking Quality? *Front. Plant Sci.* **2018**, *9*, 1356. [CrossRef] [PubMed]
46. Derkx, A.P.; Mares, D.J. Late-maturity α-amylase expression in wheat is influenced by genotype, temperature and stage of grain development. *Planta* **2020**, *251*, 51. [CrossRef] [PubMed]
47. Morris, C.F. Puroindolines: The molecular genetic basis of wheat grain hardness. *Plant Mol. Biol.* **2002**, *48*, 633–647. [CrossRef] [PubMed]
48. Obadi, M.; Li, C.; Li, Q.; Li, X.; Qi, Y.; Xu, B. Relationship between starch fine molecular structures and cooked wheat starch digestibility. *J. Cereal Sci.* **2020**, *95*, 103047. [CrossRef]
49. Lin, S.; Gao, J.; Jin, X.; Wang, Y.; Dong, Z.; Ying, J.; Zhou, W. Whole-wheat flour particle size influences dough properties, bread structure and in vitro starch digestibility. *Food Funct.* **2020**, *11*, 3610–3620. [CrossRef]
50. Kaufman, R.C.; Wilson, J.D.; Bean, S.R.; Herald, T.J.; Shi, Y.C. Development of a 96-well plate iodine binding assay for amylose content determination. *Carbohydr. Polym.* **2015**, *115*, 444–447. [CrossRef]
51. Perez-Moral, N.; Plankeele, J.-M.; Domoney, C.; Warren, F.J. Ultra-high performance liquid chromatography-size exclusion chromatography (UPLC-SEC) as an efficient tool for the rapid and highly informative characterisation of biopolymers. *Carbohydr. Polym.* **2018**, *196*, 422–426. [CrossRef]
52. Toutounji, M.R.; Butardo, V.M.; Zou, W.; Farahnaky, A.; Pallas, L.; Oli, P.; Blanchard, C.L. A High-Throughput In Vitro Assay for Screening Rice Starch Digestibility. *Foods* **2019**, *8*, 601. [CrossRef]
53. Cave, R.A.; Seabrook, S.A.; Gidley, M.J.; Gilbert, R.G. Characterization of Starch by Size-Exclusion Chromatography: The Limitations Imposed by Shear Scission. *Biomacromolecules* **2009**, *10*, 2245–2253. [CrossRef]
54. AACC. AACC method 46-30.01, Crude protein—Combustion method. *AACC Approv. Methods Anal.* **2010**. [CrossRef]